MICROCOPY RESOLUTION TEST CHART
NATIONAL BUREAU OF STANDARDS-1963-A

NAVAL POSTGRADUATE SCHOOL
Monterey, California

THESIS

BANK-TO-TURN CRUISE MISSILE TERMINAL
GUIDANCE AND CONTROL LAW COMPARISON

by

Kent B. Watterson

June 1983

Thesis Advisor: Marle D. Hewett

Approved for public release, distribution unlimited

83 09 19 093

REPORT DOCUMENTATION PAGE	READ INSTRUCTIONS BEFORE COMPLETING FORM

1. REPORT NUMBER	2. GOVT ACCESSION NO. AD A132595	3. RECIPIENT'S CATALOG NUMBER

4. TITLE (and Subtitle)	5. TYPE OF REPORT & PERIOD COVERED
Bank-To-Turn Cruise Missile Terminal Guidance and Control Law Comparison	Master's Thesis June 1983
	6. PERFORMING ORG. REPORT NUMBER

7. AUTHOR(s)	8. CONTRACT OR GRANT NUMBER(s)
Kent B. Watterson	

9. PERFORMING ORGANIZATION NAME AND ADDRESS	10. PROGRAM ELEMENT, PROJECT, TASK AREA & WORK UNIT NUMBERS
Naval Postgraduate School Monterey, California 93940	

11. CONTROLLING OFFICE NAME AND ADDRESS	12. REPORT DATE
Naval Postgraduate School Monterey, California 93940	June 1983
	13. NUMBER OF PAGES 189

14. MONITORING AGENCY NAME & ADDRESS(if different from Controlling Office)	15. SECURITY CLASS. (of this report)
	15a. DECLASSIFICATION/DOWNGRADING SCHEDULE

16. DISTRIBUTION STATEMENT (of this Report)

Approved for public release, distribution unlimited

17. DISTRIBUTION STATEMENT (of the abstract entered in Block 20, if different from Report)

18. SUPPLEMENTARY NOTES

19. KEY WORDS (Continue on reverse side if necessary and identify by block number)

Bank-To-Turn Terminal Homing
Proportional Navigation
Guidance and Control

20. ABSTRACT (Continue on reverse side if necessary and identify by block number)

This work consists of the development of the six degree of freedom non-linear model of a sea launched generic bank-to-turn cruise missile attacking a medium sized combatant ship. Two guidance and control schemes are compared in the terminal phase. The first, or baseline guidance scheme (pop out maneuver), uses a 50-foot altitude hold for an ingress phase, followed by a pop out maneuver, and then an attack phase which uses proportional

20. ABSTRACT (cont'd)

navigation in elevation and azimuth planes along with bank-to-turn maneuvering. The second scheme (sea skimmer) uses identical ingress and attack phases but eliminates the pop out maneuver. Miss distances for both schemes are compared while varying missile roll rate limit, ECM blinking frequency, and burn through ranges.

Accession For	
NTIS GRA&I	X
DTIC TAB	☐
Unannounced	☐
Justification	
By	
Distribution/	
Availability Codes	
Dist	Avail and/or Special
A	

Bank-To-Turn Cruise Missile Terminal
Guidance and Control Law Comparison

by

Kent B. Watterson
Lieutenant Commander, United States Navy
B.S., Findlay College, 1969

Submitted in partial fulfillment of the
requirements for the degree of

MASTER OF SCIENCE IN ENGINEERING SCIENCE

from the

NAVAL POSTGRADUATE SCHOOL
June 1983

Author: _____

Approved by: _____
                                    Thesis Advisor

_____
                                    Second Reader

_____
Chairman, Department of Electrical Engineering

_____
Dean of Science and Engineering

ABSTRACT

This work consists of the development of the six degree
of freedom non linear model of a sea launched generic bank-to-
turn cruise missile attacking a medium sized combatant ship.
Two guidance and control schemes are compared in the terminal
phase. The first, or baseline guidance scheme (pop out
maneuver), uses a 50-foot altitude hold for an ingress phase,
followed by a pop out maneuver, and then an attack phase which
uses proportional navigation in elevation and azimuth planes
along with bank-to-turn maneuvering. The second scheme
(sea skimmer) uses identical ingress and attack phases but
eliminates the pop out maneuver. Miss distances for both
schemes are compared while varying missile roll rate limit,
ECM blinking frequency, and burn through ranges.

TABLE OF CONTENTS

LIST OF TABLES

LIST OF FIGURES

SYMBOLS AND ABBREVIATIONS

U	Linear Velocity along body x axis
V	Linear Velocity along body y axis
W	Linear Velocity along body z axis
P	Roll rate
Q	Pitch rate
R	Yaw rate
X	Aerodynamic force in body x direction
Y	Aerodynamic force in body y direction
Z	Aerodynamic force in body z direction
Φ	Bank angle
Θ	Pitch angle
Ψ	Yaw angle
X_E	Earth coordinate of missile (Latitude)
Y_E	Earth coordinate of missile (-Longitude)
$-Z_E = H_E$	Earth coordinate of missile (Altitude)
L_A	Rolling Moment about x axis (Aerodynamic)
M_A	Pitching moment about y axis (Aerodynamic)
N_A	Pitching moment about z axis (Aerodynamic)
V_T	Total missile velocity
T	Thrust
$\overline{q}$	Dynamic pressure $(\frac{1}{2} \rho V_T^2)$
α	Angle of attack
β	Side slip angle

γ	Flight path angle ($\theta + \alpha$)
ρ	Air density (0.002377)
S	Wing area (12 ft.^{2})
b	Wing span (8.485 ft.)
$\bar{c}$	Mean aerodynamic chord (1.414 ft.)
η	Elevator Deflection
ξ	Aileron Deflection
ζ	Rudder Deflection
η_L	Left Stabilator Deflection
η_R	Right Stabilator Deflection
L	Lift force
D	Drag force
N	Normal force
C	Chord wise force
m	Missile mass (68.38 slugs)
g	Acceleration due to gravity (32.17 ft/sec^2)
ST	Static coefficient
DYN	Dynamic coefficient
n_z	Normal load factor (body fixed axis system)*
n_y	Lateral load factor (body fixed axis system)*
n_Z	Vertical load factor (earth fixed axis system)*
n_Y	Horizontal load factor (earth fixed axis system)*
u	Perturbed linear velocity x axis *
v	Perturbed linear velocity y axis *
w	Perturbed linear velocity z axis *

14

p	Perturbed angular velocity about x axis [*]
q	Perturbed angular velocity about y axis [*]
r	Perturbed angular velocity about z axis[*]
ϕ	Perturbed Euler angle Φ [*]
θ	Perturbed Euler Angle Θ [*]
ψ	Perturbed Euler Angle Ψ [*]
*	Laplace transforms of these variables are shown in capital letters

SUBSCRIPTS

SS	Steady State
E	Earth
B	Body
x,y,z	In body fixed axes
X,Y,Z	In earth fixed axes
T	Due to thrust/Target
A	Due to Aerodynamic Forces
xx,yy,zz	About the axis specified
ST	Steady State
DYN	Dynamic
EL	Eleration
AZ	Azimuth
c	Commanded

ACKNOWLEDGMENT

The author wishes to express his sincere appreciation to Professor M. D. Hewett for his guidance, direction and understanding in completing this work.

I. INTRODUCTION

The relative merits of bank-to-turn versus skid-to-turn missiles have been argued for years. Bank-to-turn missiles which must roll to a commanded bank angle before a lateral acceleration can be commanded in the appropriate direction are inherently slower to respond to target maneuvering than skin-to-turn missiles of comparable lateral acceleration capabilities. This is particularly true if the bank-to-turn missile has limited roll authority or limited roll rate capability. On the other hand, as discussed in Gonzalez, {Ref. 1}, it is sometimes difficult to build a skid-to-turn missile which meets certain operational goals and performance criteria and also has sufficient control authority in both the y and z directions to generate the large lateral accelerations required to perform skid-to-turn.

In this thesis the terminal guidance accuracy of a bank-to-turn cruise missile is studied for a sea launched, sea target cruise missile of conventional wing-tail configuration. It is assumed that roll authority is extremely limited due to operational design restrictions which impose the use of low authority ailerons or differential stabilator (no ailerons) for rolling. Lateral acceleration is also assumed to be extremely limited in the y direction due to the presence of only a small vertical surface at the tail (vertical stabilizer and rudder).

17

Two bank-to-turn guidance schemes are compared for accuracy against a medium sized combatant ship employing electronic countermeasures (an ECM blinker mounted aft on the ship). The first baseline scheme employs a pop-out maneuver consisting of a low altitude run in, azimuth offset, pop-up and roll into the target using proportional navigation in azimuth and elevation. The second, or sea-skimmer scheme, employs a straight-in low altitude attack. Miss distances for both schemes are compared while varying missile roll rate limit, ECM blinking frequency and burn through ranges.

A CSMP III simulation was coded to perform the study. Missile dynamics were represented by 6 degree of freedom nonlinear equations of motion with table look-up aerodynamic coefficients. These coefficients are representative of a generic cruise missile with a conventional wing-tail configuration of limited roll authority. Inner loop augmentation and autopilot modes were designed to improve missile damping in all axes, provide commanded load factor, commanded bank angle, and turn coordination. Autopilot outer loops were designed to provide altitude hold, and vertical flight path angle hold. Guidance loops were designed to provide proportional navigation in elevation and azimuth.

Since this study involves the influence of flight dynamic parameters (roll rate limits) on terminal guidance accuracy, no extensive tracker modeling is employed in the simulation. It is assumed that the seeker always tracks

18

the point target perfectly. The point target is, however,
moved by an ECM blinker and contaminated with a glint model.

In Chapter II the equations used to represent missile
dynamics are presented along with the methodology used to
build up aerodynamic forces and moments. In Chapter III
the development, design and simulation of the missile auto-
pilot modes are presented. In Chapter IV the design of the
guidance systems and a complete description of the two
guidance schemes is presented. In Chapter V the CSMP
simulation is presented followed by the results and conclusions
of this study.

II. DEVELOPMENT AND SIMULATION OF MISSILE DYNAMICS

In this chapter the linear and nonlinear mathematical models are developed which are used to describe the flight dynamics of a generic bank-to-turn cruise missile. The linearized mathematical model of missile dynamics is used to design the missile autopilot control laws and guidance laws. The nonlinear mathematical model is used to accurately represent missile dynamics in a CSMP computer simulation of a sea launched generic cruise missile attacking a medium sized combatant ship. Since the purpose of this investigation is to perform a detailed evaluation of terminal control laws, it was decided that a linear dynamic simulation would not adequately represent missile motion; hence a full six degree of freedom (6 DOF) nonlinear dynamic simulation was encoded. The overall system that is modeled in this study is depicted in block diagram format in Figure 2-1 and will be developed in this thesis.

A. MISSILE EQUATIONS OF MOTION

The full nonlinear six degree of freedom rigid body, dynamic equations of motion are used to represent the motion of a generic bank-to-turn cruise missile. The aerodynamic forces and moments are built up from representative tabular coefficient data for the generic missile. These tabular

20

data are given in Appendix A in graphical form along with the generic missile's physical and geometric characteristics.

1. Assumptions

The assumptions used in the development of the equations of motion are given below.

a. The earth is flat, does not rotate, and is fixed in inertial space.

b. The mass of the missile is constant.

c. The missile is a rigid body.

d. The mass distribution of the missile is constant.

e. Engine angular momentum is neglected.

f. The missile is symmetric about the body's xy plane. Therefore, the products of inertia I_{xy} and I_{yz} are zero.

g. The engine thrust line is parallel to the missile body x axis. Thus, the thrust components T_y and T_z are zero.

h. The density of the atmosphere is constant.

i. The engine thrust line passes through the missile center of mass. Therefore, the moments due to thrust L_T, M_T and N_T are zero.

j. The wind is calm.

k. Right aileron trailing edge down is positive deflection. Negative elevator deflection yields nose up pitching moment (positive).
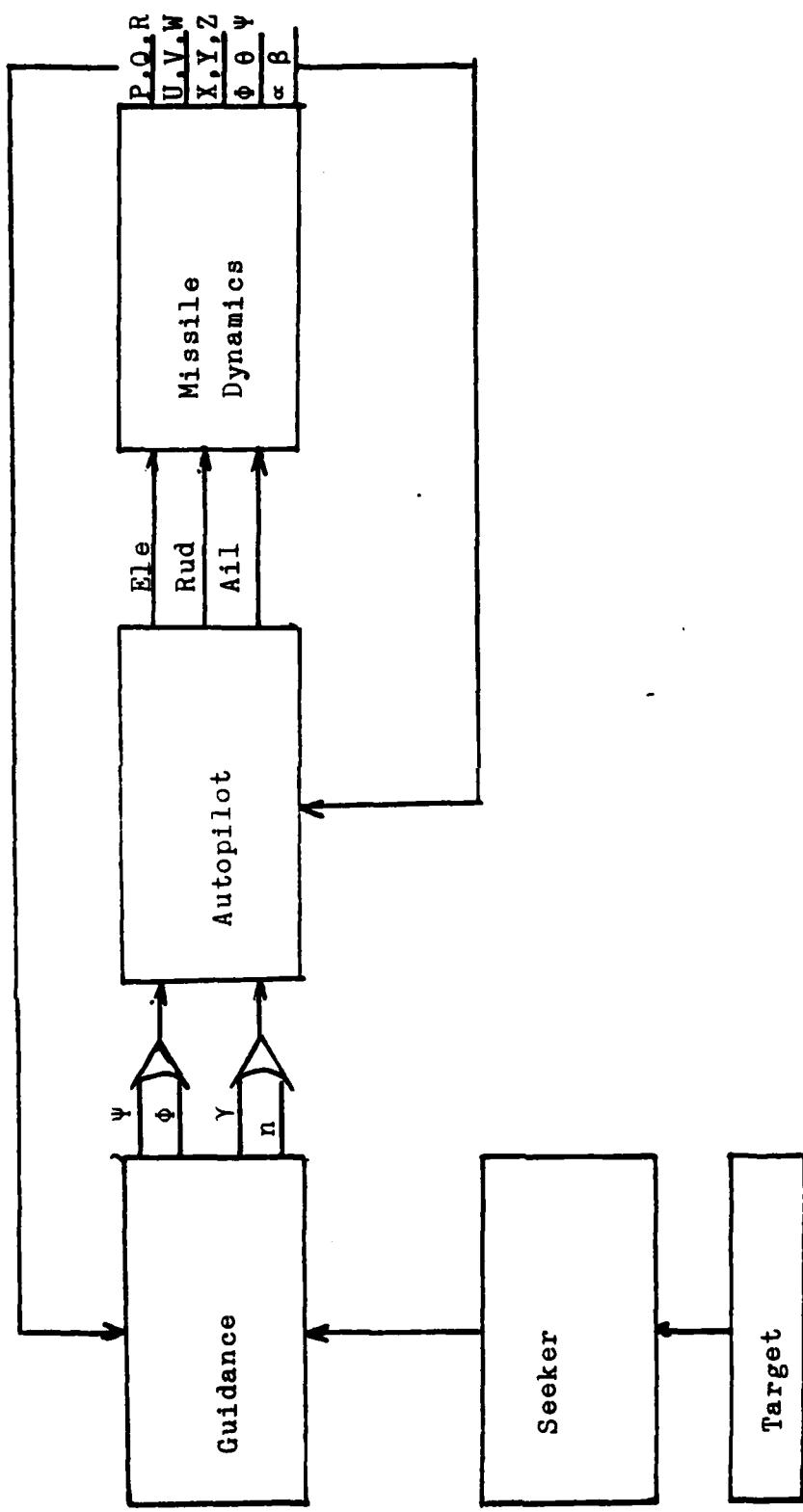
Figure 2-1   Missile System Flow Diagram

22

2. Coordinate System

An earth fixed coordinate system is established with its origin fixed at the initial position of the missile. The X_E axis points to true north, the Y_E axis points east, and the Z_E axis points toward the center of the earth. Altitude (H) therefore equals the negative of Z_E. The system is considered to be an inertial system.

A stability axis coordinate system is used with coordinates x, y, z fixed at the missile center of mass and oriented such that the x axis lies along the vehicle's forward velocity vector in steady state balanced cruise flight at 0.75 Mach number. The y axis is chosen perpendicular to the plane of symmetry and is oriented out the right wing. The z axis is chosen perpendicular to the x axis in the down direction and in the plane of symmetry.

3. The Equations of Motion

The following nonlinear equations as developed by Hewett {Ref. 2} describe the motion of the missile in 6 degrees of freedom.

$$m(\dot{U}-VR+WQ) = -mg \sin\theta + X + T \tag{1a}$$

$$m(\dot{V}+UR-WP) = mg \sin\phi \cos\theta + Y \tag{1b}$$

$$m(\dot{W}-UQ+VP) = mg \cos\phi \cos\theta + Z \tag{1c}$$

$$\dot{P}I_{xx}-(\dot{R}+PQ)I_{xz}+ RQ(I_{zz}-I_{yy}) = L_A \tag{2a}$$

$$\dot{Q}I_{yy}+PR(I_{xx}-I_{zz}) + (P^2-R^2)I_{xy} = M_A \tag{2b}$$

$$\dot{R}I_{zz}-\dot{P}I_{xz}+PQ(I_{yy}-I_{xx})+QRI_{xz} = N_A \tag{2c}$$

$$\dot\phi = P+(Q \sin \phi + R \cos \phi) \tan \theta \qquad (3a)$$

$$\dot\theta = Q \sin \phi - R \sin \phi \qquad (3b)$$

$$\dot\psi = (Q \sin \phi + R \cos \phi) \sec \theta \qquad (3c)$$

Equations (1a), (1b) and (1c) describe the translational motion of the missile. Equations (2a), (2b), and (2c) represent the rotational motion. Equations (3a), (3b) and (3c) are the Euler relations for bank, pitch and yaw angles.

Equations (4a), (4b), and (4c) describe the missile's position referenced to the earth fixed system (X_E, Y_E, Z_E).

$$\dot X_E = U \cos \psi \cos \theta + V(\cos\psi\sin\theta\sin\phi - \sin\psi\cos\phi) \qquad (4a)$$
$$+ W(\cos\psi\sin\theta\cos\phi + \sin\psi\sin\phi)$$

$$\dot Y_E = U \sin \psi \cos \theta + V(\sin\psi\sin\theta\sin\phi + \cos\psi\cos\phi) \qquad (4b)$$
$$+ W(\sin\psi\sin\theta\cos\phi - \cos\psi\sin\phi)$$

$$\dot Z_E = U\sin\theta - V\cos\theta\sin\phi - W\cos\theta\cos\phi \qquad (4c)$$

Equations (5), (6) and (7) are also required. Equations (5) and (6) yield angle of attack and side slip angle respectively in terms of velocity components U, V and W. Equation (7) represents the total velocity of the missile.

$$\alpha = \arctan \frac{W}{U} = \arcsin \frac{W}{(U^2+W^2)^{\frac{1}{2}}} \qquad (5)$$

$$\beta = \arctan \frac{V}{U^2+w^2} = \arcsin \frac{V}{(U^2+V^2+W^2)^{\frac{1}{2}}} \qquad (6)$$

$$V_T = (U^2+V^2+W^2)^{\frac{1}{2}} \qquad (7)$$

Figure 2-2 illustrates the positive directions and locations of forces, moments and velocities in the body coordinate system (x, y, z).
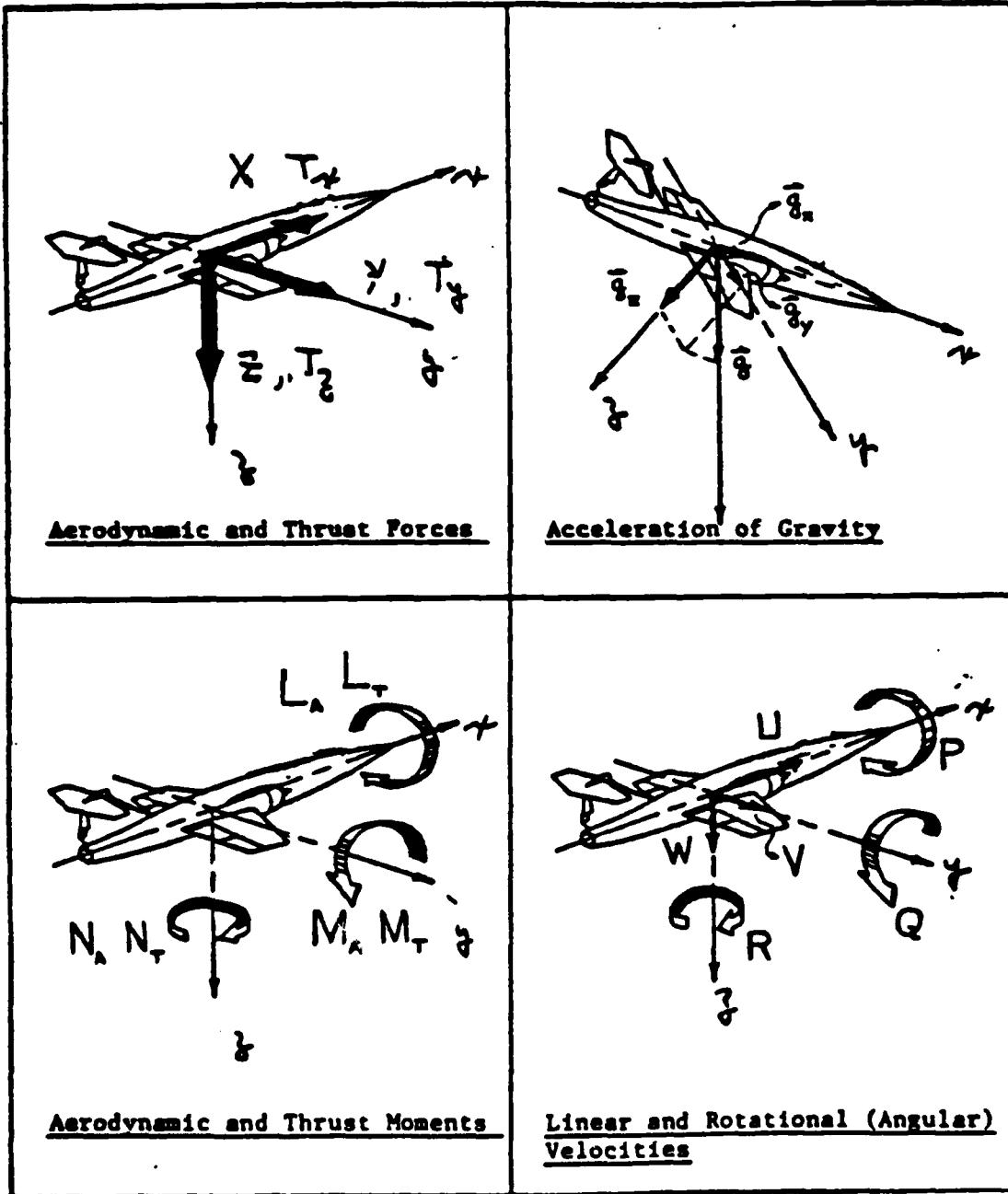
Figure 2-2   Body Coordinate System Description

Equations (1a), (1b), (1c) and (2a), (2b), (2c) can be rewritten in state format as follows:

$$\dot{U} = -g\sin\theta + VR - WQ + \frac{X}{m} + \frac{T}{m} \tag{8a}$$

$$\dot{V} = g\sin\Phi\cos\theta - UR + WP + \frac{Y}{m} \tag{8b}$$

$$\dot{W} = g\cos\Phi\cos\theta + UQ - VP + \frac{Z}{m} \tag{8c}$$

$$\dot{P} = \left[L_A I_{zz} + N_A I_{xz} - PQ(I_{yy} - I_{xx} - I_{zz})I_{xz} - RQ(I_{zz}^2 - I_{yy}I_{zz} + I_{xz}^2) \right] /$$
$$(I_{xx}I_{zz} - I_{xz}^2) \tag{9a}$$

$$\dot{Q} = \left[M_A - PR(I_{xx} - I_{zz}) - (P^2 - R^2)I_{xz} \right] / I_{yy} \tag{9b}$$

$$\dot{R} = \left[L_A I_{xz} + N_A I_{xx} - PQ(I_{yy}I_{xx} - I_{xx}^2 - I_{xz}^2) - RQ(I_{xx} + I_{zz} - I_{yy})I_{xz} \right] /$$
$$(I_{xx}I_{zz} - I_{xz}^2) \tag{9c}$$

Now integrating equations (3), (4), (8) and (9) results in U, V, W, P, Q, R, Φ, θ, Ψ, X_E, Y_E and Z_E ($-H$). The missile's velocities, angular rates, and angles and positions have thus been described.

4. Trim Equations

For straight and level flight at constant velocity the following variables are all zero: $\dot{U}$, $\dot{V}$, $\dot{W}$, $\dot{P}$, $\dot{Q}$, $\dot{R}$, Φ, θ, Ψ, Z_E, P_{SS}, Q_{SS}, R_{SS}, Φ_{SS}, $L_{A_{SS}}$, $N_{A_{SS}}$, Y_{SS}, Y_{SS}, β_{SS}, V_{SS}, $M_{A_{SS}}$ Thus the trim equations reduce to:

$$X_{SS} + T_x = mg\sin\theta_{SS}$$

$$Z_{SS} = -mg\cos\theta_{SS}$$

$$\dot{X}_{E_{SS}} = U_{SS}\cos\Psi_{SS}\cos\theta_{SS} - V_{SS}\sin\Psi_{SS} + W_{SS}\cos\Psi_{SS}\sin\theta_{SS}$$

$$\dot{Y}_{E_{SS}} = U_{SS}\sin\Psi_{SS}\cos\theta_{SS} + V_{SS}\cos\Psi_{SS} + W_{SS}\sin\Psi_{SS}\sin\theta_{SS}.$$

$$\tan\theta_{SS} = W_{SS}/U_{SS}$$

$$V_{T_{SS}} = (U_{SS}^2 + W_{SS}^2)^{\frac{1}{2}}$$

Since bank angle equals zero and the sum of flight path angle and angle of attack equal the pitch angle, then in steady state pitch angle equals angle of attack.

$$\theta_{SS} = \alpha_{SS}$$

These equations are used to define the initial cruise condition of the missile which is low level straight and level cruise flight at 0.75 Mach number. The precise initial flight condition and initial target position is described in Appendix 3.

5. Other Useful Relations

Components of load factor at the missile center of mass in the y and -z directions are given below:

$$n_z = \frac{-Z}{mg} = \frac{V_T}{g} \ (Q - \dot{\alpha}) \tag{10a}$$

$$n_y = \frac{Y}{mg} = \frac{V_T}{g} \ (\dot{\beta} + R) \tag{10b}$$

6. Definition of Controls and Control Limits

The control configuration considered in the thesis is a conventional wing and tail with conventional rudder (ζ), aileron ($\S$) and elevator (η) control surfaces. In addition, to cover a missile configuration which uses

27

differential horizontal stabilizer (stabilator) for roll control as opposed to aileron, the quantities left stabilator deflection (η_L) and right stabilator deflection (η_R) are defined and calculated.

Limits are imposed on rudder, elevator, and aileron travel. Limits are not imposed on differential stabilator travel but stabilator travel is presented for all simulations to show the stabilator travel required if indeed that were the control configuration. The aileron power coefficient data presented in Appendix A reflects the limited control authority in roll typical of a missile configured with differential stabilator for roll control as opposed to aileron.

The following control definitions and limits are applied:

a) Thrust (T) is a constant and is oriented along the x axis.

$$T = T_x = \text{constant}$$

b) Rudder deflection (ζ) is defined as positive trailing edge left from the rear and is limited to

$$-15° \leq \zeta \leq 15°$$

c) Elevator deflection (η) is defined as positive trailing edge down (produces a nose down moment) and is limited to

$$-15° \leq \eta \leq 15°$$

d) Aileron deflection (ξ) is defined as positive
with trailing edge of the right aileron up (produces a
positive (clockwise from the rear) roll) and is limited to

$$-15 \le \xi \le 15^o$$

e) Left horizontal stabilizer deflection (η_L) is
positive trailing edge down.

$$\eta_L = \eta + \xi$$

f) Right horizontal stabilizer deflection (η_R) is
positive trailing edge down.

$$\eta_R = \eta - \xi$$

B. AERODYNAMIC COEFFICIENT BUILD UP

Aerodynamic forces and moments are built up from coefficient data in standard fashion using the following relations:

$$D = C_D \bar{q} S \qquad\qquad L = C_L \bar{q} S \qquad\qquad Y = C_y \bar{q} S$$

$$M_A = C_M \bar{q}S\bar{c} \qquad\qquad L_A = C_l\bar{q}S\bar{b} \qquad\qquad N_A = C_n \bar{q} Sb$$

1. Definition of Coefficients

Each coefficient is partitioned into two parts; a
static term and a dynamic term as follows:

$$C_D = C_{D_{ST}} + C_{D_{DYN}}$$

$$C_L = C_{L_{ST}} + C_{L_{DYN}}$$

$$C_Y = C_{Y_{ST}} + C_{Y_{DYN}}$$

$$C_m = C_{m_{ST}} + C_{m_{DYN}}$$

$$C_l = C_{l_{ST}} + C_{l_{DYN}}$$

$$C_n = C_{n_{ST}} + C_{n_{DYN}}$$

2. Coefficient Build Up

The static terms are constructed from coefficient data stored in tables (Appendix A) as functions of two or three variables (either α, β, M, η, ζ, ξ) as follows:

$$C_{L_{basic}} = f\ (\alpha, \beta, M)$$

$$\Delta C_{L_{ST}}(\eta) = f\ (\alpha, \beta, \eta)$$

$$C_{D_{basic}} = f\ (\alpha, \beta, M)$$

$$\Delta C_{D_{ST}}(\eta) = f\ (\alpha, \beta, \eta)$$

$$\Delta C_{D_{ST}}(\xi) = f\ (\alpha, \beta, \xi)$$

$$\Delta C_{D_{ST}}(\zeta) = f\ (\alpha, \beta, \zeta)$$

$$C_{Y_{basic}} = f\ (\alpha, \beta)$$

$$\Delta C_{Y_{ST}}(\zeta) = f\ (\alpha, \beta, \zeta)$$

$$\Delta C_{Y_{ST}}(\xi) = f\ (\alpha, \beta, \xi)$$

$$C_{m_{basic}} = f\ (\alpha, \beta, M)$$

$$\Delta C_{m_{ST}}(\eta) = f\ (\alpha, \beta, \eta)$$

$$C_{n_{basic}} = f\ (\alpha, \beta)$$

$$\Delta C_{n_{ST}}(\zeta) = f\ (\alpha, \beta, \zeta)$$

$$\Delta C_{n_{ST}}(\xi) = f\ (\alpha, \beta, \xi)$$

$$C_{l_{basic}} = f(\alpha, \beta)$$

$$C_{l_{ST}}(\xi) = f(\alpha, \beta, \xi)$$

$$C_{l_{ST}}(\zeta) = f(\alpha, \beta, \zeta)$$

The static coefficients are formed as:

$$C_{L_{ST}} = C_{L_{basic}} + \Delta C_L(\eta)$$

$$C_{D_{ST}} = C_{D_{basic}} + \Delta C_{D_{ST}}(\eta) + \Delta C_{D_{ST}}(\xi) + \Delta C_{D_{ST}}(\zeta)$$

$$C_{Y_{ST}} = C_{Y_{basic}} + \Delta C_{Y_{ST}}(\zeta) + \Delta C_{Y_{ST}}(\xi)$$

$$C_{m_{ST}} = C_{m_{basic}} + \Delta C_{m_{ST}}(\eta)$$

$$C_{n_{ST}} = C_{n_{basic}} + \Delta C_{n_{ST}}(\xi) + \Delta C_{n_{ST}}(\zeta)$$

$$C_{l_{ST}} = C_{l_{basic}} + \Delta C_{l_{ST}}(\xi) + \Delta C_{l_{ST}}(\zeta)$$

The dynamic terms are constructed from dynamic coefficient data stored in tables (Appendix A) as a function of angle of attack and Mach number $f(\alpha, M)$. They are

$$C_{L_{\dot\alpha}}, C_{L_q}, C_{D_{\dot\alpha}}, C_{D_q}, C_{Y_\beta}, C_{Y_r}, C_{Y_p}, C_{m_{\dot\alpha}}, C_{m_q}, C_{n_\beta}, C_{n_r}, C_{n_p},$$

$$C_{l_r}, \text{ and } C_{l_p}.$$

The dynamic coefficients are formed as:

$$C_{L_{DYN}} = \frac{\bar{c}}{2V_T}(C_{L_{\dot\alpha}}\dot\alpha + C_{L_q} q)$$

$$C_{D_{DYN}} = \frac{\bar{c}}{2V_T}(C_{D_{\dot\alpha}}\dot\alpha + C_{D_q} q)$$

$$C_{Y_{DYN}} = \frac{b}{2V_T}(C_{Y_r} r + C_{Y_p} p + C_{Y_{\dot\beta}}\dot\beta)$$

$$C_{m_{DYN}} = \frac{\bar{c}}{2V_T} (C_{m_{\dot\alpha}} \dot\alpha + C_{m_q} q)$$

$$C_{n_{DYN}} = \frac{b}{2V_T} (C_{n_{\dot\beta}} \dot\beta + C_{n_r} r + C_{n_p} p)$$

$$C_{l_{DYN}} = \frac{b}{2V_T} (C_{l_r} r + C_{l_p} p)$$

The total coefficient build up is summarized below.

$$C_L = C_{L_{basic}} + \Delta C_{L_{ST}}(\eta) + \frac{\bar{c}}{2V_T} (C_{L_{\dot\alpha}} \dot\alpha + C_{L_q} q)$$

$$C_D = C_{D_{basic}} + \Delta C_{D_{ST}}(\eta) + \Delta C_{D_{ST}}(\xi) + \Delta C_{D_{ST}}(\zeta) + \frac{\bar{c}}{2V_T} (C_{D_{\dot\alpha}} \dot\alpha + C_{D_q} q)$$

$$C_Y = C_{Y_{basic}} + \Delta C_{Y_{ST}}(\zeta) + \Delta C_{Y_{ST}}(\xi) + \frac{b}{2V_T} (C_{Y_r} r + C_{Y_r} p + C_{Y_{\dot\beta}} \dot\beta)$$

$$C_m = C_{m_{basic}} + \Delta C_{m_{ST}}(\eta) + \frac{\bar{c}}{2V_T} (C_{m_{\dot\alpha}} \dot\alpha + C_{m_q} q)$$

$$C_n = C_{n_{basic}} + \Delta C_{n_{ST}}(\xi) + \Delta C_{n_{ST}}(\xi) + \frac{b}{2V_T} (C_{n_{\dot\beta}} \dot\beta + C_{n_r} r + C_{n_p} p)$$

$$C_l = C_{l_{basic}} + \Delta C_{l_{ST}}(\zeta) + \Delta C_{l_{ST}}(\xi) + \frac{b}{2V_T} (C_{l_r} r + C_{l_p} p)$$

C. MISSILE LINEARIZED EQUATIONS OF MOTION

The linearized equations of motion used to design the missile autopilot are presented in this section. The equations are linearized about the cruise flight condition.

1. Additional Assumptions for Linearized Equations

The additional assumptions required for linearized equations are as follows:

a) Derivatives are given in stability axes which are fixed for the missile low level cruise condition.

b) Standard small perturbation assumptions apply.

1) Perturbed angles are small.

2) Products of perturbed variables are neglected.

3) There is no coupling between longitudinal and lateral directional motions.

    c) Thrust derivatives are neglected.

    d) The steady state condition is chosen as low level straight and level cruise.

2. Linearized Equations Summarized

The linear equations of motion in state variable form are shown in Tables 2-1 and 2-2. The following coefficients are defined as used in Table 2-2.

$$A = \frac{I_{zz}I_{xz}}{I_{zz}I_{xx}-I_{xz}^2} \qquad\qquad B = \frac{I_{xx}}{I_{xz}}$$

$$C = \frac{I_{xx}I_{xz}}{I_{zz}I_{xx}-I_{xz}^2} \qquad\qquad D = \frac{I_{zz}}{I_{xz}}$$

3. Definition of Stability Derivatives

The dimensional aerodynamic stability derivatives used in the equations of motion are defined by the following relations.

    a. Longitudinal Dimensional Stability Derivatives

$$X_U = -\bar{q}_{SS}S(C_{D_U}+2C_{D_{SS}})/mU_{SS} \qquad\qquad 1/sec$$

$$X_\alpha = \bar{q}_{SS}S(C_{L_{SS}}-C_{D_\alpha})/m \qquad\qquad ft/sec$$

$$X_\eta = -\bar{q}_{SS}SC_{D_\eta}/m \qquad\qquad ft/sec^2$$

$$Z_U = \bar{q}_{SS}S(C_{L_U}+2C_{L_{SS}}/mU_{SS} \qquad\qquad 1/sec$$

33

TABLE 2-1

Longitudinal Equations (Perturbed Variables) (11)

$$
\begin{bmatrix} \dot{U} \\ \dot{\alpha} \\ \dot{q} \\ \dot{\theta} \end{bmatrix}
=
\begin{bmatrix}
X_U & X_\alpha & 0 & -g\cos\gamma_{SS} \\
\dfrac{Z_w}{U_{SS}-Z_{\dot\alpha}} & \dfrac{Z_\alpha}{U_{SS}-Z_{\dot\alpha}} & \dfrac{U_{SS}+Z_q}{U_{SS}-Z_{\dot\alpha}} & \dfrac{-g\sin\gamma_{SS}}{U_{SS}-Z_{\dot\alpha}} \\
\dfrac{M_U+M_{\dot\alpha}Z_U}{U_{SS}-Z_{\dot\alpha}} & \dfrac{M_\alpha+M_{\dot\alpha}Z_\alpha}{U_{SS}-Z_{\dot\alpha}} & \dfrac{M_q+M_{\dot\alpha}(U_{SS}+Z_q)}{U_{SS}-Z_{\dot\alpha}} & \dfrac{-M_{\dot\alpha}g\sin\gamma_{SS}}{U_{SS}-Z_{\dot\alpha}} \\
0 & 0 & 1 & 0
\end{bmatrix}
\begin{bmatrix} U \\ \alpha \\ q \\ \theta \end{bmatrix}
+
\begin{bmatrix}
X_\eta \\
\dfrac{Z_\eta}{U_{SS}-Z_{\dot\alpha}} \\
\dfrac{M_\eta+M_{\dot\alpha}Z_\eta}{U_{SS}-Z_{\dot\alpha}} \\
0
\end{bmatrix}
\eta
$$

TABLE 2-2

Lateral Directional Equations (Perturbed Variables) (12)

$$
\begin{bmatrix} \dot{\beta} \\ \dot{\phi} \\ \dot{p} \\ \dot{r} \end{bmatrix}
=
\begin{bmatrix}
\dfrac{Y_\beta}{U_{SS}} & \dfrac{g\cos\gamma_{SS}}{U_{SS}} & \dfrac{Y_p}{U_{SS}} & \dfrac{Y_r-U_{SS}}{U_{SS}} \\
0 & 0 & 1 & 0 \\
A(N_\beta+BL_\beta) & 0 & A(N_p+BL_p) & A(N_r+BL_r) \\
C(L_\beta+DN_\beta) & 0 & C(L_p+DN_p) & C(L_r+DN_r)
\end{bmatrix}
\begin{bmatrix} \beta \\ \phi \\ p \\ r \end{bmatrix}
+
\begin{bmatrix}
\dfrac{Y_\xi}{U_{SS}} & \dfrac{Y_\zeta}{U_{SS}} \\
0 & 0 \\
A(N_\xi+BL_\xi) & A(N_\zeta+BL_\zeta) \\
C(L_\xi+DN_\xi) & C(L_\zeta+DN_\zeta)
\end{bmatrix}
\begin{bmatrix} \xi \\ \zeta \end{bmatrix}
$$

$$Z_\alpha = -\overline{q}_{SS}S(C_L + C_{D_{SS}})/m \qquad \text{ft/sec}^2$$

$$Z_{\dot{\alpha}} = -\overline{q}_{SS}S\overline{c}C_{L_{\dot{\alpha}}}/2mU_{SS} \qquad \text{ft/sec}$$

$$Z_q = -\overline{q}_{SS}S\overline{c}C_{L_q}/2mU_{SS} \qquad \text{ft/sec}$$

$$Z_\eta = -\overline{q}_{SS}SC_{L_\eta}/m \qquad \text{ft/sec}$$

$$M_U = \overline{q}_{SS}S\overline{c}(C_{M_U} + 2C_{M_{SS}})/I_{yy}U_{SS} \qquad \text{1/ft sec}$$

$$M_\alpha = \overline{q}_{SS}S\overline{c}C_{M_\alpha}/I_{yy} \qquad \text{1/sec}^2$$

$$M_{\dot{\alpha}} = \overline{q}_{SS}S\overline{c}^2C_{m_{\dot{\alpha}}}/2I_{yy}U_{SS} \qquad \text{1/sec}$$

$$M_q = \overline{q}_{SS}S\overline{c}^2C_{m_q}/2I_{yy}U_{SS} \qquad \text{1/sec}$$

$$M_\eta = \overline{q}_{SS}S\overline{c}C_{m_\eta}/I_{yy} \qquad \text{1/sec}^2$$

b. Lateral Directional Dimensional Stability

Derivatives

$$Y_\beta = \overline{q}_{SS}SC_{y_\beta}/m \qquad \text{ft/sec}^2$$

$$Y_p = \overline{q}_{SS}SbC_{y_p}/2mU_{SS} \qquad \text{ft/sec}$$

$$Y_r = \overline{q}_{SS}SbC_{y_r}/2mU_{SS} \qquad \text{ft/sec}$$

$$Y_\xi = \overline{q}_{SS}SC_{y_\xi}/m \qquad \text{ft/sec}^2$$

$$Y_\zeta = \overline{q}_{SS}SC_{y_\zeta}/m \qquad \text{ft/sec}^2$$

$$L_\beta = \overline{q}_{SS}SbC_{1_\beta}/I_{xx} \qquad \text{1/sec}^2$$

$$L_p = \overline{q}_{SS}Sb^2C_{1_p}/2I_{xx}U_{SS} \qquad \text{1/sec}$$

$$L_r = \overline{q}_{SS}Sb^2C_{1_r}/2I_{xx}U_{SS} \qquad \text{1/sec}$$

$$L_\xi = \bar{q}_{SS} S b C_{1_\xi} / I_{xx} \qquad 1/sec^2$$

$$L_\zeta = \bar{q}_{SS} S b C_{1_\zeta} / I_{xx} \qquad 1/sec^2$$

$$N_\beta = \bar{q}_{SS} S b C_{n_\beta} / I_{zz} \qquad 1/sec^2$$

$$N_p = \bar{q}_{SS} S b^2 C_{n_p} / 2 I_{zz} U_{SS} \qquad 1/sec$$

$$N_r = \bar{q}_{SS} S b^2 C_{n_r} / 2 I_{zz} U_{SS} \qquad 1/sec$$

$$N_\xi = \bar{q}_{SS} S b C_{n_\xi} / I_{zz} \qquad 1/sec^2$$

$$N_\zeta = \bar{q}_{SS} S b C_{n_\zeta} / I_{zz} \qquad 1/sec^2$$

4. Trim Equations

For straight and level flight at constant velocity the following variables are all zero: $\dot{U}=\dot{V}=\dot{W}=\dot{P}=\dot{Q}=\dot{R}=\dot{\theta}=\dot{\psi}=\dot{\phi}$ $=\dot{Z}_E=0$ $\quad Q_{SS}=P_{SS}=R_{SS}=\Phi_{SS}=L_{A_{SS}}=M_{A_{SS}}=N_{A_{SS}}=Y_{SS}=\gamma_{SS}=\beta_{SS}=V_{SS}=W_{SS}=\dot{\zeta}_{SS}=\zeta_{SS}=0$

The trim equations reduce to:

$$T \sin\alpha_{SS} = mg - (C_{L_o} + C_{L_\alpha}\alpha_{SS} + C_{L_\eta}\eta_{SS})\bar{q}_{SS} S$$

$$T \cos\alpha_{SS} = (C_{D_o} + C_{D_\alpha}\alpha_{SS} + C_{D_\eta}\eta_{SS})\bar{q}_{SS} S$$

$$0 = (C_{m_o} + C_{m_\alpha}\alpha_{SS} + C_{m_\eta}\eta_{SS})\bar{q}_{SS} S \bar{c}$$

III. DEVELOPMENT AND SIMULATION OF THE MISSILE AUTOPILOT

The missile is assumed to be equipped with an autopilot capable of providing closed loop control which consists of the following:

   a) normal acceleration (n_z)

   b) lateral acceleration (n_y)

   c) bank angle (ϕ).

In addition, an outer closed loop control, which serves as the outer autopilot, is as follows:

   a) altitude (H)

   b) vertical flight path angle (γ)

These two outer loops are employed as required during certain phases of the attack mission.

It is assumed that the missile possesses accelerometer sensors in the y and z body axes located at the missile center of gravity, rate gyros and rate integrating gyros about the x, y, and z axes, and a radar altimeter. Sensor noise is neglected in this simulation.

A. AUTOPILOT INNER LOOP REQUIREMENTS AND DESIGNS

1. Description of the Autopilot Inner Loops

The autopilot is assumed to employ three inner loops as depicted in Table 3-1.

TABLE 3-1

Autopilot Inner Loop Description

LOOP	COMMANDED VARIABLE	CONTROL	CONSTRAINTS
1 Normal Acceleration Command	n_z (normal acceleration)	η Elevator	$-15^{\circ} \leq \eta \leq 15^{\circ}$ $-2 \leq N_z \leq 4$
2 Bank Angle Command	Φ (Bank Angle)	ξ Aileron	$-15^{\circ} \leq \xi \leq 15^{\circ}$ $\phi \leq 60^{\circ}*$ $p \leq 50,100,200^{\circ}/sec$
3 Turn Coordinator	n_y (Lateral Acceleration)	ζ Rudder	$-15^{\circ} \leq \zeta \leq 15^{\circ}$ $N_y = 0$

* Applies in certain mission phases only

2. Normal Acceleration Command System

The purpose of normal acceleration command (NAC)
system is to provide a vertical load factor (n_z) response to
a commanded load factor (n_{z_c}). An accelerometer is used to
provide the primary feedback and a rate gyro is used to
provide inner loop pitch rate feedback for improved damping.

a. Block Diagram

The block diagram of the normal acceleration
command autopilot is shown in Figure 3-1. Limiter a allows
the commanded acceleration to a range from -2.0 to +4.0 g's.
Limiter b allows the elevator control to vary from -15
degrees to +15 degrees.

b. Assumptions

1) The rate gyro and accelerometer dynamic lags
are negligible.

2) The accelerometer is mounted at the center
of gravity. Therefore the moment arm is zero and the
feedback load factor is totally n_z. (C=0)

3) The fix servo can be represented by a first
order lag.

4) The missile dynamics can be represented by
a short period approximation.

5) Commanded normal acceleration is limited from
-2.0 to +4.0 g's.

c. Design

The following transfer function was developed
from equation (11):

39
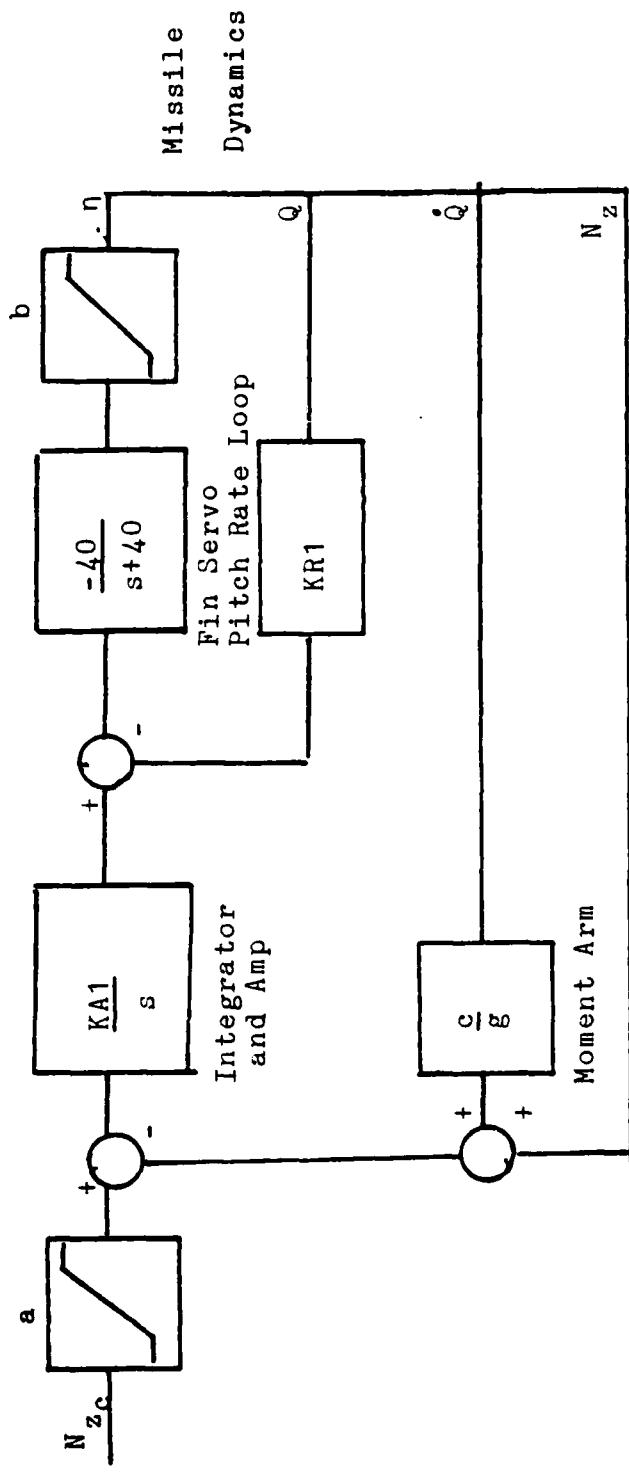
Figure 3-1   Normal Acceleration Command Autopilot Description

$$\frac{Q(s)}{\eta(s)} = \frac{(V_T M_\eta + Z_\eta M_{\dot{\alpha}})s + (M_\alpha Z_\eta - Z_\alpha M_\eta)}{V_T\{s^2 - (M_q + \frac{Z_\alpha}{V_T} + M_{\dot{\alpha}})s + \frac{(Z_{\dot{\alpha}} M_q - M_\alpha)}{V_T}\}}$$

From this transfer function and equation (10a)

$$n_z = \frac{V_T}{g}(Q - \dot{\alpha})$$

the following θ to n_z transfer function was obtained.

$$\frac{N_z(s)}{Q(s)} = \frac{V_T}{g} \frac{-Z_\eta s^2 + (M_q Z_\eta + Z_\eta M_{\dot{\alpha}})s + (M_\alpha Z_\eta - Z_\alpha M_\eta)}{(V_T M_\eta + Z_\eta M_{\dot{\alpha}})s + (M_\alpha Z_\eta - Z_\alpha M_\eta)}$$

Utilizing the characteristics listed in Appendix A
for this cruise missile at 0.75 Mach number, the above transfer
functions become

$$\frac{Q(s)}{\eta(s)} = \frac{-26.99(s+1.009)}{s^2 + 1.289s + 27.13} \quad \text{and} \quad \frac{N_z(s)}{Q(s)} = \frac{-0.08(s^2 + 0.1985s - 328.9)}{(s+1.009)}$$

Evaluating the characteristic polynomial of
the $Q(s)/\eta(s)$ transfer function yields the natural frequency
of 0.829 Hz and a damping ratio of 0.1237. The resulting
block diagram for the normal acceleration command inner
loop autopilot for analysis purposes is shown in Figure 3-2.

(1) Root Locus Evaluation.

(a) Pitch Rate Loop. The transfer function
for the pitch rate loop is:
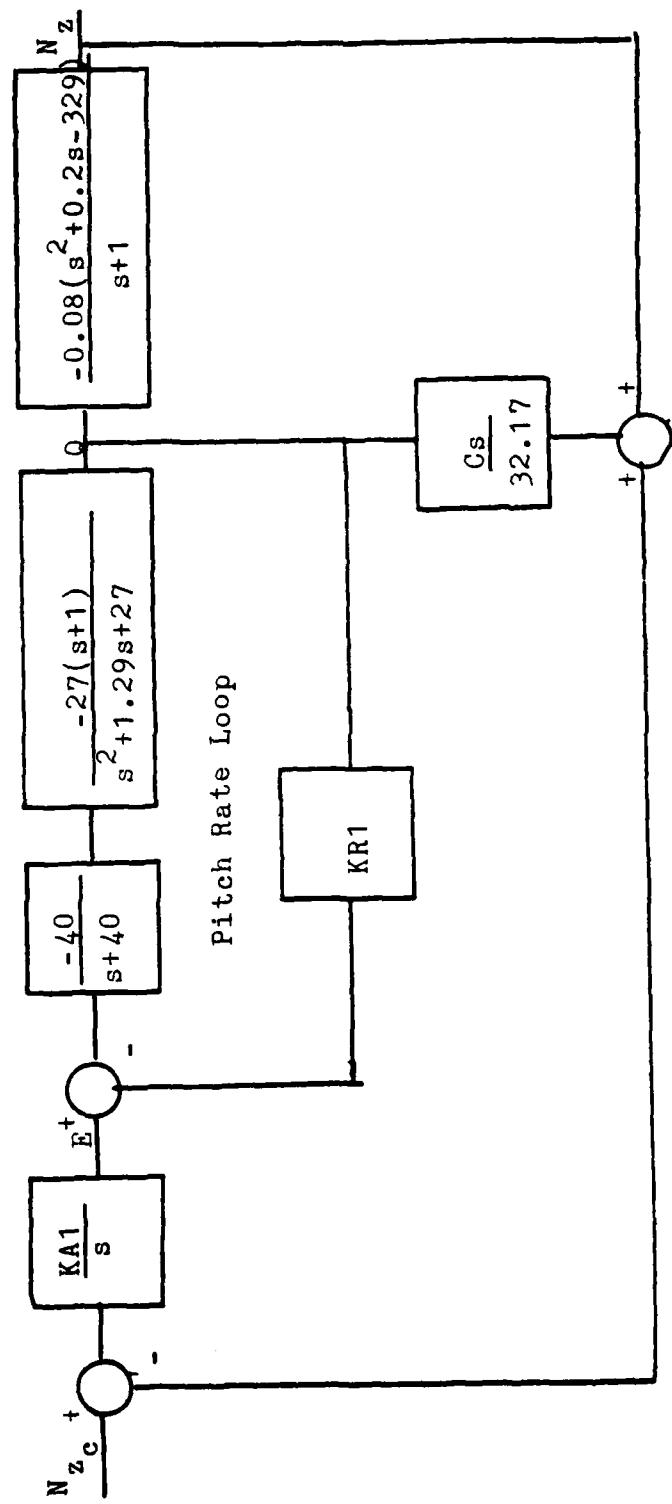
Figure 3-2 Normal Acceleration Command Autopilot Block Diagram (Analysis)

42

$$\frac{Q(s)}{E(s)} = \frac{1080\ (s+1)}{(s^3+41.29s^2+(78.7+1080KR1)s+(1084+1080KR1))}$$

Appendix C contains the root locus plot of the pitch rate loop for ranging KR1. A KR1 of 0.28 is chosen which yields the following characteristics:

$s = -5.600 \pm 3.844\ j$
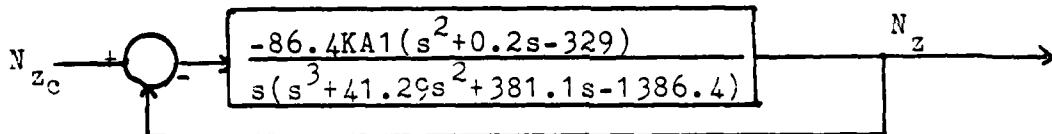
$\phi = 55.53^{\circ}$

$\zeta = 0.82$

$\omega_n = 1.08\ H_z$

(b) Normal Acceleration Command Loop.

Using a KR1 of 0.28 in the pitch rate loop and locating the acceleration at the missile center of mass (C=0), the normal acceleration command loop becomes:

$$\frac{N_z(s)}{N_{z_c}(s)} = \frac{-86.4KA1(s^2+0.2s-329)}{s(s^3+41.29s+381.1s-1386.4)-86.4KA1(s^2+0.2s-329)}$$

Appendix C contains the root locus plot of the normal acceleration command system for varying KA1. A KA1 of 0.05 is chosen which yields the following characteristics:

$s = -1.981 \pm 3.317\ j$

$\phi = 30.85^{\circ}$

$\zeta = 0.513$

$\omega_n = 0.615H_z$

43

With a KR1 of 0.28 and a KA1 of 0.05 the system transfer function relating n_{z_c} to n_z is:

$$\frac{N_z(s)}{N_{z_c}(s)} = \frac{-4.32(s^2-0.2s-329)}{s^4+41.29s^3+376.78s^2-1387.26s-1421.28}$$

The normal acceleration command autopilot has zero steady state error for a step input as it is a type 1 system. The system response to a 1g commanded load factor is shown in Figure 3-3.

3. Bank Angle Command System

The purpose of the bank angle command (BAC) autopilot is to command missile bank angle. Limits are applied to commanded roll rate and in certain mission phases commanded bank angle. A rate integrating gyro feeds back bank angle and a roll rate gyro provides feedback as a roll rate damper.

a. Block Diagram

The bank angle command autopilot is presented in block diagram in Figure 3-4. Limiter a allows the commanded bank angle to vary from 0 to 60 degrees and is active in certain flight phases. Limiter b limits the roll rate to either 50, 100, or 200 degrees/second. Limiter c limits aileron deflections to range from -15 to +15 degrees.

b. Assumptions

1) The rate gyro and displacement dynamic lags are negligible.

44
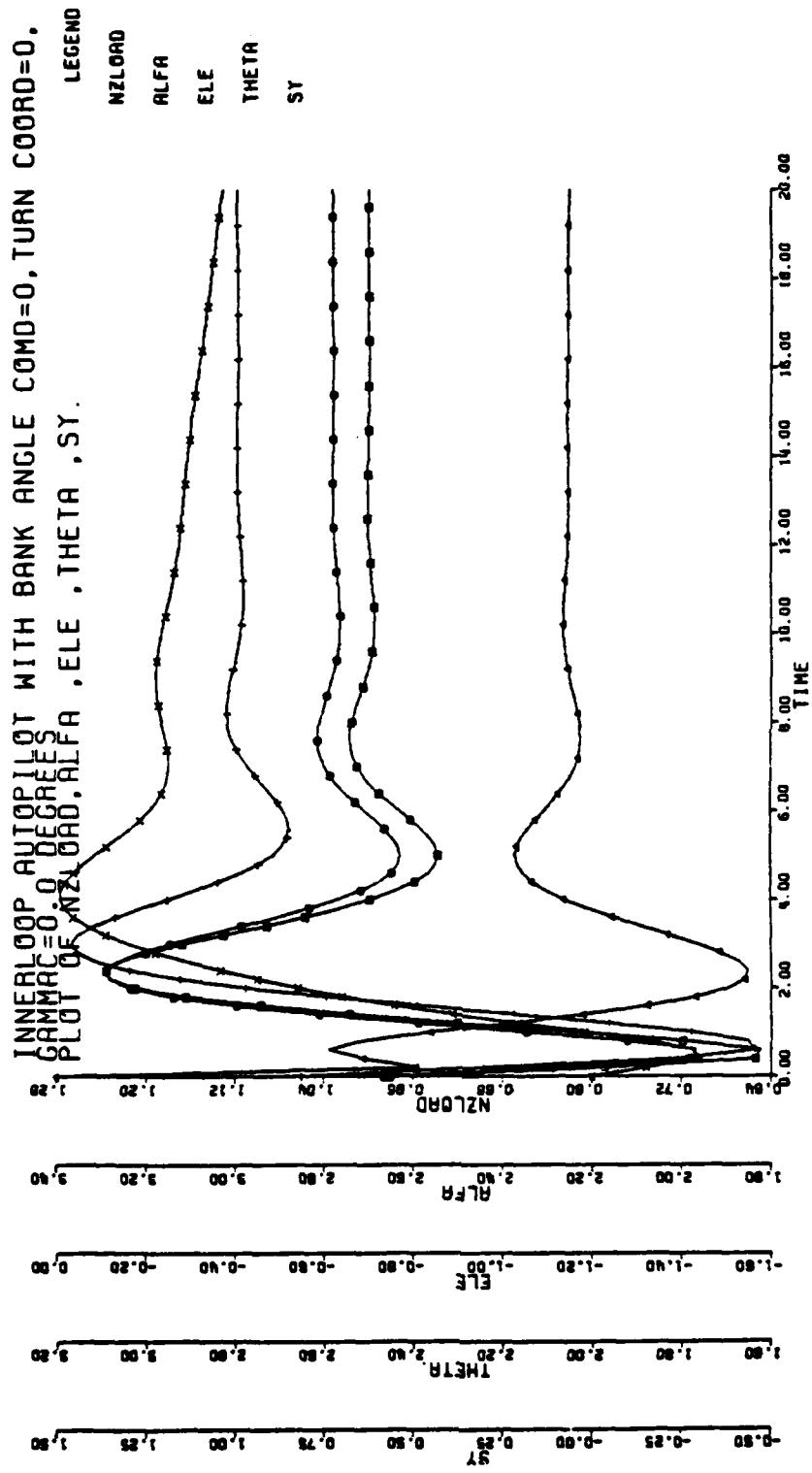
Figure 3-3   NAC Autopilot Response to 1g Commanded Load Factor

45
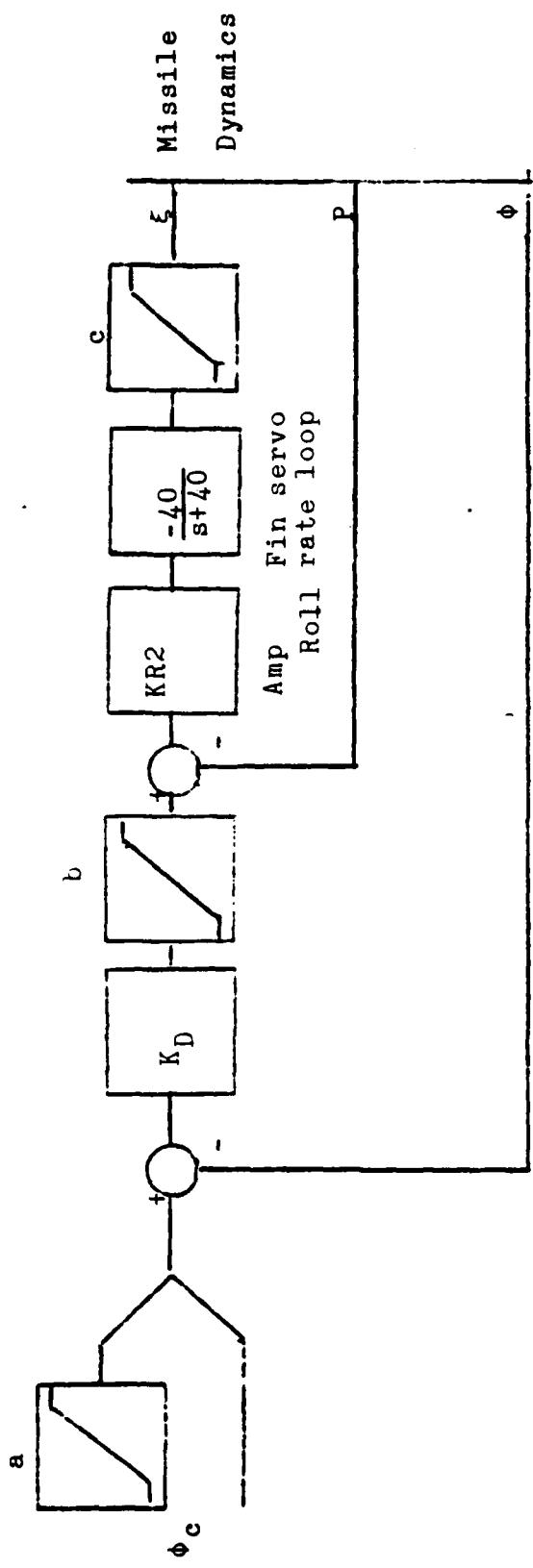
Figure 3-4 BANK ANGLE COMMAND AUTOPILOT DESCRIPTION

46

2) The fin servo can be represented by a first order lag.

3) The missile dynamics can be represented by a roll mode approximation.

4) There are limits on commanded bank angle and commanded roll rate as noted above.

c. Design

Equation (12) can be written to find the lateral transfer functions $\frac{\beta(s)}{\zeta(s)}$, $\frac{\phi(s)}{\zeta(s)}$, and $\frac{\psi(s)}{\zeta(s)}$, where $\delta = \xi$ or ζ. By allowing a roll approximation the transfer function relating aileron and bank angle becomes:

$$\frac{\phi(s)}{\xi(s)} = \frac{L_\xi}{s(s-L_p)}$$

The root at the origin indicates the missile does not have bank angle stability without autopilot stabilization. Evaluation of the transfer function coefficients results in the transfer functions $\frac{\phi(s)}{\xi(s)} = \frac{-116}{s(s+6.2)}$ and $\frac{p(s)}{\xi} = \frac{-116}{s+6.2}$. The maximum missile roll rate can be approximated by $P_{max} = \left| \frac{L_\xi \xi_{max}}{L_p} \right| = \frac{(116)(15)}{6.2} = 280.6$ degrees/second.
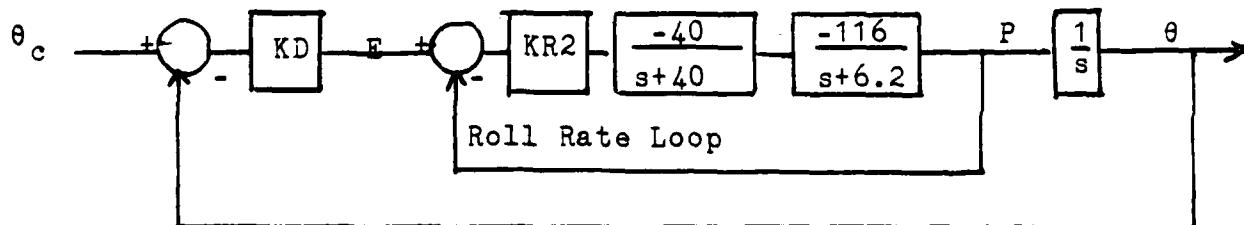
The block diagram of the bank angle command system is:

(1) <u>Root Locus Evaluation</u>.

     (a) Roll Rate Loop. The transfer function for the roll rate loop is:

$$\frac{P(s)}{E(s)} = \frac{4640 \ KR2}{s^2+46.2s+248+4640KR2}$$

     Appendix C contains the root locus plot of the roll rate loop for varying KR2. A gain KR2 of 0.10 yields the following characteristics.
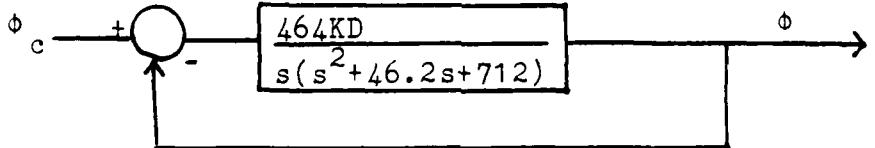
$$s = -23.10 \pm 13.36 \ s$$

$$\phi = 59.96^{\circ}$$

$$\zeta = 0.8656$$

$$\omega_n = 4.247H_Z$$

     (b) Bank Angle Command Loop. With a KR2 of 0.10 the bank angle command loop becomes:

The transfer function is:

$$\frac{\phi(s)}{\phi_c(s)} = \frac{464KD}{s^3+46.2s^2+712s+464KD}$$

     The root locus plot is shown in Appendix C for varying KD. Choosing a KD gain of 10.8 yields the following characteristics:

$$s = -9.98 \pm 9.58j$$

$$\phi = 45.056^{\circ}$$

$$\zeta = 0.718$$

$$\omega_n = 2.19 \text{ H}_Z$$

Using gains of 0.10 for the inner loop and 10.8 for the outer loop of the bank angle command system, the system transfer function $G(s)$ becomes

$$\frac{\phi(s)}{\phi_c(s)} = \frac{5011.2}{s^3 + 46.2s^2 + 712s + 5011.2}$$

and the system is a type 1 system for a step input. The transient reponse is demonstrated in Figures 3-5 and 3-6 for a commanded bank angle of 60 degrees.

4. <u>Turn Coordinator</u>

The turn coordinator (TC) is a lateral autopilot which provides a body directional load factor, n_y, to a commanded load factor, n_{y_c}. Like the normal acceleration command autopilot it employs an inner loop yaw rate damper. The outer loop uses unity accelerometer feedback and has the capability of moment arm feedback if the accelerometer is located at a different position than the missile center of mass.

a. Block Diagram

The block diagram representing the turn coordinator autopilot is shown in Figure 3-7. Limiter a limits the rudder deflection (ζ) from -15 to +15 degrees.

49
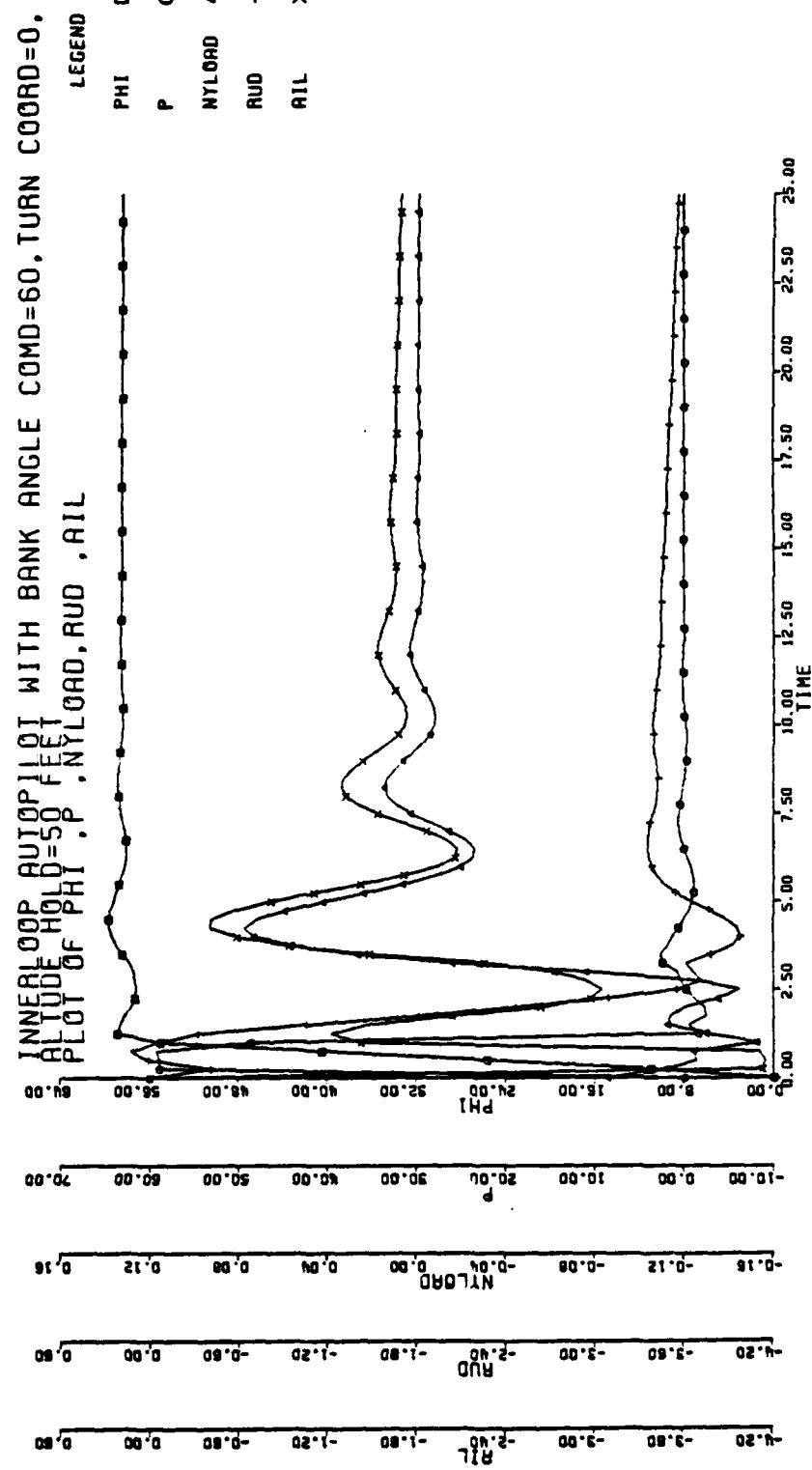
Figure 3-5 BAC Autopilot Response to 60° Commanded Bank Angle (PHI Response)
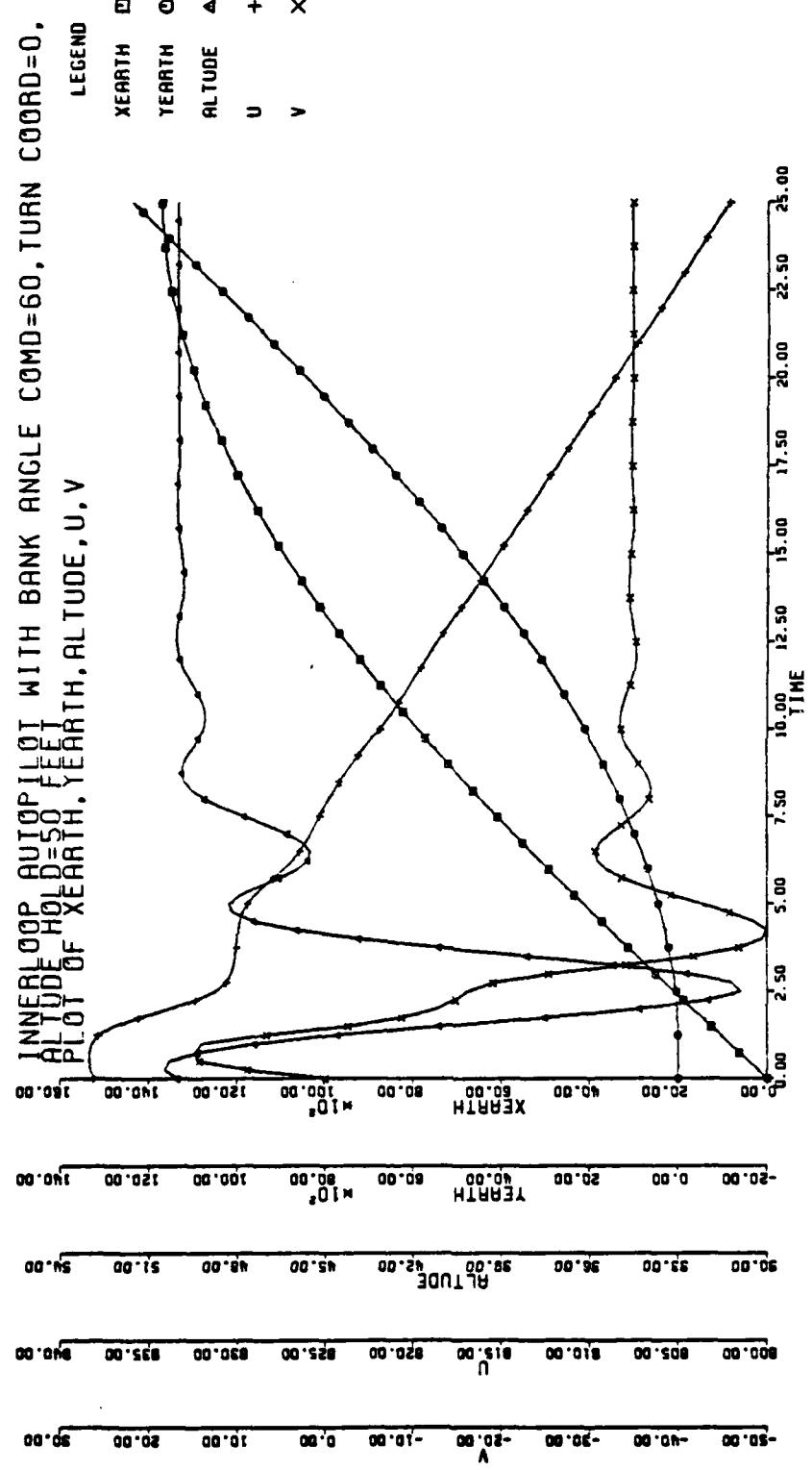
Figure 3-6 BAC Autopilot Response to 60° Commanded Bank Angle (Altitude Response)

51
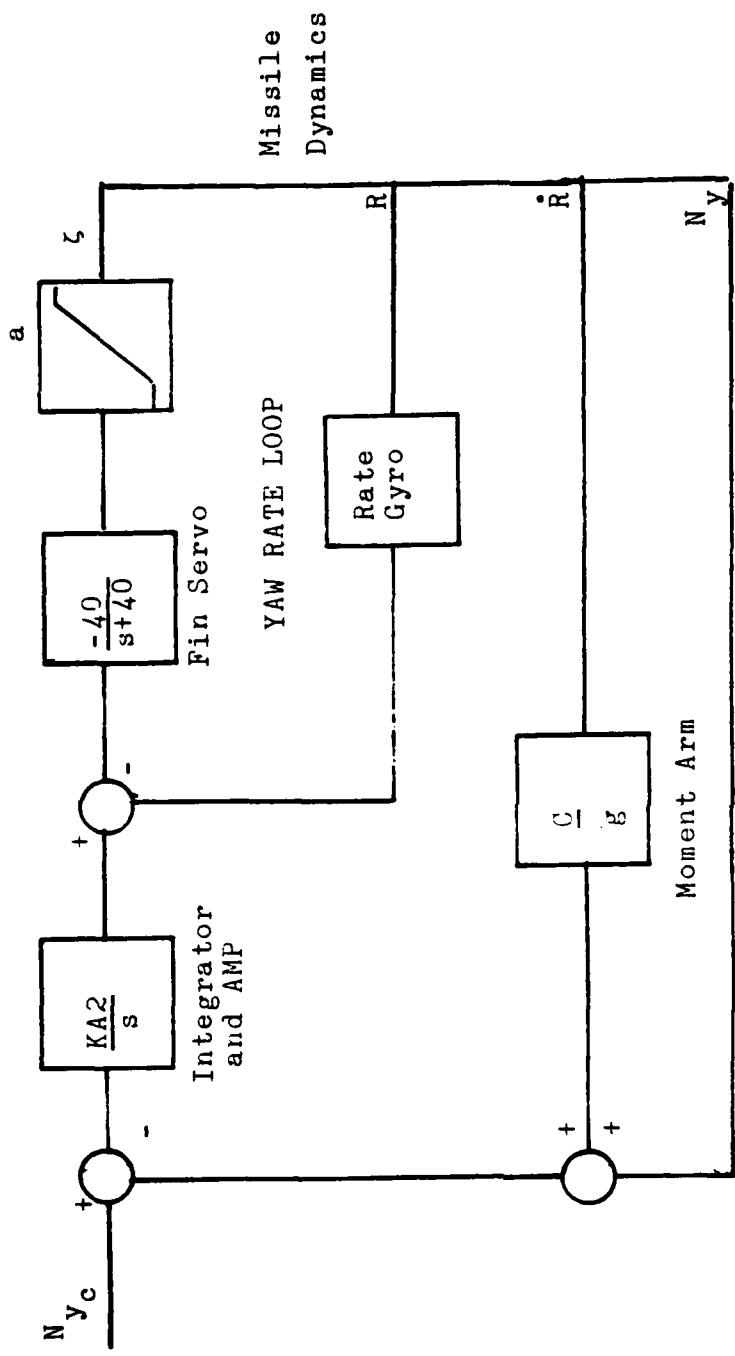
Figure 3-7 Turn Coordinator Autopilot Description

b. Assumptions

1) The rate gyro and accelerometer dynamic lags are negligible.

2) An accelerometer is mounted at the center of gravity. Therefore the moment arm is zero. C=0

3) The fin servo can be represented by a first order lag.

4) The missile dynamics can be represented by a dutch roll approximation.

c. Design

The dutch roll approximation involves side slip angle β, and yaw angle Ψ. Equation (12) with ϕ neglected (assuming a small C_{l_β} results in the following set of equations:

$$
\begin{bmatrix}
sV_T - Y_\beta & s(V_T - Y_r) \\
-N_\beta & s^2 - sN_r
\end{bmatrix}
\begin{bmatrix}
\dfrac{\beta(s)}{\zeta(s)} \\
\dfrac{\psi(s)}{\zeta(s)}
\end{bmatrix}
=
\begin{bmatrix}
Y_\zeta \\
N_\zeta
\end{bmatrix}
$$

The following transfer functions can be extracted:

$$
\frac{\beta(s)}{\zeta(s)} = \frac{Y_\zeta s + (Y_r N_\zeta - V_T N_\zeta - Y_\zeta N_r)}{V_T s^2 - (Y_\beta + V_T N_r)s + (Y_\beta N_r + V_T N_\beta - Y_r N_\beta)}
$$

$$
\frac{\psi(s)}{\zeta(s)} = \frac{V_T N_\zeta s + (Y_\zeta N_\beta - Y_\beta N_\zeta)}{s\{ V_T s^2 - (Y_\beta + V_T N_r)s + (Y_\beta N_r + V_T N_\beta - Y_r N_\beta) \}}
$$

53

$$\frac{R(s)}{\zeta(s)} = \frac{V_T N_\zeta s + (Y_\zeta N_\beta - Y_\beta N_\beta)}{V_T s^2 - Y_\beta + V_T N_r)s + (Y_\beta N_r + V_T N_\beta - Y_r N_\beta)}$$

Using the equation (10b) in Chapter I the transfer function for yaw rate to n_y is

$$\frac{N_y(s)}{R(s)} = \frac{V_T}{g} \frac{Y_\zeta s^2 + (Y_r N_\zeta - Y_\zeta N_r)s + (Y_\zeta N_\beta - Y_\beta N_\zeta)}{V_T N_\zeta s + (Y_\zeta N_\beta - Y_\beta N_\zeta)}$$

Substituting coefficient data obtained from Appendix A results in the transfer functions as:

$$\frac{R(s)}{\zeta(s)} = \frac{-14.5(s+0.11)}{s^2+0.245s+14.5}$$

$$\frac{N_y(s)}{R(s)} = \frac{-0.14(s^2-0.01s-20.9)}{s+0.11}$$

The resulting turn coordinator block diagram for analysis purposes is given in Figure 3-8.

(1) Root Locus Evaluation.

(a) Yaw Rate Loop. The loop transfer function is

$$\frac{R(s)}{E(s)} = \frac{580(s+0.11)}{s^3+40.25s^2+(24.3+580KR3)s+(580+63.8KR3)}$$

Appendix C shows the root locus plot of the yaw rate loop for varying KR3. Selecting a gain KR3 of 0.40 results in the following characteristics:

$$s = -3.581 \pm 2.339j$$

$$\phi = 56.85^\circ$$

$$\zeta = 0.8372$$

54
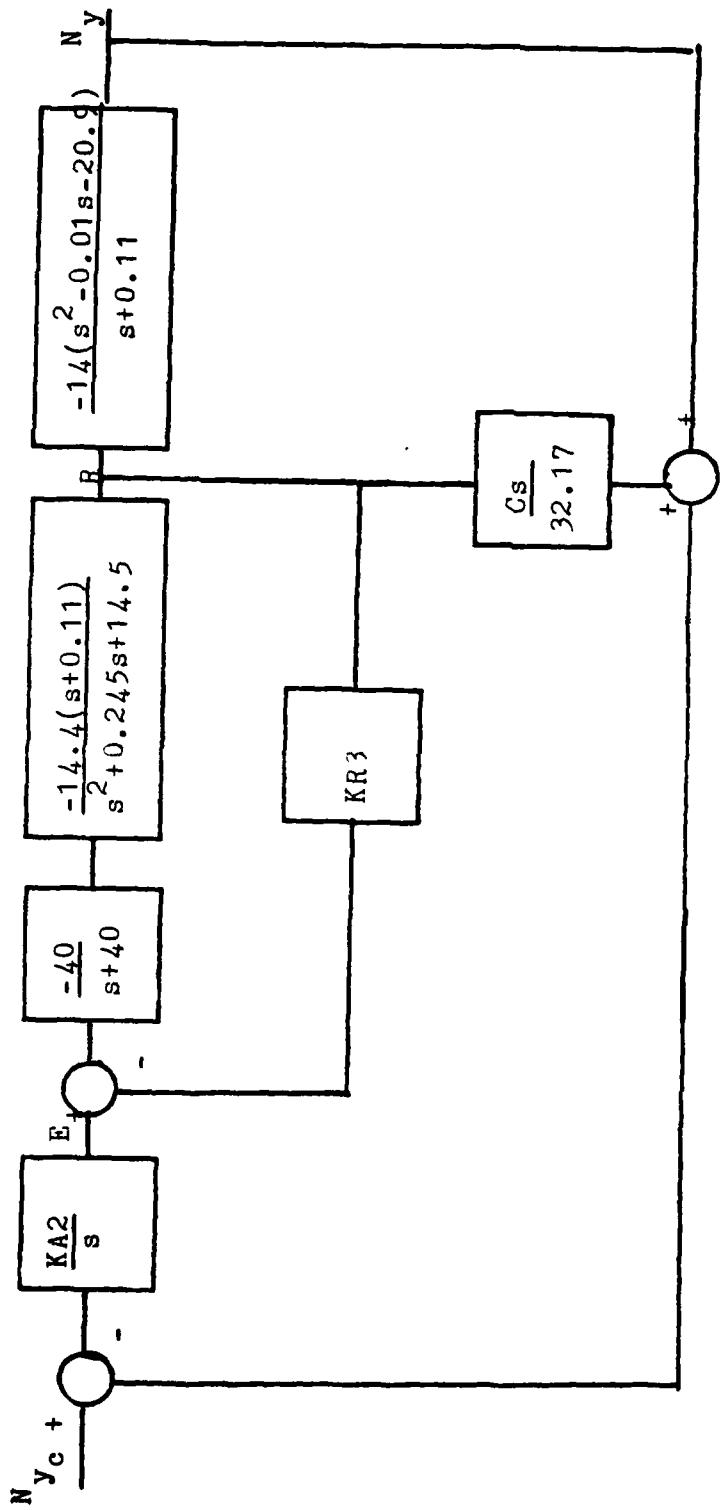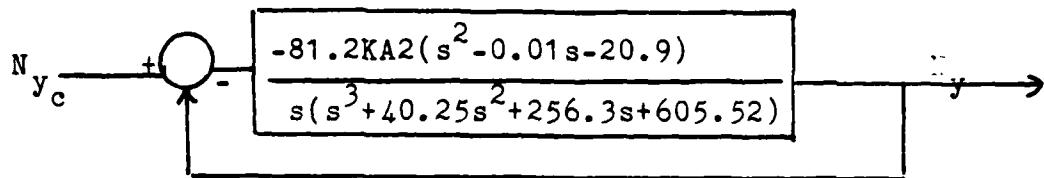
Figure 3-8 Turn Coordinator Autopilot Block Diagram (Analysis)

55

$$\omega_n = 0.6807 H_z$$

$$\phi = 56.85 \text{ degrees}$$

(b) Turn Coordinator Loop. With a KR3 of 0.40 the turn coordinator loop becomes:

$$N_{y_c} \xrightarrow{+ \bigcirc -} \boxed{\frac{-81.2 KA2(s^2 - 0.01s - 20.9)}{s(s^3 + 40.25s^2 + 256.3s + 605.52)}} \longrightarrow y$$

The transfer function is:

$$\frac{N_y(s)}{N_{y_c}(s)} = \frac{-81.2 KA2(s^2 - 0.01s - 20.9)}{s^4 + 40.25s^3 + (244.7 - 81.2 KA2)s^2 + (604.2 + 81.2 KA2)s + 1697 KA2}$$

The root locus plot for varying KA2 is shown in Appendix C. Selecting a gain KA2 of 0.25 yields characteristics as follows:

$$s = -2.206 \pm 2.807j$$

$$\phi = 38.16^o$$

$$\zeta = 0.618$$

$$\omega_n = 0.5682 Hz$$

The turn coordinator system transfer function G(s) becomes:

$$\frac{N_y(s)}{N_{y_c}(s)} = \frac{-32.48(s^2 - 0.01s - 20.9)}{s^4 + 40.25s^3 + 212.2s^2 + 604.5s + 678.8}$$

The system is type 1 and therefore has zero steady state error to a step input. Figure 2-5a shows the response

of the turn coordinator for a step aileron input. Note that an n_{y_c} of zero results in a coordinated turn.

B. AUTOPILOT OUTER LOOP REQUIREMENTS AND DESIGNS
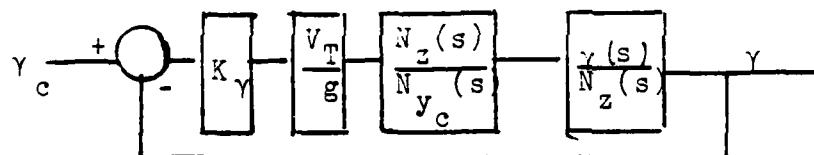
1. Description

The outer loop auto pilot has two functional loops consisting of an altitude hold and a vertical flight path angle hold.

2. Vertical Flight Path Angle System

The purpose of the vertical flight path angle hold loop or gamma command loop is to provide missile reponse to a command of 8.6 degrees during a specified phase in the terminal profile.

a. Block Diagram
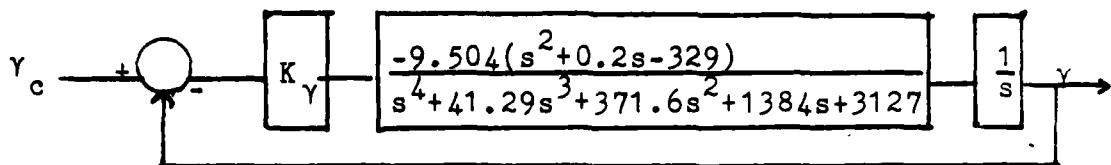
b. Assumption

1) Bank angle is zero.

c. Design

Starting with equation (10a) $n_z = \dfrac{V_T}{g}(Q - \dot{\alpha}) = \dfrac{V_T}{g}\dot{\gamma}$

the transfer function $\dfrac{\gamma(s)}{N_z(s)} = \dfrac{g}{V_T(s)}$ can be derived. Using the inner loop design previously for load factor the vertical flight path angle block diagram becomes:

57

The transfer function $\frac{\gamma(s)}{\gamma_c(s)}$ is:

$$\frac{\gamma(s)}{\gamma_c(s)} = \frac{-9.504K_\gamma(s^2+0.2s-329)}{s^5+41.29s^4+37.6s^3+(1384-9.504K_\gamma)s^2+(3127-1.9K_\gamma)s+3127K_\gamma}$$

(1) <u>Root-Locus Evaluation</u>. Appendix C shows the root locus plot of the vertical flight path angle loop for varying gain K_γ. A gain K_γ of 1.0 yields the following characteristics:

$$s = 1.2725 \pm 2.5407j$$

$$\phi = 26.6°$$

$$\zeta = 0.4478$$

$$\omega_n = 0.45H_Z$$

The system transfer function $G(s)$ with a gain of 1.0 becomes:
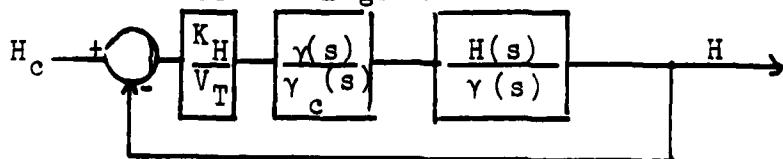
$$\frac{\gamma(s)}{\gamma_c(s)} = \frac{-9.504(s^2+0.2s-329)}{s^5+41.29s^4+371.6s^3+1374.5s^2+3125.1s+3127}$$

Figure 3-9 depicts the system response to a commanded vertical flight path angle of 8.6 degrees.

3. <u>Altitude Hold System</u>

The purpose of the altitude hold autopilot is to hold altitude at 50 feet during specified flight phases.

a. Block Diagram
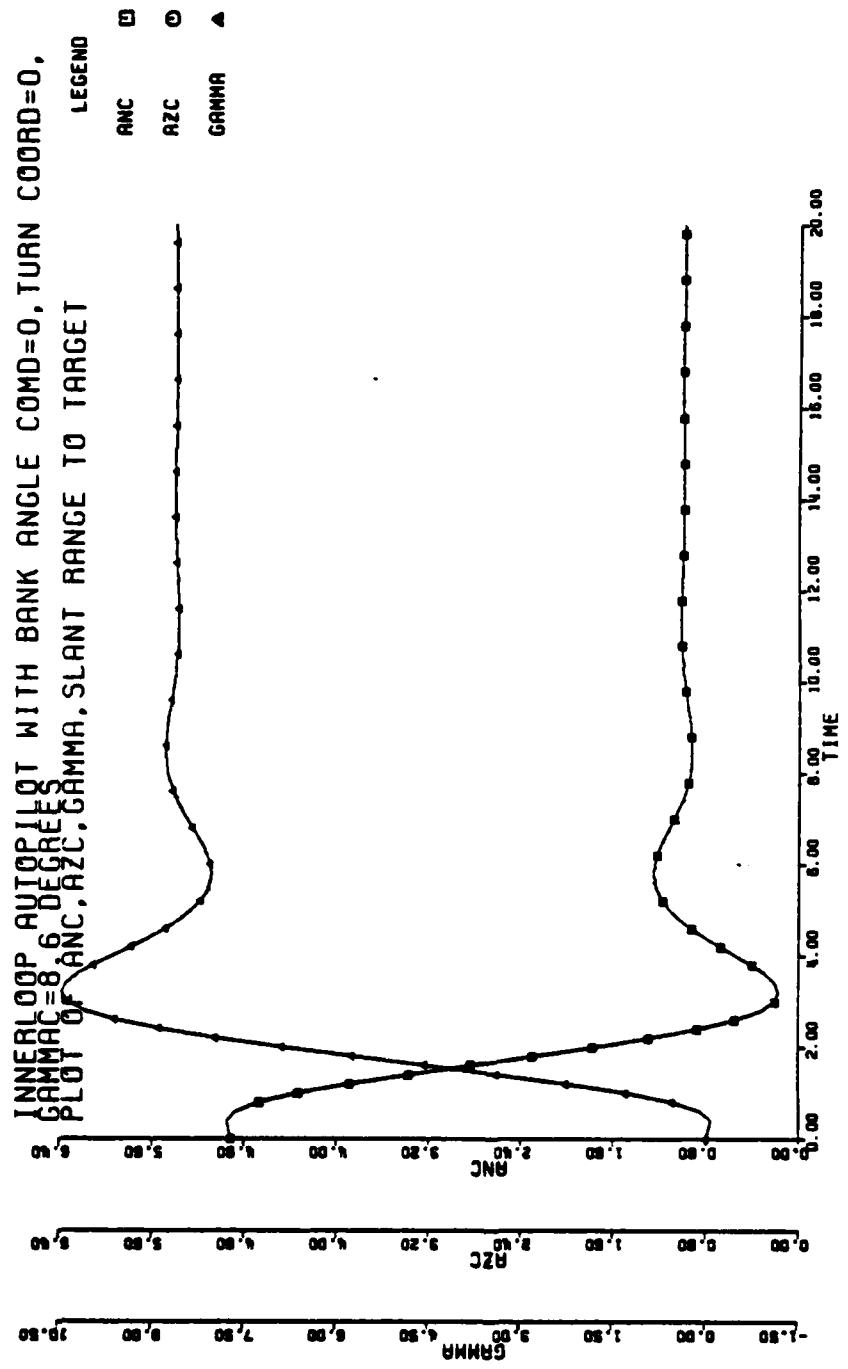
Figure 3-9 System Response to Commanded 8.6° Vertical Flight Path Angle

b. Assumptions

1) Vertical rate of climb (or desent) subtends a small angle (γ is less than 20°), therefore $H = V_T \sin \gamma = V_T \gamma$.

2) Bank angle equals zero.

c. Design

Let altitude command and altitude be designated H_c and H respectfully. The design is based upon the following two relations:

$$H = K_H (H_c - H)$$

$$\gamma_c = \frac{K_H}{V_T}(H_c - H)$$

From the vertical flight path angle development,
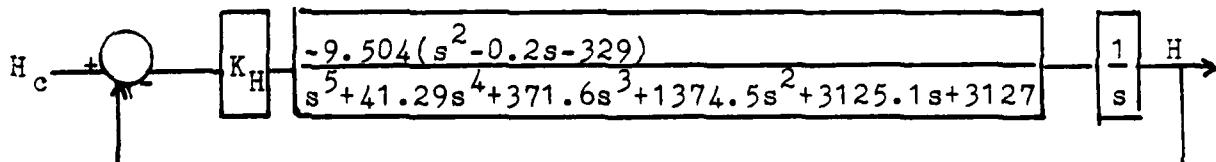
$$\frac{\gamma(s)}{N_z(s)} = \frac{g}{V_T s}$$

$$sH(s) = V_T \gamma(s) \qquad \text{(Divide both sides by } a_n(s)\text{)}$$

$$\frac{sH(s)}{N_z(s)} = V_T \frac{\gamma(s)}{N_z(s)} = V_T \frac{g}{V_T s}$$

$$\frac{H(s)}{\gamma(s)} = \frac{V_T}{s}$$

The altitude hold block diagram becomes:

The transfer function $H(s)/H_c(s)$ is:

$$\frac{H(s)}{H_c(s)} = \frac{-9.504KH(s^2+0.2s-329)}{s^6+41.29s^5+371.6s^4+1374.5s^3+(3125.1-9.504KH)s^2+(3127-1.9KH)s+3127KH}$$

(1) <u>Root Locus Evaluation</u>. Appendix C contains the root locus plot of the altitude hold loop for a varying gain KH. Again KH of 0.3 results in characteristics:

$$s = -1.4045 \pm 2.424j$$

$$\phi = 30.08^{\circ}$$

$$\zeta = 0.501$$

$$\omega_n = 0.445 \text{ Hz}$$

The altitude hold loop transfer function G(s) with KH of 0.3 is:

$$\frac{H(s)}{H_c(s)} = \frac{2.8512(s^2+0.2s-329)}{s^6+41.29s^5+371.6s^4+1374.5s^3+3122.25s^2+3126.4s+938.1}$$

and Figure 3-10 shows the response to a γ_c of 50 feet.
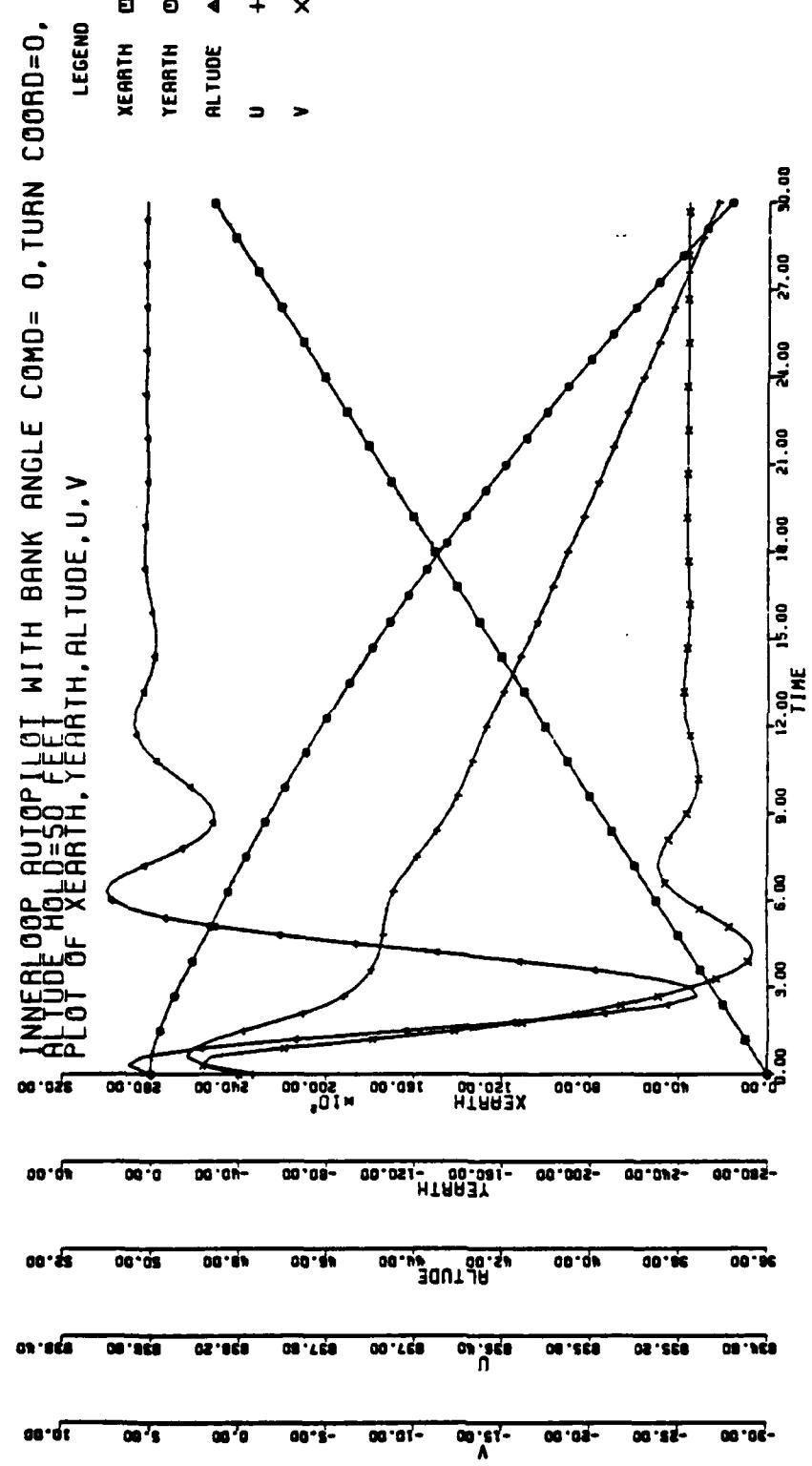
Figure 3-10 System Response to 50 ft. Altitude Hold Command

IV. DEVELOPMENT AND SIMULATION OF MISSILE GUIDANCE SYSTEM

The purpose of this study is to evaluate the effect of limited roll rate and various guidance laws on the terminal performance of a bank-to-turn cruise missile using proportional navigation in the terminal (attack) phase against a medium to large combatant ship. A baseline guidance and control scheme is designed and studied which uses a pop out maneuver, proportional navigation, and bank-to-turn maneuvering in the attack phase. The trajectory parameters and navigation constants are optimized for best performance against a moving ship utilizing blinking countermeasures. The missile is assumed to have limited roll performance due to the use of differential stabilizer for roll control vice ailerons. The terminal performance of this baseline system is evaluated for varying roll rate limits, electronic countermeasure blinking rates and burn through ranges.

A second control scheme is also designed and evaluated for the attack phase. This mode uses a sea skimming scheme in which a 50 foot altitude is maintained and proportional navigation is used in azimuth during ingress until a specified range is reached at which time proportional navigation is used in both azimuth and elevation to attack the target.

A. MISSION DESCRIPTION

1. Baseline Guidance Scheme (Pop Out Maneuver)

The mission is divided into four phases:

a) ingress

b) offset

c) popup

d) attack

The mission commences with target ship located 25,000 feet
north of the missile and moving east at 21 knots. The
missile initial heading is north.

The ingress phase commences with the missile flying
at an altitude of 50 feet on altitude hold and utilizing
proportional navigation in azimuth to home in on the
target. At a given range the offset phase is initiated with
a turn to the right of approximately 12 degrees followed by
a commanded bank angle of zero degrees. No proportional
navigation is used in this phase. At another given range
a pop up maneuver is initiated which generates a low angle
climb in preparation for the attack phase. During the pop up
maneuver, proportional navigation is used to begin turning
the missile toward the target. Finally the missile enters
the attack phase at a specified range where proportional
navigation is used in both vertical and azimuth planes.
In this phase the bank angle is unlimited but roll rates are
limited and used as one of the parameters in studying miss
distances. The second parameter under study is the electronic

counter measure blinking rate frequency which is initiated
at the start at the start of the attack phase and allowed to
remain activated until a specified burn through range which
is the third miss distance study parameter. Figure 4-1 is
a geometric depiction of the missile flight path.

   2.   Alternate Guidance Scheme (Sea Skimmer)

        The mission for this guidance scheme is divided into
two phases:

        a.   ingress

        b.   attack

This mission begins with the same initial scenario as the
baseline scheme, however, the pop out maneuvers (turn and
pop up phases) is eliminated.

        The missile flies at 50 foot altitude during the
ingress phase and utilizes proportional navigation in
azimuth until a range of 3000 feet at which point the
missile enters the attack phase and dives in on the target
using proportional navigation in both azimuth and elevation.
This low altitude approach essentially resembles a sea
skimming effect. Figure 4-2 shows the geometric flight
profile of this scheme.

   3.   Electronic Counter Measures (ECM)

        It is assumed that the target has the ECM capability
of simultaneously shifting the aim point of the missile 75
feet aft and 10 feet vertically. The simulation is tested
for ECM blinking frequencies of 0.5, 1.0, and 2.0 cycles
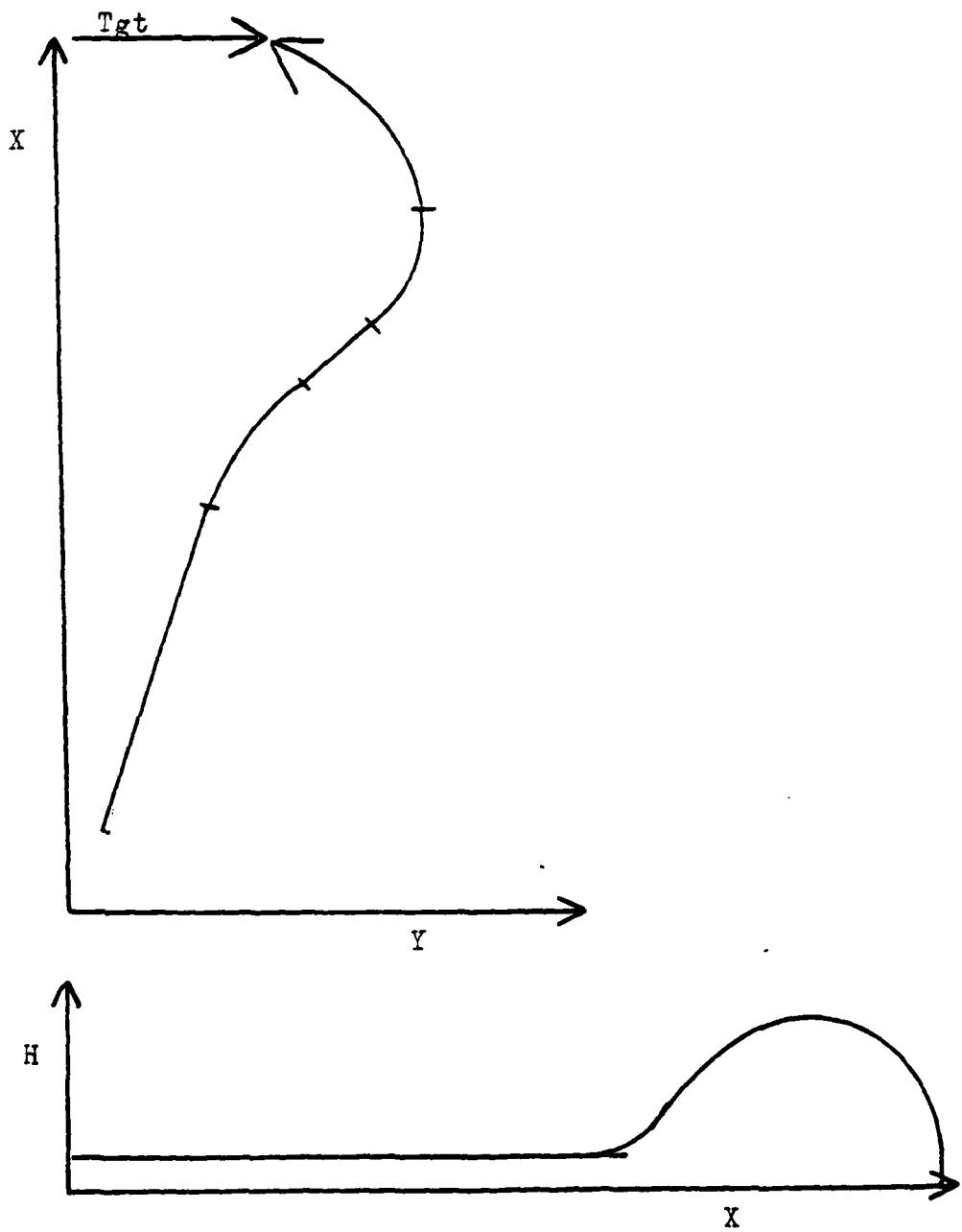
Figure 4-1   Baseline Guidance Scheme Flight Profile

66
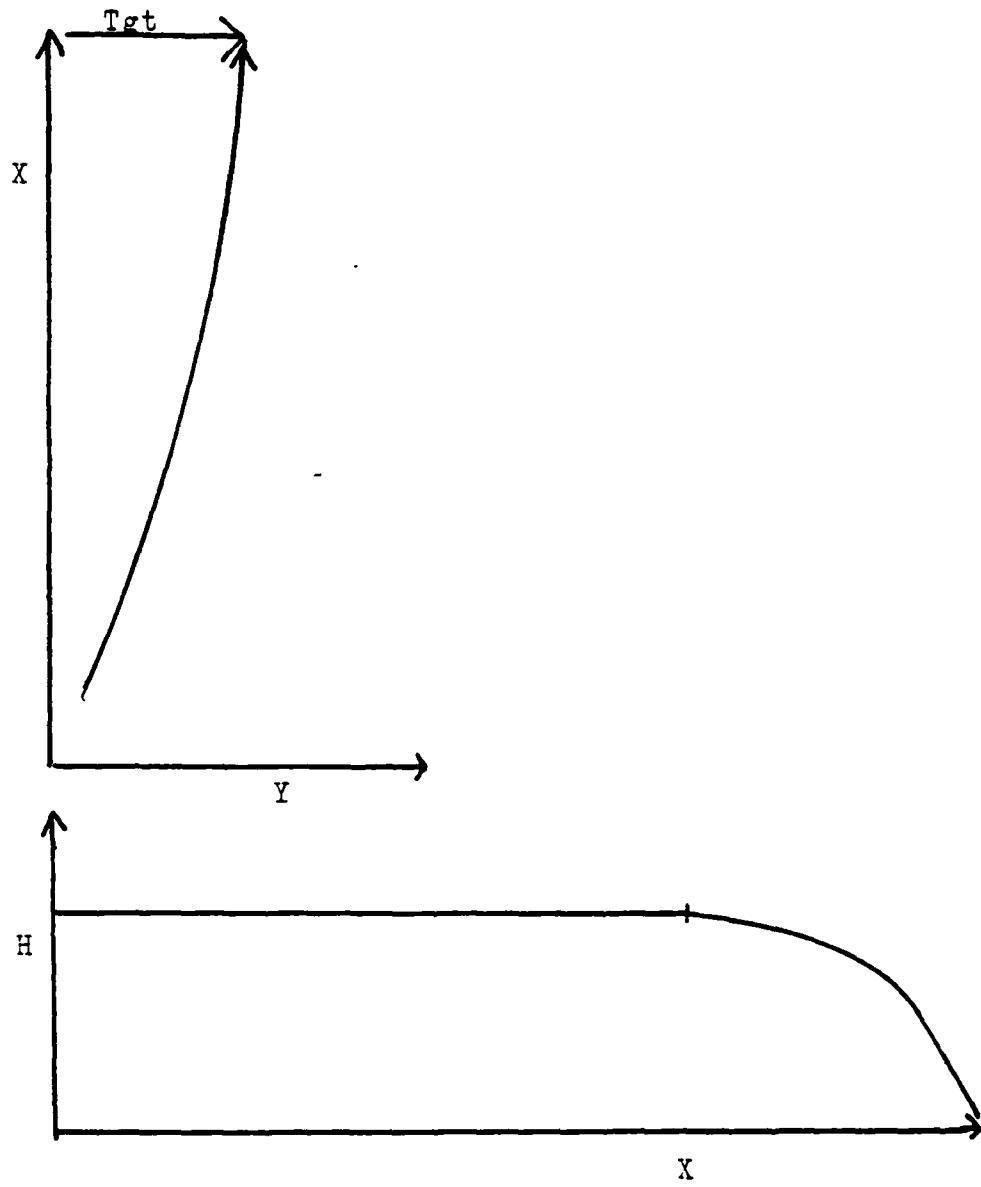
Figure 4-2   Sea Skimmer Guidance Scheme Flight Profile

per second. Blinking is commenced during the attack phase
and continues until jammer burn through occurs when the
target signal power can be seen over jammer power. Although
3800 feet (as calculated using Hosington, {Ref. 3}) is
considered a typical burn through range the missile is
tested for burn through ranges from 3800 feet down to
400 feet.

4. Glint

This study models glint with a gaussian function
that gives the aim point a random shift effect with a
variance of 25 feet in the Y axis and 4 feet in both the
X and Z axes. Since glint is imposed as a fluctuation in
target coordinates and target coordinates are used to
calculate the target line of sight angles then glint is
modeled as inversely proportional to range as required.
For ease in simulation glint is imposed only during the
attack phase. Results for runs with glint included are
presented in Chapter IV.

B. SEEKER EQUATIONS AND SIMULATION

A flow diagram of the seeker simulation is presented
in Figure 4-3.

1. Line of Sight Rates

It is assumed that the missile seeker has the ability
to sense target range and target line of sight rates in
azimuth and elevation ($\dot{\sigma}_{AZ_B}$ and $\dot{\sigma}_{EL_B}$) in the body coordinate
system out to a range of 25,000 feet.

68
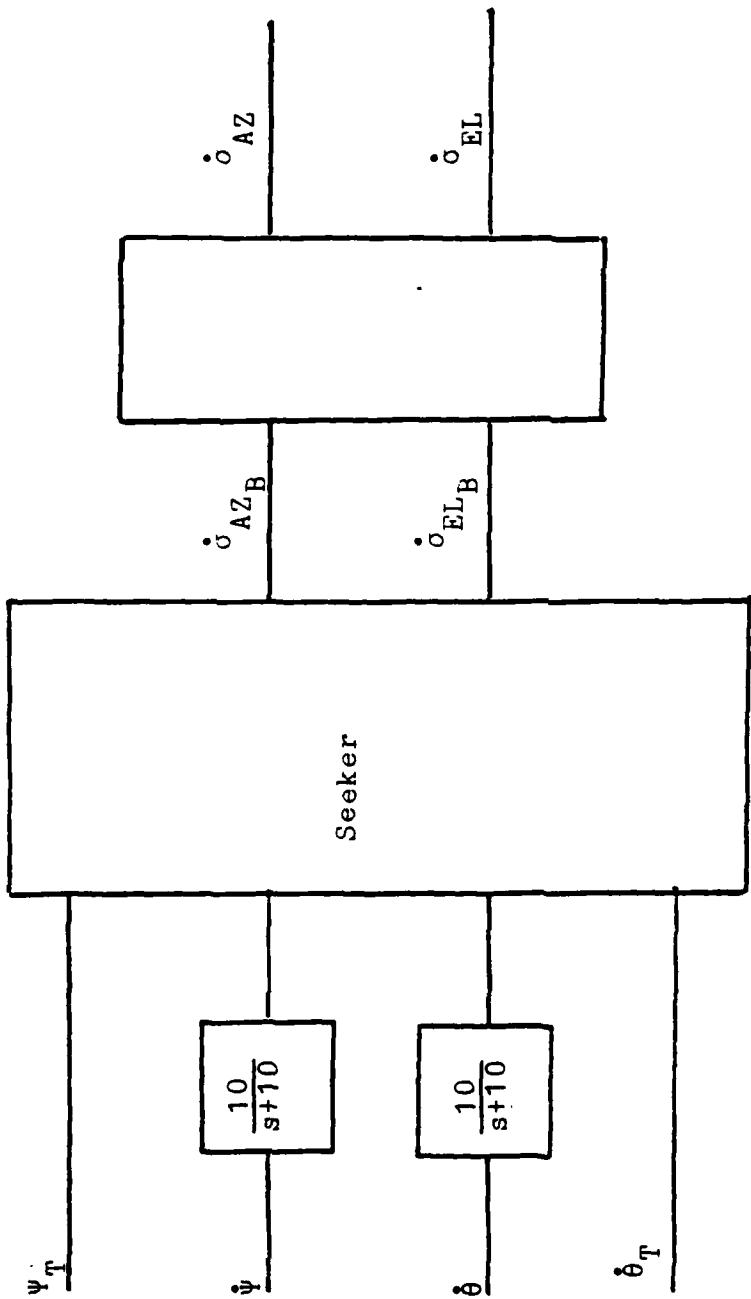
Figure 4-3   Seeker Simulation Flow Chart

69

These line of sight rates are generated in simulation by a two step procedure. First, the line of sight rates in earth referenced azimuth and elevation ($\dot{\sigma}_{AZ}$ and $\dot{\sigma}_{EL}$) are constructed by using the following relations:

$$\Psi_T = \tan^{-1} \frac{Y_T - Y_E}{X_T - X_E}$$

$$\theta_T = \tan^{-1} \frac{-H}{((X_T-X_E)^2+(Y_T-Y_E)^2)^{\frac{1}{2}}}$$

$$\sigma_{AZ} = \Psi_T - \Psi$$

$$\dot{\sigma}_{AZ} = \dot{\Psi}_T - \dot{\Psi}$$

$$\sigma_{EL} = \theta_T - \theta$$

$$\dot{\sigma}_{EL} = \dot{\theta}_T - \dot{\theta}$$

Figures 4-4 and 4-5 depict the geometry represented by the above equations.

Second, the body line of sight rates are calculated from the following transformation.
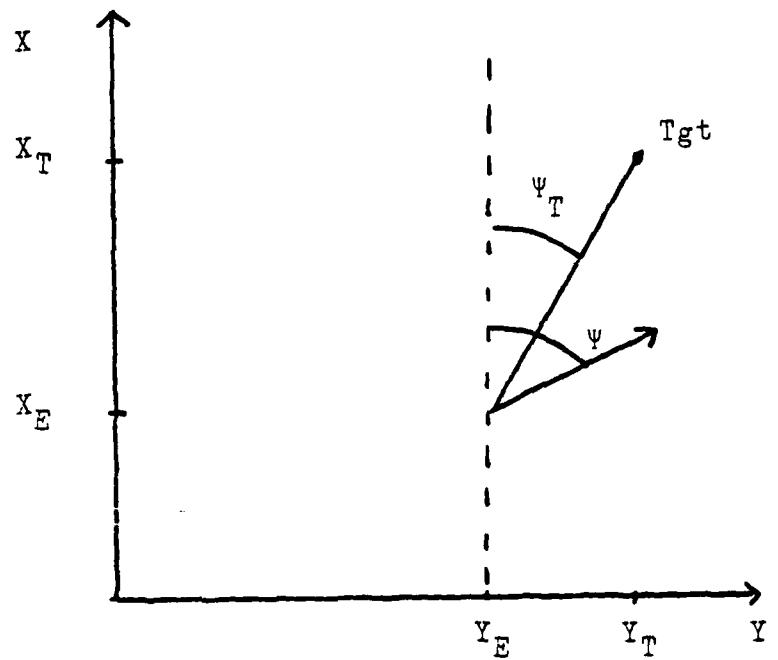
$$\dot{\sigma}_{AZ_B} = -\dot{\sigma}_{EL}\sin\phi + \dot{\sigma}_{AZ}\cos\theta\cos\phi$$

$$\dot{\sigma}_{EL_B} = \dot{\sigma}_{EL}\cos\phi + \dot{\sigma}_{AZ}\cos\theta\sin\phi$$

Once the body rates have been simulated ($\dot{\sigma}_{AZ_B}$, $\dot{\sigma}_{EL_B}$) they are transformed to earth horizontal and vertical rates through the transformation T_ϕ, defined by:

$$\dot{\sigma}_{EL} = \dot{\sigma}_{EL_B}\cos\phi - \dot{\sigma}_{AZ_B}\sin\phi$$

$$\dot{\sigma}_{AZ} = \dot{\sigma}_{EL_B}\sin\phi + \dot{\sigma}_{AZ_B}\cos\phi$$

$$\sigma_{AZ} = \Psi_T - \Psi$$

Figure 4-4 Azimuth Line of Sight Description

71
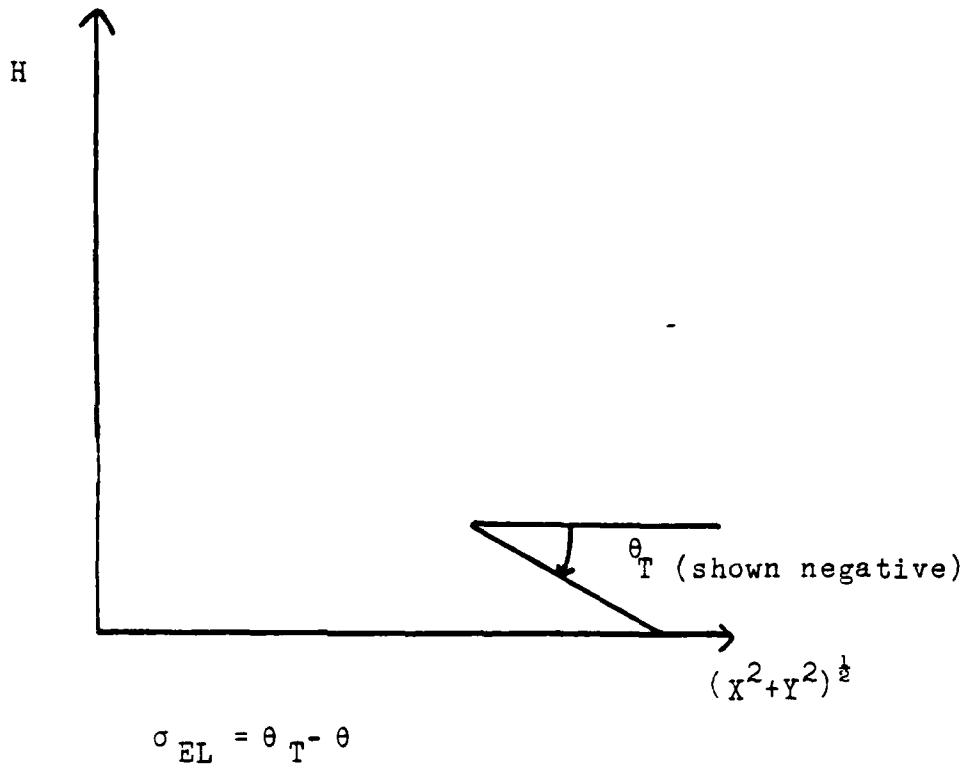
Figure 4-5   Elevation Line of Sight Description

This transformation includes the assumption that Θ is small throughout the mission. The earth horizontal and vertical line of sight rates ($\dot{\sigma}_{EL}$ and $\dot{\sigma}_{AZ}$) are then used in the appropriate guidance laws for proportional navigation.

2. Missile Dynamic Filters

In order to filter out missile dynamics from the seeker line of sight rates, a low pass filter, $10/(S+10)$, is used at the input to the seeker on $\dot{\theta}$ and $\dot{\psi}$.

C. BASELINE GUIDANCE LAW DESIGN (POPOUT MANEUVER)

A flow diagram of the baseline guidance scheme is shown in Figure 4-6. Switch positions are a function of mission phase. Each phase of the mission is described below beginning with the attack phase.

1. Attack Phase

Proportional navigation is used in azimuth and elevation to construct guidance commands to the missile autopilot commencing at a range of 9100 feet in the manner described below.

a. Proportional Navigation Constants and Guidance Commands

The earth horizontal and vertical line of sight rates ($\dot{\sigma}_{AZ}$ and $\dot{\sigma}_{EL}$) which are generated from the body rates $\dot{\sigma}_{AZ_B}$ and $\dot{\sigma}_{EL_B}$ by the transformation T_ϕ are multiplied by a navigation constant and V_T/g to generate commanded lateral accelerations in the earth vertical and horizontal planes.

73
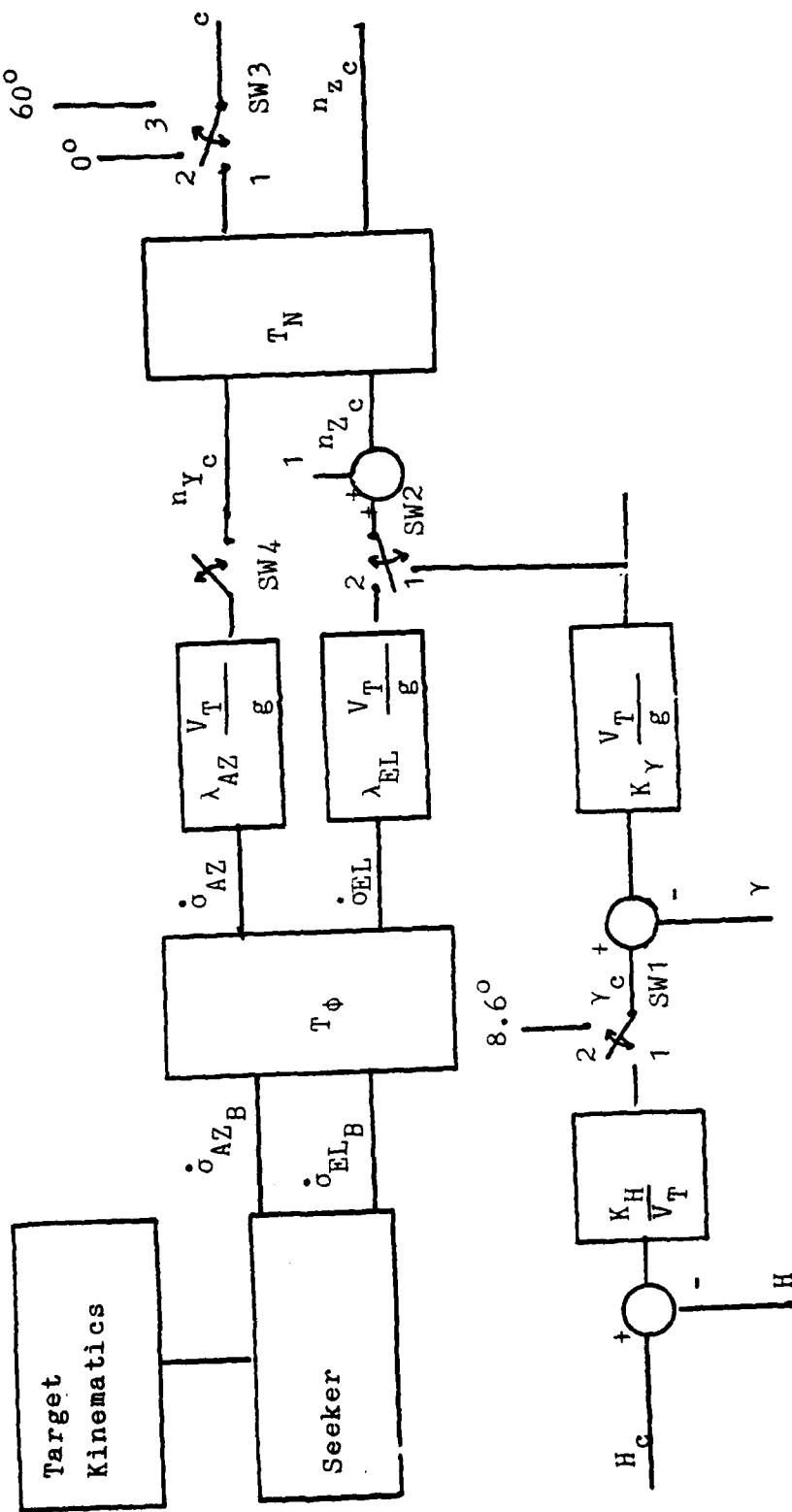
Figure 4-6 Baseline Guidance Law Flow Diagram

74

A navigation constant of 4.0 in each plane was found to
yield best results. Values from 3.0 to 4.5 were evaluated
with results of that evaluation shown in Chapter V. A one
g bias is applied to the vertical commanded lateral accelera-
tion to compensate for acceleration due to gravity. Thus
two lateral acceleration commands (n_{Y_c} and n_{Z_c}) are computed
in the earth horizontal and vertical planes.

$$n_{Y_c} = \lambda_{AZ} \; \frac{V_T}{g} \; \dot{\sigma}_{AZ} \tag{13}$$

$$n_{Z_c} = \lambda_{EL} \; \frac{V_T}{g} \; \dot{\sigma}_{EL} + 1 \tag{14}$$

These commanded lateral accelerations are subjected to a
further transformation (T_N) in order to generate commanded
bank angle and normal load factor which are required by the
missile autopilot.

$$\phi_C = \tan^{-1} \frac{n_{Y_c}}{n_{Z_c}}$$

$$n_{z_c} = n_{Z_c} \cos\phi + n_{Y_c} \sin\phi$$

Figure 4-7 depicts the geometric relationship described by
the above two equations. Commanded bank angle (ϕ_C) and
normal load factor (n_{z_c}) are used as inputs to the appropriate
autopilot outer command loops to provide closed loop bank
angle and load factor responses.
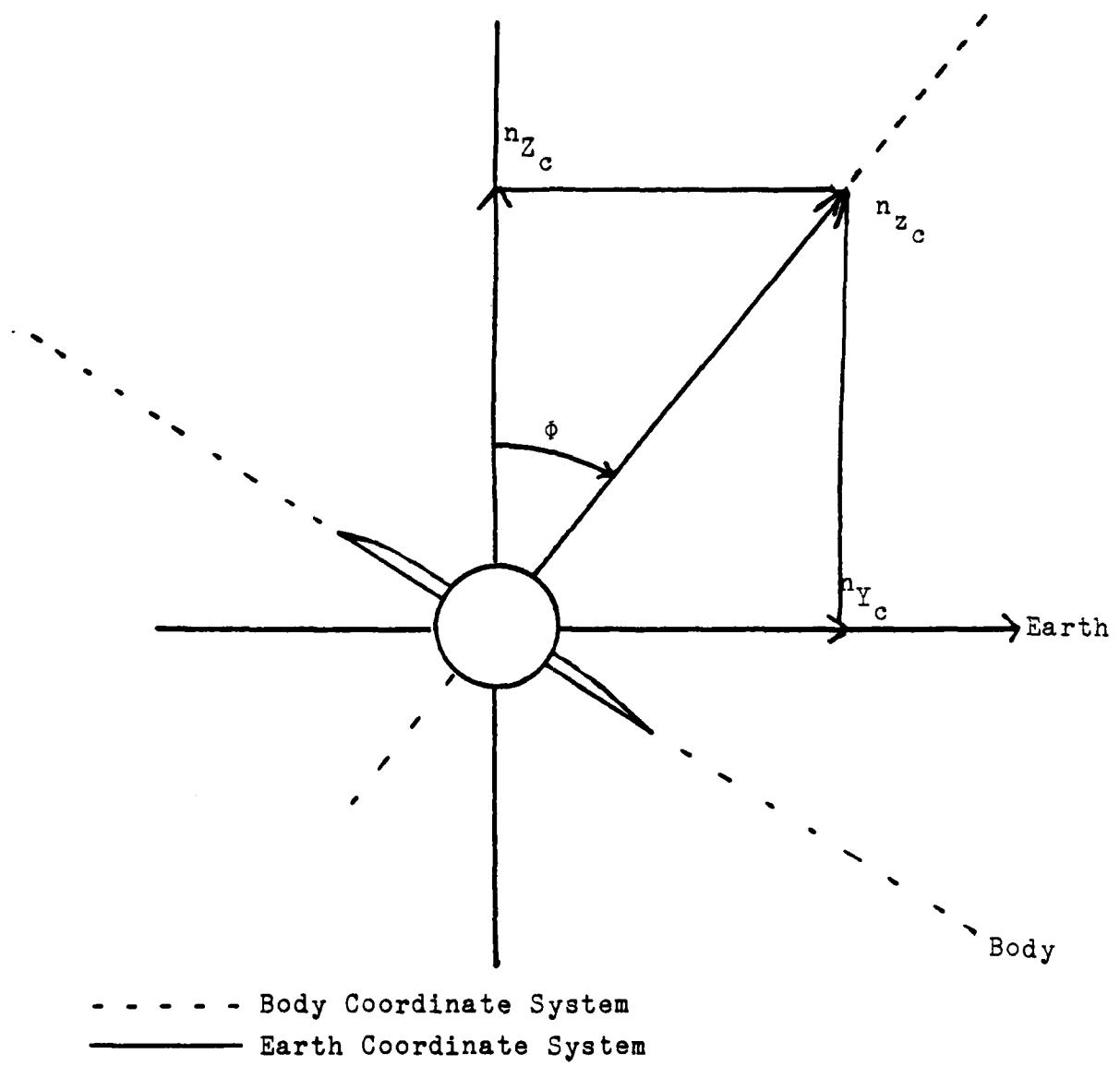
Figure 4-7 Load Factor and Bank Angle
Description

76

b. Limits on Guidance Commands

In the attack phase, the following limits are applied to commanded variables:

$$-2 \leq n_{z_c} \leq 4$$

$$|\dot{\phi}_c| \leq \dot{\phi} \text{ max}$$

Missile performance is evaluated for maximum roll rates of 50, 100 and 200 degrees per second.

c. Bank Angle Anomoly

In the attack mode there is no limit on commanded bank angle. Thus a computational scheme is required to insure that the missile always rolls the shortest way to a new commanded bank angle. This is accomplished by continuously calculating the quantity:

$$\Delta(t) = |\phi_c(t) - \phi(t)|$$

If $\Delta(t)$ is less than 180 degrees then $\phi_c(t)$ is sent to the bank angle autopilot. If $\Delta(t)$ is greater than 180 degrees then a modified bank angle command (ϕ_{c_M}) is sent to the auto pilot in accordance with the following logic:

$$\phi_{c_M} = \phi_c + 360° \text{ for } \phi_c < 0$$

$$\phi_{c_M} = \phi_c - 360° \text{ for } \phi_c > 0$$

d. Switch Positions

The switches shown in figure 4-6 are in the following positions for the attack phase:

SW1   Either position

SW2	Position 2
SW3	Position 1
SW4	Closed

e. Attack Phase Summary

In the attack phase proportional navigation is used in both azimuth and elevation to generate bank angle and normal load factor commands to the missile autopilot. The phase is commenced at a range of 9100 feet with missile offset in heading from the target at an altitude of approximately 250 feet. Roll rate is limited to ϕ_{max}. Bank angle is not limited. Normal load factor is limited from -2 to 4 g's.

2. Ingress Phase

The ingress phase commences with the beginning of the problem simulation when the missile is 25,000 feet from the target and initially heading north. The missile's Mach number is 0.75 and the ship's velocity is 21 knots to the east.

a. Altitude Hold Methodology and Guidance Commands

The missile is required to maintain altitude of 50 feet above sea level during this phase. It accomplishes this by comparing present altitude with 50 feet and multiplying the error by $\dfrac{K_H}{V_T}$ to establish a flight path angle command. K_H is assigned a value of 0.3. This calculated flight path angle command is compared with the present flight path angle

and the difference or error is multiplied by K_H and $\dfrac{V_T}{g}$ to give an elevation line of sight rate, $\dot{\sigma}_{EL}$. A value of 0.3 is assigned for K_H. Thus n_{Z_c} is computed as follows:

$$n_{Z_c} = K_H \; \frac{V_T}{g} \; (\gamma_c - \gamma) + 1$$

The lateral acceleration command n_{Y_c} is computed exactly as described in the attack phase with bank angle and roll rates limited.

The second transformation for the ingress phase (T_N) remains the same form as the attack phase.

$$\phi_c = \tan^{-1} \frac{n_{Y_c}}{n_{Z_c}}$$

$$n_{Z_c} = n_{Z_c} \cos\phi + n_{Y_c} \sin\phi$$

b. Limits on Guidance Commands

In the ingress phase the following limits are applied to commanded variables:

$$-2 \leq n_{Z_c} \leq 4$$

$$|\phi_c| \leq |\phi_{max}|$$

$$|\dot{\phi}_c| \leq |\dot{\phi}_{max}|$$

The maximum bank angle allowed is 60 degrees and roll rate is limited to 50,100 or 200 degrees per second.

c. Switch Positions

The switch positions as shown in Figure 4-6 are as follows during the ingress phase:

79

SW1, SW2, SW3   Position 1

                SW4   Closed

3. Offset Phase

The missile initiates the offset phase at 17,800 feet.
The offset phase is subdivided into two sub-phases -- turn
and level.

a. Turn and Level Sub-Phases

The missile maintains an altitude of 50 feet
throughout the offset phase in the same manner as described
during the ingress phase. Thus

$$n_{Z_c} = K_\gamma \frac{V_T}{g} (\gamma_c - \gamma) + 1$$

The missile performs the coordinated turn by
using a commanded bank angle and computing a normal load
factor as follows:

$$\phi_C = 60^\circ$$
$$n_{z_c} = \frac{n_{Z_c}}{\cos \phi}$$

At a range of 15800 feet from the target a turn of approxi-
mately 12 degrees is accomplished. The missile then performs
a straight and level maneuver by commanding zero bank angle
along with the same normal load factor as follows:

$$\phi_C = 0^\circ$$

$$n_{z_c} = \frac{n_{Z_c}}{\cos \phi}$$

b. Limits on Guidance Commands

For the offset phase normal load factor is limited as follows:

$$-2 \leq n_{z_c} \leq 4$$

Commanded bank angle is fixed at 60 degrees during the turn sub-phase and 0 degrees during the level sub-phase.

c. Switch Positions

The switch position, as shown in Figure 4-6, are as follows during the offset phase:

1) Turn sub-phase

SW1, SW2	Position 1
SW3	Position 3
SW4	Open

2) Level sub-phase

SW1, SW2	Position 1
SW3	Position 2
SW4	Open

4. Pop Up Phase

The missile enters the pop up phase when the range becomes 10,200 feet. The purpose of this phase is to pop up the missile to an altitude of approximately 250 feet so that a dive into the target will give acceptable deck penetration.

a. Vertical Flight Path Angle Methodology and Guidance Commands

The missile achieves the pop up effect by commanding a vertical flight path angle of 8.6 degrees.

This commanded climb angle is compared with the actual γ and the error is multiplied by K_γ and $\frac{V_T}{g}$ to give an elevation line of sight rate. A value of 1.0 is assigned for $K\gamma$ in this simulation. Thus n_{Z_c} is computed as follows:

$$n_{Z_c} = K_\gamma \; \frac{V_T}{g} \; (\gamma_{climb} - \gamma) + 1$$

The lateral acceleration commanded n_{y_c} is computed exactly as described in the ingress phase.

The second transformation T_N is as follows:

$$\phi_c = \tan^{-1} \frac{n_{y_c}}{n_{Z_c}}$$

$$n_{z_c} = n_{Z_c} \cos\phi + n_{Y_c} \sin\phi$$

The missile is free to start rolling into the target using proportional navigation during the pop up phase and thus aids in the attack phase which follows the pop up phase.

b. Limits on Guidance Commands

In the pop up phase the following limits are applied to commanded variables:

$$-2 \leq n_{z_c} \leq 4$$

$$|\phi_c| \leq |\phi_{max}|$$

$$|\phi_c| \leq |\phi_{max}|$$

The maximum bank angle is limited to 60 degrees
and the maximum roll rate is limited to 50, 100 or 200 degrees
per second.

c. Switch Positions

The switch positions as shown in Figure 4-6 are
as follows during the pop up phase:

SW1	Position 2
SW2, SW3	Position 1
SW4	Closed

5. Guidance Summary (Baseline)

The following matrix indicates the horizontal and
vertical controls during each phase of missile flight.

PHASE	AZIMUTH CONTROL	ELEVATION CONTROL
Ingress	PN*	Altitude Hold
Offset	Φ Command	Altitude Hold
Popup	PN	Flight Path Angle Hold
Attack	PN	PN

*Proportional Navigation

D. ALTERNATE GUIDANCE LAW DESIGN SEA-SKIMMER

The sea skimmer scheme differs only from the baseline
guidance scheme in that the offset and popup phases are
eliminated. In essence this scheme is composed of an ingress
phase and an attack phase.

1. Ingress Phase

The ingress phase commences with problem initialization
which locates the missile 25,000 feet from the target with

83.

identical initial conditions as the baseline guidance scheme.
The vertical load factor is computed as

$$n_{Z_c} = K_H \frac{V_T}{g} (\gamma_c - \gamma) + 1$$

The lateral acceleration command is computed as

$$n_{Y_c} = \lambda_{AZ} \frac{V_T}{g} \dot{\sigma}_{AZ}$$

The second transformation (T_N) is as follows:

$$\phi_C = \tan^{-1} \frac{n_{Y_c}}{n_{Z_c}}$$

and

$$n_{z_c} = n_{Z_c} \cos\phi + n_{Y_c} \sin\phi$$

Limits on guidance commands and switch positions
for the ingress phase are identical to the ingress phase
for the baseline scheme.

2. <u>Attack Phase</u>

The attack phase commences at 3000 feet range and
uses proportional navigation in both elevation and azimuth.
The missile dives into the target from 50 foot altitude.

The bank angle command and normal load factor are
computed exactly as in the baseline scheme attack phase
and are:

$$\phi_C = \tan^{-1} \frac{n_{Y_c}}{n_{Z_c}}$$

$$n_{z_c} = n_{Z_c} \cos\phi + n_{Y_c} \sin\phi$$

Limits on guidance commands and switch positions are also identical to the attack phase in the baseline guidance scheme.

3. <u>Guidance Summary (Sea Skimmer)</u>

The following matrix shows the horizontal and vertical controls during each phase of the sea skimmer guidance scheme.

PHASE	AZIMUTH CONTROL	VERTICAL CONTROL
Ingress	PN	Altitude Hold
Attack	PN	PN

V. PROBLEM SIMULATION, RESULTS, CONCLUSIONS AND RECOMMENDATIONS

This chapter describes the computer simulation special language used and presents the results of test runs in which roll rate, ECM blinking rate and burn through range are all varied in both the baseline guidance scheme and the sea skimming guidance scheme. From these results optimum parameters are chosen to yield minimum miss distance for each guidance scheme. Miss distance ranges are also presented for the baseline scheme with Glint imposed.

A. CSMP SIMULATION

The Continuous System Modeling Program III (CSMP III), an IBM developed system, is the modeling technique chosen for this study. CSMP, as discussed in Speclchart and Green {Ref. 4}, is compatable with the Fortran IV language, has six selectable integration methods (fourth order Runge-Kutta is used for this simulation), and has multiple special function codes that can solve a large variety of control engineering problems.

The special functions used for this simulation are:

a. FUNGEN - This function extracts the value of a function of one variable from a stored table in memory. It is used for aerodynamic coefficients.

b. TWOVAR - This function extracts the value of a function of two variables from a stored table in memory. It is used for aerodynamic coefficients.

c. INSW - Y = INSW (X1, X2, X3) assigns Y = X2 for $X_1 < 0$, $Y = X_3$ for $X_1 \geq 0$. It is used to accomplish ECM blinking action.

d. GAUSS - This function is a random number generator with normal distribution. It is used to realize glint.

e. REALPL - This function simulates a first order lag $1/(\tau S++1)$ filter. It is used in autopilot and seeker equations as low pass filters.

f. DEBUG - This is a computer program aid that evaluates all output parameters and variables at requested times.

In addition to the special functions, trigonometric, integral, derivative and square root functions are used to perform necessary steps with one invocation. CSMP also has the ability to perform calculations in either a sort section, where the order of computation is not considered, or a nosort section, where ordered sequential fortran statements are required. The program is structured as shows below:

<u>MISSILE SIMULATION PROGRAM</u>

INITIAL

      CONSTANTS
      AERODYNAMIC COEFFICIENT TABLES

DYNAMIC
   NOSORT

      MISSION PHASE LOGIC
      GUIDANCE EQUATIONS
      ECM (BLINKING) EQUATIONS

   SORT

      6 DOF MISSILE DYNAMIC EQUATIONS

INNER LOOP AUTOPILOTS
SEEKER EQUATIONS

TERMINAL

OUTPUT GRAPHS

The CSMP initially sets up the two and three variable coefficients in tabular form in memory. The run commences with the missile in steady state flight with steady state variables established. These steady state variables are used to enter the tables in memory and extract coefficients which are used to calculate aerodynamic derivatives, forces, moments, and other relations. From the steady state flight condition small perturbations are made and new table entries produced. This process is repeated for all phases of flight.

B. RESULTS

Both the baseline guidance scheme and the sea skim guidance scheme were tested under the same conditions and quantitative results obtained. All scenarios started from the following initial conditions:

1. Target position - 25,000 feet north of the missile.

2. Target speed - east at 21 knots.

3. Missile speed - north at 0.75 Mach number

4. Missile altitude - 50 feet above sea level.

The simulation was run for 31 seconds. Miss distance data was obtained for varying roll rate limits, ECM blinking frequencies, and burn through ranges. The following matrix of parameters was tested:

Burn through range (feet)

    2000
    1500
    1200
     800
     400

Roll rate limit (degrees per second)

    200
    100
     50

ECM blinking frequency (Hertz)

    2
    1
    0.5

The resulting miss distances are shown in Tables 5-1 and 5-2 for all runs. Figure 5-1 through figure 5-6 are the graphical results of simulation runs. Each run is presented in 6 consecutive figures a through f and depict the following.

a. Commanded roll rate (PCMD) and roll rate (P) vs time.

b. Commanded bank angle (PHICMD) and bank angle (PHI) vs time.

c. Range, X Range, Y Range and Z Range vs time.

d. Left and right stabilizers (LSTAB and RSTAB) vs time.

e. Rudder position vs time.

f. Map of YMISLE and HMISLE vs XMISLE.

The following matrix indicates the test conditions used to generate each figure:

TABLE 5-1

Baseline Guidance and Control Scheme

Miss Distance (feet)

ECM Blinking Rate	Roll Rate Limit	Burnthrough Ranges				
		400	800	1200	1500	2000
.5 cps	50	19.9	15.7	16	16	6.28
	100	17	11.3	6.95	6.95	18.16
	200	27	30	29	29	26.1
1 cps	50	24	23	11.3	9.8	10.7
	100	12.6	13.7	12.5	11	6.9
	200	5.4	3	4.9	2.9	6.57
2 cps	50	25	20	8.9	6.6	4.34
	100	23.7	15.7	2.2	1.69	6.8
	200	13.3	7.9	1.5	4.2	6.81
0 cps	50	2.5				
	100	4.4				
	200	4.5				

TABLE 5-2

Sea-Skimmer Guidance and Control Scheme

Miss Distance (feet)

ECM Blinking Rates	Roll Rate Limit	Burnthrough Ranges				
		400	800	1200	1500	2000
.5	50	43	37.7	37.7	37.7	2.8
	100	72	61	61	61	1.56
	200	44.64	28.7	37.7	28.7	1.77
1	50	54	54	38.62	28.8	1.48
	100	52	52	20	20.6	3.9
	200	65	63	26	26	3.09
2	50	34.6	31.20	37.7	37.7	2.87
	100	32.9	27.9	61	61	1.56
	200	43.5	37.35	28.8	28.8	1.77
0	50	3.9				
	100	2.7				
	200	2.6				

91

BASE GUIDANCE SCHEME

5-1 (a-f)   NO ECM, 100°/sec roll rate

5-2 (a-f)   ECM (1Hz), 100°/sec roll rate

5-3 (a-f)   ECM (1Hz), 50°/sec roll rate

5-4 (a-f)   ECM (1Hz), 200°/sec roll rate

SEA SKIMMER SCHEME

5-5 (a-f)   NO ECM, 100°/sec roll rate

5-6 (a-f)   ECM (1Hz), 100°/sec roll rate

1. Analysis of Baseline Scheme Results

   a. Varying Burn Through Range

   Miss distances generally decrease as the burn
through range increases. For runs beyond 1500 feet burn
through ranges, the miss distances are close enough to be
considered as hits since most of the miss distance is in the
Y component of range which has the largest offset (75 feet)
applied during ECM.

   b. Varying ECM Blinking Frequency

   The miss distance decreases as blinking rate
increases for the same burn through range. Miss distances
for burn through ranges beyond 1200 feet are particularly
good for all three roll rates.

   c. Varying Roll Rate Limit

   Varying roll rate limit results in the largest
variation in miss distance. For 200 degree per second
roll rate limit and 0.5 Hertz ECM blinking frequency the

92

NOGLINT,LAMDA=4.0,ECM=0.0 CPS,ROLL RATE=100 DEG/SEC
BANK ANGLE (DEGREES) VS TIME
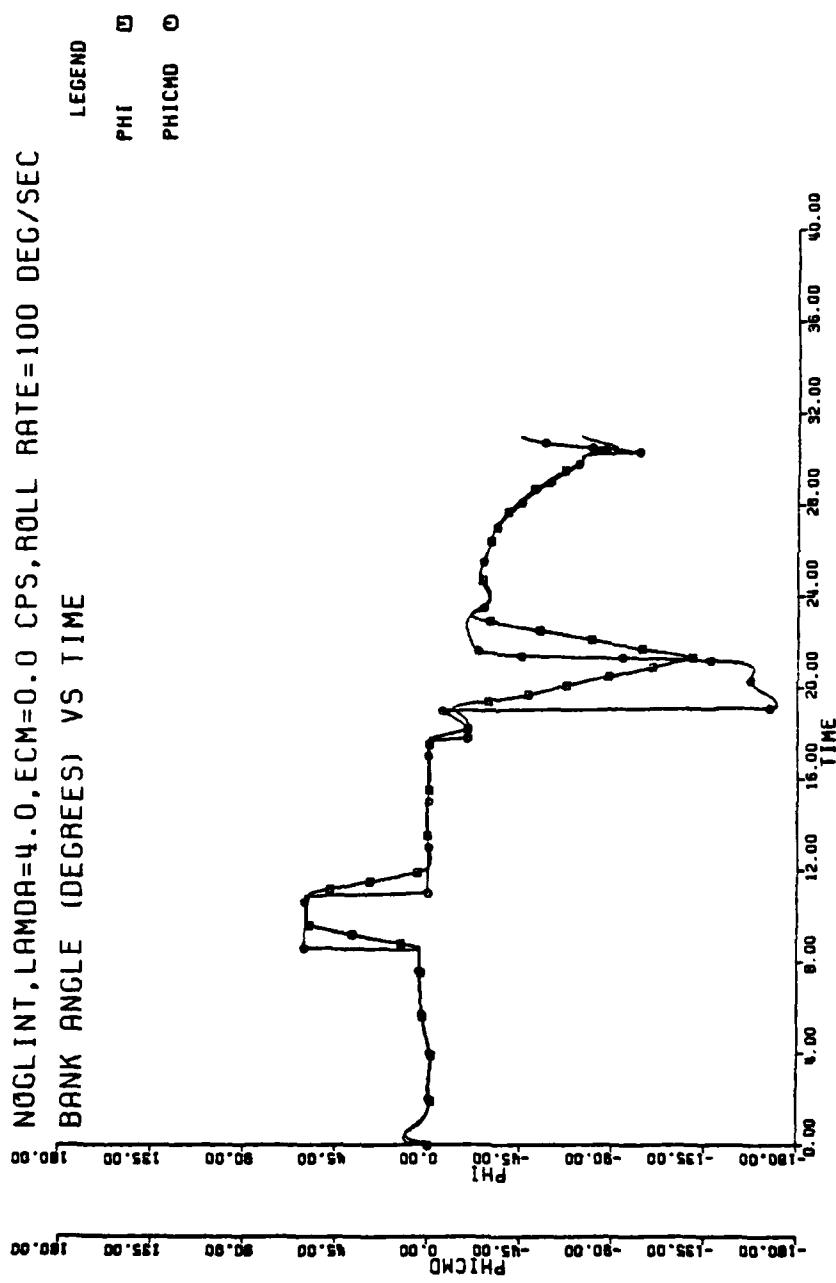
Figure 5-1a   Baseline Response for No ECM, Roll Rate Limit 100 deg/sec
(PHICMD, PHI   vs   TIME)
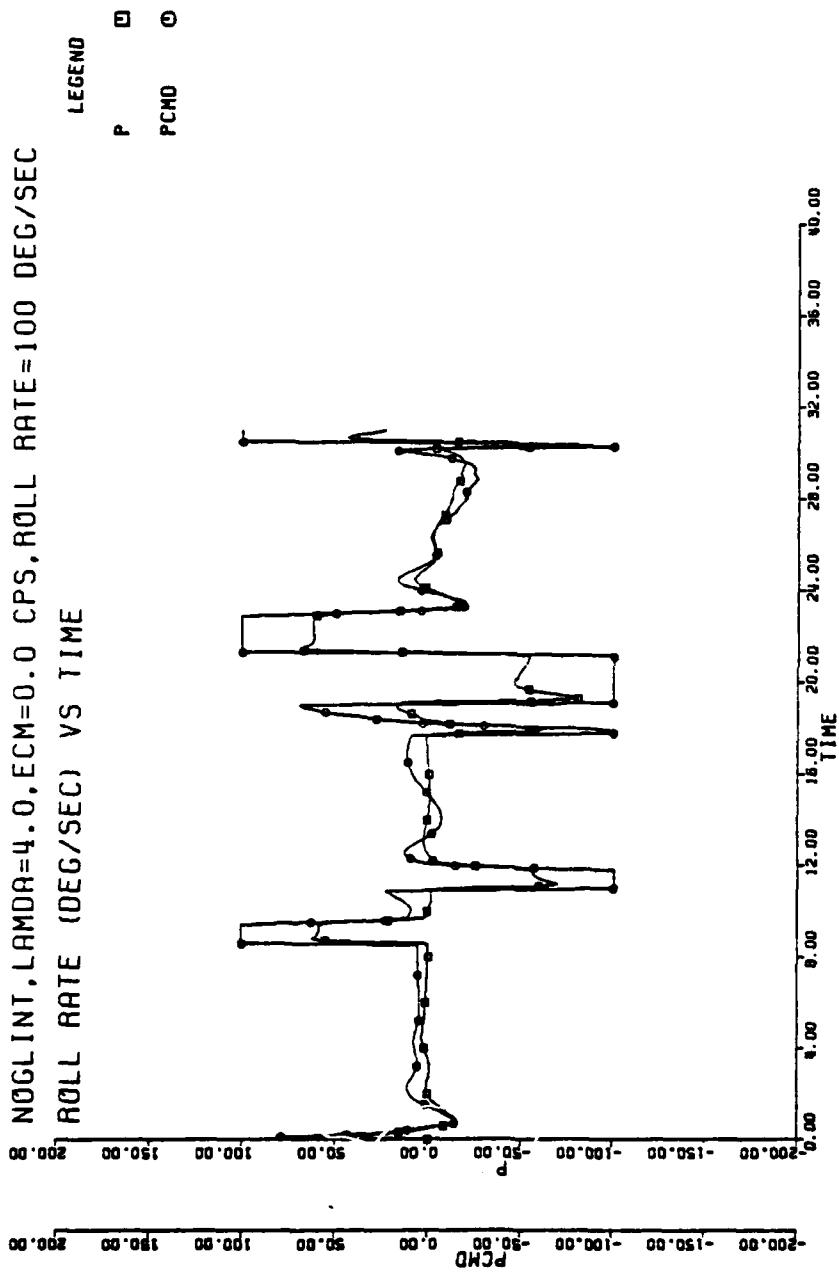
Figure 5-1b Baseline Response for No ECM, Roll Rate Limit 100 deg/sec

(PCMD, P vs TIME)

94

NOGLINT,LAMDA=4.0,ECM=0.0 CPS,ROLL RATE=100 DEG/SEC
RANGE,XRANGE,YRANGE,ZRANGE (FEET) VS TIME
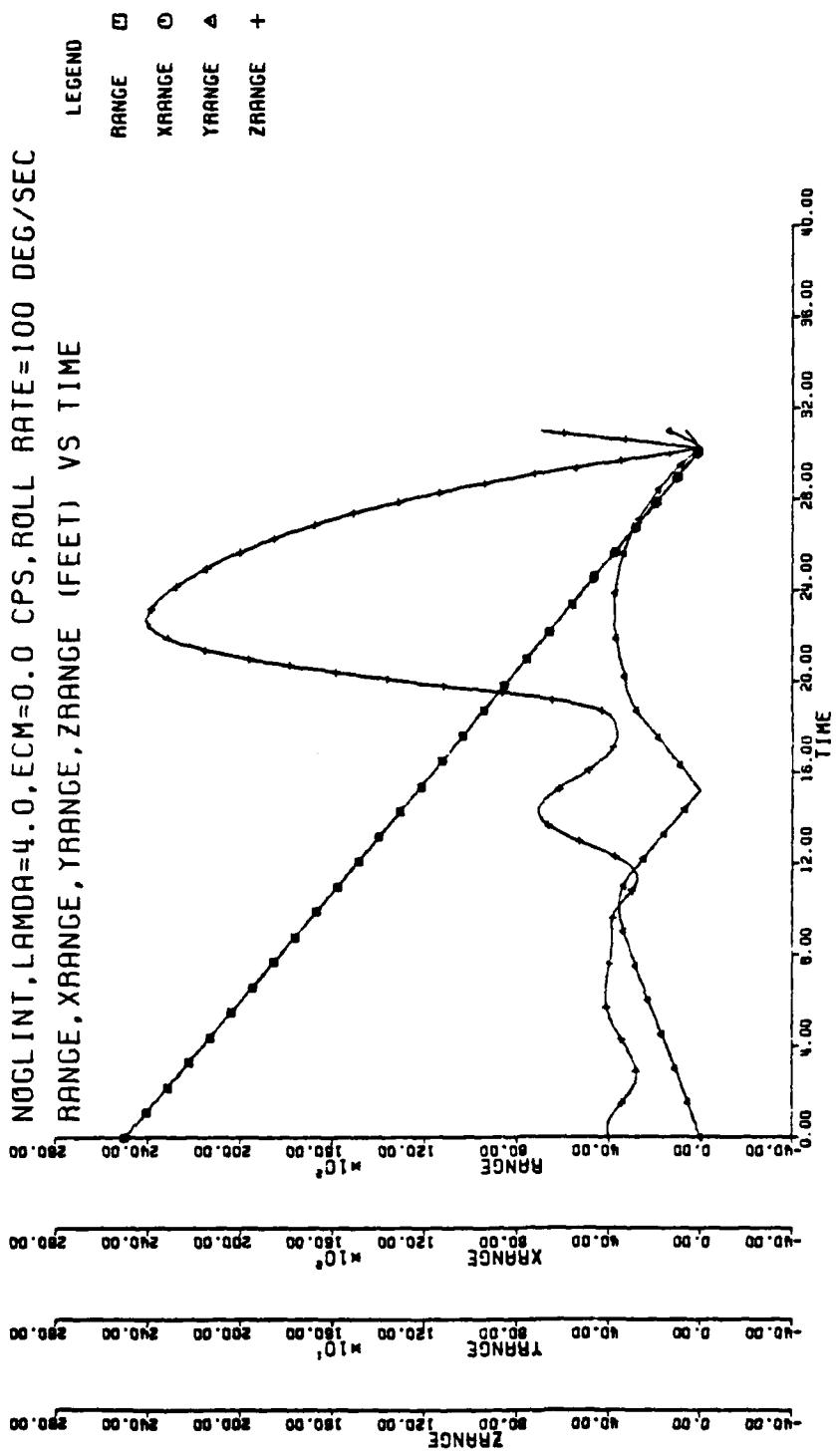
Figure 5-1c Baseline Response for No ECM, Roll Rate Limit 100 deg/sec
(RANGE, XRANGE, YRANGE, ZRANGE vs TIME)

95

MICROCOPY RESOLUTION TEST CHART

NATIONAL BUREAU OF STANDARDS-1963-A

NOGLINT,LAMDA=4.0,ECM=0.0 CPS,ROLL RATE=100 DEG/SEC
LEFT & RIGHT STABILIZERS (DEGREES) VS TIME

LEGEND
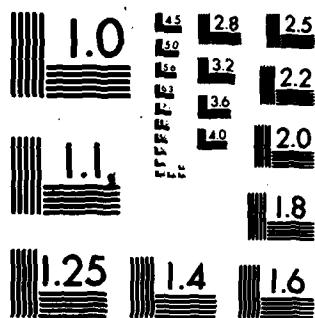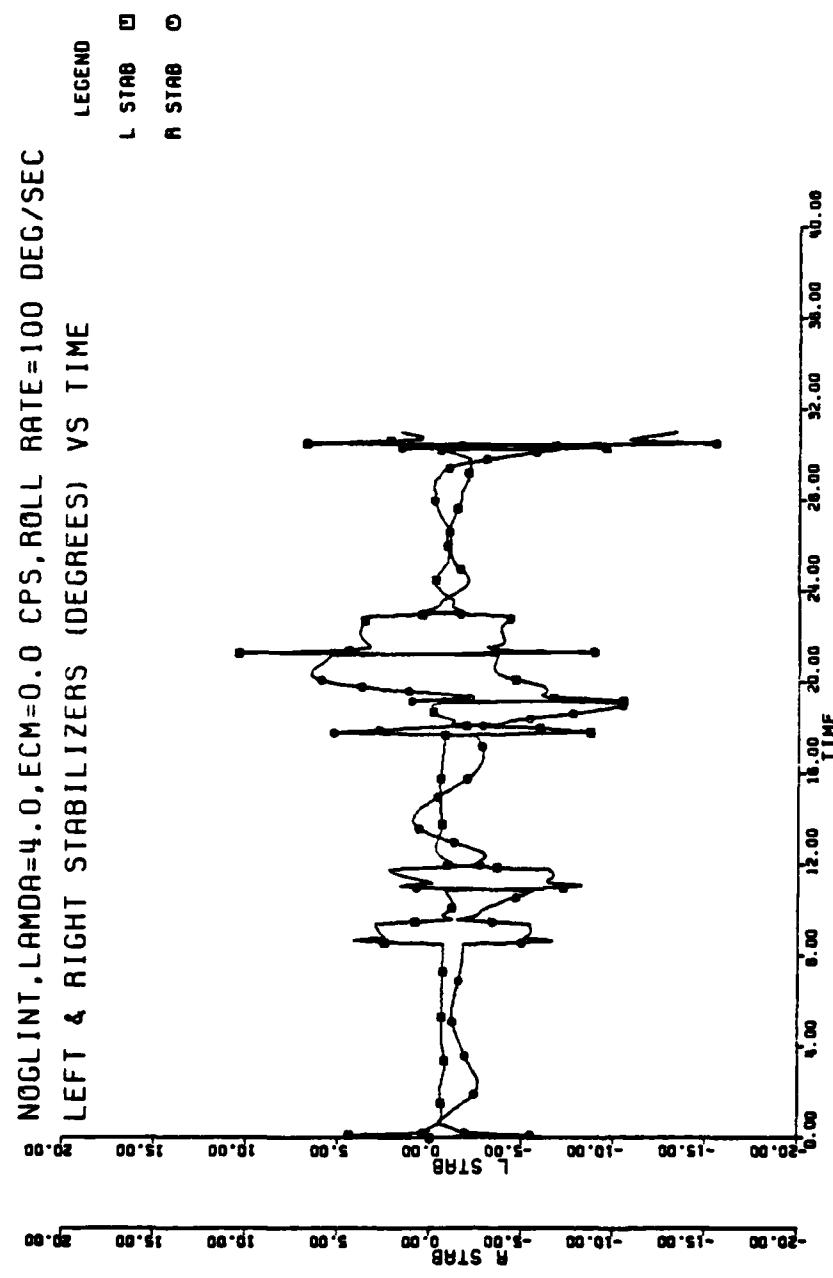
L STAB ▣

R STAB ◉

Figure 5-1d Baseline Response for No ECM, Roll Rate Limit 100 deg/sec

(L STAB, R STAB vs TIME)

96

NOGLINT,LAMDA=4.0,ECM=0.0 CPS,ROLL RATE=100 DEG/SEC
RUDDER POSITION (DEGREES) VS TIME

LEGEND
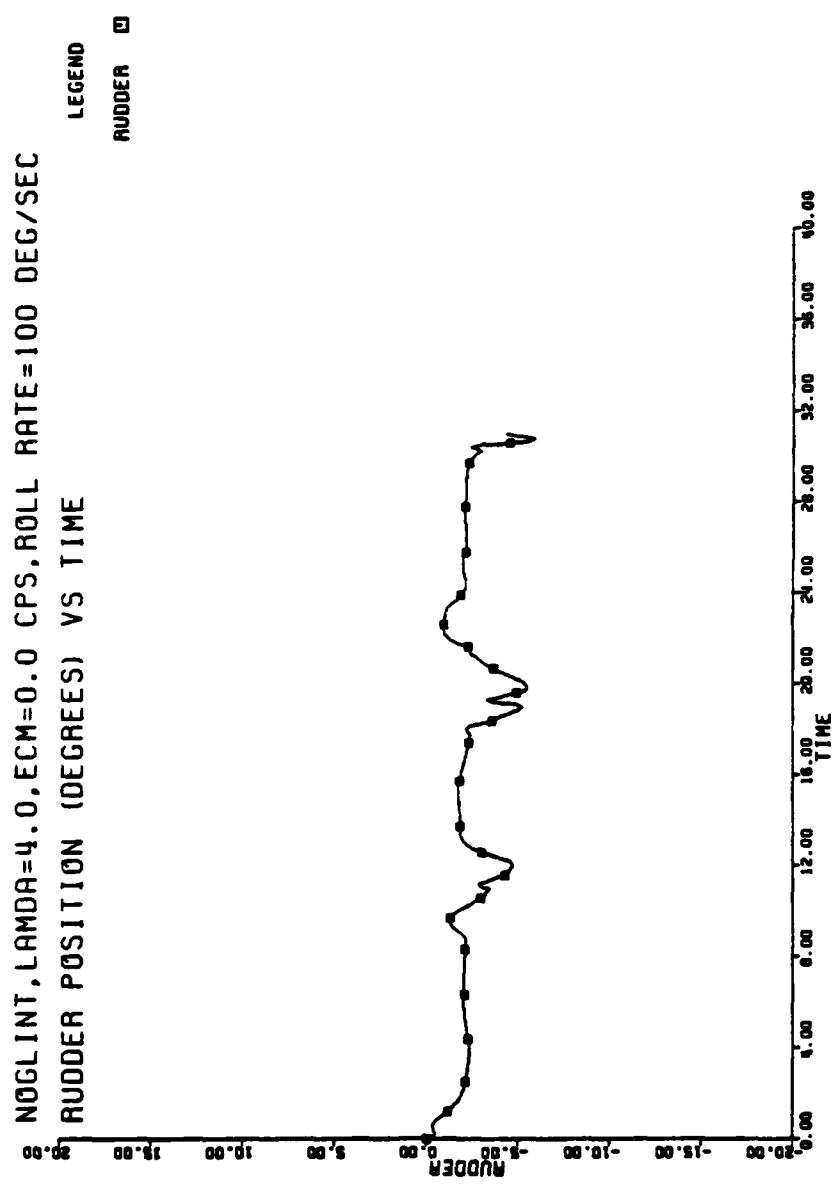
RUDDER □

Figure 5-1e   Baseline Response for No ECM, Roll Rate Limit 100 deg/sec

(RUDDER vs TIME)

97
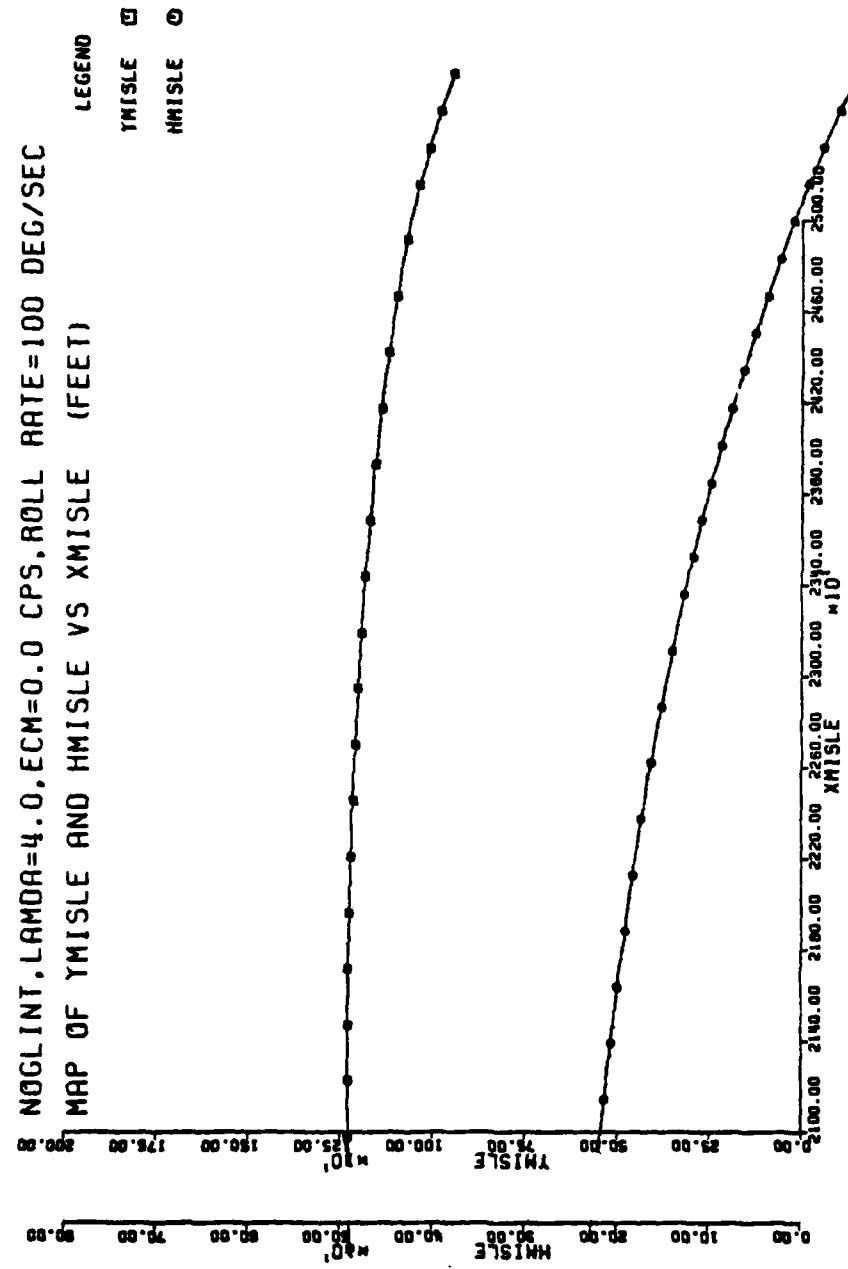
Figure 5-1f Baseline Response for No ECM, Roll Rate Limit 100 deg/sec
YMISLE, HMISLE vs XMISLE)
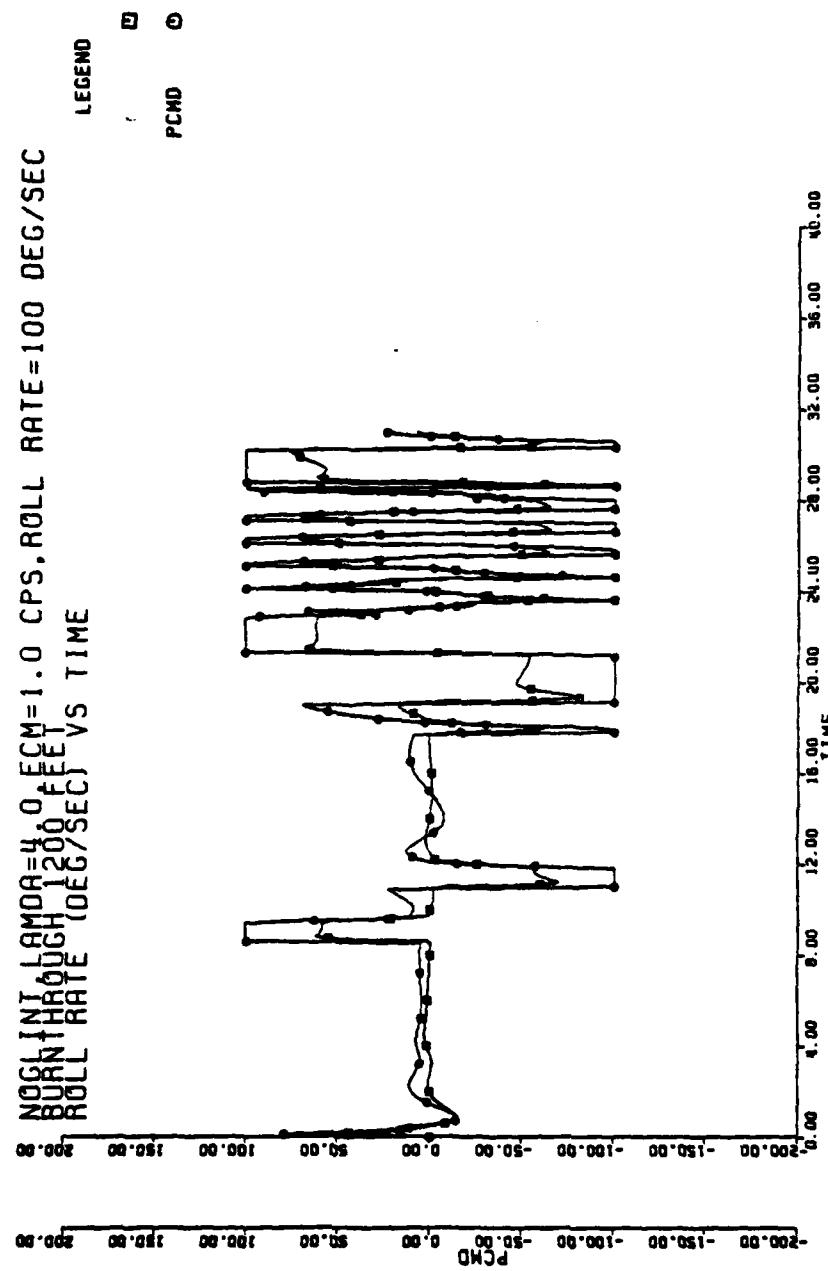
Figure 5-2a Baseline Response for ECM 1 CPS, Roll Rate Limit 100 deg/sec

(PCMD,P vs TIME)

99
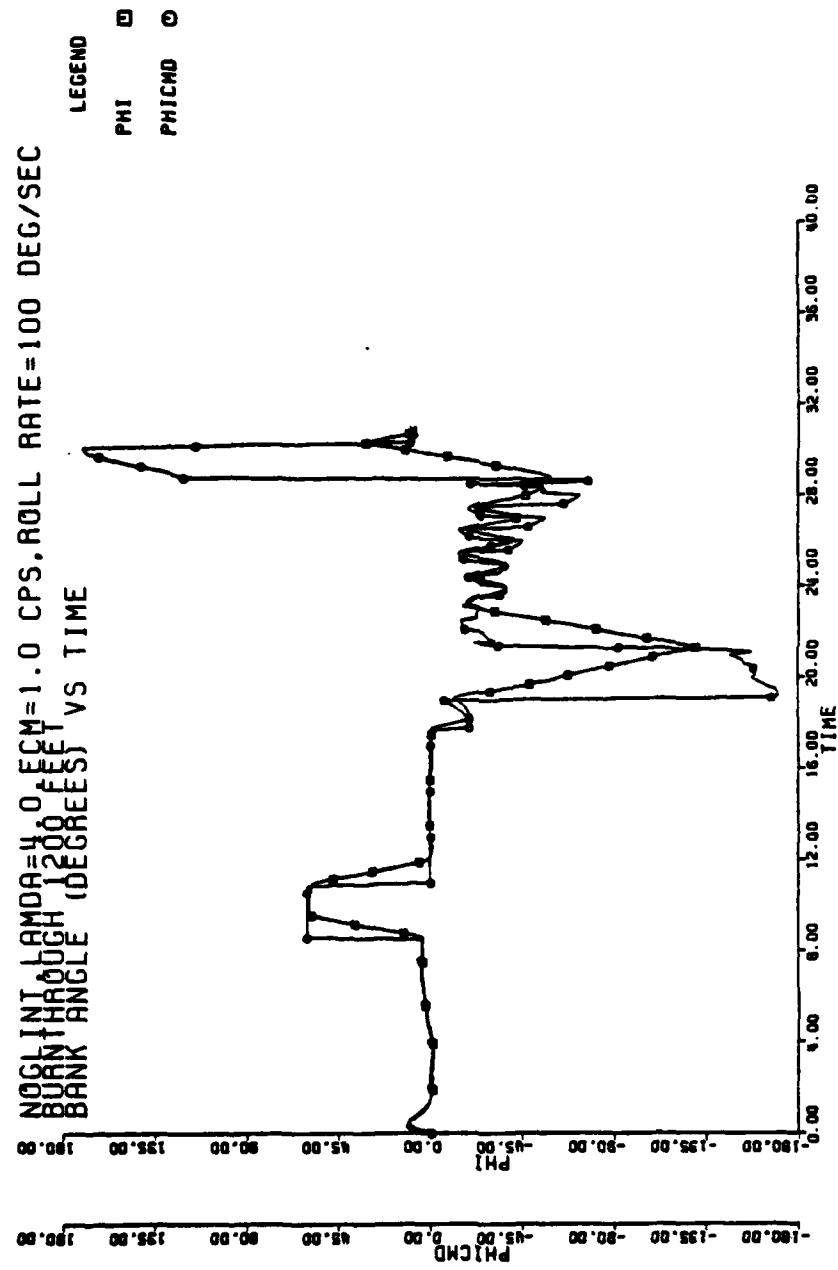
Figure 5-2b Baseline Response for ECM 1 CPS, Roll Rate Limit 100 deg/sec

(PHICMD, PHI vs TIME)
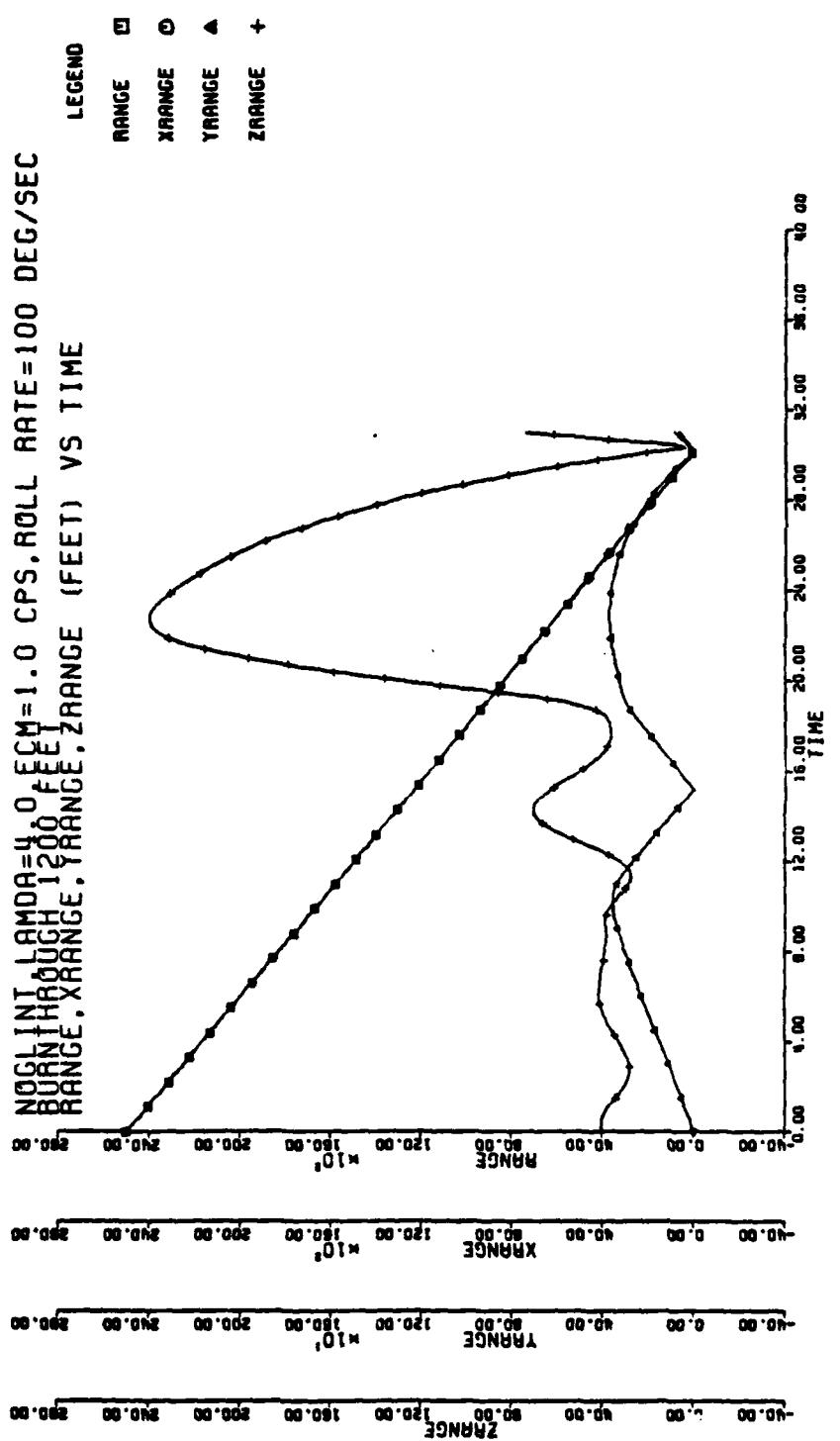
Figure 5-2c   Baseline Response for ECM 1 CPS, Roll Rate Limit 100 deg/sec

(RANGE, XRANGE, YRANGE, ZRANGE vs TIME)

101
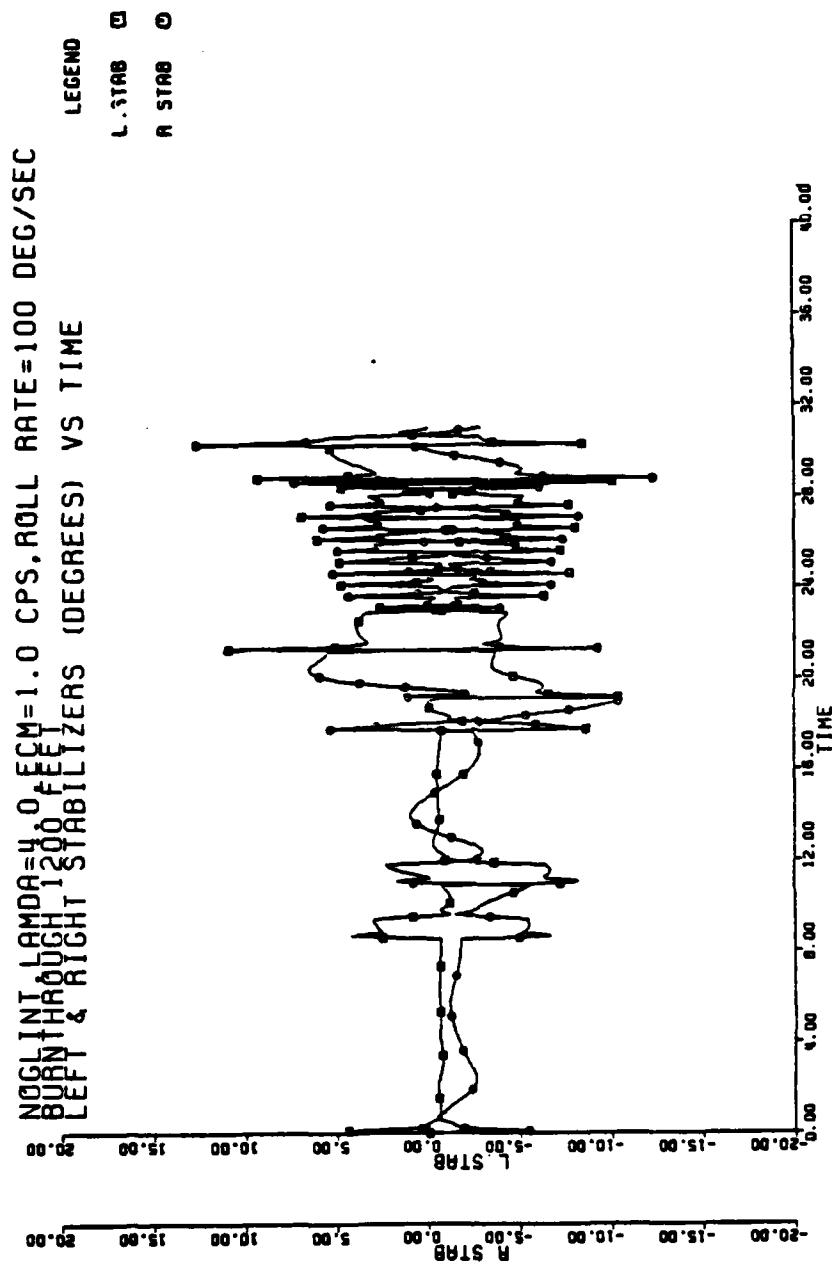
Figure 5-2d Baseline Response for ECM 1 CPS, Roll Rate Limit 100 deg/sec

(L STAB, R STAB vs TIME)

102

NOGLINT LAMDA=4.0 ECM=1.0 CPS,ROLL RATE=100 DEG/SEC
BURNTHROUGH 1200 FEET
RUDDER POSITION (DEGREES) VS TIME

LEGEND
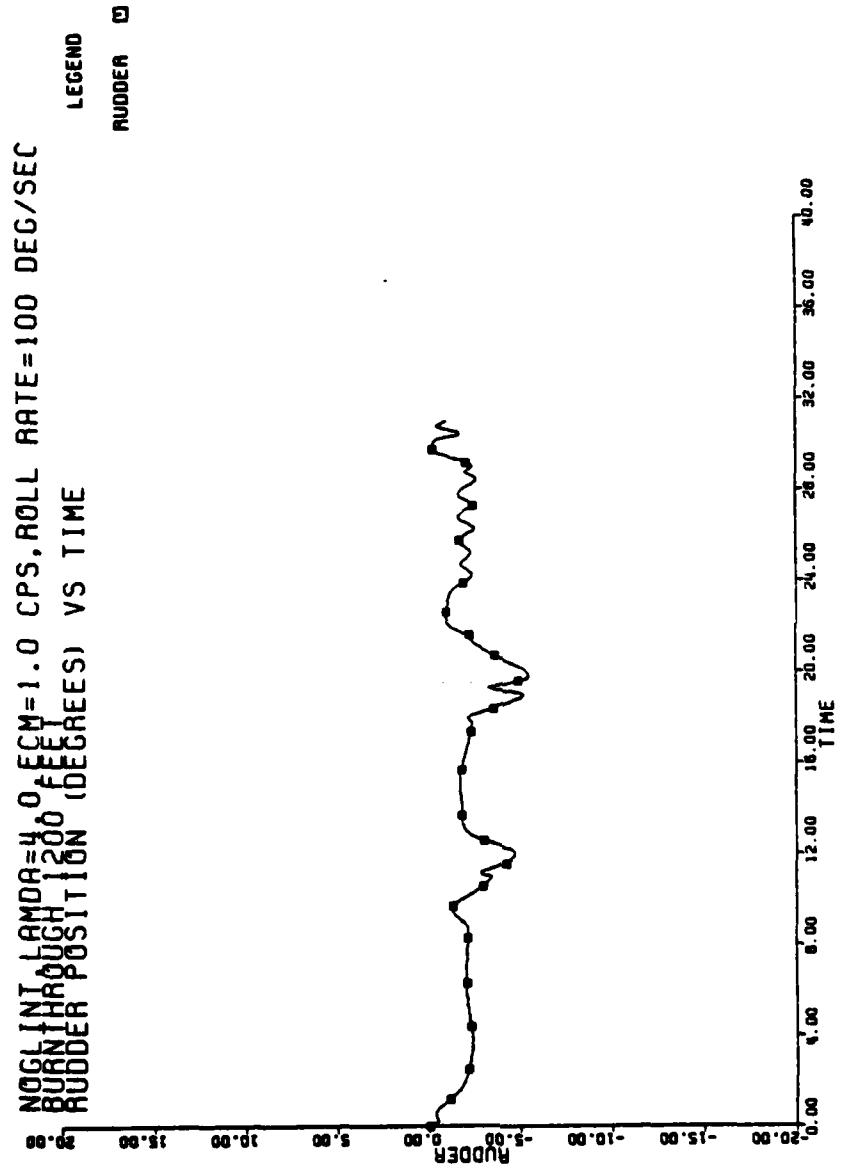
RUDDER ▣

Figure 5-2e Baseline Response for ECM 1 CPS, Roll Rate Limit 100 deg/sec

(RUDDER vs TIME)
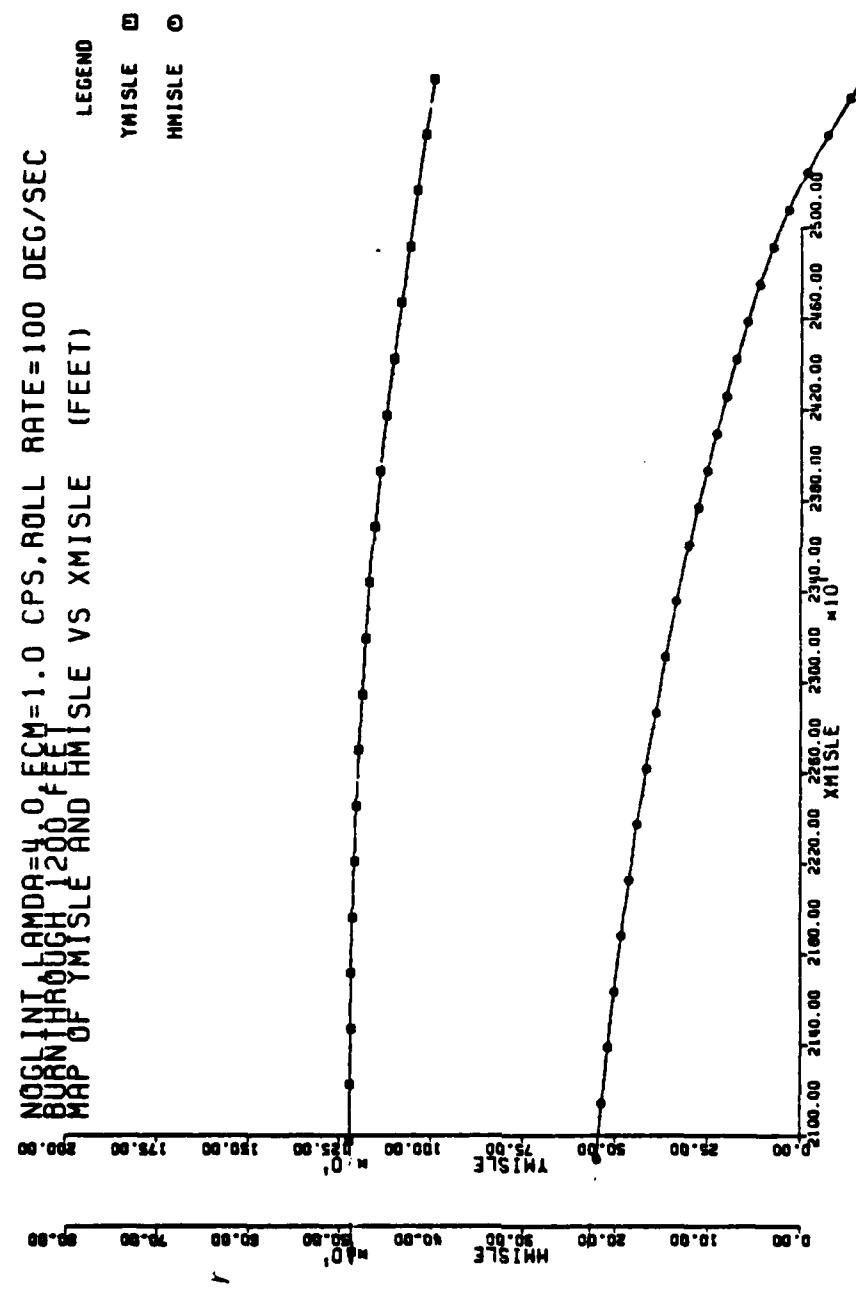
Figure 5-2f   Baseline Response for ECM 1 CPS, Roll Rate Limit 100 deg/sec

(YMISLE, HMISLE vs XMISLE)

104
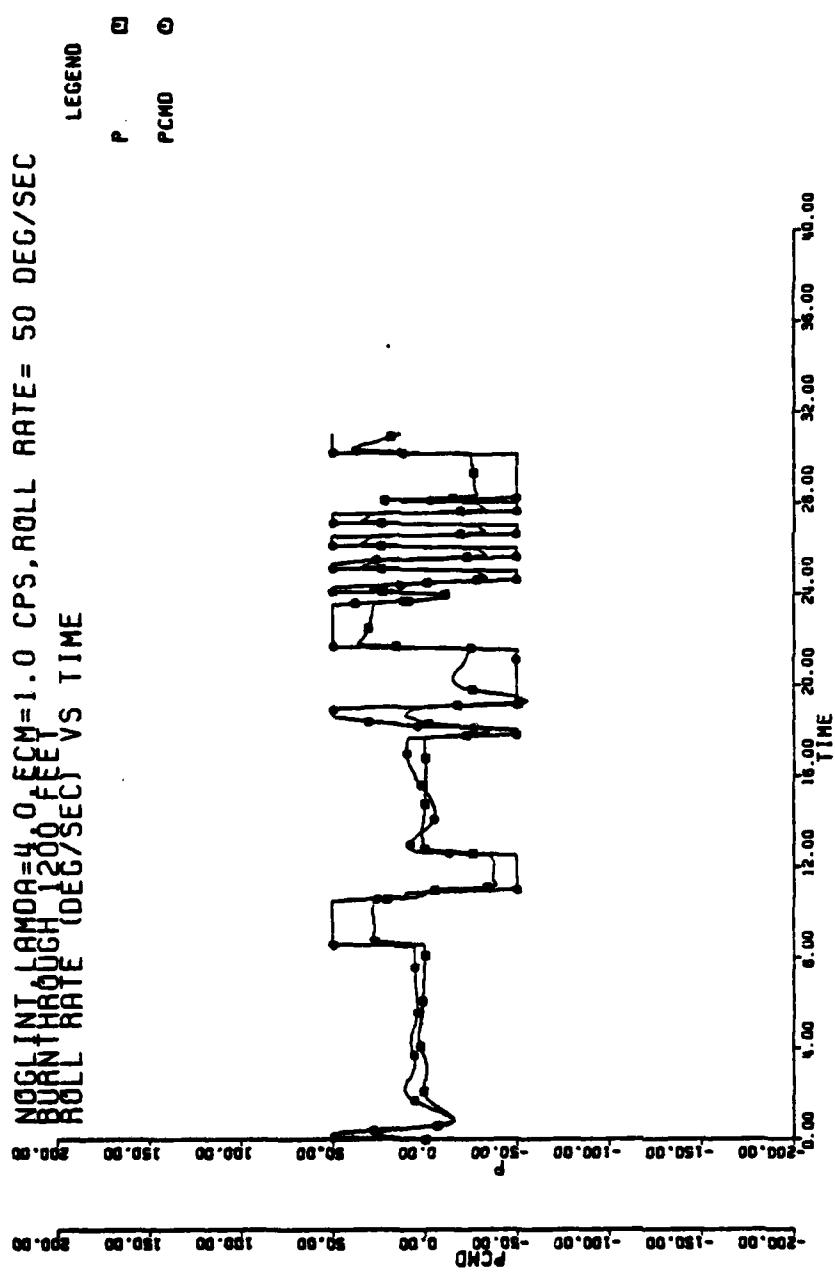
Figure 5-3a Baseline Response for ECM 1 CPS, Roll Rate Limit 50 deg/sec

(PCMD, P vs TIME)

105
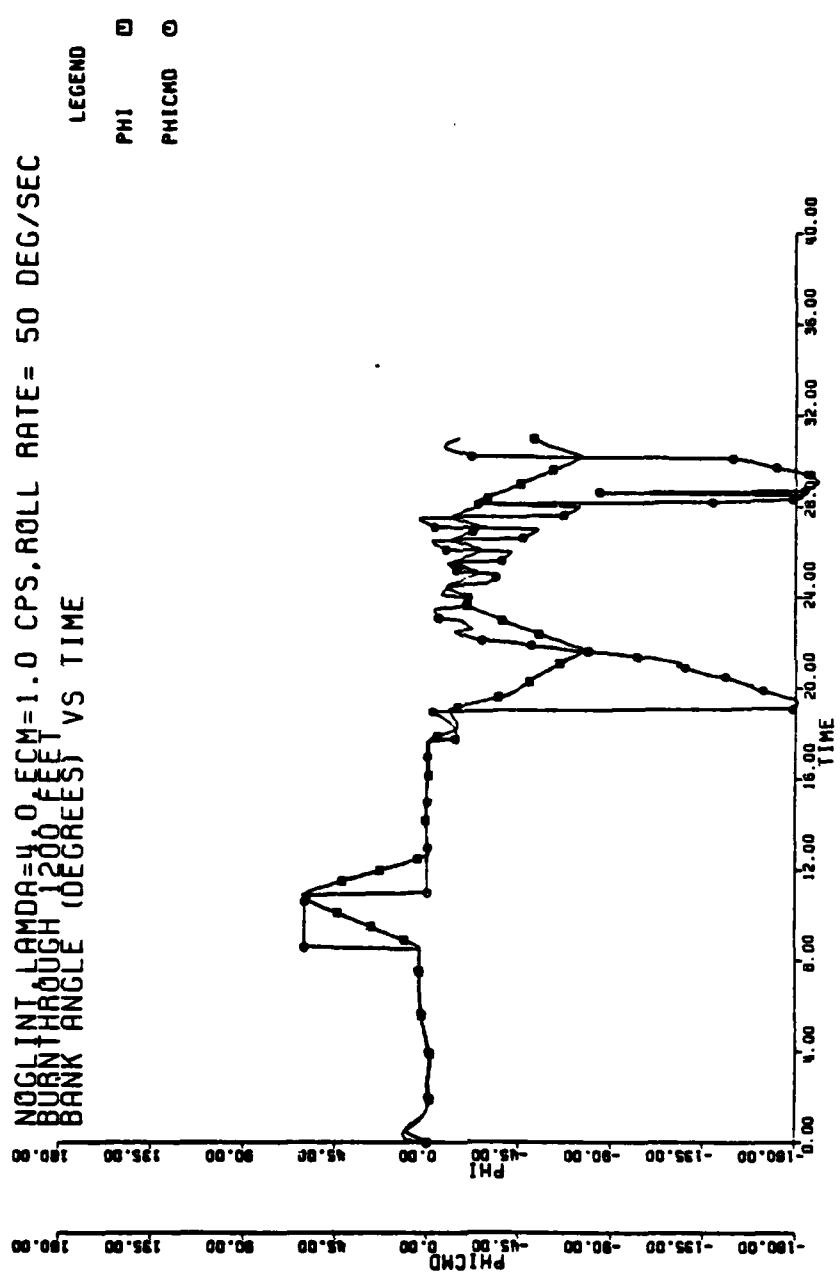
Figure 5-3b Baseline Response for ECM 1 CPS, Roll Rate Limit 50 deg/sec

(PHICMD, PHI vs TIME)
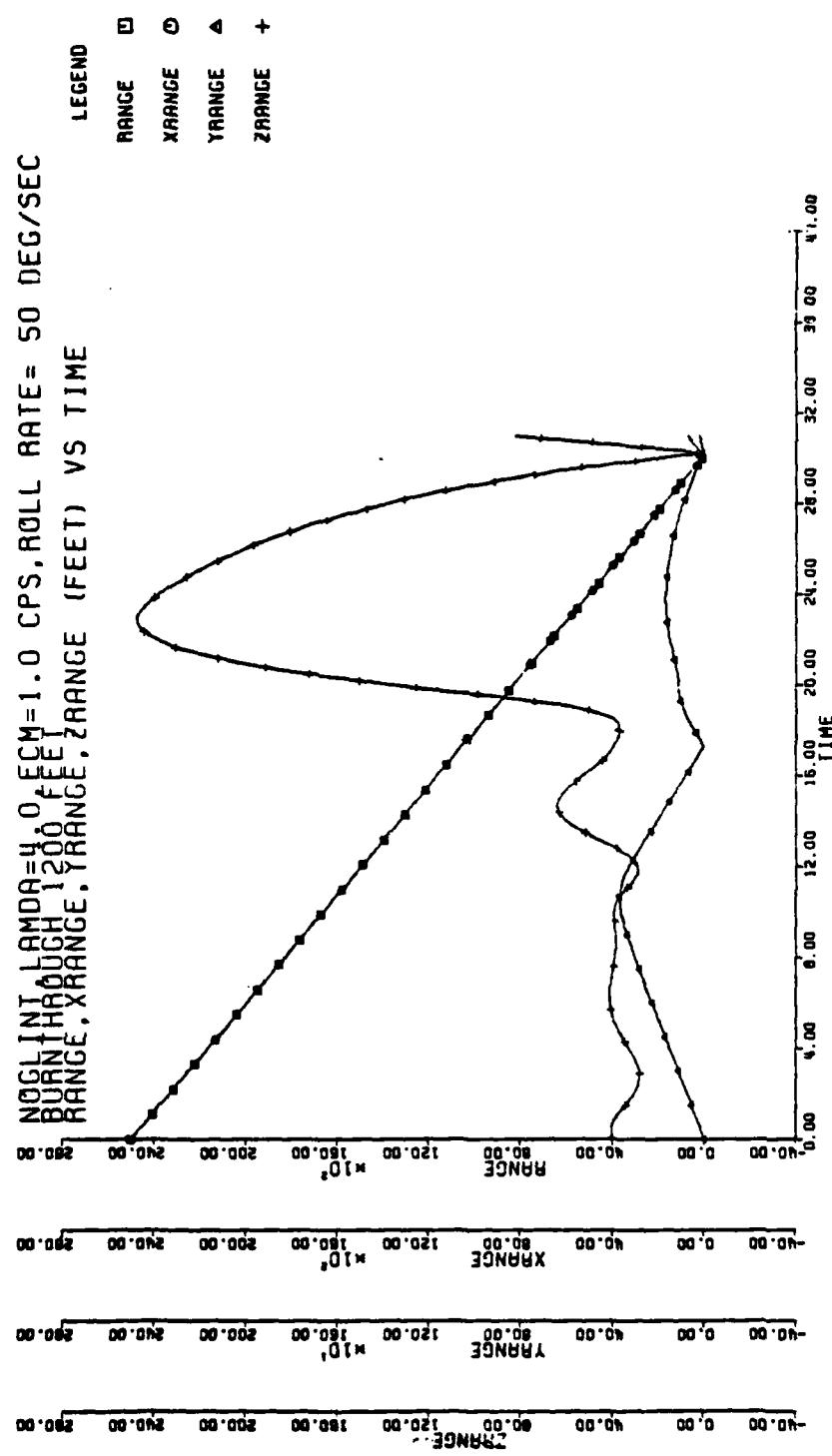
Figure 5-3c   Baseline Response for ECM 1 CPS, Roll Rate Limit 50 deg/sec

(RANGE, XRANGE, YRANGE, ZRANGE vs TIME)
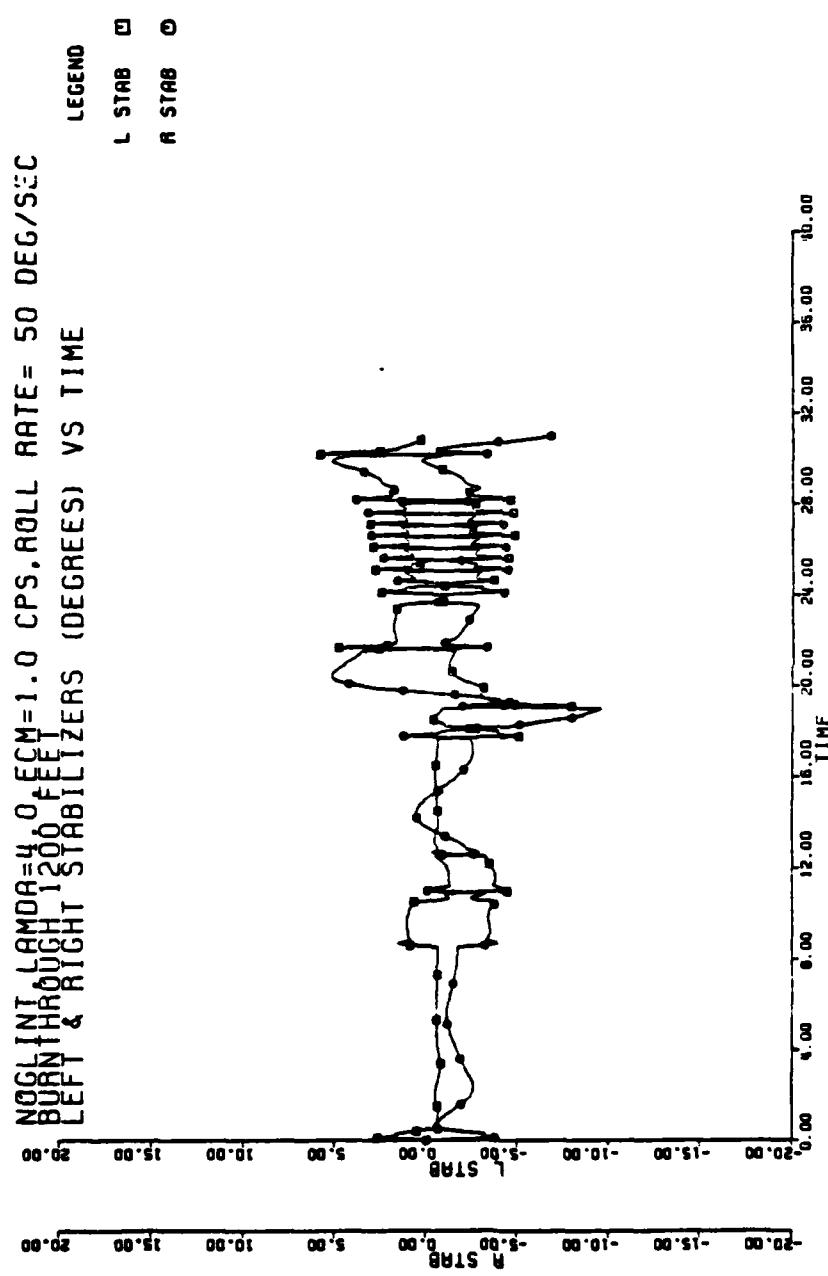
Figure 5-3d Baseline Response for ECM 1 CPS, Roll Rate Limit 50 deg/sec

(L STAB, R STAB vs TIME)

108

NOGLINT LAMDA=4.0 ECM=1.0 CPS, ROLL RATE= 50 DEG/SEC
BURNTHROUGH 1200 FEET
RUDDER POSITION (DEGREES) VS TIME

LEGEND
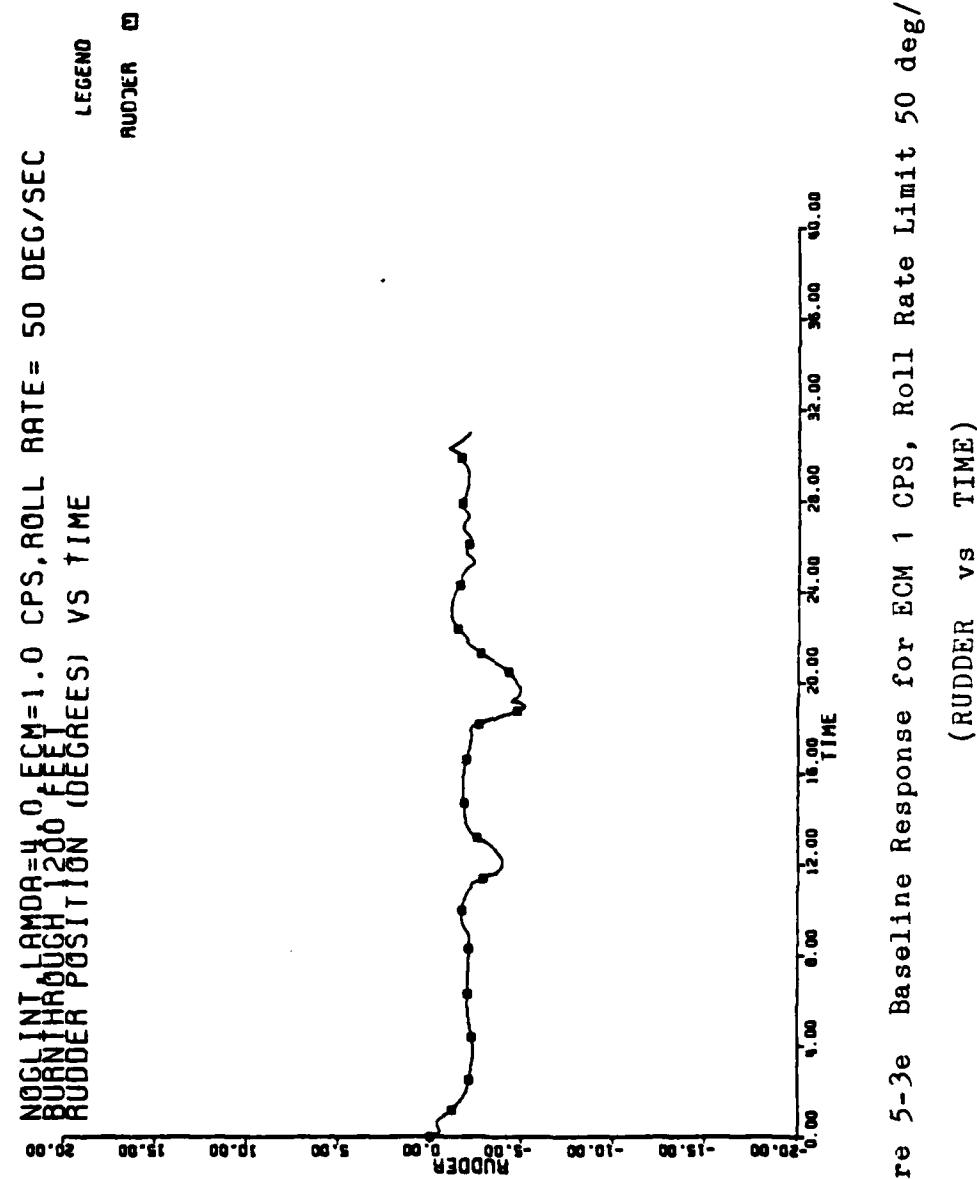
RUDDER □

Figure 5-3e   Baseline Response for ECM 1 CPS, Roll Rate Limit 50 deg/sec

(RUDDER   vs   TIME)

109
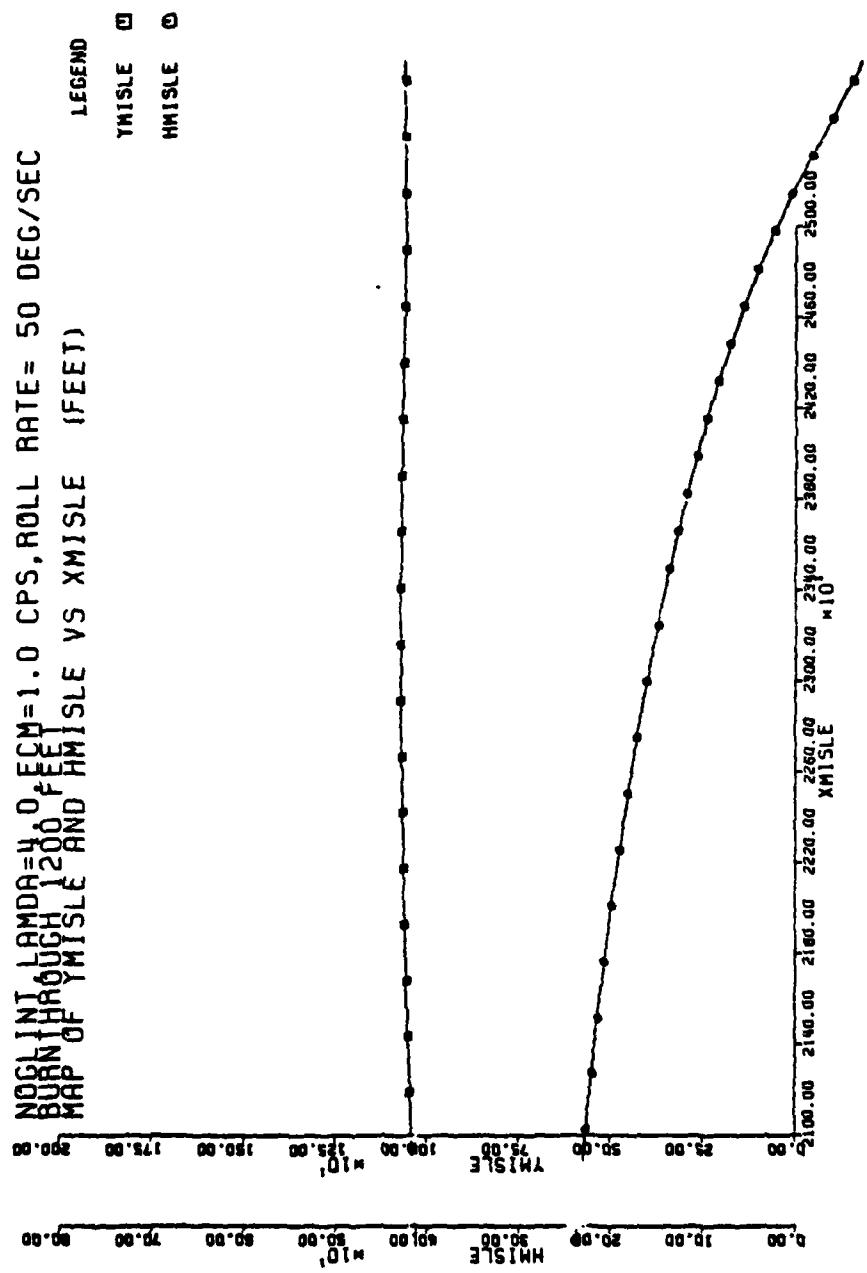
Figure 5-3f Baseline Response for ECM 1 CPS, Roll Rate Limit 50 deg/sec

(YMISLE, HMISLE vs XMISLE)
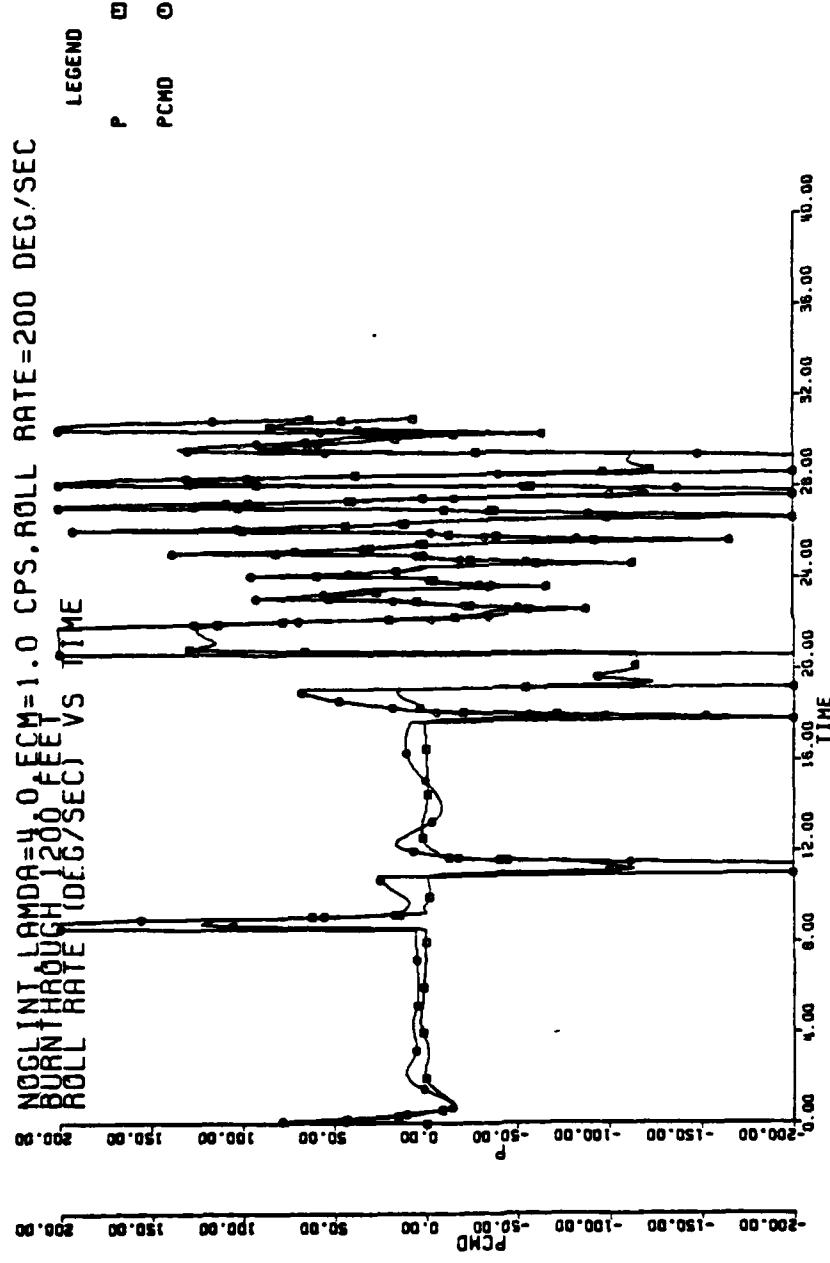
Figure 5-4a   Baseline Response for ECM 1 CPS, Roll Rate Limit 200 deg/sec

PCMD,P vs TIME)

111
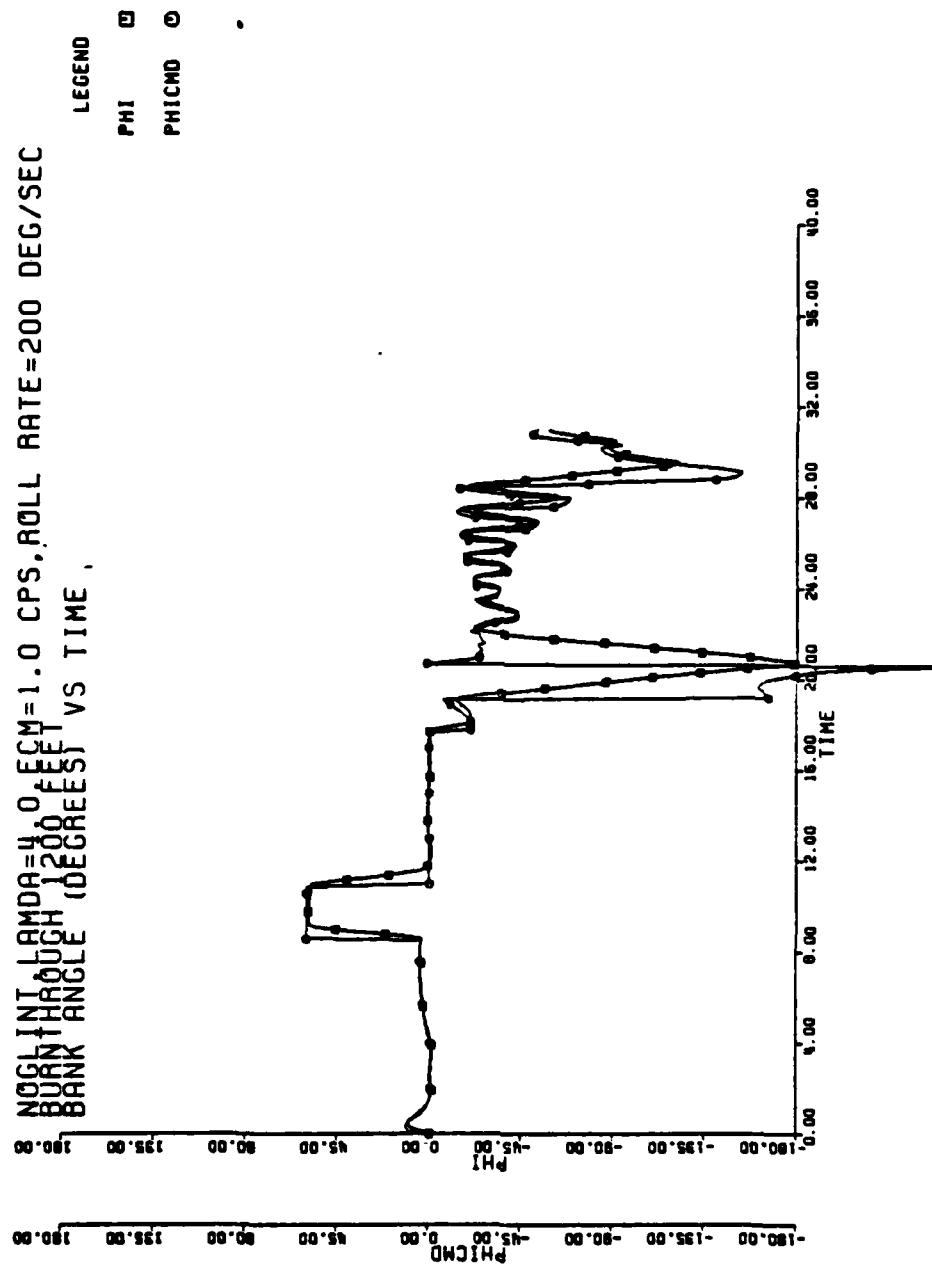
Figure 5-4b Baseline Response for ECM 1 CPS, Roll Rate Limit 200 deg/sec
(PHICMD, PHI vs TIME)

NOGLINT LAMDA=40.0 ECM=1.0 CPS,ROLL RATE=200 DEG/SEC
BURNTHROUGH 1200 FEET
RANGE,XRANGE,YRANGE,ZRANGE (FEET) VS TIME
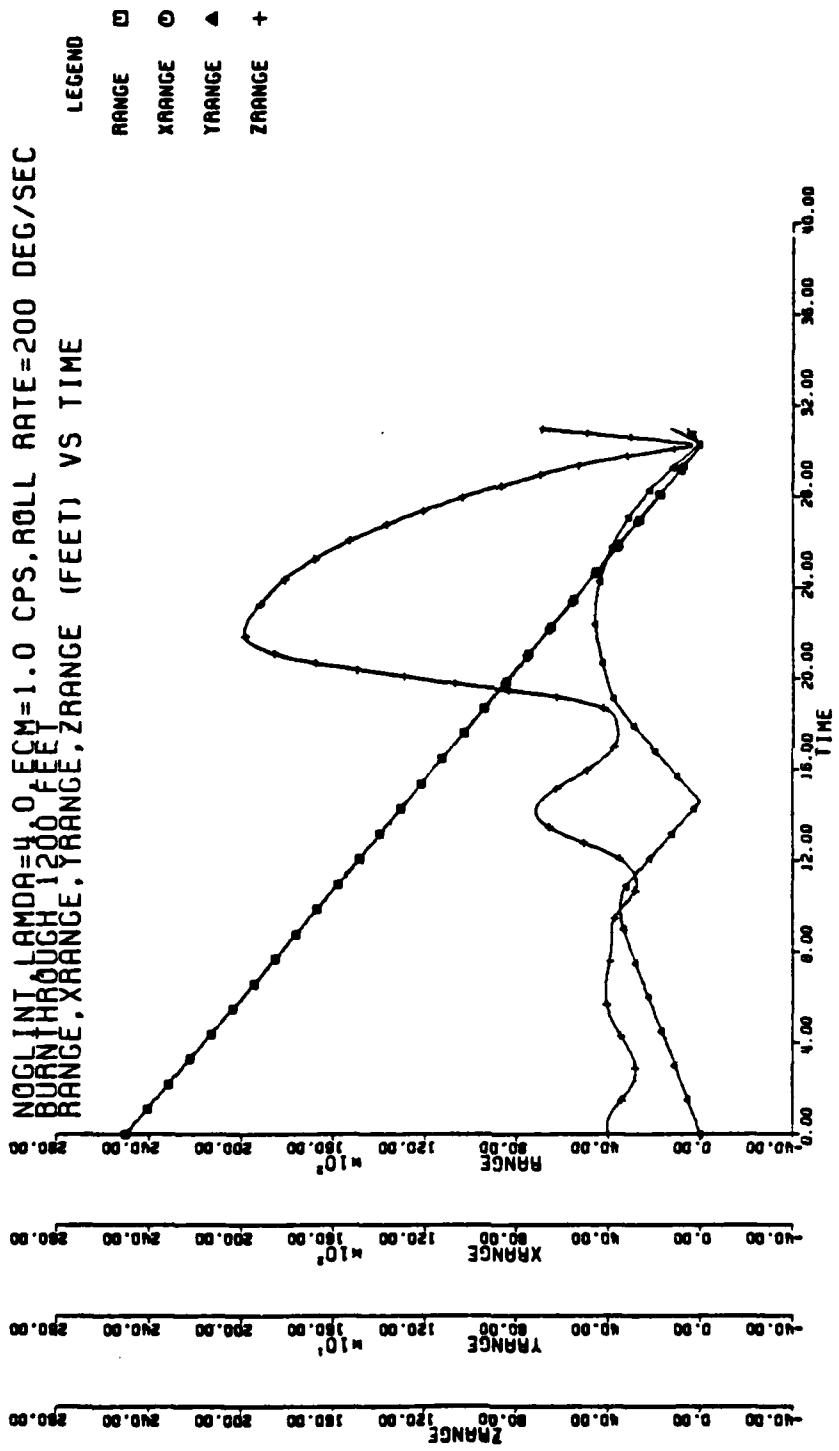
Figure 5-4c Baseline Response for ECM 1 CPS, Roll Rate Limit 200 deg/sec

(RANGE, XRANGE, YRANGE, ZRANGE vs TIME)
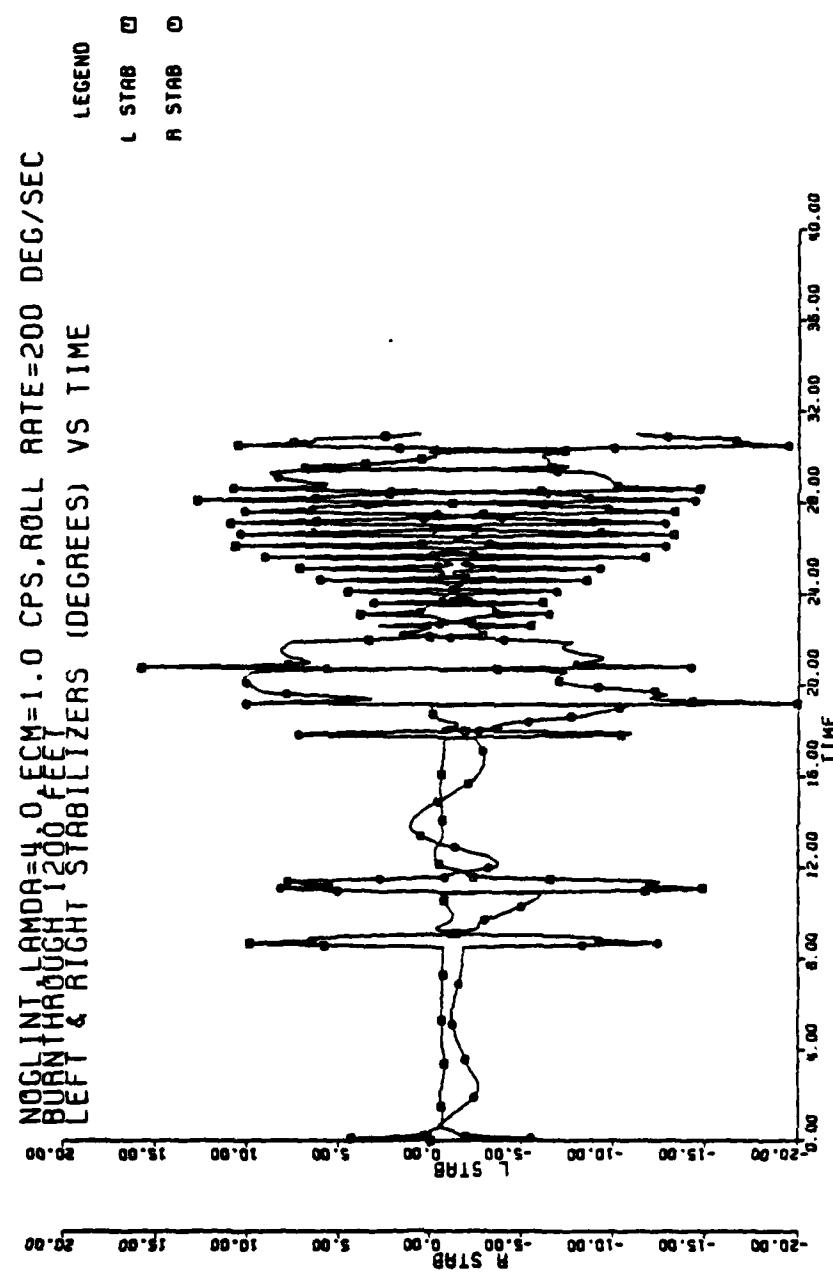
Figure 5-4d Baseline Response for ECM 1 CPS, Roll Rate Limit 200 deg/sec

(L STAB, R STAB vs TIME)

114
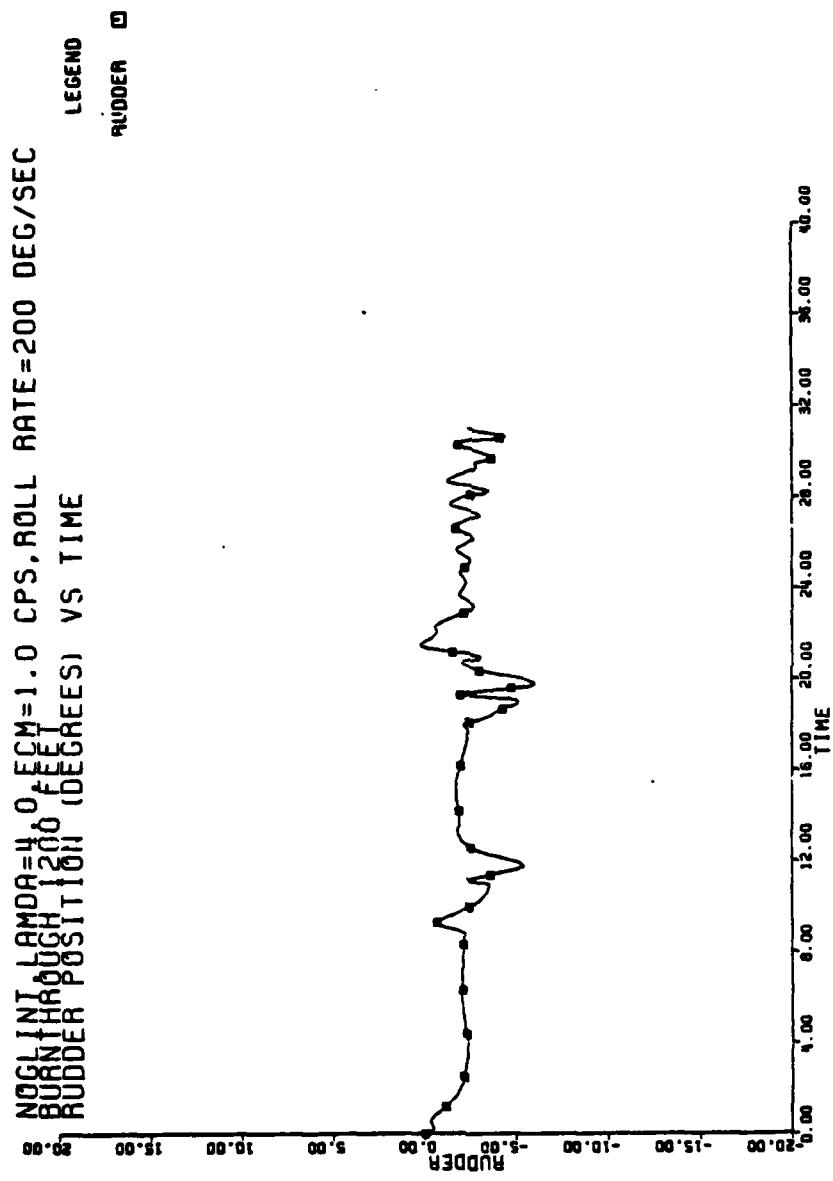
Figure 5-4e Baseline Response for ECM 1 CPS, Roll Rate Limit 200 deg/sec

(RUDDER vs TIME)

115
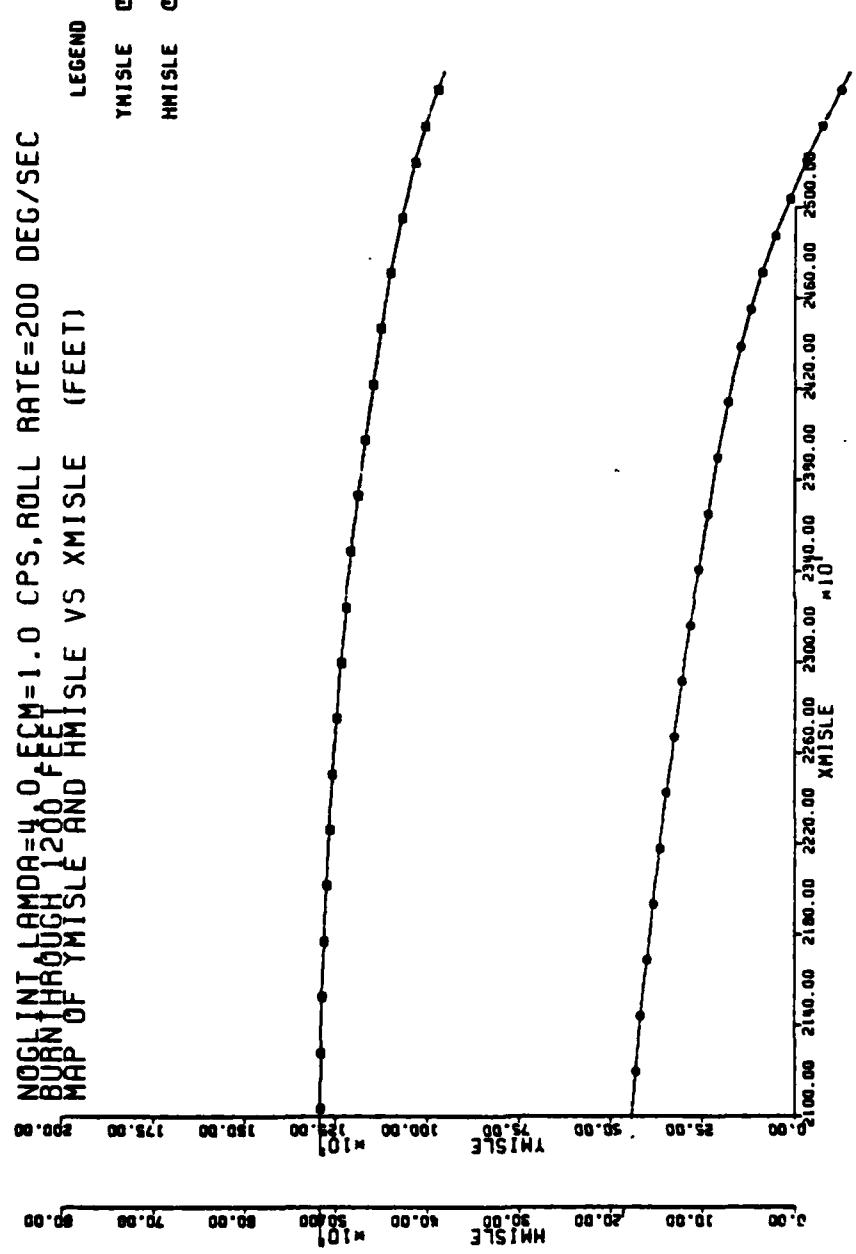
Figure 5-4f Baseline Response for ECM 1 CPS, Roll Rate Limit 200 deg/sec

(YMISLE, HMISLE vs XMISLE)
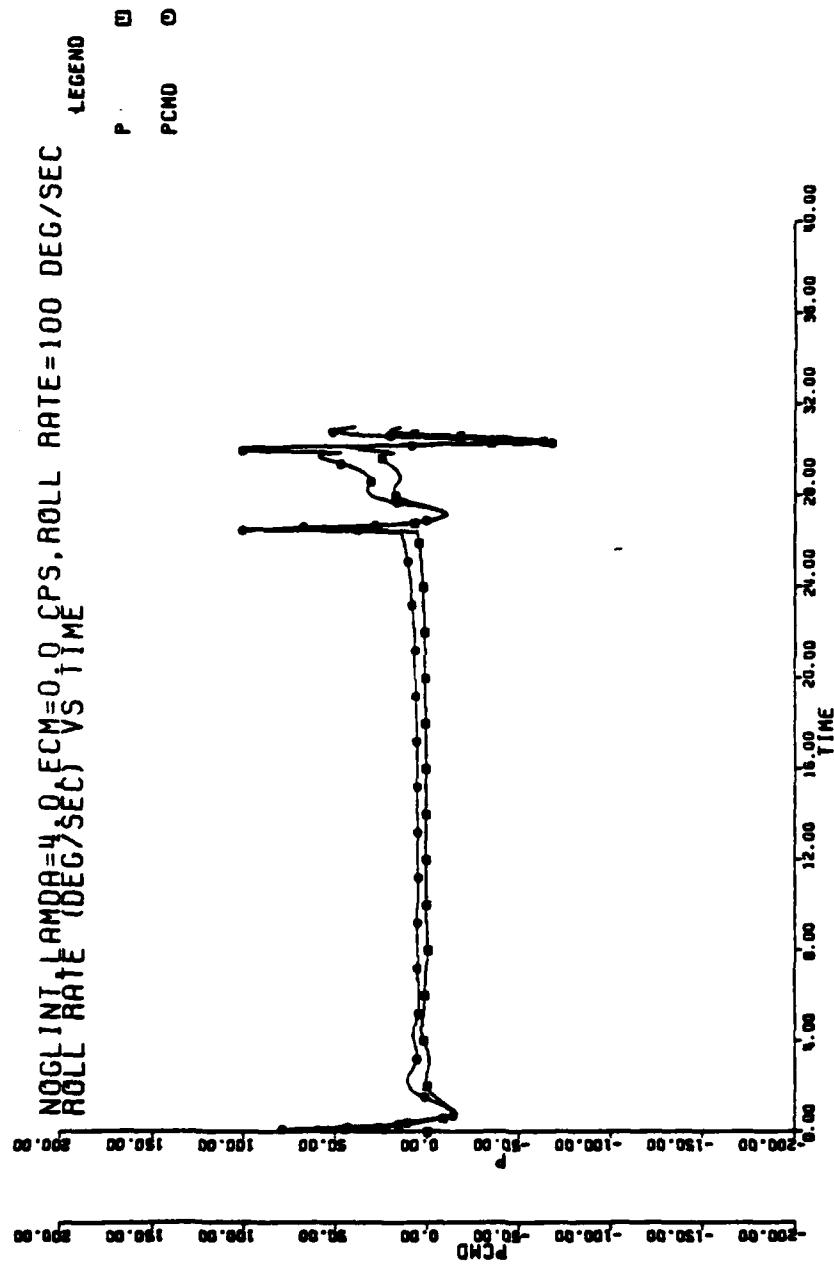
Figure 5-5a   Sea Skimmer Response for No ECM, Roll Rate Limit 100 deg/sec
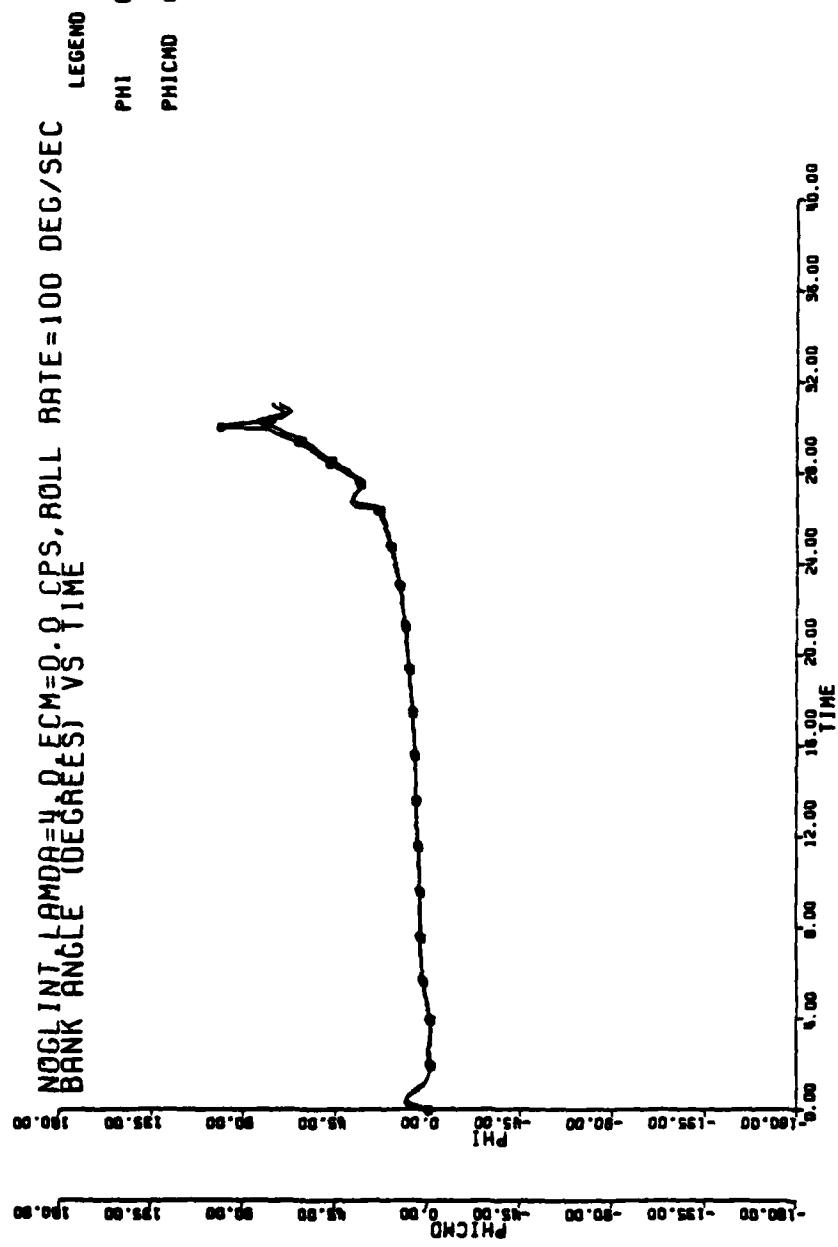
(PCMD, P vs TIME)

117

Figure 5-5b Sea Skimmer Response for No ECM, Roll Rate Limit 100 deg/sec

(PHICMD, PHI vs TIME)
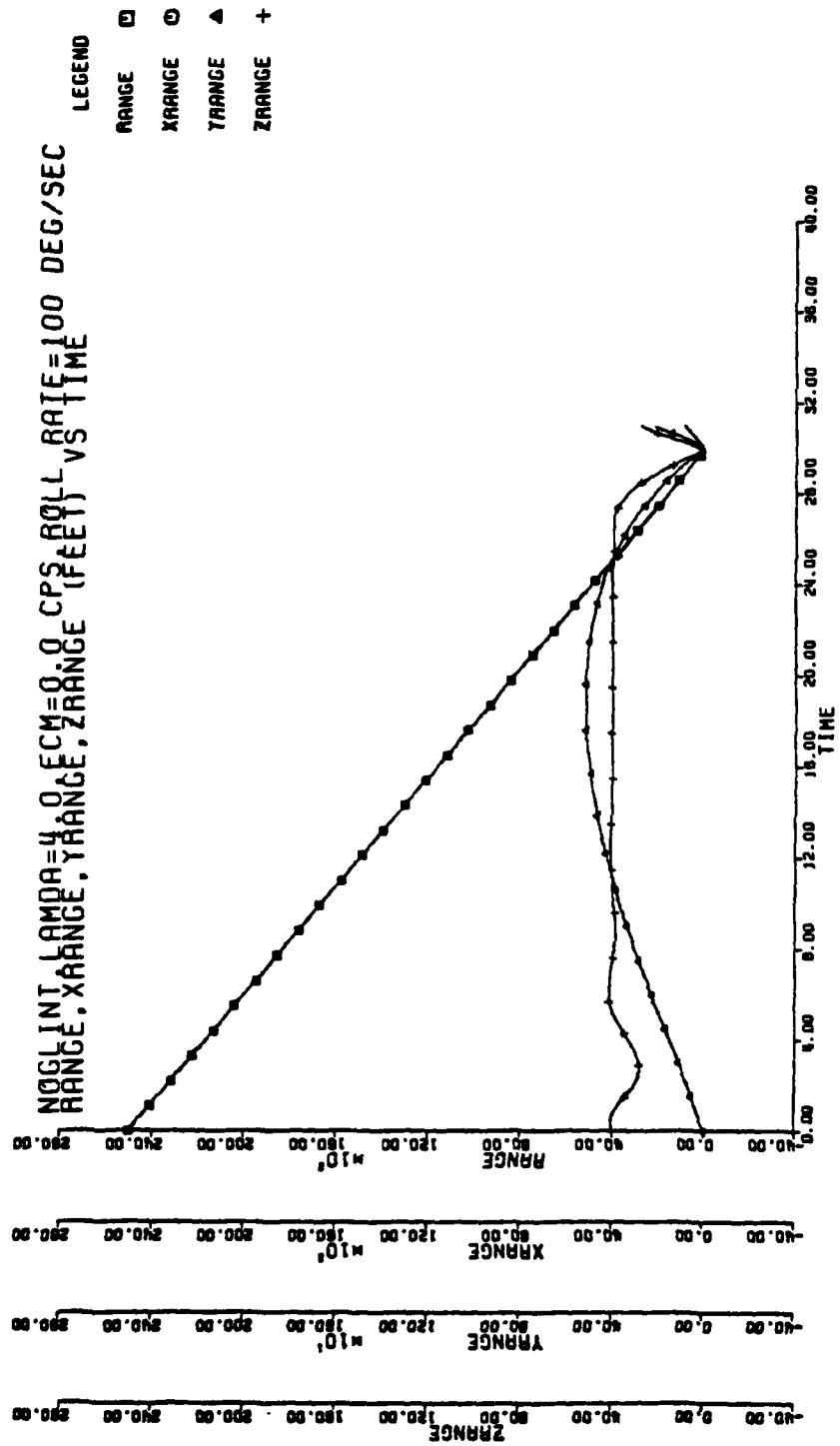
Figure 5-5c Sea Skimmer Response for No ECM, Roll Rate Limit 100 deg/sec

(RANGE, XRANGE, YRANGE, ZRANGE vs TIME)

119
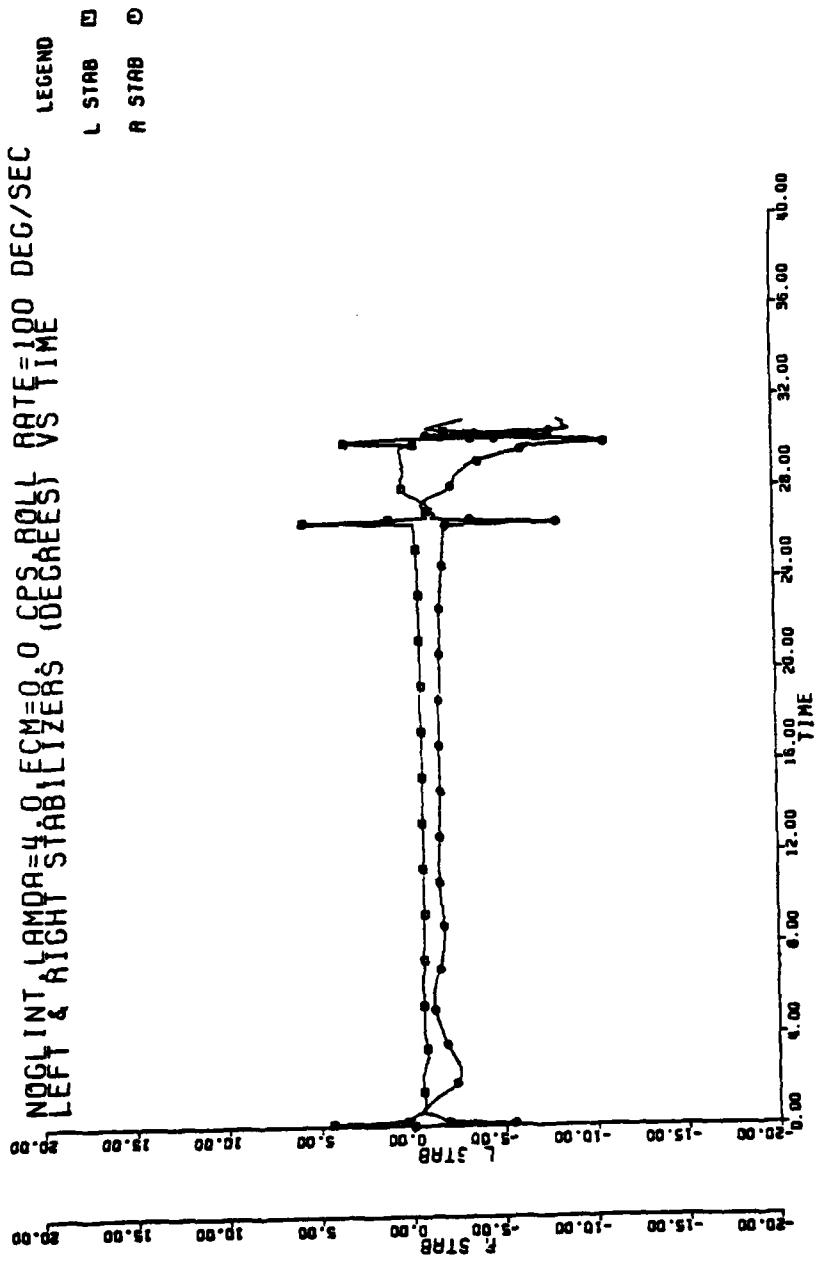
Figure 5-5d Sea Skimmer Response for No ECM, Roll Rate Limit 100 deg/sec

(L STAB, R STAB vs TIME)
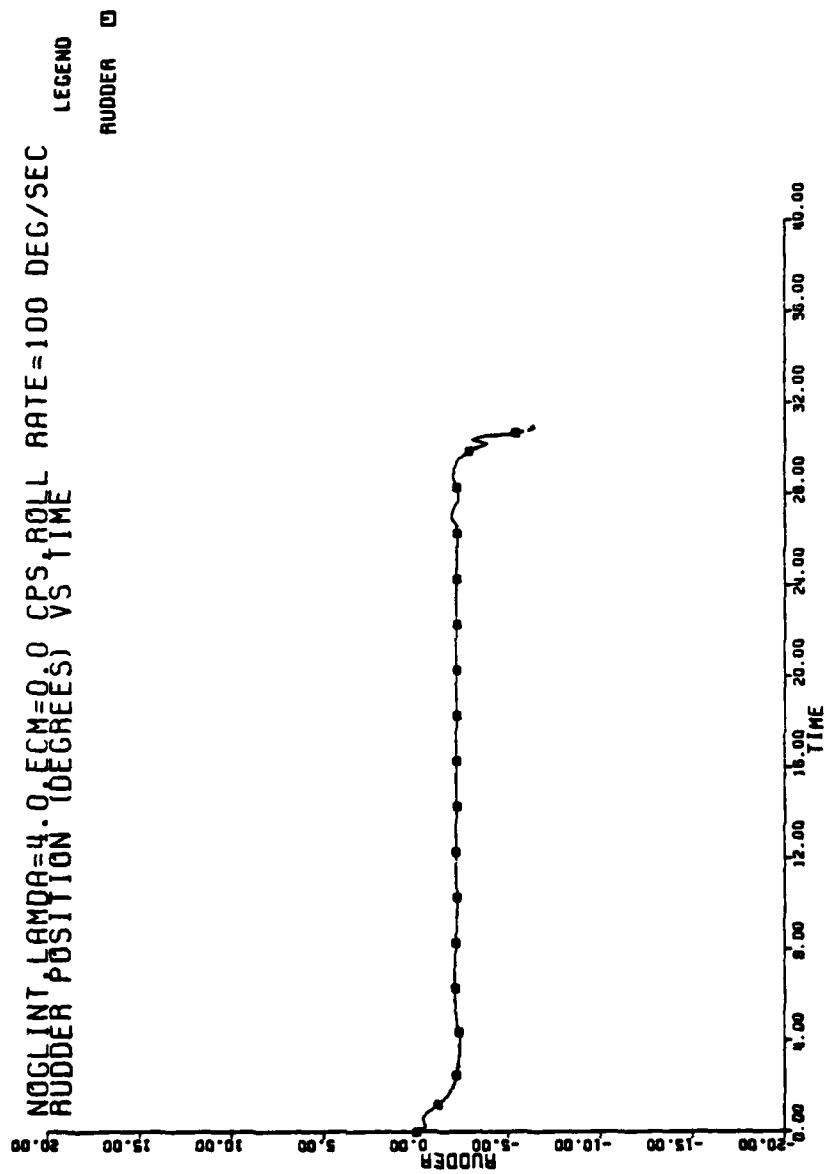
Figure 5-5e Sea Skimmer Response for No ECM, Roll Rate Limit 100 deg/sec

RUDDER vs TIME)

121
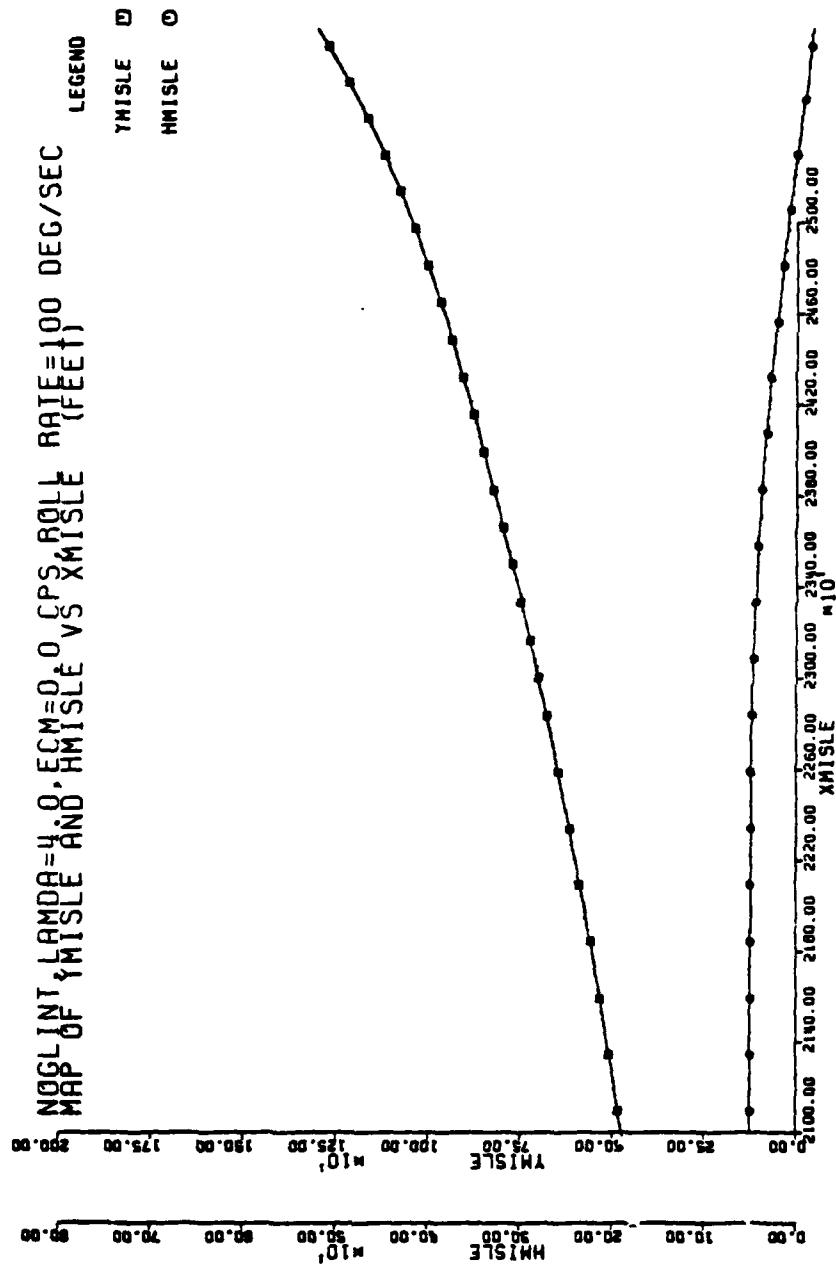
Figure 5-5f Sea Skimmer Response for No ECM, Roll Rate Limit 100 deg/sec
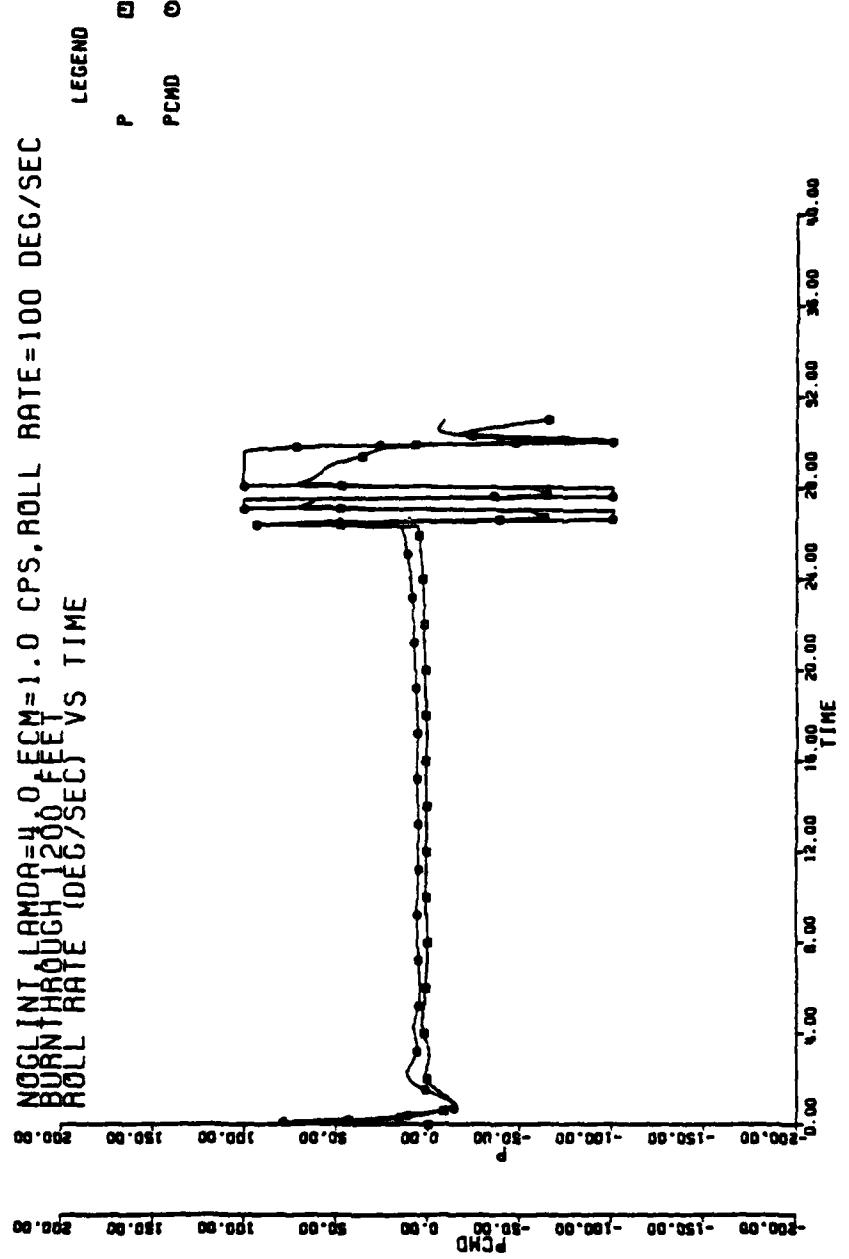
YMISLE, HMISLE vs XMISLE)

Figure 5-6a   Sea Skimmer Response for ECM 1 CPS, Roll Rate Limit 100 deg/sec

(PCMD, P vs TIME)

123
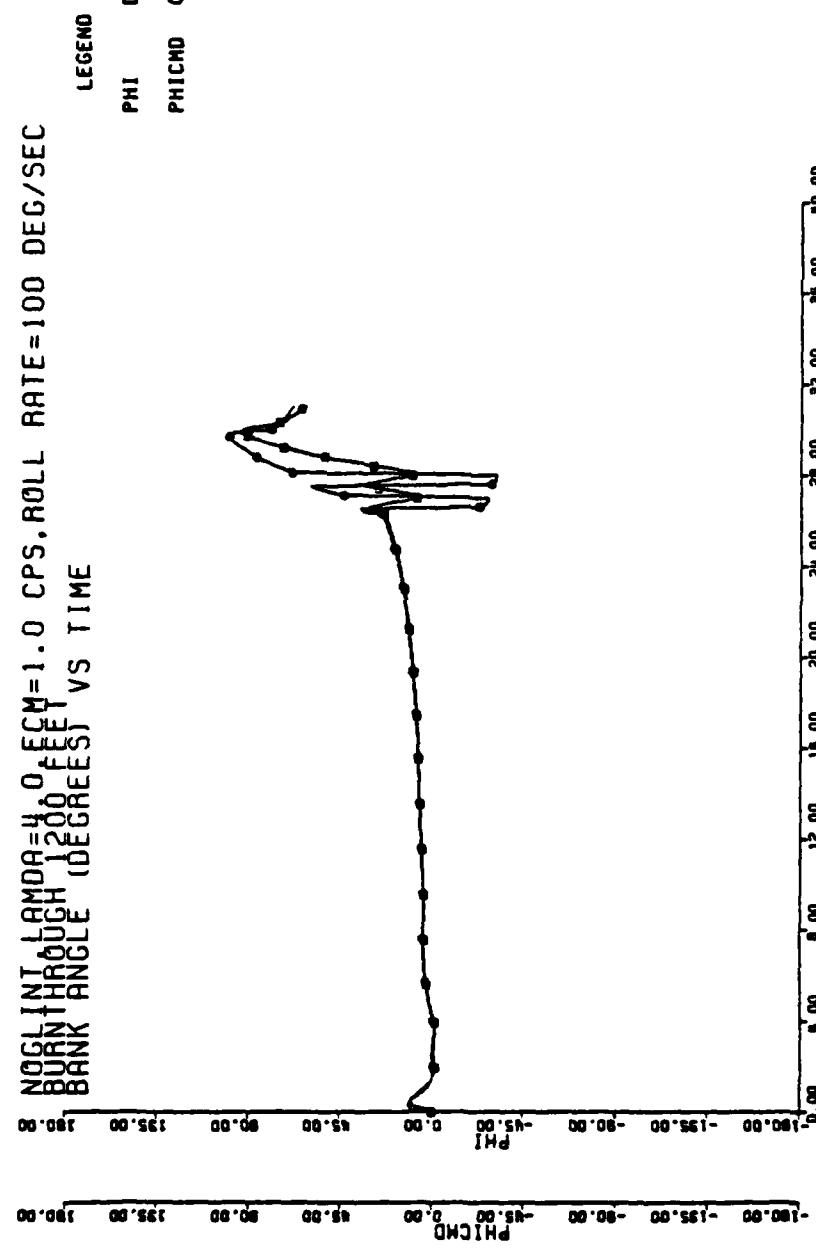
Figure 5-6b Sea Skimmer Response for ECM 1 CPS, Roll Rate Limit 100 deg/sec

(PHICMD, PHI vs TIME)

124
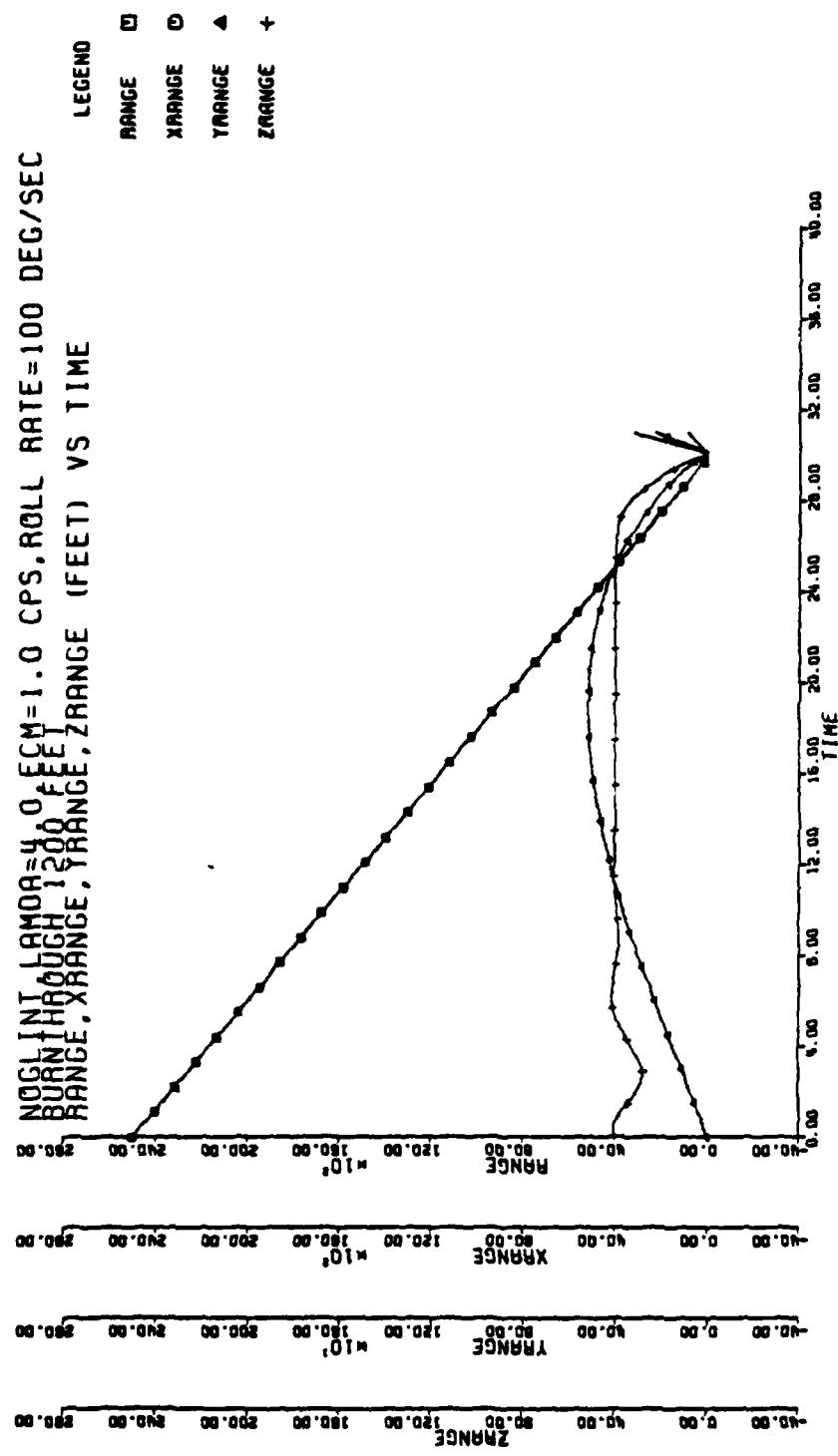
Figure 5-6c Sea Skimmer Response for ECM 1 CPS, Roll Rate Limit 100 deg/sec

(RANGE, XRANGE, YRANGE, ZRANGE vs TIME)

125
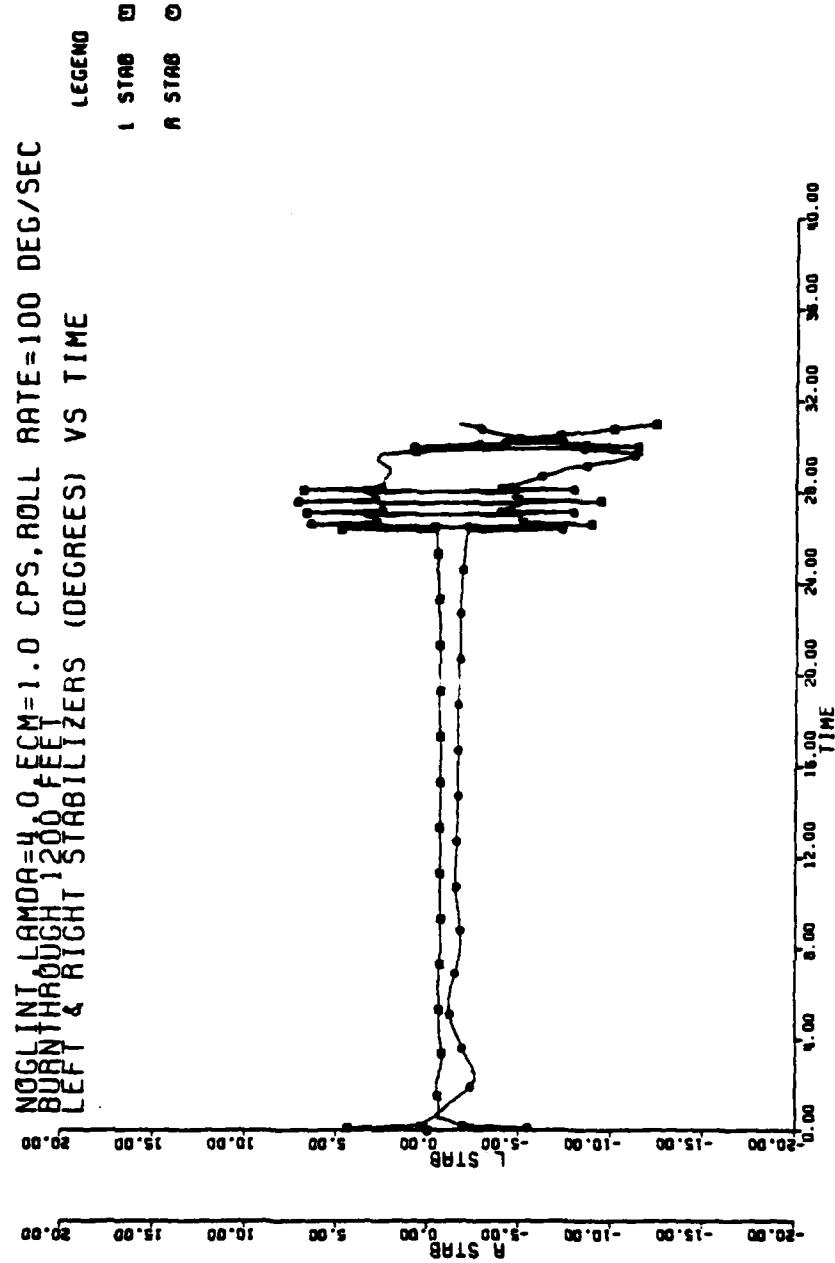
Figure 5-6d Sea Skimmer Response for ECM 1 CPS, Roll rate Limit 100 deg/sec

(L STAB, R STAB vs TIME)

126
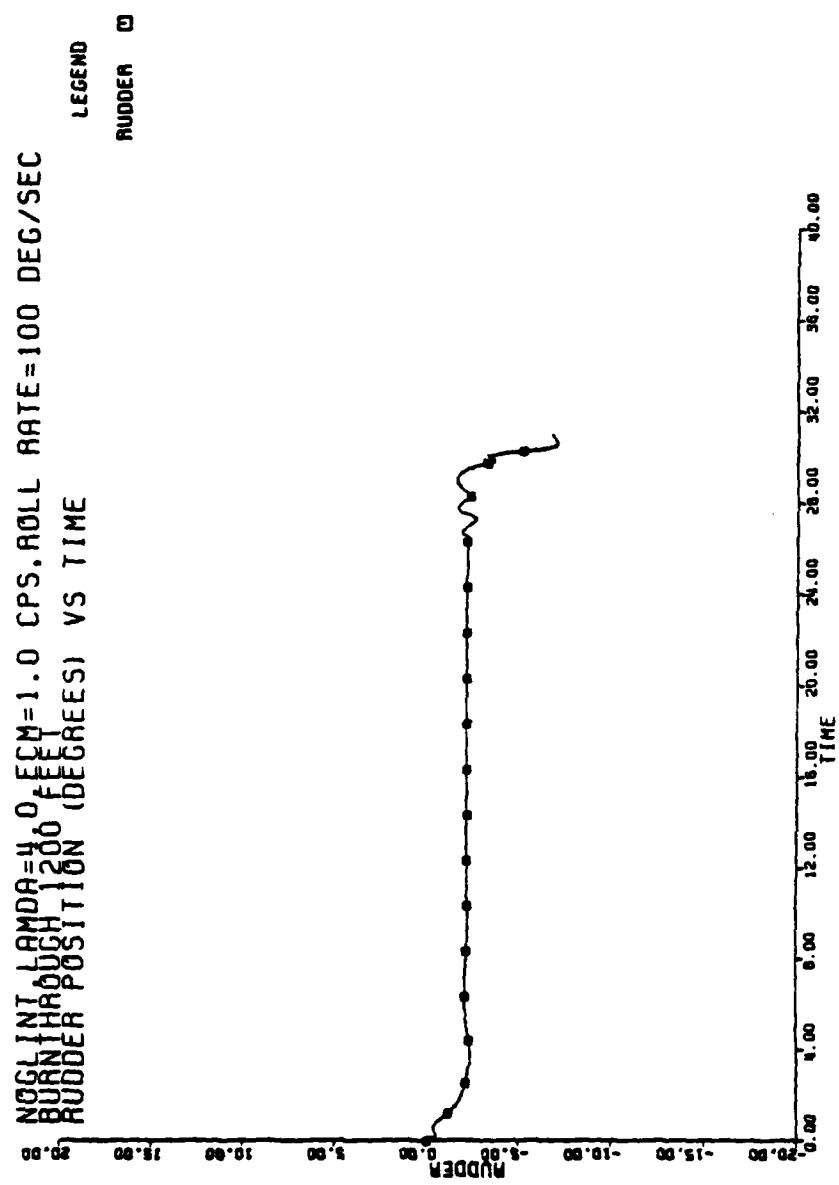
Figure 5-6e   Sea Skimmer Response for ECM 1 CPS, Roll Rate Limit 100 deg/sec

(RUDDER vs TIME)
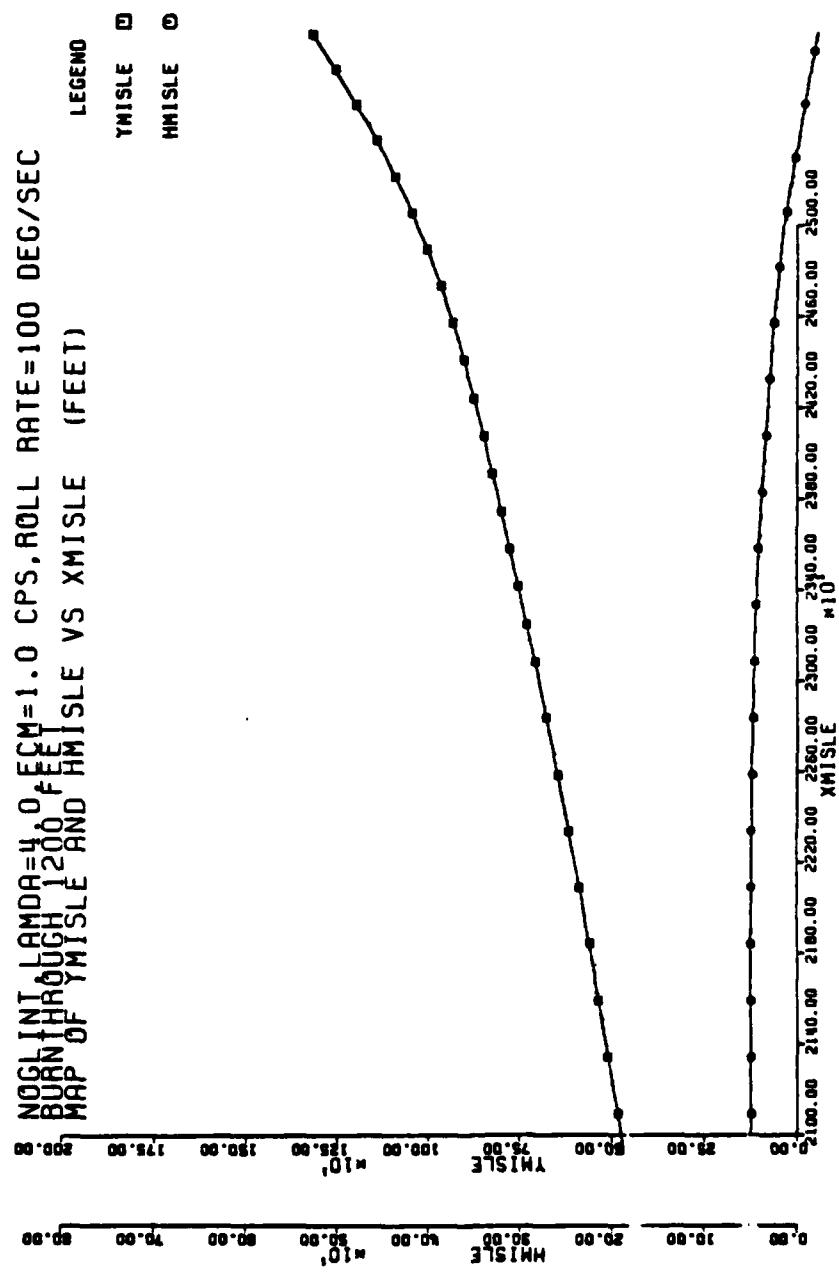
Figure 5-6f Sea Skimmer Response for ECM 1 CPS, Roll Rate Limit 100 deg/sec
(YMISLE, HMISLE vs XMISLE)

128

miss distance remains high for all burn through ranges out to 2000 feet. But, for the remaining blinking frequencies and burn through ranges the miss distances improve significantly for increasing roll rate limits. A miss distance of 7.9 feet for a burn through range of 800 feet and 2 Hertz blinking frequency is excellent.

2. Analysis of Sea Skimmer Scheme Results

The results for the sea skimmer scheme are quite different than the baseline scheme.

Burn through range seems to be the single most controlling variable. Miss distances for a burn through range of 1500 feet are marginally satisfactory for all roll rate limits and ECM blinking rates. However, at a burn through range of 2000 feet, miss distances for varying roll rate limits and ECM blinking frequencies are extremely low and considered quite good.

Varying the ECM blinking rate produces little effect on the miss distances. However, a unique roll rate limit of 100 degrees per second produces miss distances double the miss distances for roll rate limits of 50 or 200 degrees per second.

3. Analysis of Glint Simulation Results

Figure 5-7 shows the random introduction of glint in the target position and line of sight rate. The miss distance for the run in this figure is 15 feet, but analysis from other runs show that glint increases the miss distance 30 to 50 percent.
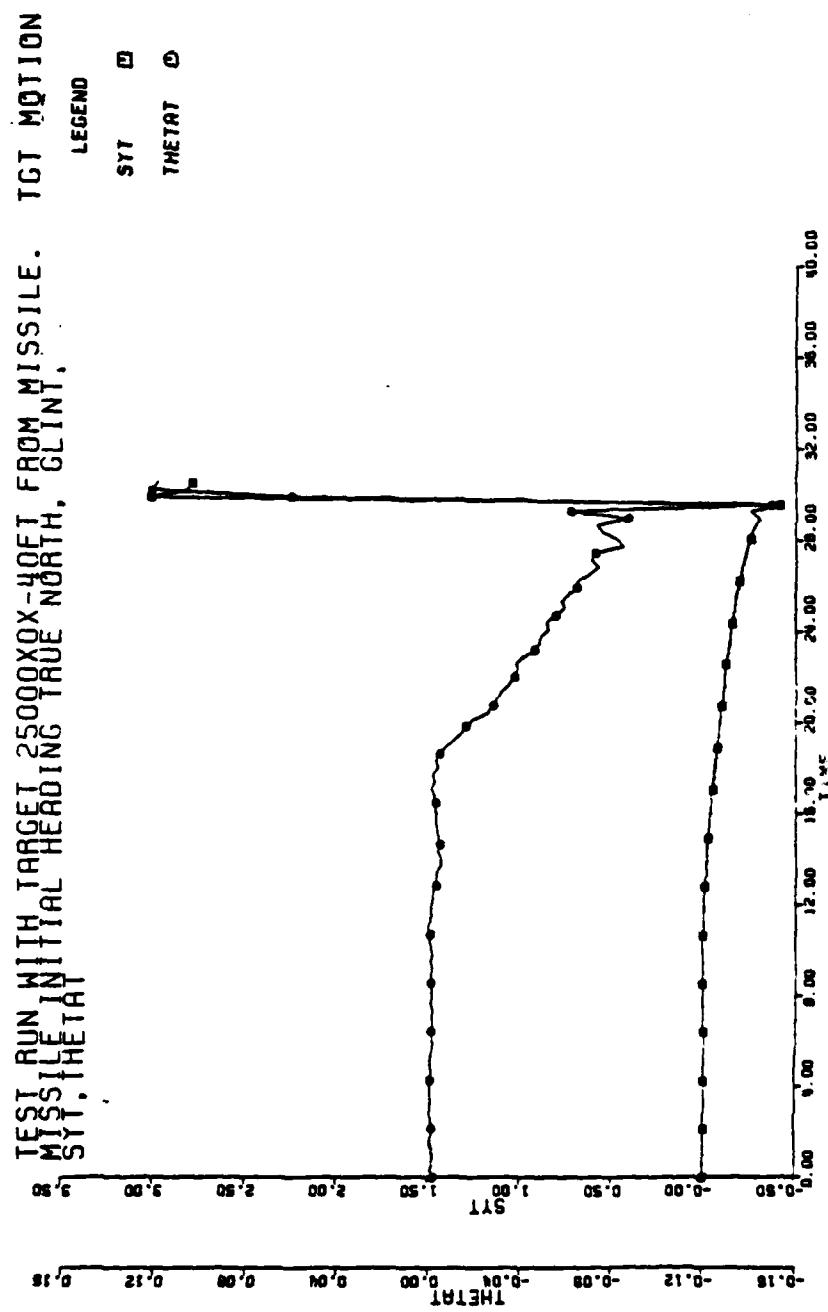
Figure 5-7a Baseline Response with Glint
(SYT, THEATAT vs TIME)

130
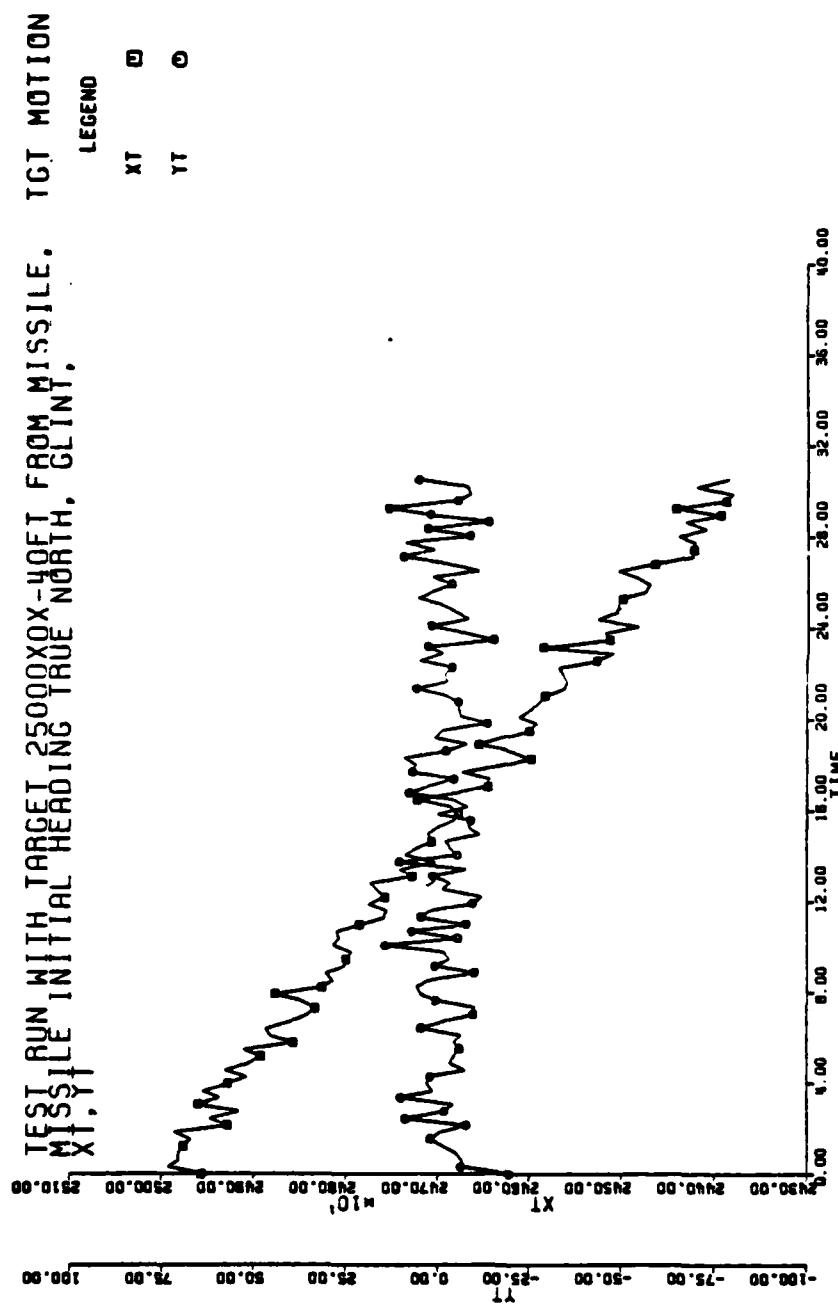
Figure 5-7b Baseline Response with Glint
(XT, YT vs Time)

4. <u>Proportional Navigation Ratio Selection</u>

The following matrix shows the result of miss distance in a no ECM environment for varying proportional navigation constant (PN).

PN	Miss Distance (feet)
3	10.6
3.5	6.9
4	4.4
4.5	3.2

Although a proportional navigation constant (PN) of 4.5 results in the smallest miss distance excessive over shoot to step inputs results in this proportional navigation constant as being an unsatisfactory choice. A PN of 4.0 was chosen based upon satisfactory system responses and the small miss distance achieved.

C. CONCLUSIONS AND RECOMMENDATIONS

Based upon the results of this study it can be concluded that miss distance is a function of roll rate limit, ECM blinking rate, burn through range, and the guidance scheme chosen. The guidance scheme chosen is most significant of these factors.

For the baseline guidance and control scheme, roll rate limit is the most significant variable affecting miss distance. One exception to this is the 0.5 Hertz blinking

rate set of runs which shows a miss distance improvement when roll rate is increased from 50 to 100 degrees per second, but yields poor miss distances for 200 degrees per second.

The most significant variable affecting miss distance for the sea-skimmer scheme is burn through range. Nevertheless, a 100-degree-per-second roll rate limit appears to be unacceptable at all burn through ranges simulated.

In summary, given that the target controls ECM blinking frequency and burn through range, the optimum selections are:

Baseline Scheme - Roll rate limit = 200 degrees per second

Sea-Skimmer - Roll rate limit = 50 or 200 degrees per second

The following additional studies are recommended:
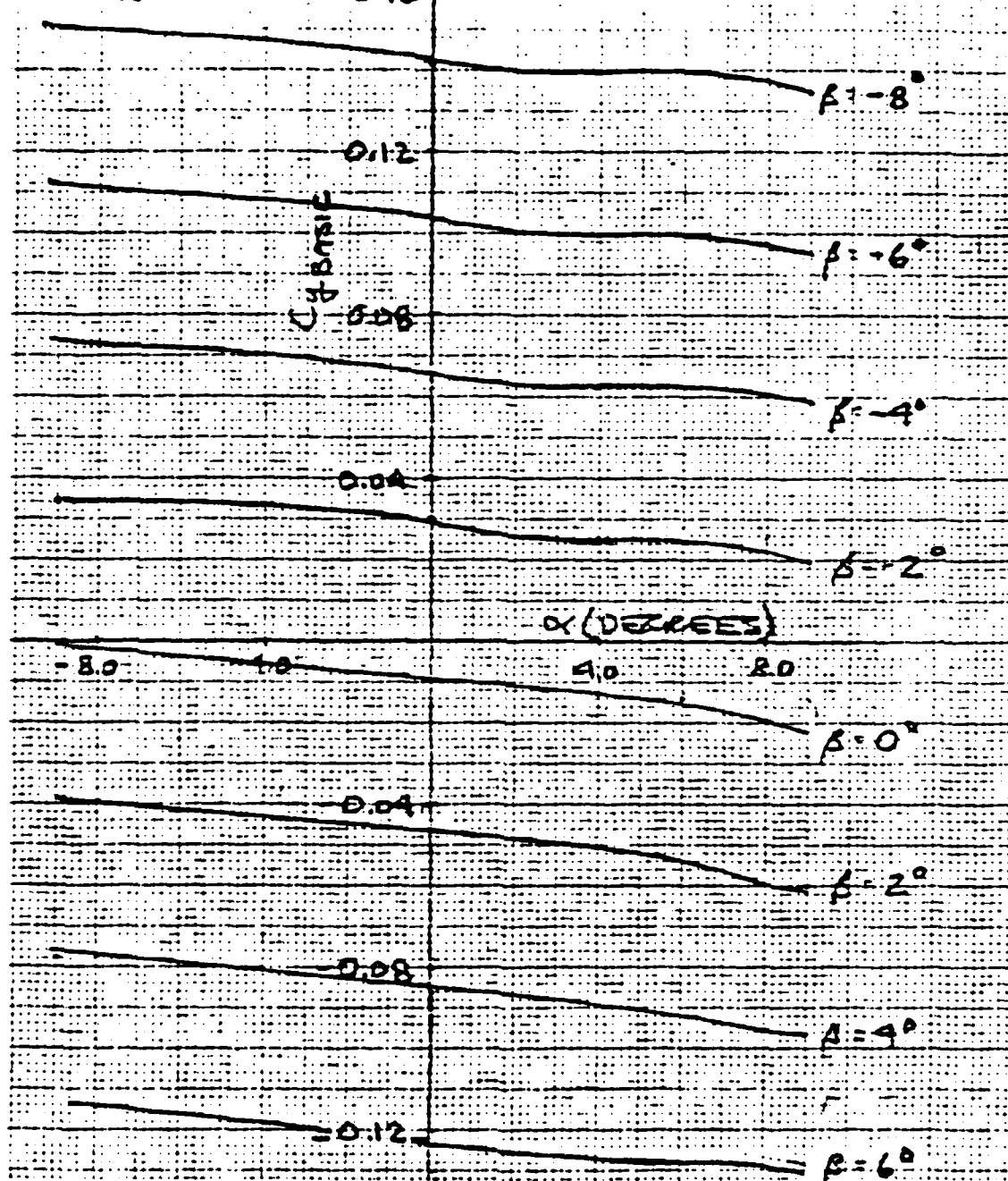
a. Further modeling with glint.

b. Variation of the direction and magnitude of the ECM shift.

c. Alteration of the decision variable used in the simulation to switch phases from range to line of sight rate.

d. Variations in flight path geometry.

e. Comparison of control laws using skid-to-turn with control laws using bank-to-turn maneuvering.
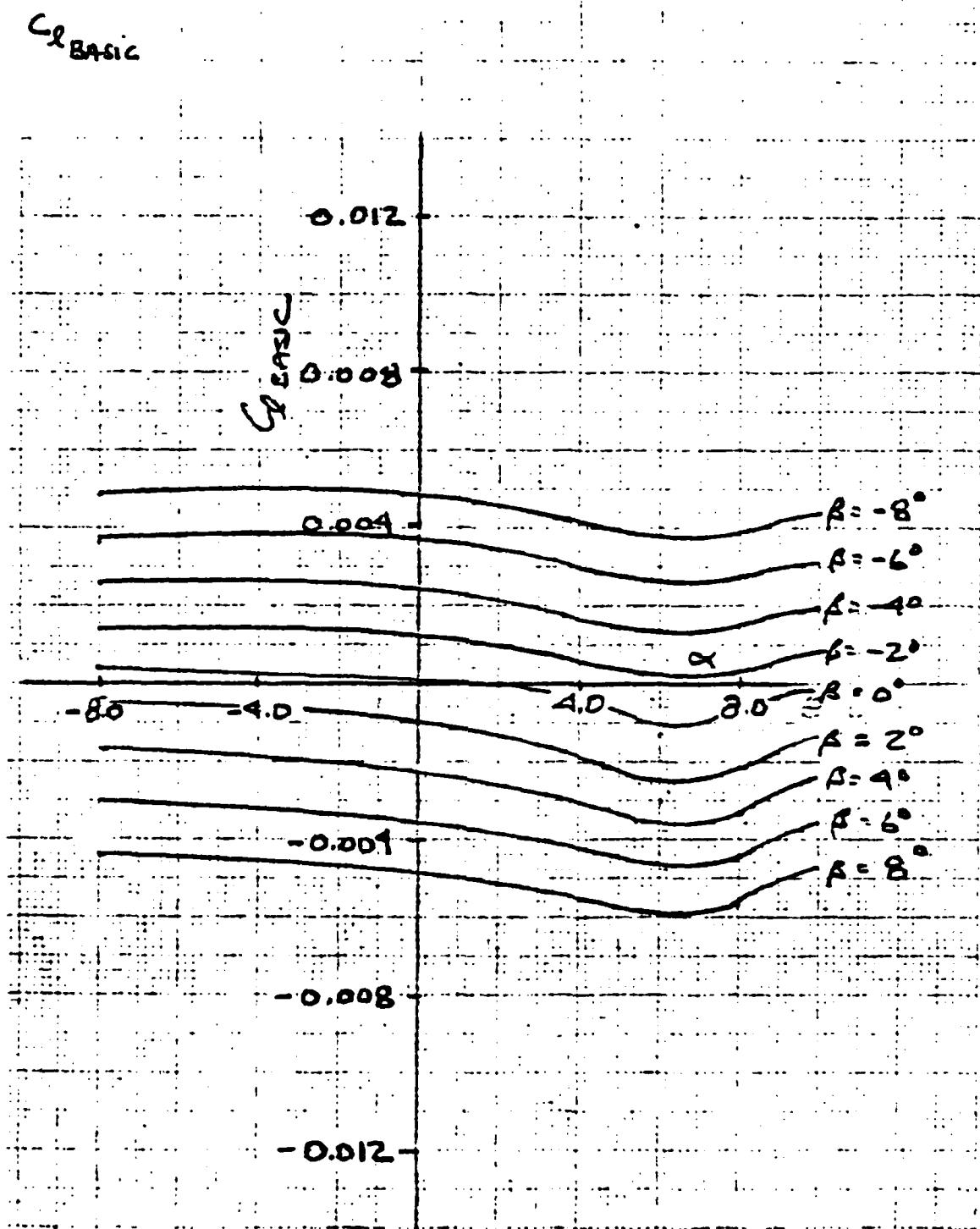
Side Slip Characteristics

α vs β vs $C_{y_{basic}}$

134
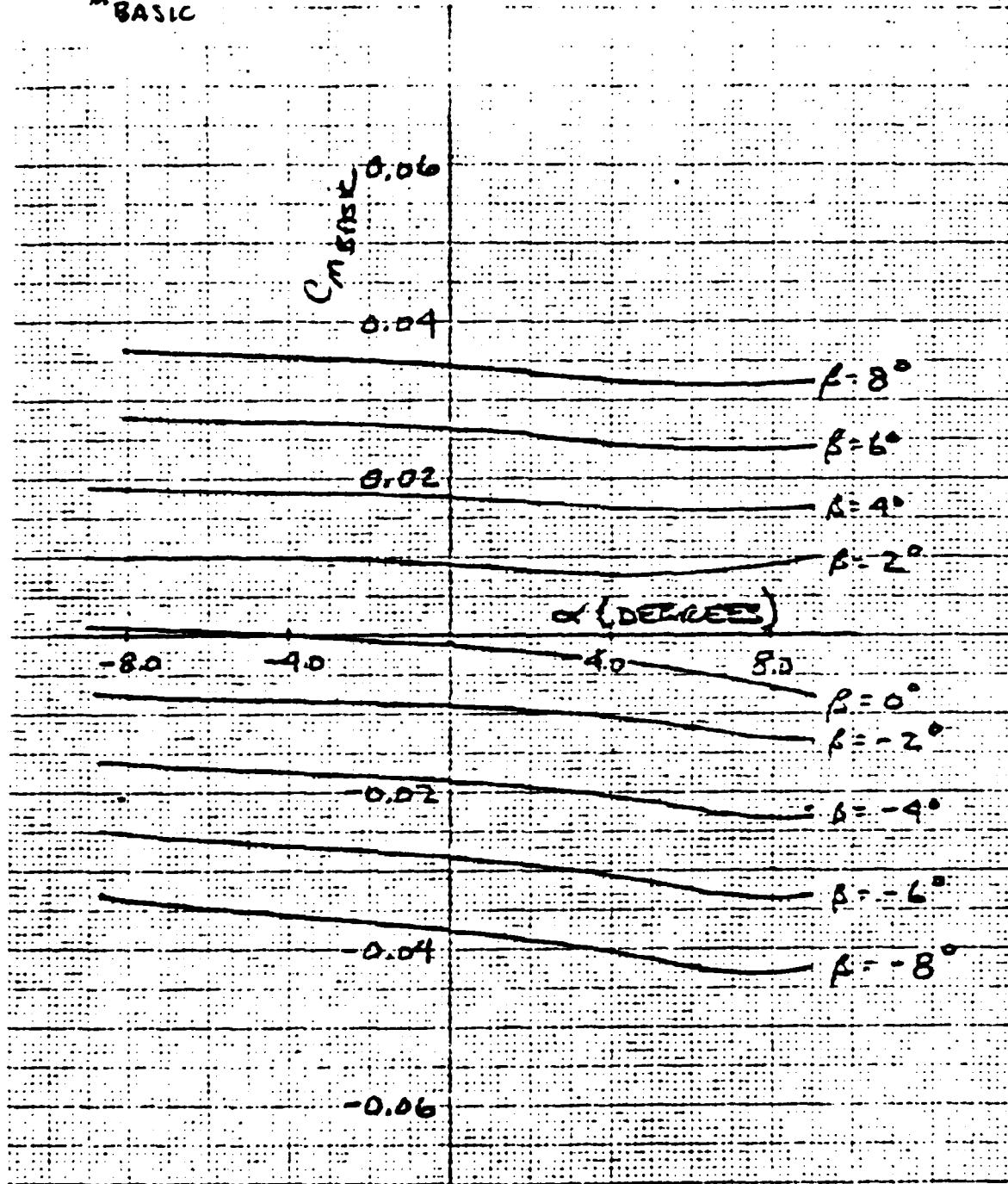
Side Slip Characteristic

α vs β vs $C_{l_{basic}}$

135

$C_{M_{BASIC}}$

$C_{M_{BASIC}}$ 0.06

0.04

$\beta = 8°$

$\beta = 6°$

0.02

$\beta = 4°$

$\beta = 2°$

α (DEGREES)

-8.0   -4.0   4.0   8.0

$\beta = 0°$

$\beta = -2°$

0.02

$\beta = -4°$

$\beta = -6°$

-0.04

$\beta = -8°$

-0.06
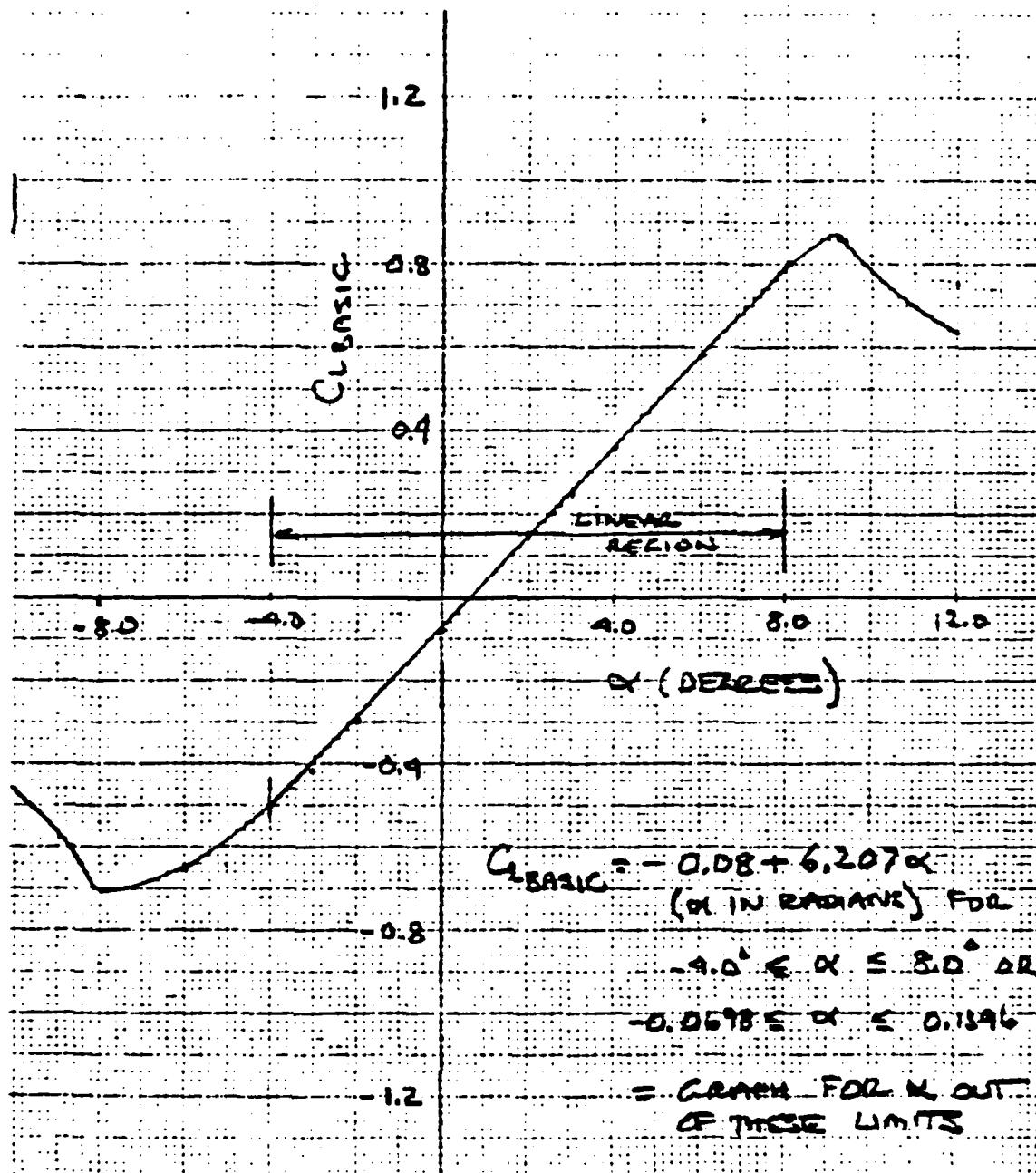
Side Slip Characteristics

α vs β vs $C_{n_{basic}}$

136
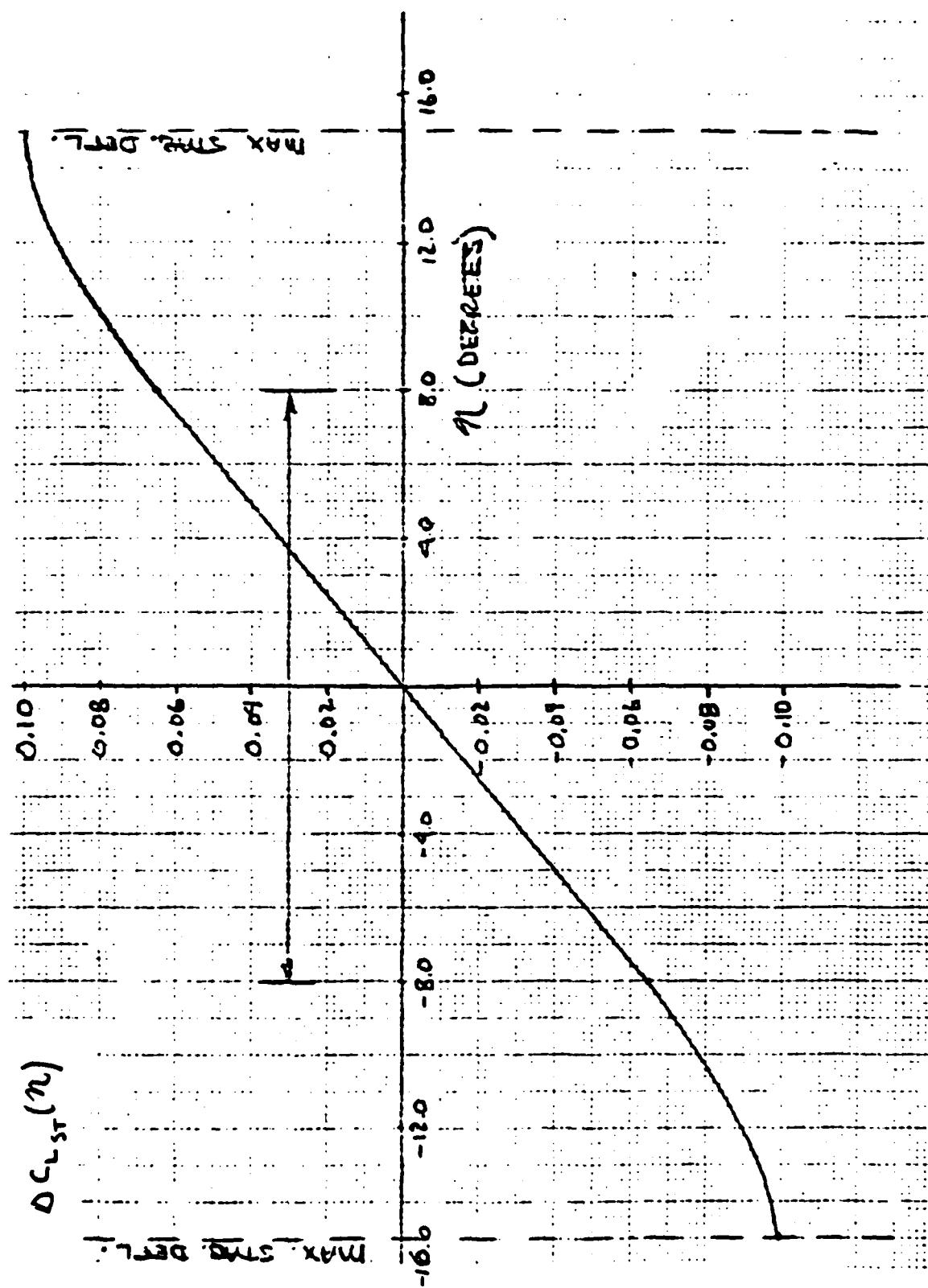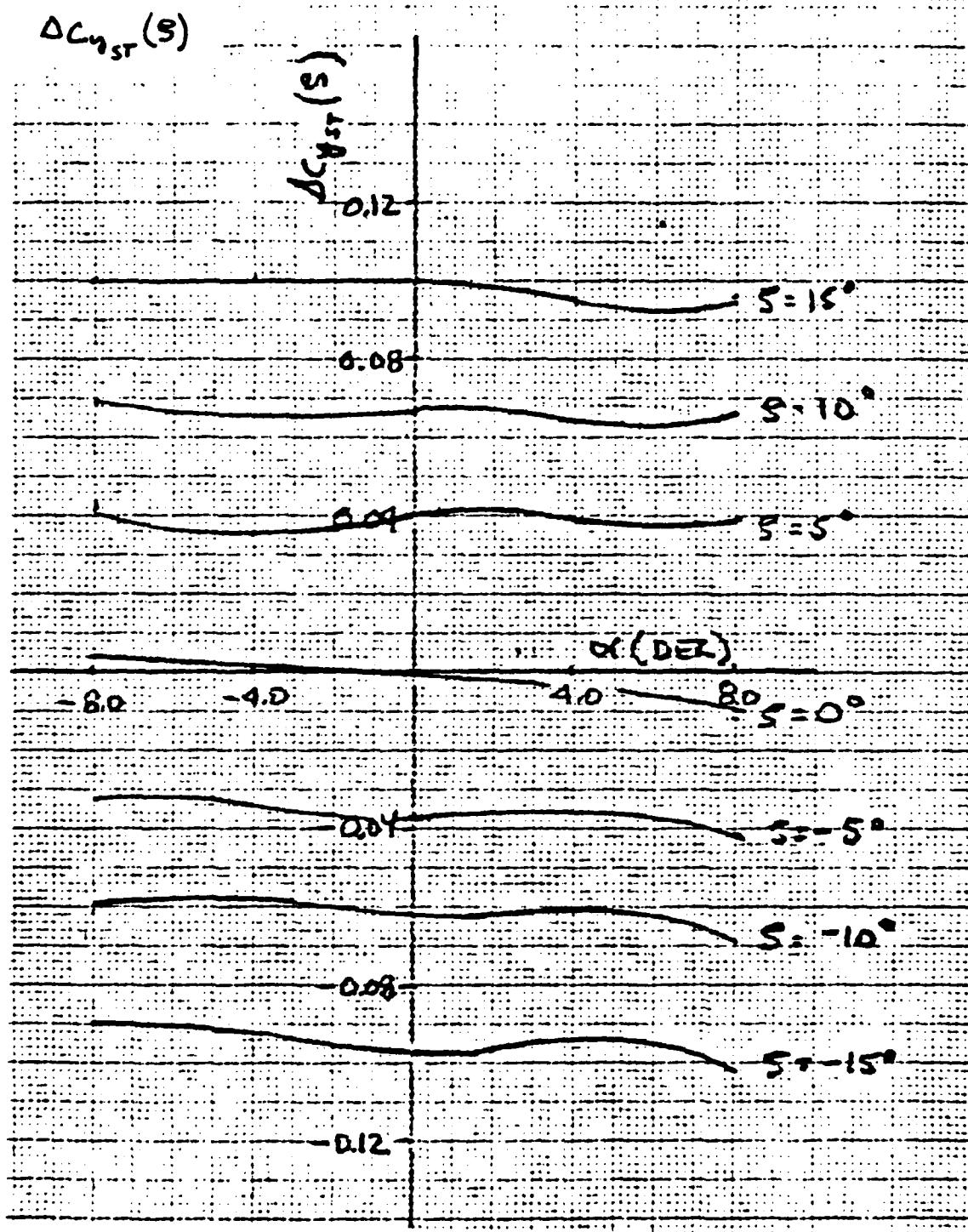
$C_{L_{BASIC}}$

Lift Characteristics

α vs $C_{L_{basic}}$

137

Lift Characteristics

η vs $\Delta C_{L_{ST}}$ (η)

138

Directional Control Characteristics

α vs ζ vs $\Delta C_{Y_{ST}}$ (ζ)

139
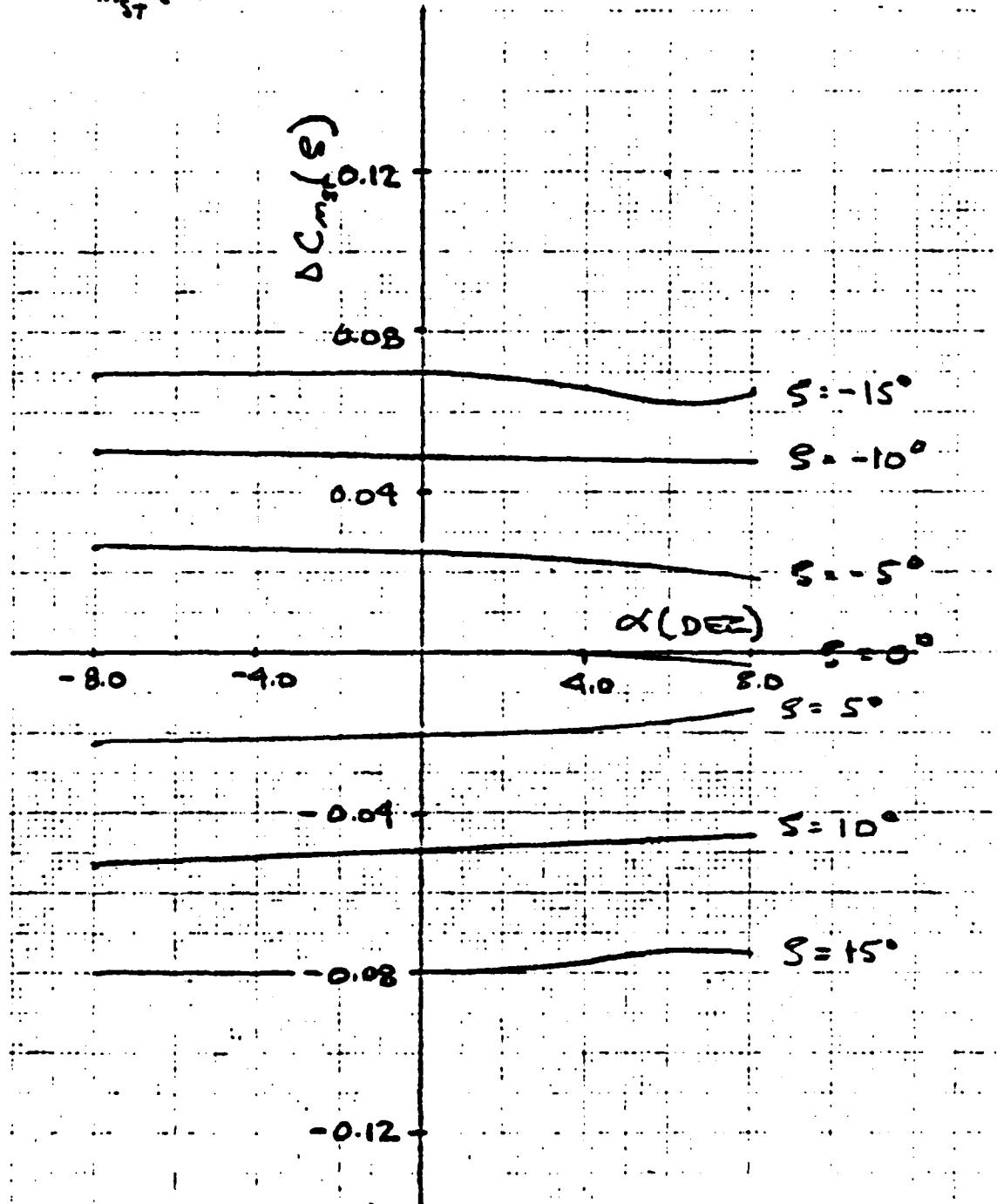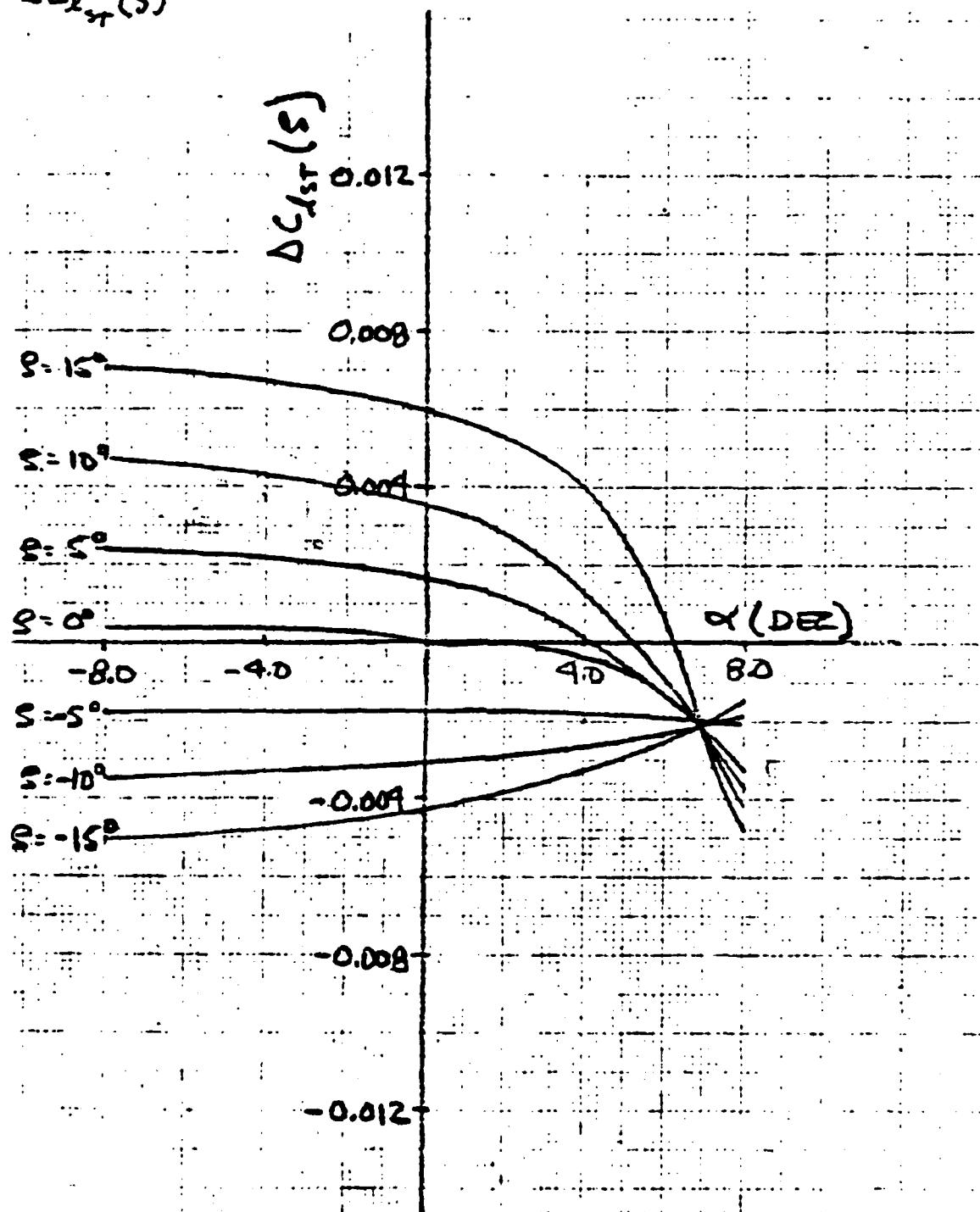
$\Delta C_{m_{ST}} (S)$

Directional Control Characteristics
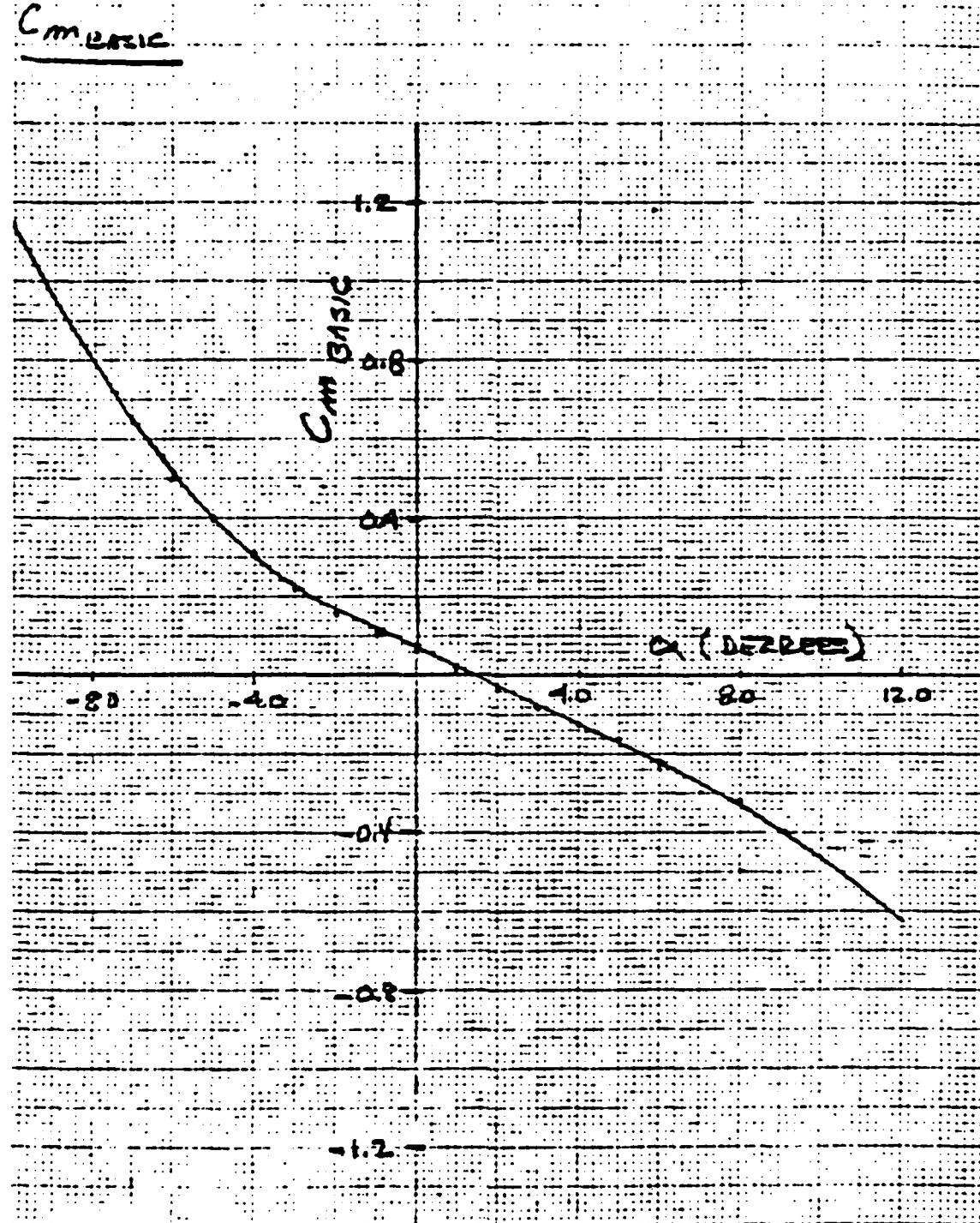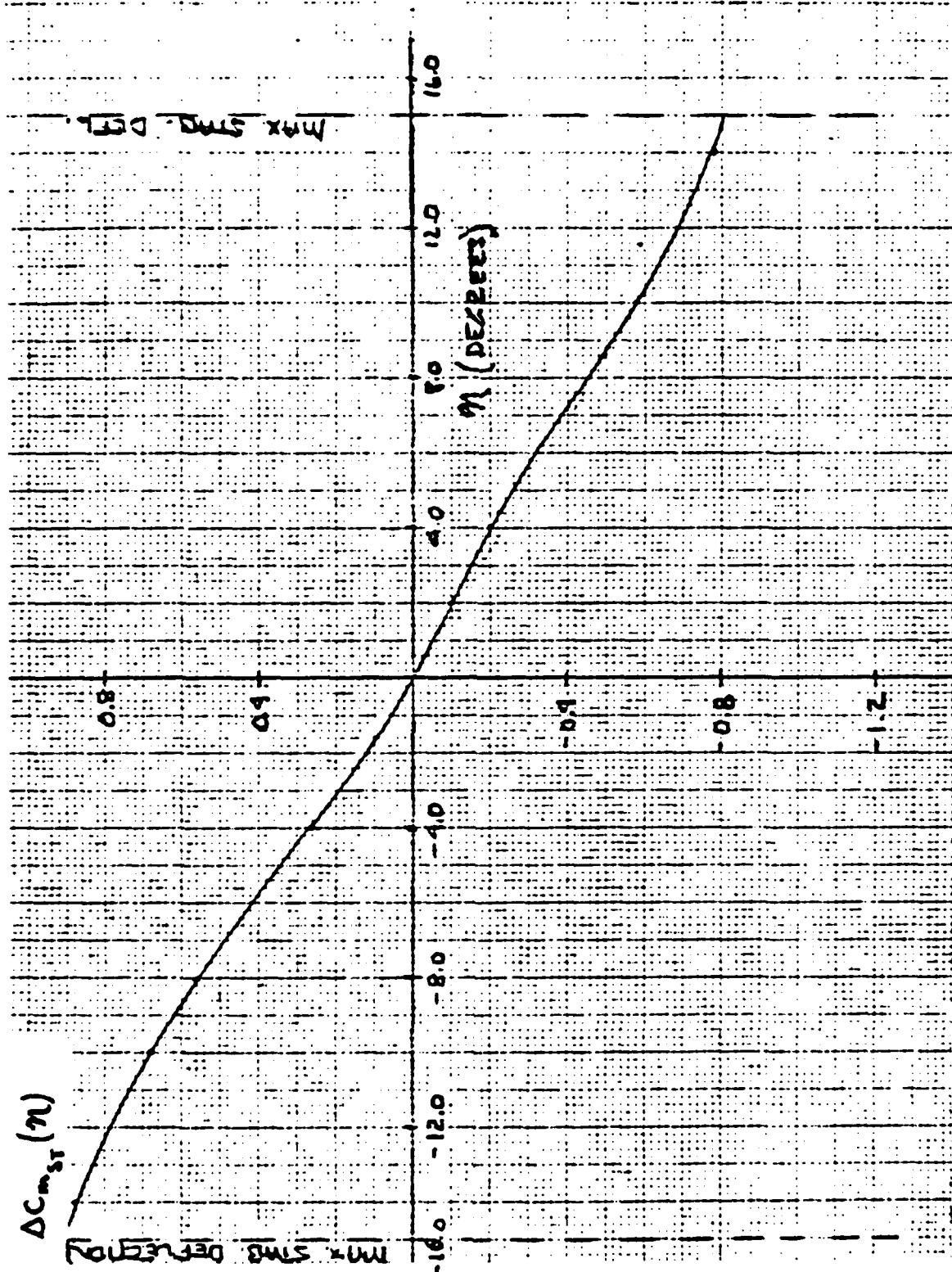
α vs ζ vs $\Delta C_{n_{ST}} (\zeta)$

140

Directional Control Characteristics

α vs ζ vs $\Delta C_{l_{ST}}$ (ζ)

141
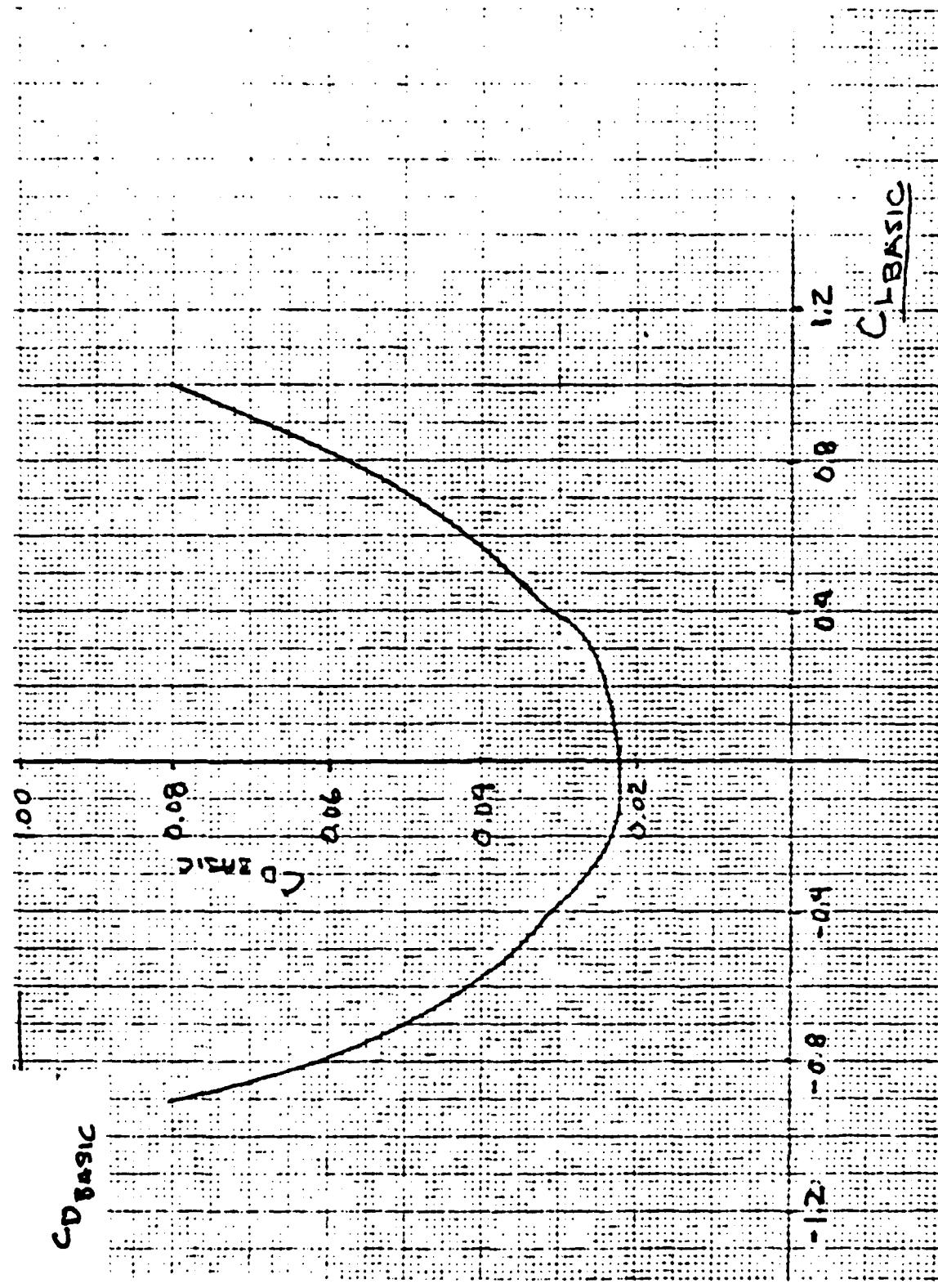
Pitching Moment Characteristics

α vs $C_{M_{basic}}$

142
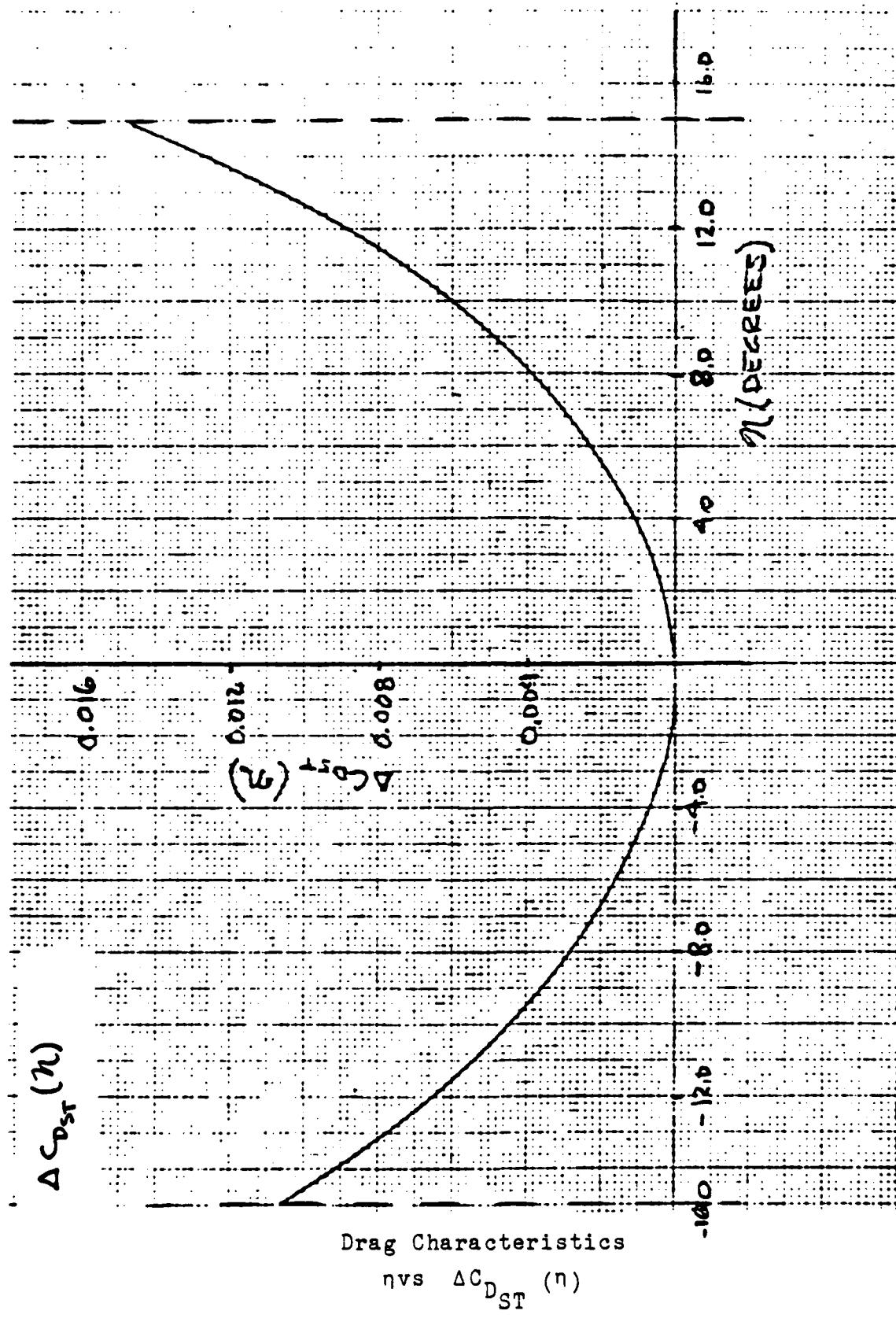
Pitching Moment Characteristics

η vs $\Delta C_{m_{ST}}$ (η)

143
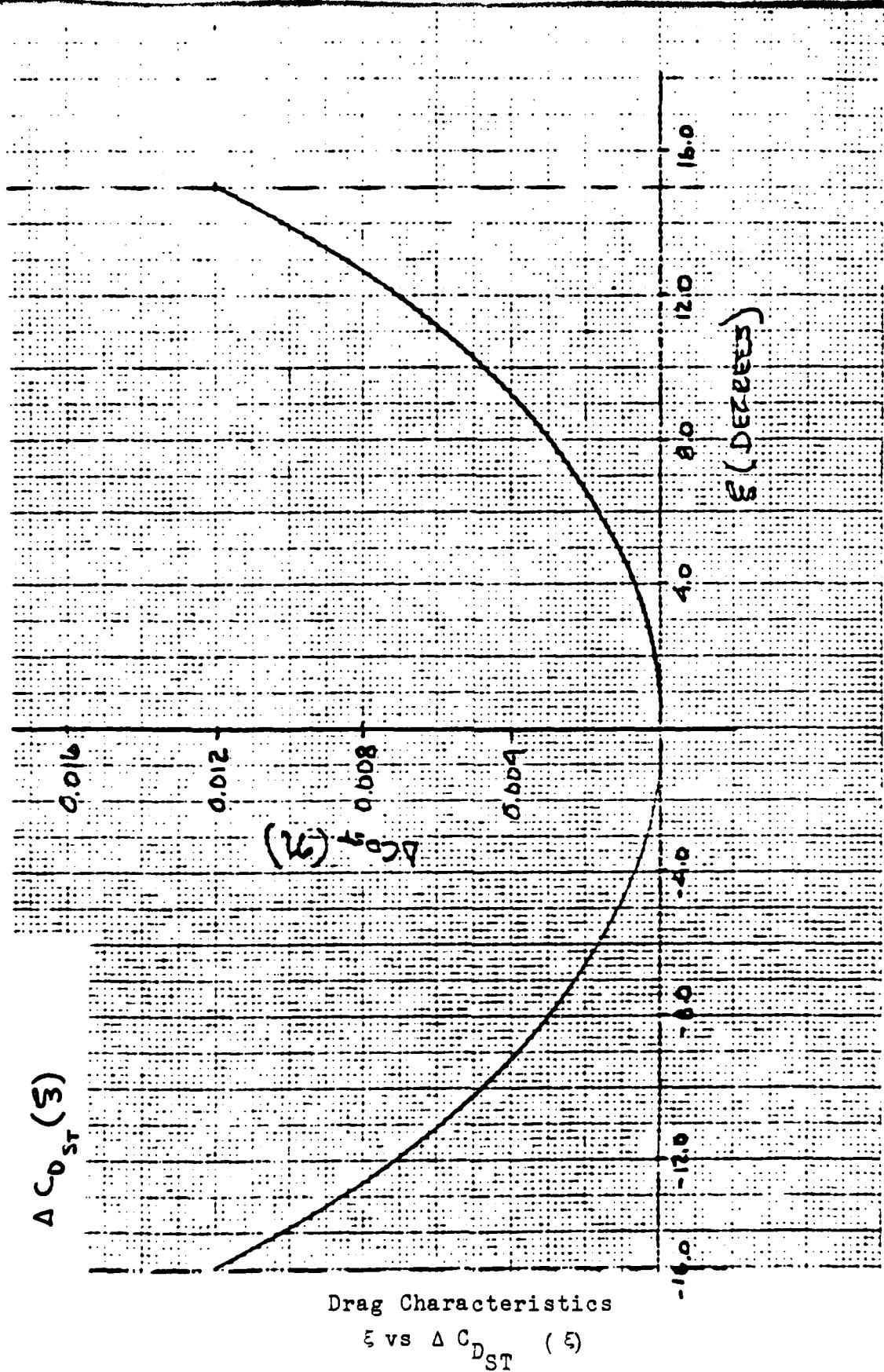
Drag Characteristics

$C_{L_{basic}}$ vs $C_{D_{basic}}$

144

Drag Characteristics

η vs $\Delta C_{D_{ST}}$ (η)

145

Drag Characteristics

ξ vs $\Delta C_{D_{ST}}$ (ξ)

146
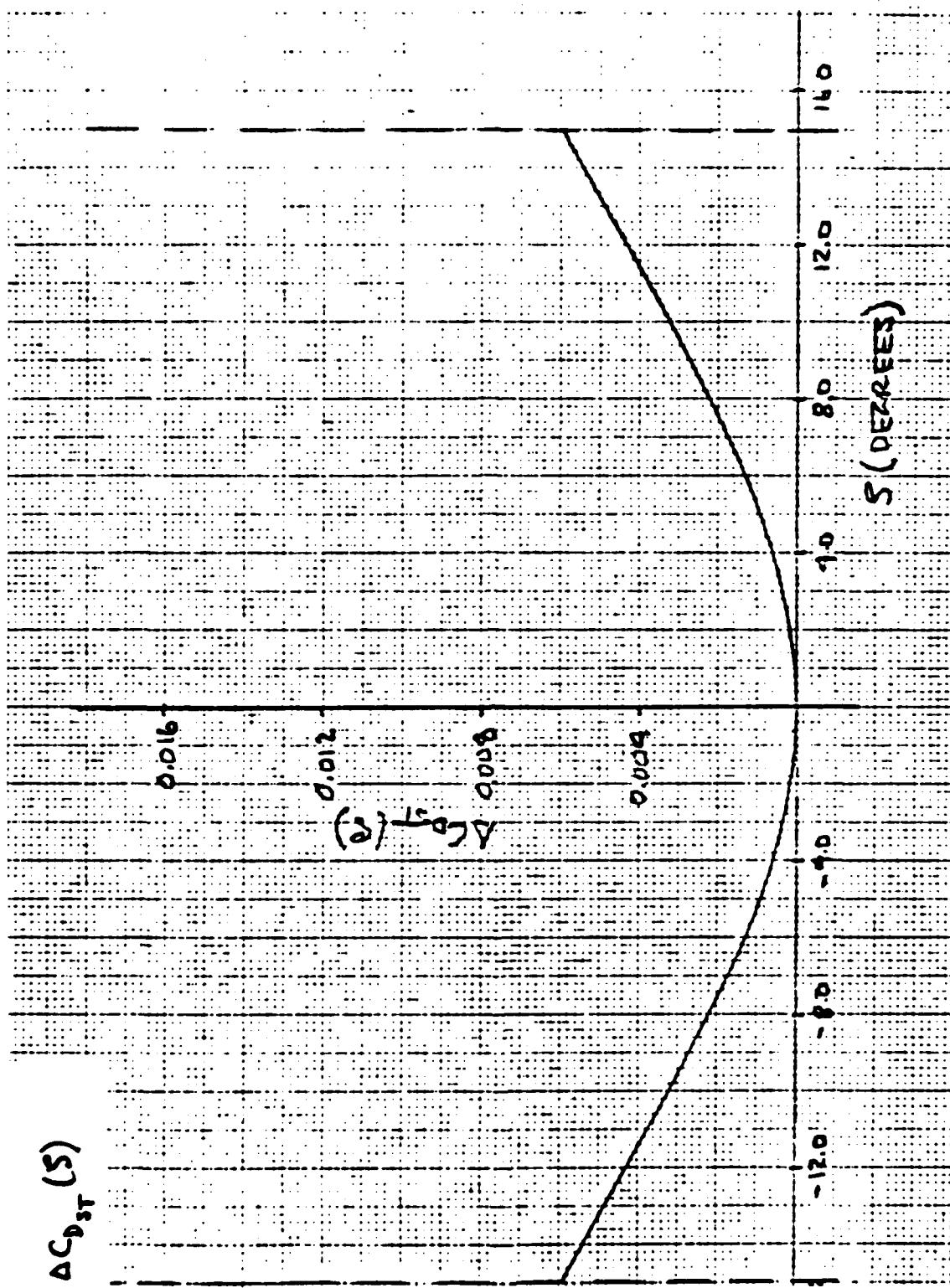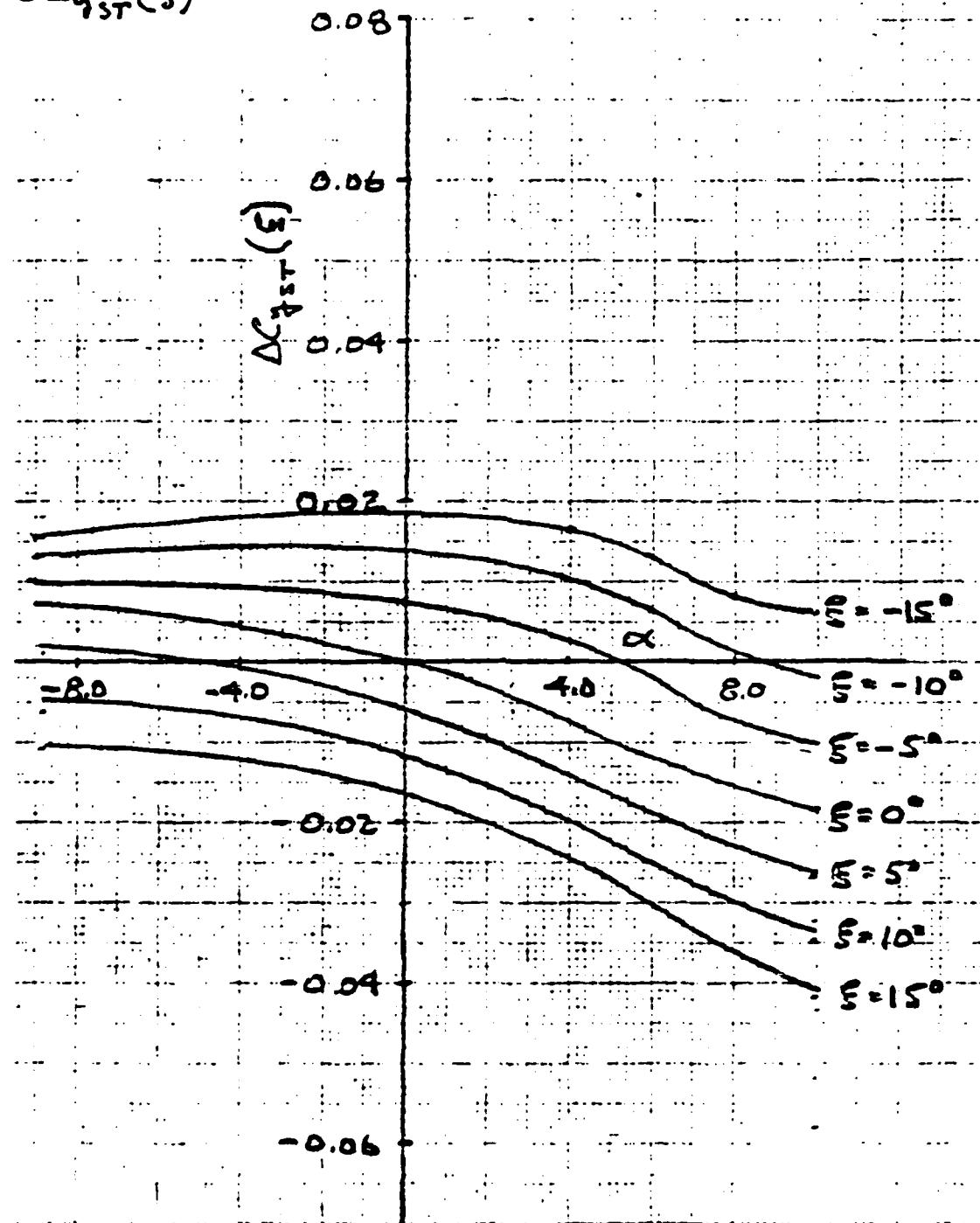
Drag Characteristics

ζ vs $\Delta C_{D_{ST}}$ (ζ)

147
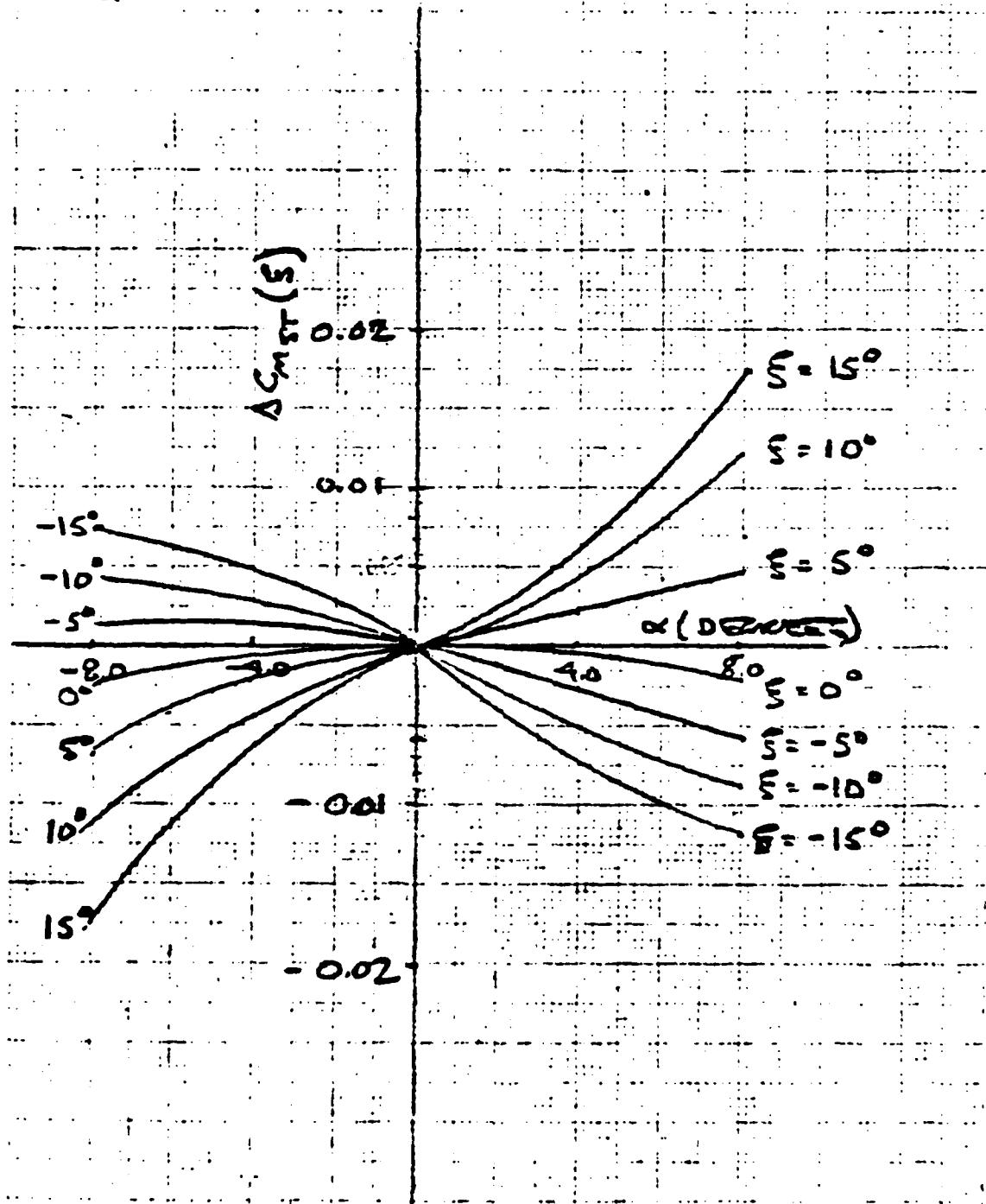
Lateral Control Characteristics

α vs ξ vs $\Delta C_{y_{ST}}(\xi)$

148
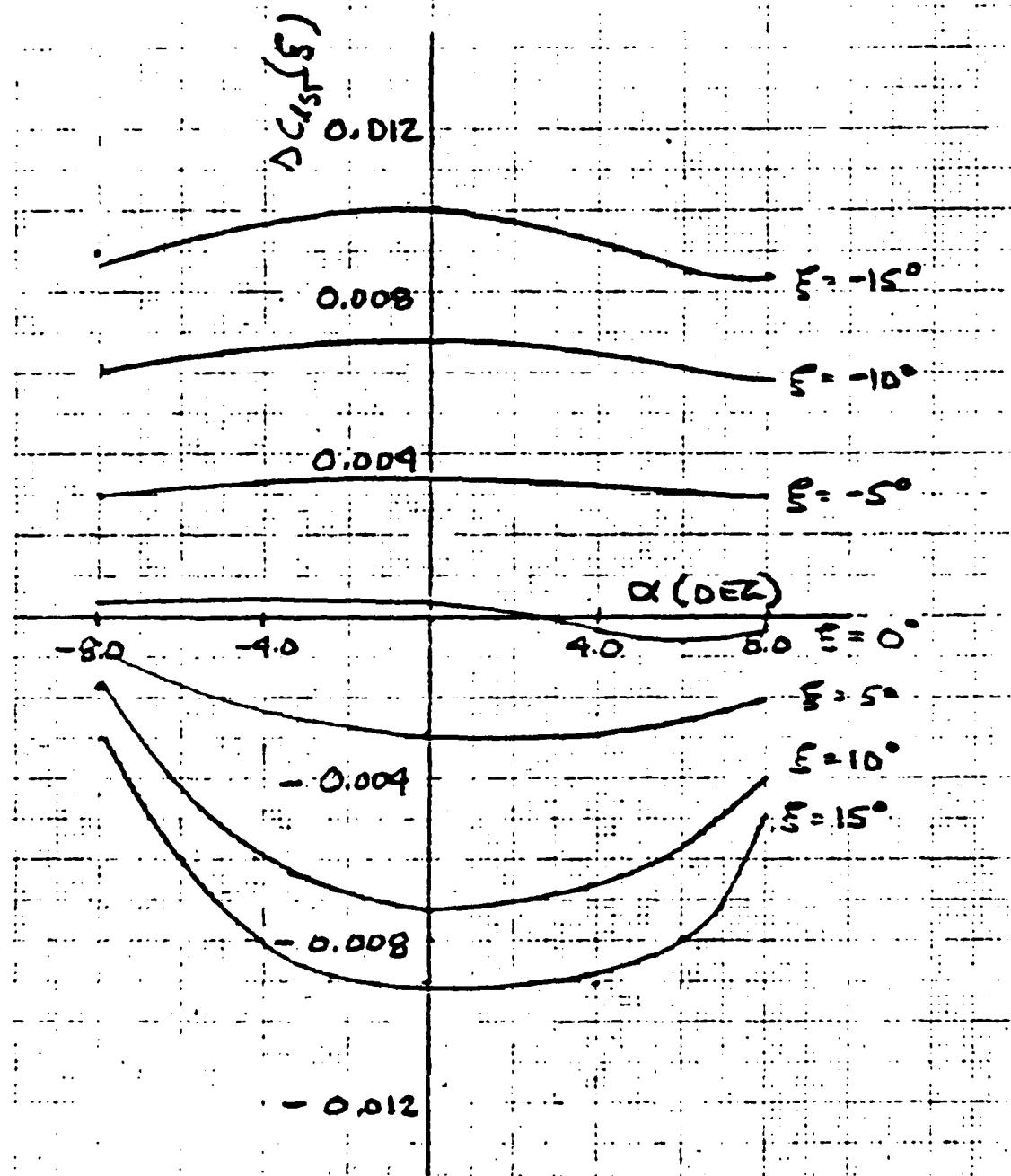
Lateral Control Characteristics

α vs ξ vs $\Delta C_{n_{ST}}$ (ξ)

149

$\Delta C_{\ell_{ST}}(\xi)$

Lateral Control Characteristics

α vs ξ vs $\Delta C_{1_{ST}}$ (ξ)

150

APPENDIX B

STEADY STATE DATA

W =   2200 LBS (At end of cruise flight)

m =   68.38 Slugs

S =   12 feet^2

$\bar{b}$ =   8.485 Feet

$\bar{c}$ =   1.414 Feet

I_{xx} =   27.8 Slug feet^2

I_{yy} =   1507 Slug feet^2

I_{zz} =   1512 Slug feet^2

I_{xz} =   11.7 Slug feet^2

$T_x = T$ =   600 LBS

M =   0.75

$V_{T_{SS}}$ =   839 Feet/Sec

$\bar{q}_{SS}$ = $\frac{1}{2}\,\rho_{SL} V_{T_{SS}}$ = 837 LBS/feet^2

$C_{L_{SS}}$ = $\dfrac{W}{q_{SS}S}$ = 0.219

$C_{D_{SS}}$ = 0.0242

α_{SS} = θ_{SS} = 2.65° = 0.04625 Radian

T_{SS} = $\dfrac{C_{D_{SS}}\,\bar{q}_{SS}S}{\cos\alpha_{SS}}$ = 243.3 LBS

W_{SS} = $V_{T_{SS}}\sin\alpha_{SS}$ = 38.79 Feet/sec

$$U_{SS} = V_{T_{SS}} \cos \alpha_{SS} = 838.1 \text{ Feet/sec}$$
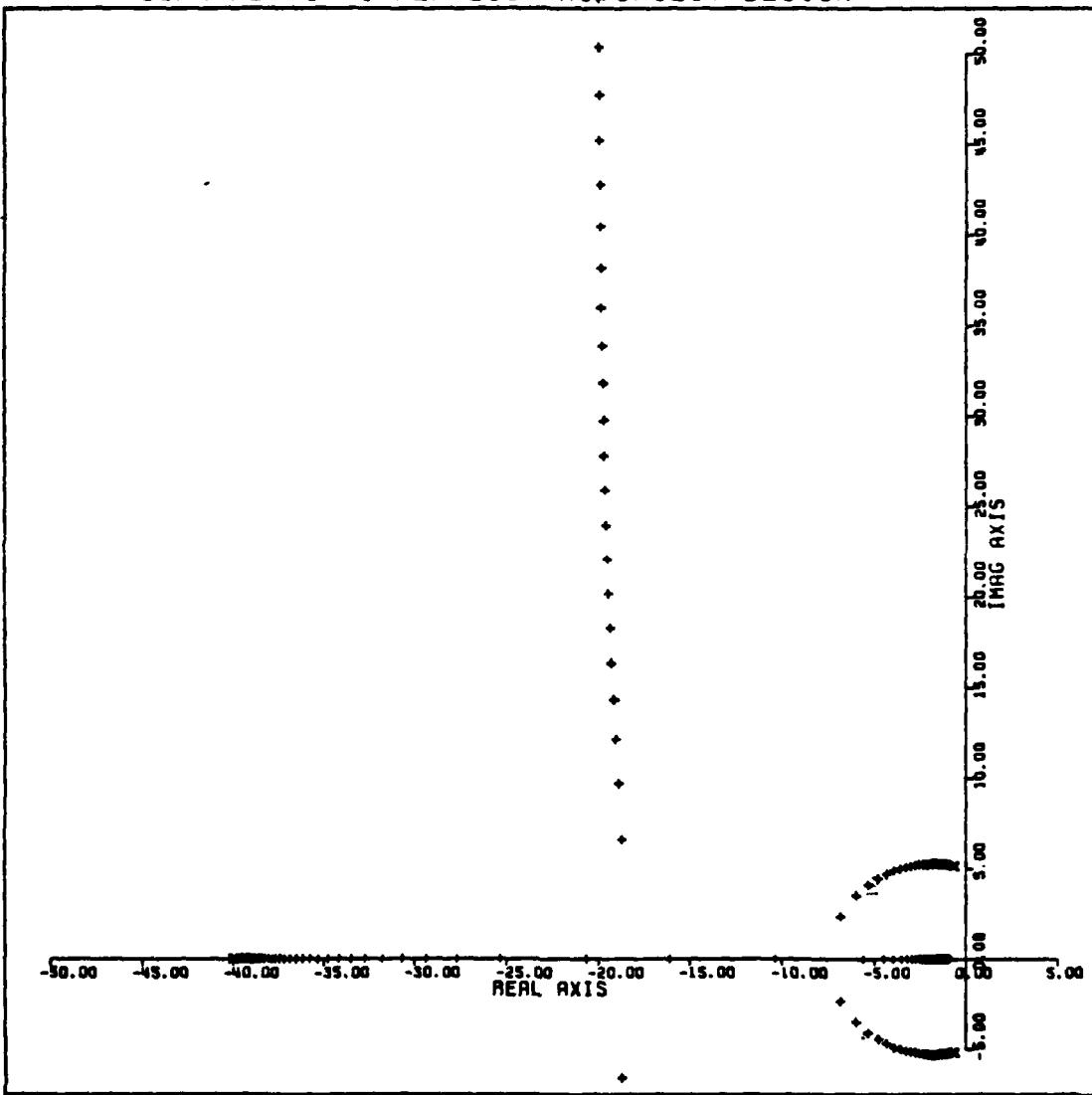
$$C_{m_{basic_{SS}}} = -0.06$$

$$C_{m_{ST_{SS}}} = 0$$

$$\eta_{SS} = -1.0^\circ = 0.01745 \text{ Radian}$$
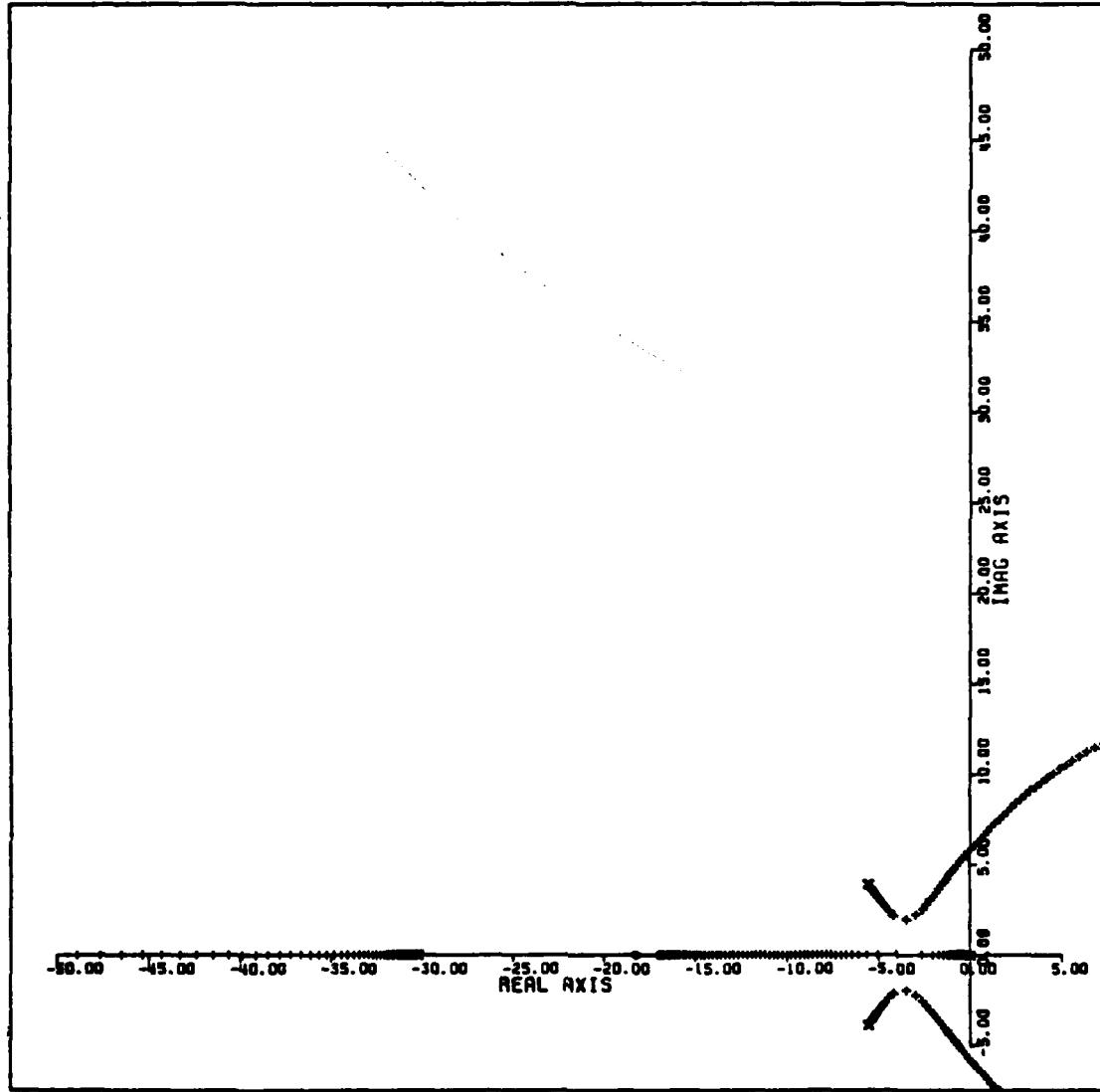
APPENDIX C

AUTOPILOT ROOT LOCUS PLOTS

REAL AXIS (UNITS PER INCH) = 5.0000
IMAG AXIS (UNITS PER INCH) = 5.0000
ROOT LOCUS OF PITCH RATE LOOP OF NORMAL ACCEL
COMMAND FOR INNER LOOP AUTOPILOT DESIGN
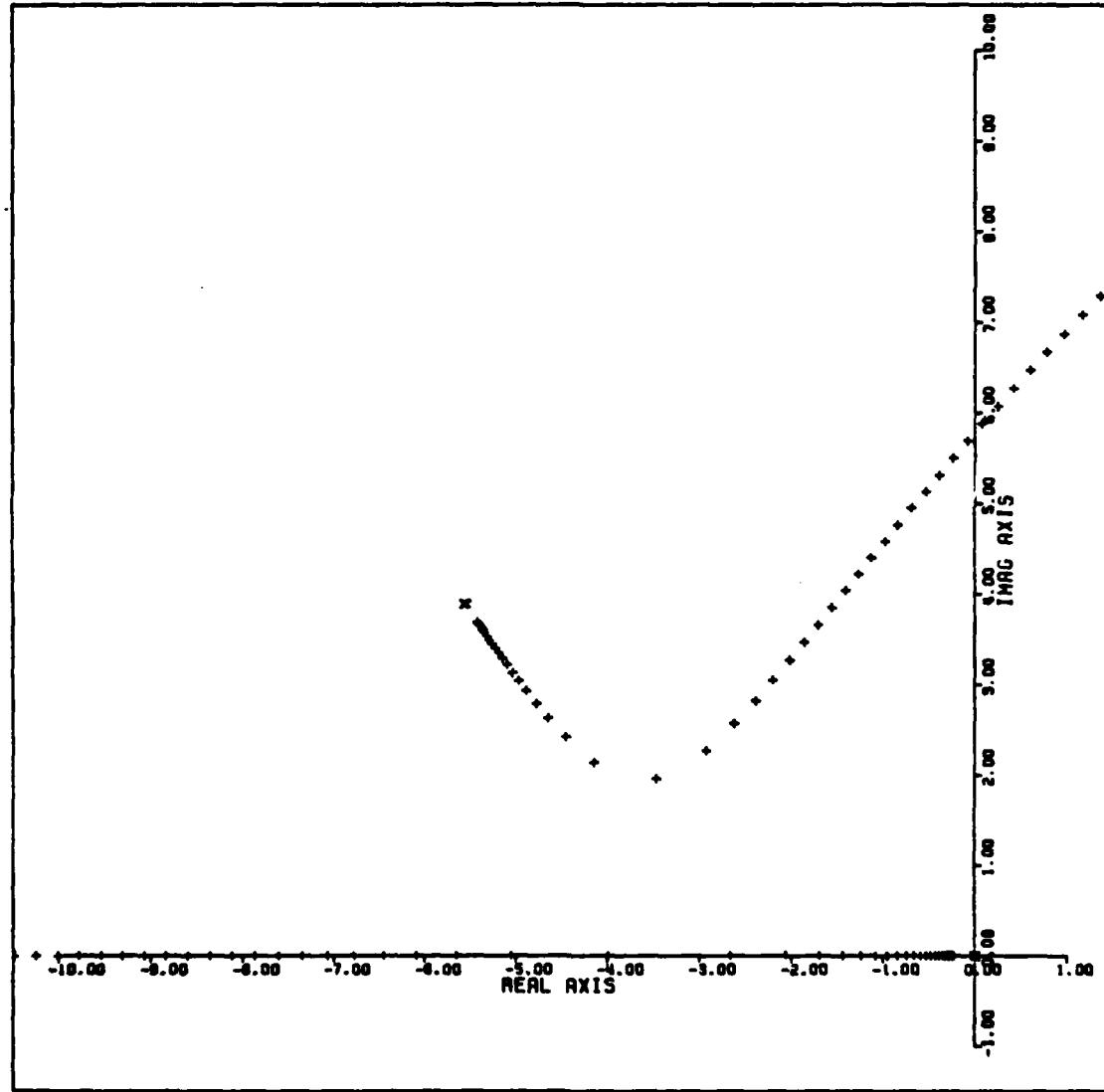
ROOT LOCUS OF NORMAL ACCELERATION COMMAND
FOR INNER LOOP AUTOPILOT DESIGN

REAL AXIS (UNITS PER INCH) = 1.0000
IMAG AXIS (UNITS PER INCH) = 1.0000
ROOT LOCUS OF NORMAL ACCELERATION
COMMAND FOR INNER LOOP AUTOPILOT DESIGN
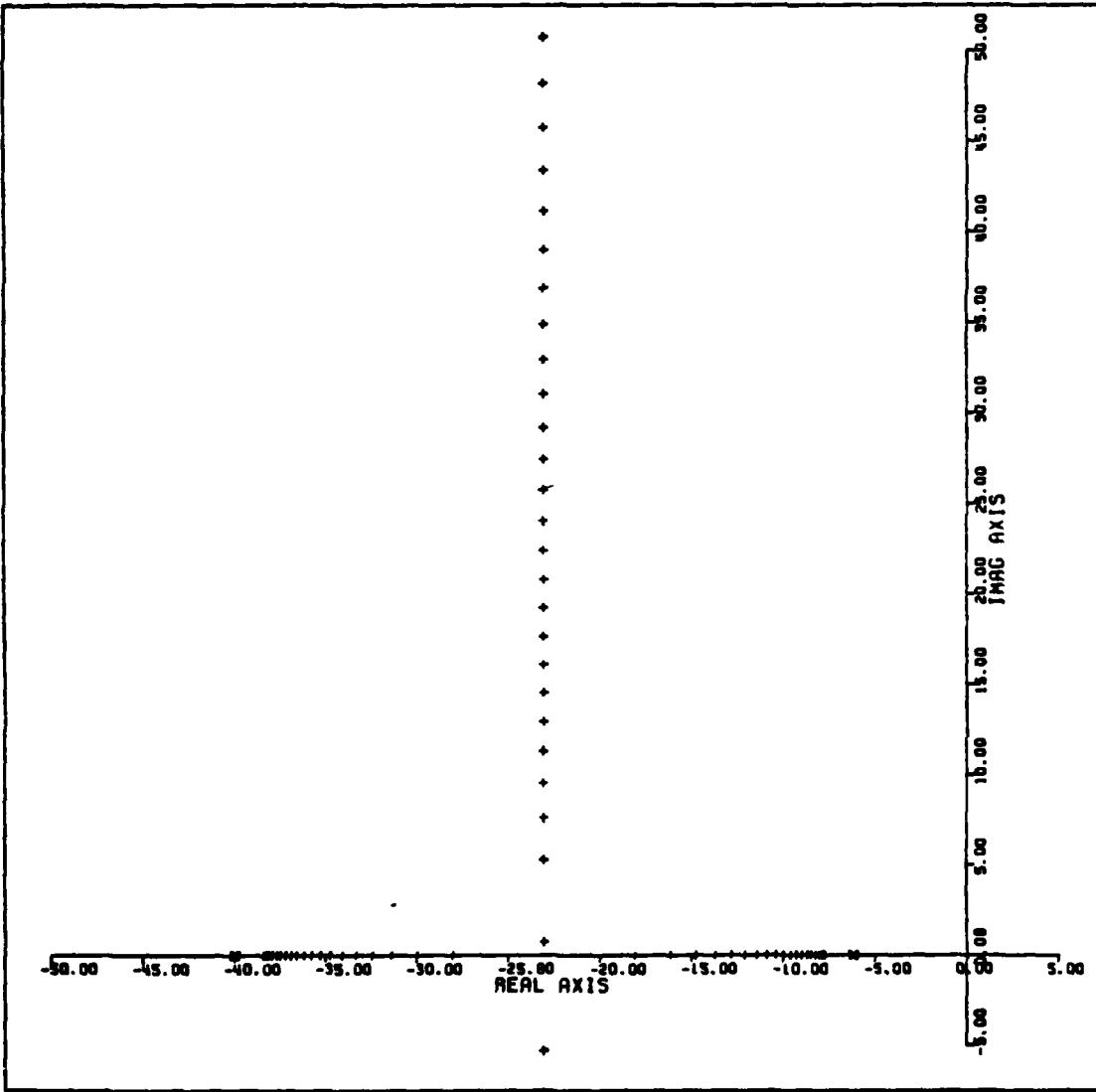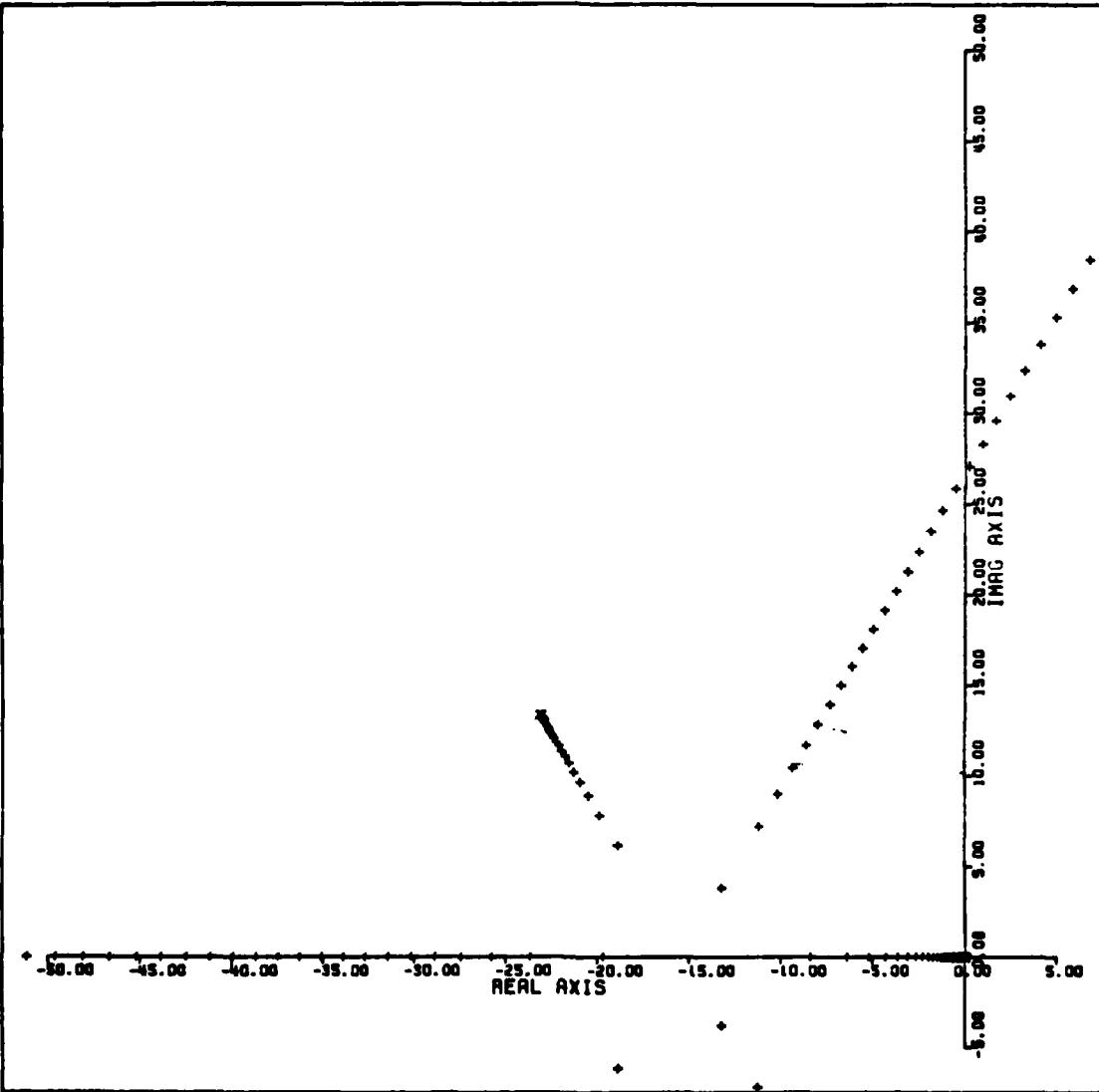
REAL AXIS(UNITS PER INCH) = 5.0000
IMAG AXIS(UNITS PER INCH) = 5.0000
ROOT LOCUS OF ROLL RATE LOOP OF BANK ANGLE
COMMAND FOR INNER LOOP AUTOPILOT DESIGN
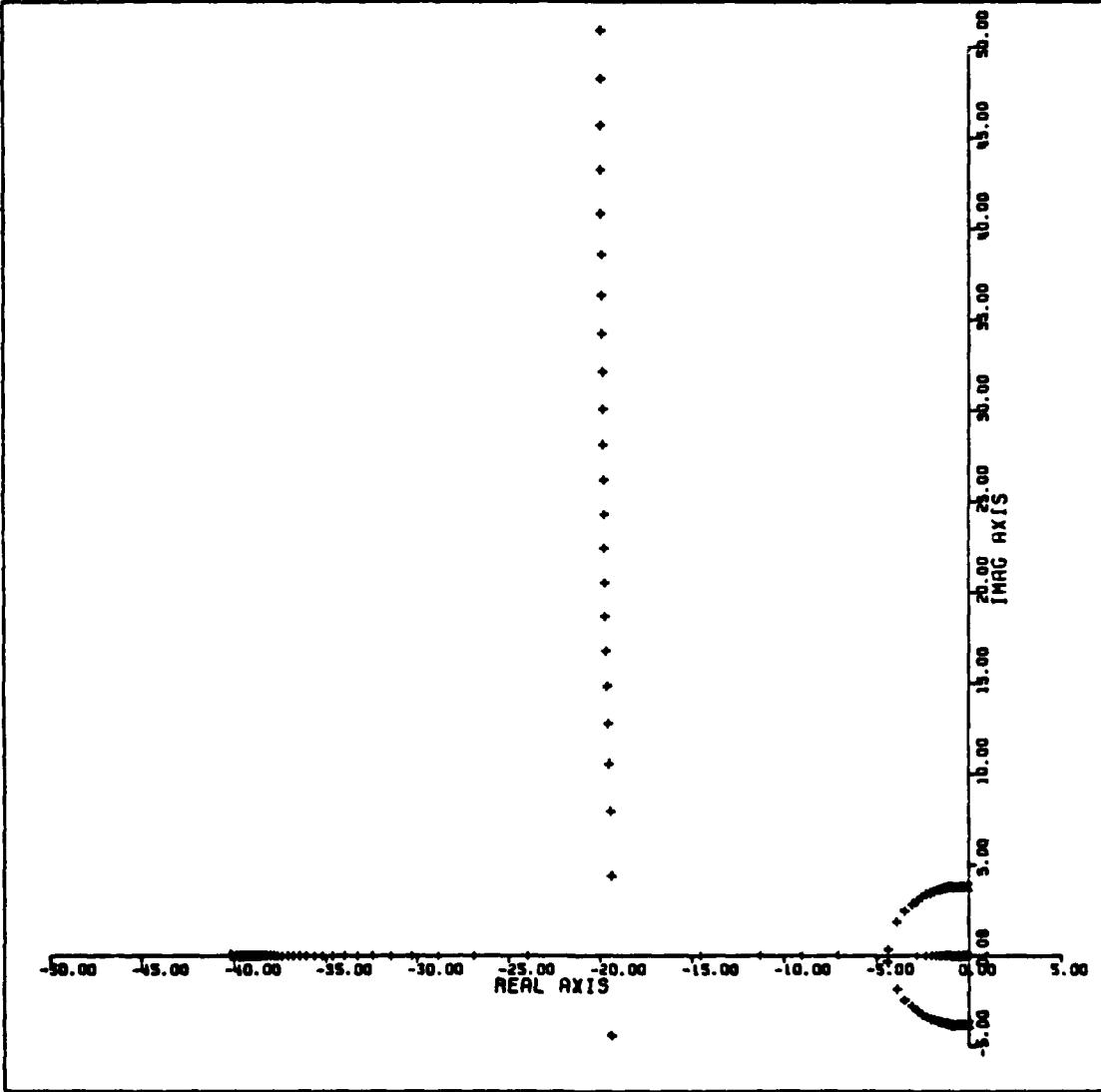
REAL AXIS(UNITS PER INCH) = 5.0000
IMAG AXIS(UNITS PER INCH) = 5.0000
ROOT LOCUS OF BANK ANGLECOMMAND
FOR INNER LOOP AUTOPILOT DESIGN

REAL AXIS (UNITS PER INCH) = 5.0000
IMAG AXIS (UNITS PER INCH) = 5.0000
ROOT LOCUS OF YAW RATE LOOP OF TURN
COORDINATOR FOR INNER LOOP AUTOPILOT DESIGN

REAL AXIS(UNITS PER INCH) = 1.0000
IMAG AXIS(UNITS PER INCH) = 1.0000
ROOT LOCUS OF YAW RATE LOOP OF TURN
COORDINATOR FOR INNER LOOP AUTOPILOT DESIGN

159

ROOT LOCUS OF TURN COORDINATOR
FOR INNER LOOP AUTOPILOT DESIGN
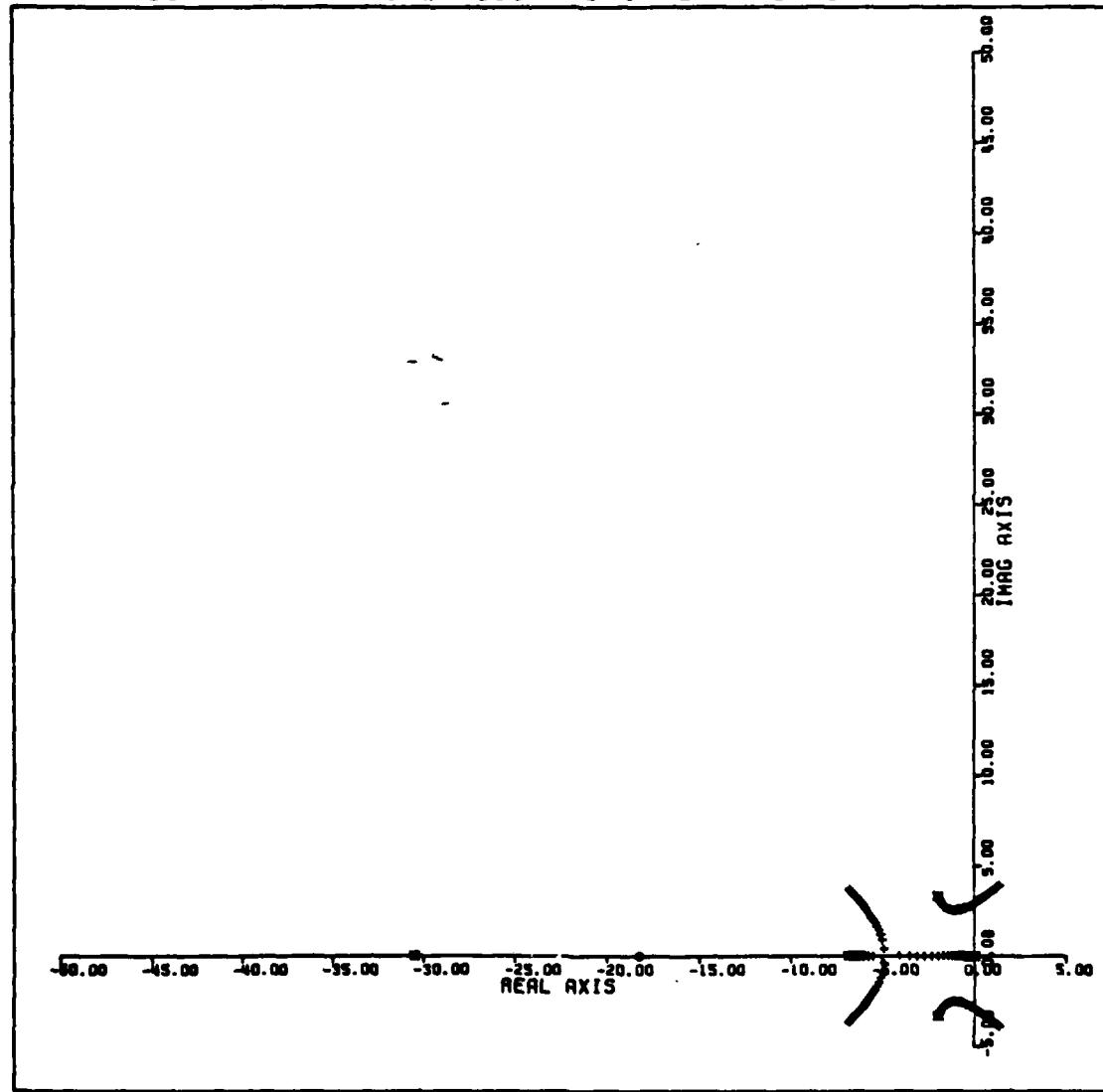
REAL AXIS(UNITS PER INCH) = 1.0000
IMAG AXIS(UNITS PER INCH) = 1.0000
ROOT LOCUS OF TURN COORDINATOR
FOR INNER LOOP AUTOPILOT DESIGN

ROOT LOCUS OF FLIGHT PATH ANGLE
COMMAND FOR OUTER LOOP AUTOPILOT DESIGN

162

REAL AXIS(UNITS PER INCH) = 1.0000
IMAG AXIS(UNITS PER INCH) = 1.0000
ROOT LOCUS OF FLIGHT PATH ANGLE
COMMAND FOR OUTER LOOP AUTOPILOT DESIGN

ROOT LOCUS OF ALTITUDE HOLDCOMMAND
FOR OUTER LOOP AUTOPILOT DESIGN

REAL AXIS(UNITS PER INCH) = 1.0000
IMAG AXIS(UNITS PER INCH) = 1.0000
ROOT LOCUS OF ALTITUDE HOLDCOMMAND
FOR OUTER LOOP AUTOPILOT DESIGN

BASELINE GUIDANCE LAW SIMULATION

```
//WATI562 JOB (1562,0198),'THESIS2',CLASS=G                        THEO00010
// EXEC CSMPX                                                      THEO00020
//X.PLOTPARM CD *                                                  THEO00030
&PLOT SCALE=.5 &END                                                THEO00040
//X.SYSIN DD *                                                     THEO00050

NOTE: 2 DEGREES=.0349065 RADIANS  10 DEG=.174532954               THEO00070
NONLINEAR BANK TO TURN CRUISE MISSLE (VARYING COEFFICIENTS)        THEO00080
WITH BANK TO TURN OR POLAR COORDINATE SYS GUIDANCE LAW             THEO00090
SEA SKIMMER GUIDANCE SCHEME                                        THEO00100
LABEL NCGLINT,LAMDA=4.0,ECM=2.0 LPS,ROLL RATE=100 DEG/SEC          THEO00110
LABEL BURNTHROUGH 400 FEET                                         THEO00120
INITIAL                                                            THEO00130
PARAM G=32.17, T=242.3, WT=2200.0, S=12.0, K2=57.29577951, M=68.38,...  THEO00140
C=0.0, KRI=0.28, KAI=0.05, KR2=0.10, K0=10.8, KR3=0.40, KA2=0.25,...    THEO00150
KGAMMA=1.0, KFA=1.25, KFE1=1.0, KFE2=2.0, LAMDA2=4.00, LAMDEL=4.0,...   THEO00160
KALT=0.0, XI=25000.0, YTI=0.0, HTI=10.0, CLIMBA=0.1580983,...           THEO00170
PI=3.1415926 54, FREQ=2.00, SHIFTY=75.0, SHIFTH=15.0                    THEO00180
* TABLE OF COEFFICIENTS STORED AS FUNCTION OF TWO OR THREE VARIABLES    THEO00190
* TWO VARIABLE COEFFICIENT TABLES                                       THEO00200
* LIFT CHARACTERISTICS                                                  THEO00210
* ALFA VS CLBASIC                                                       THEO00220
FUNCTION LIFTI=-12.0,-.32,-11.0,-.57,-35.,-10.0,-.46,-9.0,-.57,...      THEO00230
-8.0,-.70,-7.0,-.65,-6.0,-.65,-5.0,-.58,-4.0,-.50,-3.0,-.42,...         THEO00240
-2.0,-.30,-1.0,-.18,0.0,-.08,1.0,0.0,2.0,.15,3.0,.25,4.0,.36,...        THEO00250
5.0,.47,6.0,.58,7.0,.65,8.0,.80,9.0,.87,10.0,.78,11.0,.73,...           THEO00260
12.0,.64                                                               THEO00270
* ELE VS DELTA CLST(ELE)                                                THEO00280
FUNCTION LIFT2=-15.0,-.100,-14.0,-.097,-13.0,-.094,-14.0,0.,...         THEO00290
-.090,-11.0,-.084,-10.0,-.078,-9.0,-.071,-8.0,-.065,-7.0,0.,...         THEO00300
-.056,-6.0,-.048,-5.0,-.040,-4.0,-.032,-3.0,-.024,-2.0,-.016,...        THEO00310
-1.0,-.008,0.0,0.0,1.0,.008,2.0,.016,3.0,.024,4.0,.033,5.0,0.,...       THEO00320
-.041,6.0,.049,7.0,.057,8.0,.065,9.0,.073,10.0,.080,11.0,0.,...         THEO00340
.086,12.0,.092,13.0,.098,14.0,.100                                     THEO00350
* DRAG CHARACTERISTICS                                                  THEO00360
* CLBASIC VS CDBASIC                                                    THEO00370
FUNCTION DRAG1=.9,.080,-8.0,.061,-7.,.050,-6.,.042,-5.,.035,...         THEO00380
-.042,-.031,.026,-2.,.021,.023,-1.,.024,0.,.023,0.,.024,0.,.054,...     THEO00390
-.024,-.03,.026,0.04,-.031,.036,0.6,.042,0.7,.049,0.8,.054,...          THEO00400
0.9,.06,1.0,.080                                                        THEO00410
* ELE VS DELTA CDST(ELE)                                                THEO00420
FUNCTION DRAG2=-15.,.0106,-14.,.0091,-13.,.0077,-12.,.0065,...          THEO00430
-13.,.0044,-9.,.0036,-8.,.0028,-7.,.0022,-6.,.0016,-5.,.0011,...        THEO00440
.0011,-4.,.0007,-3.,.0003,-2.,.0001,-1.,.0001,0.,.0001,2.,.0011,...     THEO00450
.0049,1.0,.006,.0011,.0073,12.,.0089,13.,.0126,14.,.0146,...            THEO00460
* AILERON VS DELTA CDST(AIL)                                            THEO00470
FUNCTION DRAG3=-15.,.0120,-14.,.0102,-13.,.0085,-12.,.0071,...          THEO00480
```

```
-10.,.0048,-5.,.0038,-8.,.0030,-7.,.0023,-6.,.0016,-5.,.0011,...   THEO0490
-4.,.0007,-3.,.0003,-2.,.0011,6.,.0017,7.,.0023,8.,.0030,9.,.0038,... THEO0500
.0003,4.,.0007,5.,.0011,6.,.0039,12.,.0071,13.,.0085,14.,.0100,15.,.0120 THEO0510
10.,.0048,-11.,.0039,12.,CDSF(RUD)                                 THEO0520
RUDDER VS DELTA CDSF(RUD)                                           THEO0530
FUNCTION DRAG4=-15.,.0059,-14.,.0054,-13.,.0048,-12.,.0043,...      THEO0540
-10.,.0032,-9.,.0027,-8.,.0022,-7.,.0017,-6.,.0013,-5.,.0009,...    THEO0550
-4.,.0006,-3.,.0003,-2.,.0001,6.,.0011,7.,.0019,0.0.0017,8.,.0022,9.,.0027,... THEO0560
.0001,4.,.0006,5.,.0009,6.,.0015,7.,.0017,8.,.0022,9.,.0027,...     THEO0570
10.,.0016,.0037,12.,.0043,13.,.0048,14.,.0054,15.,.0059            THEO0580
PITCHING MOMENT CHARACTERISTICS                                    THEO0590
ALFA VS CMBASIC                                                     THEO0600
FUNCTION PITCH1=-10.,-1.,13.,-8.,.00,-6.,.50,-4.,.31,-2.,.16,...    THEO0610
0.,.08,.2.,.03,4.,.13,6.,-.22,8.,-.32,10.,-.46,12.,-.62            THEO0620
ELEV VS DELTA CMST(ELE)                                            THEO0630
FUNCTION PITCH2=-15.,.90,-14.,.80,-12.,.78,-10.,.68,-8.,.56,...     THEO0640
-6.,.42,-4.,.27,-2.,.12,0.,.2.,.10,4.,.20,6.,-.32,8.,-.45,...       THEO0650
10.,.58,.12,.,.69,14.,-.78,15.,-.80                                THEO0660
                                                                    THEO0670
THREE VARIABLE COEFFICIENT TABLES                                   THEO0680
SIDESLIP CHARACTERISTICS                                            THEO0690
ALFA VS BETA VS CYBASIC                                            THEO0700
FUNCTION SIDE1=-8.,0=(-8.,.140),(-6.,.111),(-4.,.073),(-2.,.151)   THEO0710
.0341,(C.,.002),(2.,.340),(4.,.077),(6.,.114),(8.,-.151)          THEO0720
FUNCTION SIDE1=-6.,0=(-8.,.149),(-6.,.118),(-4.,.072),(-2.,.153)   THEO0730
.0341,(C.,.003),(2.,.342),(4.,.078),(6.,.116),(8.,-.153)          THEO0740
.0325,(C.,.013),(2.,.140),(4.,.100),(-4.,.063),(8.,-.162)          THEO0750
FUNCTION SIDE1=8.,0=(-8.,.137),(-6.,.089),(-4.,.127),(8.,-.162)     THEO0760
.0220,(C.,.020),(2.,.130),(4.,.060),(4.,.077),(6.,-.060),(8.,-.162) THEO0770
ALFA VS BETA VS CRLLBASIC                                          THEO0780
FUNCTION SIDE2=-8.,0=(-8.,.048),(-6.,.0038),(-4.,.0020),(-2.,...   THEO0790
.0014,(C.0.,.0004),(2.,.0005),(4.,.0016),(6.,-.0301),(8.,...        THEO0800
FUNCTION SIDE2=-6.,0=(-8.,.040),(-6.,.0036),(-4.,.0022),(-2.,...   THEO0810
.0010,(C.,.0004),(2.,.0014),(4.,.0026),(6.,-.0038),(8.,...          THEO0820
.0052,(C.,.0004),(2.,.0014),(4.,.0026),(6.,-.0038),(8.,...          THEO0830
FUNCTION SIDE2=6.,0=(-8.,.038),(-6.,.0026),(-4.,.0026),(-2.,...    THEO0840
.0000,(C.0.,.0031),(2.,.0025),(4.,-.0036),(6.,-.0047),(8.,...       THEO0850
.0059,(C.,.0002),(2.,.0002),(4.,-.0036),(6.,-.0025),(8.,...         THEO0860
FUNCTION SIDE2=16.,0=(-8.,.044),(-6.,.0030),(-4.,.0020),(-2.,...   THEO0870
.0008,(C.0.,.0002),(2.,-.0014),(4.,-.0025),(6.,-.0036),(8.,...      THEO0880
ALFA VS BETA VS CNBASIC                                            THEO0890
FUNCTION SIDE3=-8.,0=(-8.,-.0034),(-6.,-.0025),(-2.,.0161,...      THEO0900
(-2.,.0077),(C.,.0001),(2.,.0101),(4.,.049),(6.,.028),(8.,.036)   THEO0910
FUNCTION SIDE3=0.,0=(-8.,-.0057),(-6.,-.028),(-4.,.028),(8.,.0191,...  THEO0920
(-2.,-.0091),(C.,.0001),(2.,-.009),(4.,-.009),(6.,.026),(8.,.034)  THEO0930
```

```
FUNCTION SI(C3,   6.0=(-8.,-.042),(-6.,-.033),(-4.,-.024),(8.,.022)
(-12=(C12),(0.,.005),(2.,.008),(4.,.016),(6.,.024),(8.,.032)
FUNCTION SI(C3,   8.0=(-8.,-.042),(-6.,-.033),(-4.,-.025),(8.,.032)
DIRECTIONAL CONTROL CHARACTERISTICS
ALFA VS RUDDER DIREC VS DELTA CYST(RUD)
FUNCTION DIREC1,-8.0=(-15.,.090),(-10.,.060),(-5.,-.032),...
(0.=DIREC1,-4.0=(-15.,-.070),(-10.,.062),(-5.,-.036),...
FUNCTION DIREC1, 2.0=(-15.,-.097),(-15.,.098),(-5.,-.057),...
(0.=DIREC1,      4.0=(-10.,-.060),(-10.,.062),(-5.,-.042),...
FUNCTION DIREC1, 6.0=(-15.,-.095),(-10.,.092),(-5.,-.042),...
(0.=DIREC1,-.026),8.0=(-10.,-.062),(-10.,.048),(-5.,-.018),...
FUNCTION DIREC1, 8.0=(-10.,-.040),(-10.,.066),
(0.=DIREC1,-.010),(-10.,-.066),
ALFA VS RUDDER DIREC2 DELTA CNST(RUD)
FUNCTION DIREC2,-8.0=(-15.,-.070),(-10.,-.050),(-5.,.026),...
(0.=DIREC2,      2.0=(-15.,-.052),(-10.,-.080),(-5.,-.024),...
FUNCTION DIREC2, 2.0=(-15.,-.068),(-15.,-.049),(-5.,-.024),...
(0.=DIREC2,      4.0=(-15.,-.020),(-10.,-.079),(-5.,-.022),...
FUNCTION DIREC2, 6.0=(-15.,-.062),(-10.,-.048),(-5.,-.022),...
(0.=DIREC2,-.018),(-15.,-.047),(-10.,-.074),
FUNCTION DIREC2, 8.0=(-10.,-.065),(-15.,-.048),(-5.,-.018),...
(0.=DIREC2,-.014),(-10.,-.065),(-15.,-.075),
ALFA VS RUDDER DIREC3 CRGLL ST(RUD)
FUNCTION DIREC3,-8.0=(-15.,-.050),(-10.,-.0034),(-5.,-.0018),...
(0.=DIREC3,      2.0=(-10.,-.048),(-15.,-.0070),(-5.,-.0018),...
FUNCTION DIREC3, 2.0=(-15.,-.038),(-10.,-.0029),(-5.,-.0018),...
(0.=DIREC3,      4.0=(-15.,.0012),(-10.,.028),(-15.,.0053),
FUNCTION DIREC3, 4.0=(-10.,-.0033),(-15.,.0040),(-5.,-.0027),...
(0.=DIREC3,-.004),(-5.,-.0012),(-10.,-.0040),
FUNCTION DIREC3, 7.0=(-10.,-.0032),(-15.,-.0022),(-5.,-.0002),...
(0.=DIREC3,      8.0=(-15.,-.0022),(-10.,-.002),
FUNCTION DIREC3,-.002),(-10.,-.0044),(-15.,-.0018),(-5.,-.0020),...
(0.=DIREC3,      8.0=(-15.,-.0034),(-15.,.0048),
LATERAL CONTROL CHARACTERISTICS
ALFA VS AILERON VS CELTA CYST(AIL)
FUNCTION LATRL1,-8.0=(-15.,.015),(-10.,.0013),(-5.,.0010),...
(0.=LATRL1,      .02=(-15.,-.035),(-15.,.0010),(-5.,.0090),...
FUNCTION LATRL1,  1.0=(-15.,-.0012),(-15.,.014),(-5.,-.0024),...
(0.=LATRL1,      3.0=(-10.,.0017),(-15.,.001C),
FUNCTION LATRL1,(5.,-.014),(-10.,-.020),(-15.,.025),
(0.=LATRL1,      10.0=(-10.,.006),(-15.,-.0062),(-5.,-.010),...
(0.=LATRL1,      (5.,-.018),(-10.,-.023),(-15.,-.042)
ALFA VS AILERON VS DELTA CNST(AIL)
FUNCTION LATRL2,-8.0=(-15.,-.0075),(-10.,-.0040),(-5.,-.0015),...
(0.=LATRL2,     05=(-10.,-.0120),(-15.,-.0175),
FUNCTION LATRL2,-4.0=(-15.,-.0050),(-10.,-.0030),(-5.,.0020),...
```
THEO0970
THEO0980
THEO0990
THEO1000
THEO1010
THEO1020
THEO1030
THEO1040
THEO1050
THEO1060
THEO1070
THEO1080
THEO1090
THEO1100
THEO1110
THEO1120
THEO1130
THEO1140
THEO1150
THEO1160
THEO1170
THEO1180
THEO1190
THEO1200
THEO1210
THEO1220
THEO1230
THEO1240
THEO1250
THEO1260
THEO1270
THEO1280
THEO1290
THEO1300
THEO1310
THEO1320
THEO1330
THEO1340
THEO1350
THEO1360
THEO1370
THEO1380
THEO1390
THEO1400
THEO1410
THEO1420
THEO1430
THEO1440

168

```
         (0.,.0010)(15.,.0030)(10.,.0030)(15.,.0045),(15.,.0070)
FUNCTICN LATRL2,(0.,0.)=(-15.,.0.),(-10.,0.),(0.,0.),(0.,0.),...
         (5.,0.),(10.,0.),(15.,0.)
FUNCTICN LATRL2, 4.0=(-15.,.0075)(-10.,-.0050),(-5.,-.0025),...
         (0.,-.0008)(5.,.0025)(10.,.0040)(15.,.0070)
FUNCTICN LATRL2, 8.0=(-15.,.0120)(-10.,-.0085),(-5.,-.0060),...
         (0.,-.0020)(5.,.0050)(10.,.0160)(15.,.0175)
ALFA VS AILERON VS DELTA CROLLST(AIL)
FUNCTICN LATKL3, -8.0=(-15.,.0087)(-10.,-.0060)(-5.,.0050),...
         (0.,.0004)(5.,.0008)(10.,-.0018)(15.,-.0030)
FUNCTICN LATRL3, -4.0=(-15.,.0023)(-10.,-.0056)(-5.,-.0066)(-15.,-.0033)...
         (0.,.0023)(5.,-.0023)(10.,-.0059)(15.,-.0080)
FUNCTICN LATRL3,  0.0=(-15.,.0050)(-10.,-.0100)(-5.,-.0068)(-5.,.0034)...
         (0.,-.0050)(5.,-.0050)(10.,-.0072)(15.,-.0092)
FUNCTICN LATRL3,  4.0=(-15.,.0030)(-10.,-.0046)(-15.,-.0064)(-5.,.0036)...
         (0.,-.0030)(5.,-.0030)(10.,-.0046)(15.,-.0084)
FUNCTICN LATRL3,  8.0=(-15.,.0020)(-10.,-.0084)(-15.,.0058)(-5.,.0050)...
         (0.,-.0020)(5.,-.0020)(10.,-.0040)
(10.0,-.0G04),(5.,-.0020),(10.,-.0040),(15.,-.0050)

DYNAMIC
NOSORT
IF (TIME.EQ.0.0) RNGMIN =100.0
IF (RNGMIN.LE.RANGE) GO TO 10
    RNGMIN = RANGE
    TIMMIN = TIME
    DXTGTM = DXTGT
    DYTGTM = DYTGT
    DZTGTM = DZTGT
10  CONTINUE
*   ALGORITHM THAT PROCEEDS FROM INGRESS TO 3000,THEN ATTACK UNTIL
*   HIT. IT ALLOWS ECM TO ACTIVATE FROM 3000-BURN THROUGH RANGE.
    IF(RANGE.GT.3000.0) GO TO 20
    IF(RANGE.GT.3000.0) GO TO 60
INGRESS INT(3000.0 FEET
    DXTGT = XT-XEARTH
    DYTGT = YT-YEARTH
    DZTGT = HT-ALTUDE
    AYC = LAMDAZ*VT*SIGOZ2/6
    ANC = AZC*COS(PHI)+AYC*SIN(PHI)
    IF(AYC.EQ.0.0.AND.AZC.EQ.0.0) PHIC = 0.0
    IF(AYC.NE.0.0.OR.AZC.NE.0.0) PHIC=ATAN2(AYC,AZC)
    PHIC = LIMIT(-1.047,1.047,PHIC)
20  TC 20C
*   ATTACK PHASE INTO THE TARGET
60  IF (RANGE.GT.2900.) GO TO 65
    IF (RANGE.LT.40C.0) GO TO 65
*   ALLOW ECM TO OCCUR BETWEEN 2900 AND BURN THROUGH RANGE
```

```
THEO1450
THEO1460
THEO1470
THEO1480
THEO1490
THEO1500
THEO1510
THEO1520
THEO1530
THEO1540
THEO1550
THEO1560
THEO1570
THEO1580
THEO1590
THEO1600
THEO1610
THEO1620
THEO1630
THEO1640
THEO1650
THEO1660
THEO1670
THEO1680
THEO1690
THEO1700
THEO1710
THEO1720
THEO1740
THEO1750
THEO1760
THEO1770
THEO1780
THEO1790
THEO1800
THEO1810
THEO1820
THEO1830
THEO1840
THEO1850
THEO1860
THEO1870
THEO1880
THEO1900
THEO1910
THEO1920
```

169

```
*       PUT ECM BLANKING OF 75FT HORIZONTAL SHIFT AT FREQ(.5,1,2 CPS)       THEO1930
        Y1 = SIN(2*PI*FREQ*TIME)                                           THEO1940
        YY = INSW(Y1,SHIFTY,0.0)                                           THEO1950
        YTT = YT-YY                                                        THEO1960
*       PUT ECM BLANKING OF 15FT VERTICAL SHIFT AT FREQ(.5,1,2 CPS)        THEO1970
        H1 = SIN(2*PI*FREQ*TIME)                                          THEO1980
        HH = INSW(H1,SHIFTH,0.0)                                           THEO1990
        HTT = HT+HH                                                        THEO2000
        DXTGT = XT-XEARTH                                                  THEO2010
        DYTGT = YTT-YEARTH                                                 THEO2020
        DZTGT = HT-ALTUDE                                                  THEO2030
        GO TO 66                                                           THEO2040
65      DXTGT = XT-XEARTH                                                  THEO2050
        DYTGT = YT-YEARTH                                                  THEO2060
        DZTGT = HT-ALTUDE                                                  THEO2070
*66     PROPORTIONAL ELEVATION                                            THEO2080
        PNEL1 = LAMDEL*VT*SIGDEL/G                                         THEO2090
        AZCPR3 = PNEL1 + 1.0                                               THEO2100
        AYC = LAMDAZ*VT*SIGDZ1/G                                           THEO2110
        ANC = AZCPR3*COS(PHI)+AYC*SIN(PHI)                                 THEO2120
        PHIC1 = ATAN2(AYC,AZCPR3)                                          THEO2130
*       THIS ROUTINE KEEPS PHIC FROM ROTATING 360 DEG WHEN                 THEO2140
*       TAN FUNCTION PASSES THROUGH 180 DEG.                               THEO2150
        DELTA = PHIC1-PHI                                                  THEO2160
        DELTA1 = ABS(DELTA)                                                THEO2170
        IF (DELTA1.LT.3.14159265470) GO TO 70                             THEO2180
        IF (PHIC1.GE.0.0) GO TO 200                                        THEO2190
        PHIC1 = PHIC1 + 6.2831853                                         THEO2200
        GO TO 200                                                          THEO2210
200     PHIC1 = PHIC1 - 6.2831853                                         THEO2220
70      CONTINUE                                                           THEO2230
230     SORT                                                               THEO2240
        QS =12.*C*.002377*(VT**2)/2                                       THEO2250
        PHIDOT = P+TAN(THETA)*(Q*SIN(PHI)+R*COS(PHI))                      THEO2260
        THETAD = Q*COS(PHI)-R*SIN(PHI)                                     THEO2270
        SYDCT = (Q*SIN(PHI)+R*COS(PHI))/COS(THETA)                        THEO2280
        PHI = INTGRL(0.0,PHIDOT)                                           THEO2290
        THETA = INTGRL(0.04880,THETAD)                                    THEO2300
        SY = INTGRL(0.0,SYDCT)                                            THEO2310
        UDOT = -G*SIN(THETA)+V*K-W*Q+X/M+T/M                              THEO2320
        VDOT = G*SIN(PHI)*COS(THETA)-U*K+W*P+Y/M                          THEO2330
        WDOT = G*COS(PHI)*COS(THETA)+U*Q-V*P+Z/P                          THEO2340
        U = INTGRL(E38.1,UDOT)                                             THEO2350
        V = INTGRL(0.0,VDOT)                                              THEO2360
        W = INTGRL(8.75,WDOT)                                             THEO2370
        XEDCT=U*COS(SY)*COS(THETA)+V*(COS(SY)*SIN(THETA)*SIN(PHI)...      THEO2380
        -SIN(SY)*COS(PHI))+W*(COS(SY)*SIN(THETA)*COS(PHI)+...             THEO2390
        SIN(SY)*SIN(PHI))                                                 THEO2400
```

170

```
YEDOT=U*SIN(SY)*COS(THETA)+V*(SIN(SY)*SIN(THETA)*SIN(PHI)...          THEO02410
+COS(SY)*COS(PHI))+W*(SIN(SY)*SIN(THETA)*COS(PHI)-...                 THEO02420
COS(SY)*SIN(PHI))                                                     THEO02430
ZEDOT=-L*SIN(THETA)-V*COS(THETA)*SIN(PHI)-W*COS(THETA)*COS(PHI)       THEO02440
XEARTH=INTGRL(0.0,XEDOT)                                              THEO02450
YEARTH=INTGFL(0.0,YEDOT)                                              THEO02460
NOTE: ALTITUDE AND Z FUNCTIONS ARE DEFINED AS POSITIVE GOING UP       THEO02470
ALTUDE=INTGFL(50.,ZEDOT)                                              THEO02480
PDOT = 0.03608*LA+0.000279*NA+0.009160*P*Q-0.1837 11**Q              THEO02490
RDOT = 0.00279*LA+0.000064*NA-0.97823*P*Q-0.009160*R**Q              THEO02500
QDOT = (MA+1484.2*P*R-11.7*(P**2-R**2))/1507.0                        THEO02510
P = INTGRL(0.0,PDOT)                                                  THEO02520
Q = INTGRL(0.0,QDOT)                                                  THEO02530
R = INTGRL(0.0,RDOT)                                                  THEO02540
ALFA=ATAN(W/U)                                                        THEO02550
BETA=ASIN(V/VT)                                                       THEO02560
ALFADT=DERIV(0.6480,ALFA)                                             THEO02570
BETADT=DERIV(0.0,BETA)                                                THEO02580
VT=SQRT(L**2+V**2+W**2)                                               THEO02590
CLBAS=FUNGEN(LIFT1,1,ALFA)                                            THEO02600
DCLSTE=FUNGEN(LIFT2,1,ELE1)                                           THEO02610
DCDBAS=FLAGEN(DRAG1,1,CLBAS)                                          THEO02620
DCDSTE=FUNGEN(DRAG2,1,ELE1)                                           THEO02630
DCCSTA=FUNGEN(DRAG3,1,AILI)                                           THEO02640
DCDSTR=FUNGEN(DRAG4,1,RUDI)                                           THEO02650
CMBAS=FLNGEN(PITCH1,1,ALFA)                                           THEO02660
DCMSTE=FUNGEN(PITCH2,1,ELE1)                                          THEO02670
CYDAS=THGVAR(SIDE1,BETA,ALFA)                                         THEO02680
CRBAS=THGVAR(SIDE2,BETA,ALFA)                                         THEO02690
CNBAS=THGVAR(SIDE3,BETA,ALFA)                                         THEO02700
DCYSTR=THGVAR(DIREC1,RUDI,ALFA)                                       THEO02710
DCNSTR=THGVAR(DIREC2,RUDI,ALFA)                                       THEO02720
DCRSTR=THGVAR(DIREC3,RUDI,ALFA)                                       THEO02730
DCYSTA=THGVAR(LATRL1,AILI,ALFA)                                       THEO02740
DCNSTA=THGVAR(LATRL2,AILI,ALFA)                                       THEO02750
DCRSTA=THGVAR(LATRL3,AILI,ALFA)                                       THEO02760
CL=CLBAS+DCLSTE+.707/VT*(2.0*ALFADT+5.0*Q)                            THEO02770
CD=CDBAS+DCDSTE+DCDSTR+DCDSTK+.707/VT*(0.1*ALFADT+0.1*Q)              THEO02780
CY=CYBAS+DCYSTR+DCYSTA+DCOSTK+4.24/VT*(0.4C*R-C.10*P-0.10*BETADT)     THEO02790
CM=CMBAS+DCMSTE+0.707/VT*(-10.0*ALFADT-15.0*Q)                        THEO02800
CN=CNBAS+DCASIR+DCNSTA+4.24/VT*(0.15*BETADT-0.20*R-0.01*P)            THEO02810
CRULL=CRBAS+DCRSTA+DCRSTR+4.24/VT*(0.20*R-0.40*P)                     THEO02820
L=CL*QS                                                               THEO02830
D=CD*QS                                                               THEO02840
LA=6.485*CRCLL*CS                                                     THEO02850
MA=1.414*CM*QS                                                        THEO02860
NA=8.485*CN*QS                                                        THEO02870
X=L*SIN(ALFA)-D*COS(ALFA)                                             THEO02880
```

171

```
Y=CY*QS                                                          THE02890
Z=-L*CCS(ALFA)-D*SIN(ALFA)                                       THE02900
NZLGAD=-Z/(P*G)                                                  THE02910
NYLCAD=Y/(M*G)                                                   THE02920
ALFA1=ALFA*K2                                                    THE02930
BETA1=BETA*K2                                                    THE02940
PHII=PHI*K2                                                      THE02950
THETA1=THETA*K2                                                  THE02960
P1=P*K2                                                          THE02970
Q1=C*K2                                                          THE02980
R1=R*K2                                                          THE02990
SY1=SY*K2                                                        THE03000
ELE1=ELE*K2                                                      THE03010
RUDI=RUC*K2                                                      THE03020
AIL1=AIL*K2                                                      THE03030
GAMMA1=GAMMA*K2                                                  THE03040

INNER LCGP AUTOPILOT                                             THE03050

NORMAL ACCELERATION CGMMAND                                     THE03060
                                                                 THE03070
ANC1 = LIMIT(-2.0,4.0,ANC)                                       THE03080
ERRCRN = ANC1-(NZLQAD+C*QDOT/G)                                  THE03090
NSERVI =-1.C*(KA1*INTGRL(0.0,ERRCRN)-KR1*Q)                      THE03100
NSERVO = REALPL(0.0,0.025,NSERVI)                                THE03110
ELE = LIMIT(-0.262,0.262,NSERVO)                                 THE03120
                                                                 THE03130
BANK ANGLE CCMMAND SYSTEM                                        THE03140
60 DEGREE LIMIT ON BANK ANGLE = 1.047 RADIANS(DGNE IN ALGORITHM) THE03150
ROLL RATE (FCL) IS VARIED AS 50,100,&200 DEG/SEC                 THE03160
50=.87,  100=1.75,  200=3.49                                     THE03170
                                                                 THE03180
ERRBA1 = (PHIC1-PHI)*KD                                          THE03190
PCL1 = LIMIT(-1.75,1.75,ERRBA1)                                  THE03200
PCL1 = PCL*K2                                                    THE03210
PHIC2 = PHIC1*K2                                                 THE03220
BASRVI = -1.0*KR2*(PCL-P)                                        THE03230
BASRVO = REALPL(0.0,0.025,BASRVI)                                THE03240
AIL = LIMIT(-0.262,0.262,BASRVO)                                 THE03250
                                                                 THE03260
TURA CCCRDINATOR                                                 THE03270
                                                                 THE03280
ALC = 0.0                                                        THE03290
EN = ALC-(C*RDOT/G+NYLGAD)                                       THE03300
EN1 = KA2*(INTGRL(0.0,EN))                                       THE03310
TSERVI = -1.0*(EN1-KR3*R)                                        THE03320
TSERVO = REALPL(0.0,0.025,TSERVI)                                THE03330
RUD = LIMIT(-0.262,0.262,TSERVO)                                 THE03340
                                                                 THE03350
                                                                 THE03360
```

172

```
*     GUIDANCE.
*
*     GUIDANCE SCHEME IS DIVIDED INTO TWO PHASES-INGRESS AND ATTACK.
*     PROPORTIONAL NAVIGATION IS USED FOR HEADING CONTROL DURING INGRESS,
*     (WITH BANK ANGLE LIMITED TO 60 DEG)AND DURING ATTACK PHASE
*     (BANK ANGLE UNLIMITED).
*     AN ALTITUDE HOLD OF 50 FEET IS USED FOR INGRESS PHASE.
*     PROPORTIONAL NAVIGATION IN ELEVATION IS USED DURING ATTACK PHASE.
*
*     OUTER LCCP AUTOPILOT
*
*     FLIGHT PATH ANGLE
      AZC = 1.0+KGAMMA*VT/G*(GAMMAC-GAMMA)
      GAMMA = ASIN(ZEDOT/VT)
*     ALTITUDE HOLD
      ALTCMD = 50.0
      GAMMAC = KALT/VT*(ALTCMD-ALTUDE)
*
*     SEEKER EQUATIONS
*
      YT2 = YTI+35.0*TIME
      RANGE = SQRT((XTI-XEARTH)**2+(YT2-YEARTH)**2+(HTI-ALTUDE)**2)
      SIGDZB = -SIGDEL*SIN(PHI)+SIGDAZ*COS(THETA)*COS(PHI)
      SIGDEB = SIGDEL*COS(PHI)+SIGDAZ*COS(THETA)*SIN(PHI)
      SIGDZI = SIGDZB*COS(PHI)+SIGDEB*SIN(PHI)
      SIGDEI = -SIGDZB*SIN(PHI)+SIGDEB*COS(PHI)
*     THIS SECTION CHANGES PROGRAM VARIABLES TO MORE COMMON NAMES
      XRANGE = ABS(XTI-XEARTH)
      YRANGE = ABS(YT2-YEARTH)
      ZRANGE = ABS(HTI-ALTUDE)
      PCMD = FCL1
      PHICMD = PHIC2
      XMISLE = XEARTH
      YMISLE = YEARTH
      HMISLE = ALTUDE
      XTGT = XTI
      YTGT = YT2
      HTGT = HTI
      VECM = VTT
      HECM = HTT
      RUDDER = RUC1
      LISTAB = ELE1-AIL1
      RISTAB = ELE1+AIL1
      NZ = NZLCMD
      NZ1CMD = ANC1
      NY = NYLCAD
      NY1CMD = ALC
```

173

```
      ELLCSR  = SIGDEL*K2                                              THEO3850
      AZLCSR  = SIGDAZ*K2                                              THEO3863

      THETDT = (-2EDOT*(DXTGT**2+DYTGT**2)-DZTGT*(-XEDOT*DXTGT+...     THEO3880
     (35.0-YEDOT*DYTGT))/(RANGE**2*SQRT(DXTGT**2+DYTGT**2))           THEO3893
      THETDF = REALPL(0.0,10.,THETAD)                                  THEO3900
      SIGDEL = THETDT-THETDF                                           THEO3910
      SYDOTT =(XELOT*CYTGT+(35.-YEDOT)*DXTGT)/(DXTGT**2+DYTGT**2)      THEO3920
      SYDOIF = REALPL(0.0,10.0,SYDOT)                                  THEO3953
      SIGDAZ = SYLOTT-SYDLTF                                           THEO3940

                                                                      THEO3950
C     TARGET GLINT FACTOR WITH SHIP MOVING AT 21 KNOTS TO EAST        THEO3560
      YTR= GAUSS(0.0,20.0)                                            THEO3570
      XTR = GALSS(3.0,0.6.0)                                          THEO3980
      HTR = GAUSS(1.0,0.6.0)                                          THEO3590
      XT = XTI+XTR                                                    THEO4000
      YT = YTI+YTR                                                    THEO4010
      HT = HTI+HTF                                                    THEO4020
      XT = XTI                                                        THEO4030
      YT = YTI                                                        THEO4043
      HT = HTI                                                        THEO4050

                                                                      THEO4060
      NOSCRT                                                          THEO4070
      CALL DEBUG(1,29.82)                                            THEO4080
      CALL DEBUG(1,29.84)                                            THEO4090
      CALL DEEBUG(1,29.86)                                           THEO4103
      CALL DEBUG(1,29.88)                                            THEO4110
      CALL DEBUG(1,29.90)                                            THEO4120
      CALL DEBLG(1,29.95)                                            THEO4130
      TERMINAL                                                        THEO4143
      OUTPUT TIMMIN,RAGMIN,DXTGTM,DYTGTM,CZTGTM                       THEO4150
      LABEL MINIMUM RANGE,DXTGT,DYTGT, & CZTGT AND TIME OF MIN RANGE  THEO4160
      PAGE NPLCT=5                                                    THEO4173
      TIMER FINTIM=31.00, OUTDEL=0.100, DELT=0.01525                  THEO4180
      OUTPUT TIME,PI(-200.0,200.0),PCMD(-200.0,20C.0)                 THEO4190
      LABEL RCLL FATE (DEG/SEC) VS TIME                              THEO4200
      PAGE XYFLOT                                                    THEO4213
      OUTPUT TIME ,PHI1(-180.0,180.0) ,PHICMD(-180.0,180.0)          THEO4223
      LABEL BANK ANGLE (DEGREES) VS TIME                            THEO4233
      PAGE XYFLOT                                                    THEO4240
      OUTPUT TIME,RANGE(-4000.,28000.),XRANGE(-4000.,28000.),...     THEO4250
      YRANGE(-400.,2800.),ZRANGE(-40.,280.)                          THEO4260
      LABEL RANGE,XRANGE,YRANGE,ZRANGE (FEET) VS TIME               THEO4273
      PAGE XYFLCT                                                    THEO4280
      OUTPUT TIME(29.5,30.5),RANGE(0.,800.),XRANGE(0.,800.),...      THEO4290
      YRANGE(0.,8C.),ZRANGE(0.,8C.)                                 THEO4303
      LABEL RANGE,XRANGE,YRANGE,ZRANGE (FEET) VS TIME               THEO4310
      PAGE XYFLOT                                                    THEO4320
```

174

```
OUTPUT TIME,XMISLE(0.,3200.0),XTGT(0.,3200.0)                       THEO4330
LABEL MISSILE AND TARGET X COORDINATE (FEET) VS TIME                THEO4340
PAGE XYFLOT                                                         THEO4350
OUTPUT TIME,YMISLE(-400.,2800.),YTGT(-400.,2800.),YECM(-400.,2800.) THEO4360
LABEL MISSILE AND TARGET Y COORDINATE (FEET) VS TIME                THEO4370
PAGE XYFLOT                                                         THEO4380
OUTPUT TIME,HMISLE(-40.,280.),HTGT(-40.,280.),HECM(-40.,280.)       THEO4390
LABEL MISSILE AND TARGET ALTITUDE (FEET) VS TIME                    THEO4400
PAGE XYFLOT                                                         THEO4410
OUTPUT TIME,LISTAB(-20.,20.),RISTAB(-20.,20.)                       THEO4420
LABEL LEFT & RIGHT STABILIZERS (DEGREES) VS TIME                    THEO4430
PAGE XYFLOT                                                         THEO4440
OUTPUT TIME,RUDDER(-20.,20.)                                        THEO4450
LABEL RUDDER POSITION (DEGREES) VS TIME                             THEO4460
PAGE XYFLOT                                                         THEO4470
OUTPUT TIME,NZ(-3.,5.),NZICMD(-3.,5.)                               THEO4480
LABEL VERTICAL ACCELERATION (G'S) VS TIME                           THEO4490
PAGE XYFLOT                                                         THEO4500
OUTPUT TIME,NY(-2.,2.),NYICMD(-2.,2.)                               THEO4510
LABEL HORIZCNTAL ACCELERATION (G'S) VS TIME                         THEO4520
PAGE XYFLOT                                                         THEO4530
OUTPUT TIME,ELLOSR,AZLCSR                                           THEO4540
LABEL SEEKER EARTH LINE OF SIGHT RATES (DEG/SEC) VS TIME            THEO4550
PAGE XYFLOT                                                         THEO4560
OUTPUT XMISLE(21000.,25000.),YMISLE(0.,2000.),HMISLE(0.,800.)       THEO4570
LABEL MAP OF YMISLE AND HMISLE VS XMISLE (FEET)                     THEO4580
PAGE XYFLOT                                                         THEO4590
END                                                                 THEO4610
STOP                                                                THEO4620
```

ENDJOB

175

SEA SKIMMER GUIDANCE LAW SIMULATION

```
//WATL562 JOB (1562,0198),'THESIS2',CLASS=G          THEO0010
// EXEC CSMPXV                                        THEO0020
//X.FLGTPARM CC *                                     THEO0030
&PLOT SCALE=.5 &END                                   THEO0040
//X.SYSIN DD *                                         THEO0050
*                                                     THEO0060
NOTE: 2 DEGREES=.03490658 RADIANS  10 DEG=.17453292 52 THEO0070
NONLINEAR BANK TO TURN CRUISE MISSLE (VARYING COEFFICIENTS) THEO0080
WITH BANK TC TURN CR PCLAR COORDINATE SYS GUIDANCE LAW THEO0090
BASE LINE GUIDANCE LAW                                THEO0100
LABEL NCGLINT,LAMDA=4.0;ECM=0.5 CPS,ROLL RATE=100 DEG/SEC THEO0110
LABEL BURNTHROUGH 2000 FEET                           THEO0120
INITIAL                                               THEO0130
PARAM G=32.17,T=242.3,WT=2200.0,S=12.0,K2=57.29577 951,M=68.38,... THEO0140
C=0.0,KR1=0.28,KAL=0.35,KR2=0.10,KO=10.E,KR3=0.40,KA2=0.25,... THEO0150
KGAMMA=1.0,KFA=1.25,KFE1=1.0,KFE2=2.0,LAMDAZ=4.00,LAMDEL=4.0,... THEO0160
KAL=0.3,KXTI=25000.0,YTI=0.0,HTI=10.0,CLIMBA=0.1500983,... THEO0170
PI=3.141592654 FREQ=.50,SHIFTX=75.C,SHIFTH=15.0        THEO0180
TABLE OF CCEFFICIENTS STORED AS FUNCTION OF TWO OR THREE VARIABLES THEO0190
LIFT CHARACTERISTICS                                  THEO0200
ALFA VS CLBASIC                                        THEO0210
FUNCTION LIFT1=-12.0,-.32,-11.0,-.35,-10.0,-.46,-9.0,-.27,... THEO0220
-8.0,-.70,-7.0,-.69,-6.0,-.65,-5.3,-.58,-4.0,-.50,-3.0,-.42,... THEO0240
-2.0,-.3C,-1.0,-.18,0.0,-.06,1.0,0.C,2.C,.15,3.0,.25,4.0,.36,... THEO0250
5.0,.47,6.0,.58,7.0,.65,8.0,.80,9.0,.87,10.C,78,11.0,.70,... THEO0260
12.0,.84                                              THEO0270
ELE VS DELTA CLST(ELE)                                THEO0280
FUNCTION LIFT2=-15.0,-.100,-14.0,-.C97,-13.C,-.094,-14.0,-0.,... THEO0290
-.090,-11.0,-.084,-10.0,-.C78,-9.0,-.071,-8.0,-.065,-7.0,-0.,... THEO0300
-.056,-6.0,-.048,-5.0,-.040,-4.C,-.032,-3.0,-.024,-2.0,-.016,... THEO0310
-1.0,-.C08,C.0,0.0,1.0,.008,2.0,.016,3.0,.024,4.0,.033,5.0,... THEO0320
.041,6.0,.045,7.0,.057,8.0,.065,9.0,.073,10.0,.080,11.0,... THEO0330
.086,12.0,.092,13.0,.096,14.0,.098,15.C,.10C          THEO0340
DRAG CHARACTERISTICS                                  THEO0350
CLBASIC VS CDBASIC                                    THEO0360
FUNCTION DRAG1=-.9,.080,-.8,.061,-.7,.050,-.6,.042,-.5,.035,... THEO0370
-.4,.031,-.3,.026,-.2,.023,-.1,.022,0.0,.02,.1,.023,.2,.024,... THEO0380
.3,.026,.4,.031,.5,.036,.6,.042,.7,.049,.8,.057,... THEO0390
.9,.06,1.C,.080                                       THEO0400
ELE VS DELTA CDST(ELE)                                THEO0410
FUNCTION DRAG2=-15.0,.0106,-14.,.0091,-13.,.0077,-12.,.0065,... THEO0420
-10.,.CC44,-9.,.0036,-8.,.0028,-7.,.0022,-6.,.0016,-5.,.0011,... THEO0430
-.0004,-4.,.0007,-3.,.0003,-2.,.0001,-1.,.10,-C.,.0001,2.,.0012,... THEO0440
.0049,1C.,.C060,11.,.0075,12.,.0089,13.,.0106,14.,.0126,15.,.0146 THEO0450
AILERCN VS DELTA CDST(AIL)                            THEO0460
FUNCTION DRAG3=-15.,.0120,-14.,.0102,-13.,.0085,-12.,.0071,... THEO0470
                                                      THEO0480
```

THREE VARIABLE COEFFICIENT TABLES

SIDESLIP CHARACTERISTICS

ALFA VS BETA VS CYBASIC

ALFA VS BETA VS CROLLBASIC

ALFA VS BETA VS CNBASIC

PITCHING MOMENT CHARACTERISTICS

ALFA VS CMBASIC

```
FUNCTION SIDE3,   6.0=(-8.,-.042),(-6.,-.033),(-4.,-.022),...
(-2.,-.012),(0.,-.005),(2.,-.008),(4.,-.016),(6.,-.024),(8.,-.032)         THEO0670
(-2.,-.014),(0.,-.008),(2.,-.010),(4.,-.033),(6.,-.024),(8.,-.023)         THEO0980
DIRECTIONAL CONTROL CHARACTERISTICS                                        THEO0990
ALFA VS RUDDER VS DELTA CYST(RUD)                                          THEO1000
FUNCTION DIREC1,  -8.0=(-10.,-.090),(-10.,-.060),(-5.,-.042),...           THEO1010
(0.,-.04),(10.,-.040),(10.,-.070),(15.,-.101),(-5.,-.032),...             THEO1020
FUNCTION DIREC1,  2.0=(-15.,-.097),(-10.,-.062),(-5.,-.050),...            THEO1040
(0.,-.022),(5.,-.042),(10.,-.066),(15.,-.098),(-5.,-.037),...             THEO1050
FUNCTION DIREC1,  6.0=(-15.,-.095),(-10.,-.062),(-5.,-.037),...            THEO1060
(0.,-.006),(5.,-.038),(10.,-.019),(15.,-.052),(-5.,-.042),...             THEO1070
FUNCTION DIREC1,  8.0=(-15.,-.102),(-10.,-.069),(-5.,-.042),...           THEO1080
(0.,-.010),(5.,-.040),(10.,-.066),(15.,-.096),                            THEO1090
ALFA VS RUDDER VS DELTA CNST(RUD)                                          THEO1100
FUNCTION DIREC2,  -8.0=(-15.,-.070),(-10.,-.050),(-5.,-.026),...          THEO1110
(0.,-.022),(5.,-.028),(10.,-.080),(15.,-.049),                            THEO1120
FUNCTION DIREC2,  2.0=(-15.,-.048),(-10.,-.049),(-5.,-.024),...           THEO1140
(0.,-.020),(5.,-.048),(10.,-.062),(15.,-.079),(-5.,-.022),...             THEO1150
FUNCTION DIREC2,  6.0=(-10.,-.062),(-10.,-.048),(-5.,-.048),...           THEO1160
(0.,-.018),(5.,-.047),(15.,-.074),(-5.,-.018),...                         THEO1170
FUNCTION DIREC2,  8.0=(-15.,-.065),(-10.,-.048),(-15.,-.075),             THEO1180
(0.,-.003),(5.,-.014),(10.,-.046),                                        THEO1190
ALFA VS RUDDER VS DELTA CRCLLST(RUD)                                       THEO1200
FUNCTION DIREC3,  -8.0=(-15.,-.0050),(-10.,-.0034),(-5.,-.0018),...       THEO1210
(0.,-.0024),(5.,-.0048),(15.,-.0070),                                     THEO1220
FUNCTION DIREC3,  2.0=(-15.,-.0038),(-10.,-.0029),(-5.,-.0018),...        THEO1230
(0.,-.0012),(10.,-.0028),(15.,-.0053),                                    THEO1240
FUNCTION DIREC3,  4.0=(-15.,-.0033),(-10.,-.0027),(-5.,-.0018),...        THEO1250
(0.,-.0001),(5.,-.0012),(10.,-.0040),                                     THEO1260
FUNCTION DIREC3,  7.0=(-15.,-.0002),(-10.,-.0021),(-5.,-.0021),...        THEO1270
(0.,-.001),(5.,-.0020),(15.,-.0048),(-5.,-.0020),...                      THEO1280
FUNCTION DIREC3,  8.0=(-15.,-.0044),(-10.,-.0048),(-5.,-.0020),...        THEO1290
(0.,-.0036),(10.,-.0038),(1E.,-.0048),                                    THEO1300
LATERAL CONTROL CHARACTERISTICS                                           THEO1310
ALFA VS AILERON VS DELTA CYST(AIL)                                        THEO1320
FUNCTION LATIRL1, -8.0=(-15.,-.015),(-10.,-.013),(-5.,-.010),...          THEO1340
(0.,-.007),(5.,-.005),(15.,-.019),(-10.,-.014),(-5.,-.009),...            THEO1350
FUNCTION LATIRL1, -1.0=(-15.,-.003),(-10.,-.005),(-5.,-.014),...          THEO1360
(0.,-.002),(5.,-.006),(15.,-.017),(-10.,-.010),(-5.,-.002),...            THEO1370
FUNCTION LATIRL1,  4.0=(-15.,-.014),(-10.,-.006),(-15.,-.025),            THEO1380
(0.,-.007),(5.,-.010),(10.,-.006),(15.,-.002),(-5.,-.010),...            THEO1390
ALFA VS AILERON VS DELTA CNST(AIL)                                        THEO1400
FUNCTION LATIRL2, -8.0=(-15.,-.075),(-10.,-.0040),(1E.,-.0005),...        THEO1410
(0.,-.007),(10.,-.026),(10.,-.012),(1E.,-.0175),(-5.,-.0015),...          THEO1420
FUNCTION LATIRL2, -4.0=(-15.,-.007),(-10.,-.0050),(-10.,-.0030),...       THEO1430
                                                                          THEO1440
```

```
         (0.,-.0010),(5.,-.0030),(10.,-.0045),(15.,-.0070)
FUNCTION LATRL2 ,0.0=(-15.,0.),(-10.,0.),(0.,0.),...
(5.,0.),(10.,0.),(15.,0.)
FUNCTION LATRL2, 4.0=(-15.,.0075),(-10.,.0050),(-5.,-.0025),...
(0.0,.0008),(5.,.0025),(10.,.0040),(15.,.0070),...
FUNCTION LATRL2, 8.0=(-15.,.0120),(-10.,.0085),(-5.,-.0060),...
(0.0,-.0020),(5.,.0050),(10.,.0120),(15.,.0175)
ALFA VS AILERON VS DELTA CROLLST(AIL)
FUNCTION LATRL3 , -8.0=(-15.,-.0087),(-10.,-.0060),(-5.,.0030),...
(0.0,.0004),(5.,-.0008),(10.,-.0018),(15.,-.0030),...
FUNCTION LATRL3 , -4.0=(-15.,-.0096),(-10.,-.0066),(-5.,.0033),...
(0.0,.0004),(5.,.0023),(10.,.0059),(15.,-.0080),...
FUNCTION LATRL3 , 0.0=(-15.,-.0100),(-10.,-.0068),(-5.,.0034),...
(0.0,.0004),(5.,-.0030),(10.,-.0072),(15.,-.0092),...
FUNCTION LATRL3 , 4.0=(-15.,-.0030),(-10.,-.0064),(15.,.0036),...
(0.0,.0004),(5.,-.0030),(10.,.0046),(15.,.0088),...
FUNCTION LATRL3 , 8.0=(-15.,.0084),(-10.,.0058),(15.,-.0030),...
(0.0,-.0004),(5.,-.0020),(10.,-.0040),(15.,-.0050)
DYNAMIC
NOSORT
IF (TIME.EQ.0.0) RNGMIN =400.0
IF (RNGMIN.LE.RANGE) GO TO 10
RNGMIN = RANGE
TIMMIN = TIME
DXTGTM = DXTGT
CYTGTM = DYTGT
CZTGTM = DZTGT
CONTINUE
ALGORITHM THAT PROCEEDS FROM INGRESS TO POP UP TO 17800 RIGHT UP FSET TO
15800 LEVEL OFF TO 10200, POP UP TO 9100, ATTACK UNTIL HIT
IF(RANGE.GT.17800.0) GO TO 20
IF(RANGE.GT.15800.0) GO TO 30
IF(RANGE.GT.10200.0) GO TO 40
IF(RANGE.GT.9100.0) GO TO 50
INGRESS INTO 17800.0 FEET
CXTGT = XT-XEARTH
CYTGT = YT-YEARTH
CZTGT = HT-ALTUDE
AYC = LAMCAZ*VT*SIGDZL/G
ANC = AZC*COS(PHI)+AYC*SIN(PHI)
IF(AYC.EQ.0.0.AND.AZC.EQ.0.0) PHIC = 0.0
IF(AYC.NE.0.0.OR.AZC.NE.0.0) PHIC=ATAN2(AYC,AZC)
PHICL = LIMIT(-1.047,1.047,PHIC)
GO TO 20
TURN TO RIGHT UNTIL TARGET AZIMUTH ANGLE = 12 DEGREES(.16421)
CXTGT = XT-XEARTH
```

THE01450
THE01460
THE01480
THE01490
THE01500
THE01510
THE01520
THE01530
THE01540
THE01550
THE01560
THE01570
THE01580
THE01590
THE01600
THE01610
THE01620
THE01630
THE01640
THE01650
THE01660
THE01670
THE01680
THE01690
THE01700
THE01710
THE01720
THE01730
THE01740
THE01750
THE01760
THE01770
THE01780
THE01790
THE01800
THE01810
THE01820
THE01830
THE01840
THE01850
THE01860
THE01870
THE01880
THE01890
THE01900
THE01910
THE01920

```
          DYIGT = YT-YEARTH
          DZIGT = HT-ALTUDE
          ANC = AZC/COS(PHI)
          PHICI = 1.047
          GO TO 200
*  40  COMMAND 60RC DEGREES BANK ANGLE UNTIL START OF PUP UP
          DXIGT = XT-XEARTH
          DYIGT = YT-YEARTH
          DZIGT = HT-ALTUDE
          ANC = AZC/COS(PHI)
          PHICI = 0.0
          GO TO 200
*  50  PUP UP UNTIL ALTUDE = 250 FEET
          DXIGT = XT-XEARTH
          DYIGT = YT-YEARTH
          DZIGT = HT-ALTUDE
          AYC = LAMDAZ*VT*SIGDZ1/G
          ANC = AZCP*COS(PHI)+AYC*SIN(PHI)
          PHIC = -ATAN2(AYC,AZCP)
          PHICI = LIMIT(-1.047,1.047,PHIC)
          GO TO 200
*  60  ATTACK PHASE INTO THE TARGET
          IF(RANGE.GT.9000.0) GO TO 65
          IF(RANGE.LT.2000.) GO TO 65
**       ALLOW ECM BLINKING TO OCCUR BETWEEN 9000 AND 2000 FT RANGE
**       PUT ECM BLINKING OF 75FT HORIZONTAL SHIFT AT FREQ(.5,1.2 CPS)
          Y1 = SIN(2*PI*FREQ*TIME)
          YY = INSW(Y1,SHIFTY,0.0)
          YTT = YT-YY
*        PUT ECM BLINKING OF 15FT VERTICAL SHIFT AT FREQ(.5,1.2 CPS)
          H1 = SIN(2*PI*FREQ*TIME)
          HH = INSW(H1,SHIFTH,0.0)
          HTT = HT+HH
          DXIGT = XT-XEARTH
          DYIGT = YT-YEARTH
          DZIGT = HTT-ALTUDE
          GO TO 66
*  65     DXIGT = XT-XEARTH
          DYIGT = YT-YEARTH
          DZIGT = HT-ALTUDE
*        PROPORTIONAL ELEVATION
          PNELI = LAMDEL*VT*SIGDEL/G
*  66     AZCPR3 = PNELI + 1.0
          AYC = LAMDAZ*VT*SIGDZ1/G
          ANC = AZCPR3*COS(PHI)+AYC*SIN(PHI)
          PHIC = ATAN2(AYC,AZCPR3)
**       THIS ROUTINE KEEPS PHIC FROM ROTATING 360 DEG WHEN
**       TAR FUNCTION PASSES THROUGH 180 DEG.
```

THE01530
THE01540
THE01550
THE01560
THE01570
THE01580
THE01590
THE02000
THE02010
THE02020
THE02030
THE02040
THE02050
THE02060
THE02070
THE02080
THE02090
THE02100
THE02110
THE02130
THE02140
THE02150
THE02160
THE02170
THE02180
THE02190
THE02200
THE02210
THE02220
THE02230
THE02240
THE02250
THE02260
THE02270
THE02280
THE02290
THE02300
THE02340
THE02320
THE02330
THE02350
THE02390
THE02370
THE02380
THE02390
THE02400

180

```
        DELTA = PHIC1-PHI                                                    THEO02410
        DELTA1 = ABS(DELTA)                                                  THEO02420
        IF (DELTA1.LT.3.14159265) GO TO 200                                  THEO02430
        IF (PHIC1.GE.0.0) GO TO 70                                           THEO02440
        PHIC1 = PHIC1 + 6.2831853                                            THEO02450
        GO TO 200                                                            THEO02460
70      PHIC1 = PHIC1 - 6.2831853                                            THEO02470
200     CONTINUE                                                             THEO02480
        SQRT                                                                 THEO02490
        QS =12.*C*.02377*(VT**2)/2                                           THEO02500
        PHIDOT = P+TAN(THETA)*(Q*SIN(PHI)+R*COS(PHI))                        THEO02510
        THETAD = (Q*COS(PHI)-R*SIN(PHI)                                      THEO02520
        SYDCT = (Q*SIN(PHI)+R*COS(PHI))/COS(THETA)                           THEO02530
        PHI = INTGRL(0.04880,THETAD)                                         THEO02540
        THETA = INTGRL(0.0,PHIDOT)                                           THEO02550
        SY = INTGRL(0.0,SYDCT)                                               THEO02560
        UDOT = -G*SIN(THETA)+V*R-W*Q+X/M+T/M                                 THEO02570
        VDOT = G*SIN(PHI)*CGS(THETA)-U*R+W*P+Y/M                             THEO02580
        WDOT = G*COS(PHI)*CGS(THETA)+U*Q-V*P+Z/M                             THEO02590
        U = INTGRL(E38-1,UDOT)                                               THEO02600
        V = INTGRL(0.0,VDOT)                                                 THEO02610
        W = INTGRL(8.75,WDOT)                                                THEO02620
        XEDOT=L*COS(SY)*COS(THETA)+V*(COS(SY)*SIN(THETA)*SIN(PHI)...         THEO02630
        -SIN(SY)*COS(PHI))+W*(COS(SY)*SIN(THETA)*COS(PHI)+...                THEO02640
        YEDOT=U*SIN(SY)*COS(THETA)+V*(SIN(SY)*SIN(THETA)*SIN(PHI)...         THEO02650
        +COS(SY)*COS(PHI))+W*(SIN(SY)*SIN(THETA)*COS(PHI)-...                THEO02660
        ZEDCT= U*SIN(THETA)-V*COS(THETA)*SIN(PHI)-W*COS(THETA)*COS(PHI)      THEO02670
        XEARTH=INTGRL(0.0,XEDOT)                                             THEO02680
        YEARTH=INTGRL(0.0,YEDOT)                                             THEO02690
        NOTE: ALTITUDE AND Z FUNCTIONS ARE DEFINED AS POSITIVE GOING UP      THEO02700
        ALTUDE=INTGRL(50,ZEDOT)                                              THEO02710
        PDOT = 0.03608*NA+LA+0.000279*NA-0.009160*P*Q-0.183716*R*Q           THEO02720
        RDOT = 0.00229*NA+LA+0.000684*NA-0.978236*P*Q-0.009160*R*Q           THEO02730
        QDOT = (PA+148.2*P*R-11.7*(P**2-R**2))/1507.0                        THEO02740
        P = INTGRL(0.0,PDOT)                                                 THEO02750
        Q = INTGRL(0.0,QDOT)                                                 THEO02760
        R = INTGRL(0.0,RDOT)                                                 THEO02770
        ALFA=ATAN(W/U)                                                       THEO02780
        BETA=ASIN(V/VT)                                                      THEO02790
        ALFADT=DERIV(0.04880,ALFA)                                           THEO02800
        BETADT=DERIV(0.0,BETA)                                               THEO02810
        VT=SQRT(U**2+V**2+W**2)                                              THEO02820
        CLBAS=FUNGEN(LIFT1,1,ALFA)                                           THEO02830
        DCLSTE=FUNGEN(LIFT2,1,ELE1)                                          THEO02840
        CDBAS=FUNGEN(DRAG1,1,CLBAS)                                          THEO02850
        DCDSTE=FUNGEN(DRAG2,1,ELE1)                                          THEO02880
```

181

```
DCCSTA=FUNGEN(DRAG3,1,AIL1)
DCDSTR=FUNGEN(DRAG4,1,RUD1)
CMBAS=FUNGEN(PITCH1,1,ALFA1)
DCMSTE=FUNGEN(PITCH2,1,ELE1)
CYBAS=T*CVAF(SICE1,BETA1,ALFA1)
CRBAS=T*CVAF(SICE2,BETA1,ALFA1)
CNBAS=T*CVAF(SICE3,BETA1,ALFA1)
DCYSTK=T*CVAR(DIREC1,RUD1,ALFA1)
DCNSTR=T*CVAR(DIREC2,RUD1,ALFA1)
DCRSTR=T*CVAR(DIREC3,RUD1,ALFA1)
DCNSTA=T*CVAR(LATRL1,AIL1,ALFA1)
DCYSTA=T*CVAR(LATRL2,AIL1,ALFA1)
DCRSTA=T*CVAR(LATRL3,AIL1,ALFA1)
CL=CLBAS+CCLSTE+.707/VT*(2.0*ALFADT+5.0*Q)
CD=CDBAS+CCLSTE+DCDSTA+DCDSTR+.707/VT*(C.1*ALFADT+0.1*4)
CY=CYBAS+DCYSTE+DCYSTA+4.24/VT*(0.4C*R-0.10*P-0.10*BETADT)
CM=CMBAS+CCPSTE+0.707/VT*(-10.0*ALFADT-15.0*Q)
CN=CNBAS+DCNSTA+DCNSTR+4.24/VT*(0.15*BETADT-0.20*R-0.01*P)
CRDLL=CRBAS+DCRSTA+DCRSTR+4.24/VT*(0.20*R-0.40*P)
L=CL*QS
D=CD*QS
LA=8.485*CRCLL*QS
MA=1.114*CM*QS
NA=8.485*CN*QS
X=L*SIN(ALFA)-D*COS(ALFA)
Y=CY*QS
Z=-L*COS(ALFA)-D*SIN(ALFA)
NZLCAC=-Z/(M*G)
NYLCAD=Y/(M*G)
ALFA1=ALFA*K2
BETA1=BETA*K2
PHI1=PHI*K2
THETA1=THETA*K2
P1=P*K2
Q1=Q*K2
R1=R*K2
SY1=SY*K2
ELE1=ELE*K2
RUD1=RUD*K2
AIL1=AIL*K2
GAMMA1=GAMMA*K2

INNER LCCP AUTOPILOT

NORMAL ACCELERATION COMMAND

ANC1 = LIMI1(-2.0,4.0,ANC)
ERRCRN = ANC1-(NZLCAD+C*QDCT/G)
```

*****

```
NSERVI =-1.C*(KA1*INTGRL(0.0,ERROKN)-KR1*Q)                              THEO03370
NSERVO = REALPL(0.C,0.025,NSERVI)                                        THEO03380
ELE = LIMIT(-0.262,0.262,NSERVO)                                         THEO03390

BANK ANGLE COMMAND SYSTEM                                                THEO03400
60 DEGREE LIMIT ON BANK ANGLE = 1.047 RADIANS(DONE IN ALGORITHM)         THEO03410
ROLL RATE (FCL) IS VARIED AS 50,10C,&200 DEG/SEC                         THEO03420
50=.87, 10C=1.75, 200=3.49                                               THEO03430
                                                                         THEO03440
ERRBAL = (PHIC1-PHI)*KD                                                  THEO03450
PCL = LIMIT(-1.75,1.75,ERRBAL)                                           THEO03460
PCL1 = PCL*K2                                                            THEO03470
PHIC2 = PHIC1*K2                                                         THEO03480
BASRVI = -1.0*KR2*(PCL-P)                                                THEO03490
BASRVO = REALPL(0.0,0.025,BASRVI)                                        THEO03500
AIL = LIMIT(-0.262,0.262,BASRVO)                                         THEO03510

TURN COORDINATOR                                                         THEO03520
                                                                         THEO03530
ALC = C.C                                                                THEO03540
EN = ALC-(C*RDOT/G+NYLOAD)                                               THEO03550
EN1 = KA2*(INTGRL(0.0,EN))                                               THEO03560
TSERVI = -1.0*(EN1-KR3*R)                                                THEO03570
TSERVO = REALPL(0.0,0.025,TSERVI)                                        THEO03580
RUD = LIMIT(-0.262,0.262,TSERVO)                                         THEO03590

GUIDANCE.                                                                THEO03600
                                                                         THEO03610
GUIDANCE SCHEME IS DIVIDED INTO FOUR PHASES-INGRESS,TURN,POP UP,         THEO03620
AND ATTACK. PROPORTIONAL NAVIGATION IS USED FOR HEADING CONTROL          THEO03630
DURING INGRESS AND POP UP (BOTH WITH BANK ANGLE LIMITED TO 60 DEG)       THEO03640
AND DURING ATTACK PHASE (BANK ANGLE UNLIMITED). DURING THE TURN          THEO03650
PHASE THE HEADING COMMANDS ARE ACHIEVED WITH FIXED BANK ANGLES.          THEO03660
AN ALTITUDE HOLD OF 50 FEET IS USED FOR INGRESS AND TURN PHASES.         THEO03670
VERTICAL FLIGHT PATH ANGLE CONTROL (CONSTANT RATE OF CLIMB OF 8.6        THEO03680
DEGREES IS USED FOR THE POP UP MANEUVER).                               THEO03690

OUTER LCCP AUTOPILOT                                                     THEO03700
FLIGHT PATH ANGLE                                                        THEO03710
AZC = 1.0*KGAMMA*VT/G*(GAMMAC-GAMMA)                                     THEO03720
GAMMA = ASIN(ZEDGT/VT)                                                   THEO03730
ALTITUDE HOLD                                                            THEO03740
ALTCMD = 50.0                                                            THEO03750
GAMMAC = KALT/VT*(ALTCMD-ALTUDE)                                         THEO03760
POP UP MANELVER (CLIMB ANGLE=CLIMBA=8.6 DEGREES)                         THEO03770
AZCP = 1.0+KGAMMA*VT/G*(CLIMBA-GAMMA)                                    THEO03810
                                                                         THEO03820
SEEKER EQUATIONS                                                         THEO03830
```

```
       YT2 = YTI+35.0*TIME                                              THEO3850
       RANGE = SQRT((XTI-XEARTH)**2+(YT2-YEARTH)**2+(HTI-ALTUDE)**2)     THEO3860
       SIGDZB = -SIGDEL*SIN(PHI)+SIGDAZ*COS(THETA)*COS(PHI)             THEO3870
       SIGDEB = SIGDEL*COS(PHI)+SIGDAZ*COS(THETA)*SIN(PHI)             THEO3880
       SIGDZI = SIGDZB*COS(PHI)+SIGDEB*SIN(PHI)                        THEO3890
       SIGDEI = -SIGDZB*SIN(PHI)+SIGDEB*COS(PHI)                       THEO3900
C      THIS SECTION CHANGES PROGRAM VARIABLES TO MORE COMMON NAMES       THEO3910
       XRANGE = ABS(XTI-XEARTH)                                        THEO3920
       YRANGE = ABS(YT2-YEARTH)                                        THEO3930
       ZRANGE = ABS(HTI-ALTUDE)                                        THEO3940
       PCMD = PCL1                                                     THEO3950
       PHICMD = PHIC2                                                  THEO3960
       XMISLE = XEARTH                                                 THEO3970
       YMISLE = YEARTH                                                 THEO3980
       HMISLE = ALTUDE                                                 THEO3990
       XTGT = XTI                                                      THEO4000
       YTGT = YT2                                                      THEO4010
       HTGT = HTI                                                      THEO4020
       YECM = YTT                                                      THEO4030
       HECM = HTT                                                      THEO4040
       RUDDER = RUC1                                                   THEO4050
       LISTAB = ELE1-AIL1                                              THEO4060
       RISTAB = ELE1+AIL1                                              THEO4070
       NZ = NZLCAD                                                     THEO4080
       NZ1CMD = ANC1                                                   THEO4090
       NY = NYLCAD                                                     THEO4100
       NY1CMD = ALC                                                    THEO4110
       ELLCSR = SIGDEL*K2                                              THEO4120
       AZLCSR = SIGDAZ*K2                                              THEO4130
                                                                       THEO4140
       THETDT =(-ZEDOT*(DXTGT**2+DYTGT**2)-DZTGT*(-XEDOT*DXTGT+...      THEO4150
      (35.0-YEDOT)*DYTGT))/(RANGE**2*SQRT(DXTGT**2+DYTGT**2))          THEO4160
       THETDF = REALPL(0.C10,-THETAD)                                  THEO4170
       SIGDEL =(THETDT-THETDF)                                         THEO4180
       SYDOTT =(XEDOT*LYTGT+(35.-YEDOT)*DXTGT)/(DXTGT**2+DYTGT**2)     THEO4190
       SYDCTF = REALPL(0.010,-0.0,SYDOT)                              THEO4200
       SIGDAZ = SYDOTT-SYDCTF                                          THEO4210
                                                                       THEO4220
C      TARGET GLINT FACTOR WITH SHIP MOVING AT 21 KNOTS TO EAST          THEO4230
       YTR= GAUSS(30.0,20.0)                                           THEO4240
       XTR = GAUSS(30.0,6.0)                                           THEO4250
       HTR = GAUSS(10.0,6.0)                                           THEO4260
       XT = XTI+XTF                                                    THEO4270
       YT = YT2+YTF                                                    THEO4280
       HT = HTI+HTF                                                    THEO4290
       XT = XTI                                                        THEO4300
       YT = YT2                                                        THEO4310
                                                                       THEO4320
```

```
HT = HTI
NOSCRT
CALL DEBUG(1,30,16)                                                    THE04330
CALL DEBUG(1,30,17)                                                    THE04340
CALL DEBUG(1,30,18)                                                    THE04350
CALL DEBUG(1,30,19)                                                    THE04360
CALL DEBUG(1,30,20)                                                    THE04370
CALL DEBUG(1,30,21)                                                    THE04380
CALL DEBUG(1,30,22)                                                    THE04390
CALL DEBUG(1,30,23)                                                    THE04400
CALL DEBUG(1,30,24)                                                    THE04410
CALL DEBUG(1,30,25)                                                    THE04420
CALL DEBUG(1,30,26)                                                    THE04430
TERMINAL                                                               THE04440
OUTPUT TIMMIN,RAGMIN,DXTGTM,DYTGTM,DZTGTM                              THE04450
LABEL MINIMUM RANGE,DXTGT,DYTGT, & DZTGT AND TIME OF MIN RANGE         THE04460
PAGE NPLCT=6                                                           THE04470
TIMER FINTIM=31.00, OUTDEL=0.100, DELT=0.01525                         THE04480
OUTPUT TIME,PHI(-230.0,200.0),PCMD(-203.0,200.0)                       THE04490
LABEL ROLL RATE (DEG/SEC) VS TIME                                      THE04500
PAGE XYFLOT                                                            THE04510
OUTPUT TIME,PHI(-180.0,180.0),PHICMD(-180.0,180.0)                     THE04520
LABEL BANK ANGLE (DEGREES) VS TIME                                     THE04530
PAGE XYFLOT                                                            THE04540
OUTPUT TIME,RANGE(-400.,2000.),XRANGE(-400.,28000.),...               THE04550
YRANGE(-400.,2800.),ZRANGE(-40.,280.)                                 THE04560
LABEL RANGE,YRANGE,ZRANGE (FEET) VS TIME                               THE04570
PAGE XYFLOT                                                            THE04580
OUTPUT TIME(29.,5,30.5),RANGE(0.,800.),XRANGE(0.,80.),...             THE04590
YRANGE(0.,80.),ZRANGE(0.,80.)                                         THE04600
LABEL RANGE,YRANGE,ZRANGE (FEET) VS TIME                               THE04610
PAGE XYFLOT                                                            THE04620
OUTPUT TIME,XMISLE(0.,2000.0),XIGT(0.,2000.0)                          THE04630
LABEL MISSILE AND TARGET X COORDINATE (FEET) VS TIME                   THE04640
PAGE XYFLOT                                                            THE04650
OUTPUT TIME,YMISLE(-400.,2800.),YTGT(-400.,2800.),YECM(-400.,2800.)    THE04660
LABEL MISSILE AND TARGET Y COORDINATE (FEET) VS TIME                   THE04670
PAGE XYFLOT                                                            THE04680
OUTPUT TIME,HMISLE(-40.,280.),HTGT(-40.,280.),HECM(-40.,280.)          THE04690
LABEL MISSILE AND TARGET ALTITUDE (FEET) VS TIME                       THE04700
PAGE XYFLOT                                                            THE04710
OUTPUT TIME,LISTAB(-20,20),RISTAB(-20,20)                              THE04720
LABEL LEFT & RIGHT STABILIZERS (DEGREES) VS TIME                       THE04730
PAGE XYFLOT                                                            THE04740
OUTPUT TIME,RUDDER(-20,20)                                             THE04750
LABEL RUDDER POSITION (DEGREES) VS TIME                                THE04760
PAGE XYFLOT                                                            THE04770
                                                                      THE04780
                                                                      THE04790
                                                                      THE04800
```

185

```
OUTPUT TIME,NZ(-3.,5.),NZ1CMD(-3.,5.)                          THEO4810
LABEL VERTICAL ACCELERATION (G.S) VS TIME                      THEO4820
PAGE XYFLOT                                                    THEO4830
OUTPUT TIME,NY(-2.,2.),NY1CMD(-2.,2.)                          THEO4840
LABEL HORIZONTAL ACCELERATION (G.S) VS TIME                    THEO4850
PAGE XYFLOT                                                    THEO4860
OUTPUT TIME,ELLOSR,AZLGSR                                      THEO4870
LABEL SEEKER EARTH LINE OF SIGHT RATES (DEG/SEC) VS TIME       THEO4880
PAGE XYFLOT                                                    THEO4890
OUTPUT XMISLE(21000.,25000.),YMISLE(0.,2000.),HMISLE(0.,800.) THEO4900
LABEL MAP OF YMISLE AND HMISLE VS XMISLE (FEET)                THEO4910
PAGE XYFLOT                                                    THEO4920
END                                                           THEO4930
STOP                                                           THEO4940
                                                              THEO4950
* * * * * * * * *

ENDJCB
```

LIST OF REFERENCES

1. Gonzalez, J., <u>New Methods in the Terminal Guidance and Control of Tactical Missiles</u>, AGARD Lecture Series No. 101, 1979.

2. Hewett, M.D., Guidance and Control Systems Course (Class Notes), 1982.

3. Hoisington, D.B., <u>Introduction to Electronic Warfare</u> Notes, 1980.

4. Speclchart, F.H., and Green, W.L., <u>A Guide to Using CSMP-The Continuous System Modeling Program</u>, Prentice-Hall, 1976.

INITIAL DISTRIBUTION LIST

No. Copies

1. Library, Code 0142   2
    Naval Postgraduate School
    Monterey, California   93940

2. Department Chairman, Code 62   1
    Department of Electrical Engineering
    Naval Postgraduate School
    Monterey, California   93940

3. Professor M.D. Hewett, Code 67Hj   5
    Department of Aeronautics
    Naval Postgraduate School
    Monterey, California   93940

4. Professor H. A. Titus, Code 62Ts   1
    Department of Electrical Engineering
    Naval Postgraduate School
    Monterey, California   93940

5. Professor G. Thaler, Code 62Tr   1
    Department of Electrical Engineering
    Naval Postgraduate School
    Monterey, California   93940

6. Director   1
    Attention: CDR Richard Fessenden
    JCM 531
    Joint Cruise Missile Programs.
    Bldg. NC-1
    Washington, D.C.   20360

7. Professor D. J. Collins, Code 67Co   1
    Department of Aeronautics
    Naval Postgraduate School
    Monterey, California   93940

8. LCDR Kent B. Watterson   5
    Naval Sea Systems Command (SEA-62Y1F)
    Department of the Navy
    Washington, D.C.   20362

9. LT Daniel A. Forkel   1
    Naval Postgraduate School
    SMC 2088
    Monterey, Calfiornia   93940

10. Defense Technical Information Center   2
    Cameron Station
    Alexandria, Virginia   22314

ATE
LMED
8